Universidade do Minho
Escola de Medicina

José Carlos Lentilhas da Graça

Spinal Cord Injury: can recovery be achieved through the Spleen?

April, 2024

Spinal Cord Injury: can recovery be achieved through the Spleen?
José Carlos Lentilhas da Graça
Uminho | 2024

FCT Fundação para a Ciência e a Tecnologia
PhDoC Ageing and Chronic Diseases
ICVS Life and Health Sciences Research Institute, Instituto de Investigação em Ciências da Vida e Saúde
ICVS/3B's Associate Laboratory
Universidade do Minho Escola de Medicina
PD-F Programas de Doutoramento FCT
República Portuguesa
MCTES Ministério da Ciência, Tecnologia e Ensino Superior
CNC Centro de Neurociência e Biologia Celular
Universidade de Coimbra 1290
Prémios
Wings for Life Spinal Cord Research Foundation
POCH
iBiMED Universidade de Aveiro
PPBI Portuguese Platform of Bioimaging
NOVA Medical School
NOVA Universidade Nova de Lisboa
Cofinanciado por:
COMPETE 2020
Portugal 2020
União Europeia Fundo Europeu de Desenvolvimento Regional
União Europeia Fundo Social Europeu
NORTE2020 Programa Operacional Regional do Norte

Universidade do Minho
Escola de Medicina

José Carlos Lentilhas da Graça

Spinal Cord Injury: can recovery be achieved through the Spleen?

Tese de Doutoramento

Programa Interuniversitário de Doutoramento em Envelhecimento e Doenças Crónicas

Trabalho efetuado sob a orientação do

Doutor Nuno André Martins Silva

Doutor Ramiro Daniel Carvalho de Almeida

Abril de 2024

Agradecimentos

Quero começar por agradecer ao Doutor Nuno Silva, meu Orientador, por toda a compreensão, amizade, ajuda, por estar sempre presente em todos os momentos, por tudo, pois sem ele ele não teria conseguido chegar até aqui. O meus agradecimnentos Doutor ao Ramiro Almeida, também meu Orientdor, por toda a ajuda, compreensão e disponibildade. Quero também agradecer ao Doutor António Salgado, Líder da ReNeu, por toda compreensão e disponibilidade. Agradecer também ao João Afonso, Diogo Santos, Eduardo Gomes que acompanharam mais de perto os meus trabalhos e também restantes pessoas envolvidas no artigo científico presente nesta Tese, assim como todos membros atuais e passados da ReNEU/ "TóTeam". Muito obrigado à Marta S. Dias, Vera M. Mendes e Doutor Bruno Manadas por a sua ajuda no artigo científico. Agradecer à Professora Margarida Correia-Neves por todo o apoio, ao PhDOC, restantes membros da sua Comissão Diretiva e a todos os associados a este Programa Doutoral. Aos Colegas Ana Bela, Gabriela, Carla e restantes colegas da minha edição e aos colegas das restante edições dos PhDOC, o meu muito obrigado. O meu agradecimento institucional ao ICVS e Escola de Medicina, e Universidade do Minho. aos seu Diretores e a todo pessoal por todo o seu apoio. Ao CNC e Faculdade de Medicina da Universidade de Coimbra, iBiMED, Universidade de Aveiro assim como à NOVA Medical School|Faculdade de Ciências Médicas da Universidade Nova de Lisboa . À Doutora Cláudia Guimas Almeida, muito obrigado, por me ter dado a conhecer o PhDOC. Agradecer também à Fundação para a Ciência e a Tecnologia (FCT), a bolsa nacional de doutoramento (com referência PD/BD/127820/2016). A toda a Comunidade da Paróquia de São Victor, Braga, e assim como aos seus grupos onde estou envolvidos, por todo o auxílio. A todas pessoas, que não consigo mencionar, que me apoiaram. Ao saudoso Padre Leonard, pelas suas palavras de esperança. Ao meu Pai, que se encontra num lugar melhor, que intercede por mim e à minha Mãe, por tudo, e por mais palavras que escreva, não conseguiria expressar todos o meu agradecimentos e que sem ela nada teria sido possível. A Deus, por ter providenciado, o meu muito obrigado.

Apoio Financeiro

Este trabalho foi financiado através da FCT, Prémios Santa Casa Neurociências–Prize Melo e Castro, Wings For Life Spinal Cord Research Foundation. Aquisição de imagens nas instalação LiM do iBiMED e na Plataforma de Microscopia Científica do ICVS, ambos membros da infraestrtura nacional PPBI - Plataforma Portuguesa de Bioimagem (PPBI-POCI-01-0145-FEDER-022122).

STATEMENT OF INTEGRITY

I hereby declare having conducted this academic work with integrity. I confirm that I have not used plagiarism or any form of undue use of information or falsification of results along the process leading to its elaboration.

I further declare that I have fully acknowledged the Code of Ethical Conduct of the University of Minho.

Resumo

Lesão da Medula Espinhal: poderá a recuperação ser alcançada através do Baço?

A lesão da medula espinhal (LME) é uma doença neurológica devastadora com um forte impacto na vida das pessoas afetadas, sendo por isso urgente o desenvolvimento de novas estratégias terapêuticas. Após a LME, a resposta inflamatória é um importante fator para a continuação de danos secundários no tecido neural. Os macrófagos que infiltram a medula espinal podem adquirir um espectro de estados de ativação, no entanto, o microambiente no local da LME favorece a polarização dos macrófagos num fenótipo pró-inflamatório. Este é um dos principais motivos por que ensaios clínicos que transplantaram macrófagos falharam no passado. Foi anteriormente demonstrado que após a LME a medula espinhal é primeiramente infiltrada por macrófagos originados do reservatório de monócitos do baço. Deste modo, é apelativo estudar estes monócitos bem como a sua capacidade para serem polarizados em macrófagos com fenótipos anti-inflamatórios e reparadores. Portanto, nesta tese, investigamos o potencial terapêutico do secretoma de macrófagos do baço para a recuperação da LME e, em vez de transplantar as células, injetámos os fatores parácrinos e as vesículas extracelulares que eles secretam, evitando a perda do fenótipo das células transplantadas devido a sinais do microambiente local. Primeiro, investigámos o efeito do secretoma *in vitro* usando neurónios periféricos e derivados do SNC e células-tronco neurais humanas. Além disso, realizamos um ensaio pré-clínico em ratinhos e analisámos a recuperação das funções motoras, sensoriais e autonómicas. Demonstrámos que diferentes fenótipos de macrófagos têm um efeito distinto no crescimento e sobrevivência neuronal, nomeadamente, a ativação alternativa com IL-10 e TGF-β1 ($M_{(IL\text{-}10\ +\ TGF\text{-}\beta1)}$) promove regeneração axonal significativa. Observamos também que a injeção sistêmica de fatores solúveis e vesículas extracelulares derivadas de macrófagos $M_{(IL\text{-}10\ +\ TGF\text{-}\beta1)}$ promove recuperação funcional significativa após lesão medular compressiva e leva a maior sobrevivência dos neurónios da medula espinhal. Além disso, o secretoma de $M_{(IL\text{-}10\ +\ TGF\text{-}\beta1)}$ apoiou a recuperação da função da bexiga e diminuiu a ativação microglial, astrogliose e cicatriz fibrótica na medula espinhal. A análise proteómica do secretoma derivado de $M_{(IL\text{-}10\ +\ TGF\text{-}\beta1)}$ identificou grupos de proteínas envolvidas na extensão dos axónios, manutenção das espinhas dendríticas, estabelecimento da polaridade celular e regulação da ativação astrocítica. Globalmente, os nossos resultados demonstraram que os fatores solúveis e vesículas extracelulares produzidos pelos macrófagos podem ser uma terapia promissora para LME, com possíveis aplicações clínicas.

Palavras-chave: Lesão da Medula Espinhal; Macrófagos; Neuroimunologia; Neurorregeneração, Secretoma.

Abstract

Spinal Cord Injury: can recovery be achieved through the Spleen?

Spinal cord injury (SCI) constitutes a debilitating neurological disorder with a strong impact in the persons affected. Therefore, it is urgent to develop new therapeutic strategies. The inflammatory response post-SCI significantly contributes to secondary damage of the neural tissue. Infiltrating macrophages can acquire a spectrum of activation states, however, the microenvironment at the SCI site tends to polarize them towards a pro-inflammatory phenotype, hindering the success of macrophage transplantation. The first wave of macrophages that infiltrated the spinal cord originated from splenic monocyte reservoir. Thus, it is appealing to comprehend the function of these macrophages and understand the therapeutic potential of the alternatively activated anti-inflammatory phenotypes. Therefore, in this thesis, we explored the therapeutic potential of the spleen macrophage secretome for SCI recovery. Instead of transplanting the cells, we injected the paracrine factors and extracellular vesicles secreted by macrophages, mitigating the risk of phenotype loss of the transplanted cells due to local environmental cues. Initially, we investigated the effect of the secretome *in vitro* using peripheral and CNS-derived neurons as well as human neural stem cells. Subsequently, a pre-clinical trial using a mouse model with SCI compression was conducted to analyze the recovery of motor, sensory and autonomic functions. Our findings indicate that different macrophage phenotypes have a distinct effect on neuronal growth and survival. Notably, the alternative activation with IL-10 and TGF-β1 ($M_{(IL\text{-}10+TGF\text{-}\beta1)}$) significantly promotes axonal regeneration. We also observed that systemic injection of secretome derived from $M_{(IL\text{-}10+TGF\text{-}\beta1)}$ macrophages promotes significant functional recovery after compressive SCI, accompanied by increased survival of spinal cord neurons. Additionally, the $M_{(IL\text{-}10+TGF\text{-}\beta1)}$ secretome supported the recovery of bladder function and decreased microglial activation, astrogliosis and fibrotic scar in the spinal cord. Proteomic analysis of the $M_{(IL\text{-}10+TGF\text{-}\beta1)}$-derived secretome identified protein clusters crucial for axon extension, dendritic spine maintenance, cell polarity establishment, and regulation of astrocytic activation. Collectively, this thesis underscores the potential of macrophages-derived soluble factors and extracellular vesicles as a promising therapy for SCI, with possible clinical applications.

Keywords: Macrophages; Neuroimmunology; Neuroregeneration; Secretome; Spinal Cord Injury.

CONTENTS

List of Abbreviations

2D - Two Dimensional

3D - Three Dimensional

β2-Ars - β2-Adrenoceptors

ACK - Ammonium-chloride-potassium

AGM - Aorta-gonads-mesonephros

AIS - ASIA Impairment Scale

AKT - Protein kinase B

AMPA - α-amino-3-hydroxy-5-methyl-4-isoxazole propionic acid

ANOVA - Analysis of variance

AR - Aldose reductase

ARG1 - Arginase 1

ARI - AR inhibitor

ARRIVE - Animal Research: Reporting of In Vivo Experiments

ASIA - American Spinal Injury Association

ATP - Adenosine Triphosphate

BAM - Border-associated Macrophages

BDNF - Brain Derived Neurotrophic Factor

BMS - Basso Mouse Scale

BMSCs - Bone marrow-derived stem cells

BSA - Bovine serum albumin

C1q - Complement component 1q

CCL - CC motif chemokine ligand

CCR - CC motif chemokine receptor

CD - cluster of differentiation

CDC - Centers for Disease Control and Prevention

cDNA - Complementary DNA

chABC - Chondroitinase ABC

ChP - Choroid plexus

cMo - Classical monocytes

cMoP - Common Monocyte precursor

CMP - Common Myeloid progenitors

CNC—Center for Neuroscience and Cell Biology

CNS - Central nervous system

Covid-19 - Coronavirus disease 2019

COX-2 - Cyclooxygenase-2

CSF - Cerebrospinal fluid

CSF-1 - Colony Stimulating Factor-1

CSF1R - Colony stimulating factor 1 receptor (M-CSF receptor)

CSPGS - chondroitin sulfate proteoglycans

CST - Corticospinal tract

CX3CR1 - C-X3-C motif chemokine receptor 1

CXCL - Chemokine (C-X-C motif) ligand

DAMPs - Damage-associated Molecular Patterns

DAPI - 40,6-diamidino-2-phenylindoledihydrochloride

DC – Dendritic Cell

DCMo - DC-like monocytes

DDA - Data-dependent acquisition

DLL - Delta-like

DMEM - Dulbecco Modified Eagle Medium

DMSO - Dimethyl sulfoxide

DNA - Deoxyribonucleic acid

DRG - Dorsal root ganglion

DRGMacs - Macrophages in the DRG

E - Embryonic day

EBs - Embryoid Bodies

ECM - Extracellular matrix

ED-Siglec-9 - Ectodomain of sialic acid-binding Ig-like lectin-9

EGR2 - Early growth response 2

EMPs - Erythromyeloid progenitors

ERK1/2 - Extracellular signal-regulated kinase 1/2

FACS - Fluorescence-activated cell sorting

FBS - Fetal bovine serum

Fc - Fragment crystallizable

FCN1 - Ficolin-1

FCT - Foundation for Science and Technology

FCS - Fetal Calf Serum

FDC - Follicular dendritic cell

FDR - False Discovery Rate

fMRI - Functional Magnetic Resonance Imaging

Foxp3 - Forkhead box P3

GAPDH - Glyceraldehyde 3-phosphate dehydrogenase

GC - Germinal center

gDNA - Genomic DNA

GFAP - Glial fibrillary acidic protein

GFP - Green fluorescent protein

GM-1 - Monosialotetrahexosylganglioside

GM-CSF - Granulocyte-macrophage colony-stimulating factor

GMP - Granulocyte and macrophage progenitor

HIF-1α - Hypoxia-inducible factor-1α

hiPSCs - Human induced pluripotent stem cells

HBSS - Hanks' Balanced Salt Solution

HLA-DR - Human Leukocyte Antigen - DR

HMGB1 - High mobility group box 1

HNSC - Human Neural Stem Cell

HPRT - Hypoxanthine Phosphoribosyltransferase

HSC - Hematopoietic Stem Cells

Iba1 - Ionized calcium binding adaptor molecule 1

iBiMED - Institute of Biomedicine

ICAM - Intercellular adhesion molecule-1

ICVS - Life and Health Sciences Research Institute

IFN - Interferon

IFN-γR - Interferon-γ receptor

IGF - Insulin-like growth factor

IL - Interleukin

IL-1RI - Interleukin 1 receptor type I

IL-4Rα - Interleukin-4 Receptor Alpha

IL-10R - Interleukin-10 receptor

iNOS - Inducible Nitric Oxide Synthase

intMo Intermediate Monocytes

iPS - Induced Pluripotent Stem Cells

IRF - Interferon regulatory factor

KLF - Kruppel-like factor

KO - Knockout

LC-MS/MS - Liquid chromatography with mass spectrometry

LiM - Light Microscopy facility

LMPs - Lymphomyeloid progenitors

LPS - Lipopolysaccharide

LTαβ - Lymphotoxin αβ

LTB4 - Leukotriene B4

Ly6 - Lymphocyte antigen 6 complex

MΦ – Macrophage

M-CSF - Macrophage colony-stimulating factor

MAG - Myelin-associated glycoprotein

MadCAM1 - Mucosal Vascular Addressin Cell Adhesion Molecule 1

MCP-1 - Monocyte Chemoattractant Protein-1

MDP - Macrophage and Dendritic cell progenitor

MHC - major histocompatibility complex

miRNAs - MicroRNAs

MMMs - Marginal Metallophilic Macrophages

MMP7 - Matrix Metallopeptidase 7

MMP-9 - Matrix Metalloproteinase

mRNA - Messenger RNA

MSCs - Mesenchymal stem cells

mTOR - Mammalian target of rapamycin

MZ - Marginal zone

MZMs - Marginal Zone Macrophages

NADPH - Nicotinamide adenine dinucleotide phosphate

ncMo - Non-classical Monocytes

NEAA - Non-essential amino acids

NeuMo - Neutrophil-like monocytes

NeuN - NEUronal Nuclei

NF-kB - Nuclear Factor Kappa B

NK – Natural killer

NMDA - *N*-methyl-d-aspartate

NO - Nitric Oxide

NOD2 - Nucleotide-Binding Oligomerization Domain

NOS - Nitric oxide synthase

NSPCs - Neural stem/progenitor cells

Nr4a1 - Nuclear receptor 4A1

OCT- Optimal cutting temperature

P - Postnatal day

PAMPs - Pathogen-associated Molecular Patterns

PANTHER - Protein Analysis Through Evolutionary Relationships

PB-MSCs - Peripheral blood mesenchymal stem cells

PBMCs - Peripheral blood mononuclear cells

PBS - Phosphate-buffered saline

PBS-T - PBS-Triton

PD-1 - Programmed cell death 1

PDGFR - Platelet-derived growth factor receptor

pen/strep - Penicillin-streptomycin

PFA - Paraformaldehyde

PI3K - Phosphatidylinositol 3-kinase

PMs - Peripheral macrophages

PM-Exos - PM-derived exosomes

PNS - Peripheral Nervous System

PPARγ -Peroxisome proliferator-activated receptor gamma

PPARδ - Peroxisome proliferator-activated receptor delta

PPBI - Portuguese Platform of Bioimaging

PRRs - Pattern Recognition Receptors

qPCR - Quantitative PCR

RANTES - Regulated on activation, normal T cell expressed and secreted

RBP-J - Recombination signal binding protein for immunoglobulin kappa J region

RGMA - Repulsive guidance molecule A

rGMP - Revised GMPs

RNA - Ribonucleic Acid

RNA-seq - RNA-sequencing

ROS - Reactive Oxygen Species

RST - Rubrospinal tract

SatM - Segregated-nucleus-containing Atypical Monocytes

SEM - Standard error of the mean

SCI - Spinal cord injury

SCT - Spinocerebellar tract

SDS-PAGE - Sodium dodecyl-sulfate polyacrylamide gel electrophoresis

SIRPA - Signal regulatory protein alpha

SMAD - Mothers against decapentaplegic

SMP - Segregated-nucleus-containing atypical monocyte precursor

SOCS - Suppressor of cytokine signaling

solTNF - Soluble form of TNF

STAT - Signal transducer and activator of transcription

SA-PE - Streptavidin-phycoerythrin

TβRI - TGF-β type I receptor

TβRII - TGF-β type II receptor

TCA - Trichloroacetic acid

TE - Tissue-embedded

TGF-β - Transforming Growth Factor-beta

TLRs - Toll-like receptors

TNF - Tumor necrosis factor

TNF-α -Tumour necrosis factor α

TNFR1 - Tumor necrosis factor receptor 1

TRH - Thyrotropin-releasing Hormone

TUDCA - Tauroursodeoxycholic acid

USA - United States of America

u.a. - Umbilical artery

v.a. - Vitelline artery

VCAM-1 - Vascular Cell Adhesion Molecule-1

VEGF-A - Vascular endothelial growth factor A

VLA1 - Very late antigen-1

VLE-RPMI - Very Low Endotoxin Roswell Park Memorial Institute medium

WHO - World Health Organization

WT - Wild-type

YS - Yolk Sac

% - Percent

°C – Celsius degrees

μg – Micrograms

μl - Microliters

μM - Micromolar

μm - Micrometers

Ca^{2+} - Calcium

cm - Centimeters

cm^2 - Square centimeters

CO_2 - Carbon dioxide

dpi - Days post-injury

g - Grams

h – Hours

H_2O_2 - Hydrogen peroxide

kDa - Kilodalton

Kg - Kilograms

Mg^{2+} - Magnesium

mg - Milligrams

min - Minutes

mL - Milliliters

mM - Millimolar

mm - Millimeters

NaCl - Sodium chloride

ng – Nanograms

nM – Nanomolar

psi - Pounds per square inch

ROI - Region of interest

rpm - Rotations per minute

RT - Room temperature

O_2^- - Superoxide

$ONOO^-$ - Peroxynitrite

V - Volts

v/v - volume per volume

List of Figures

List of Tables

List of Videos

Thesis objectives and Layout

The objective of this thesis was to develop a therapeutic strategy for SCI repair, using spleen macrophages secretome. This strategy was evaluated *in vitro* and in an *in vivo* model of SCI, addressing both functional and histological outcomes. Additionally, the proteic analysis of the secretome was evaluated (Chapter 2).

This thesis is divided into three chapters:

Chapter 1 - General introduction to the main topics involved in this study. An overview of SCI is presented, including, SCI epidemiology, medical care, pathophysiology, immune responses, and monocytes, macrophages and secretome in SCI.

Chapter 2 - Comprehensive analysis of the therapeutic potential of spleen macrophages secretome for SCI recovery. This chapter presents an in-depth analysis of the therapeutic potential of the secretome of alternative-activated splenic macrophages for SCI repair. This chapter encompasses a comprehensive examination of the secretome effect *in vitro*, using peripheral and CNS-derived neurons, along with human neural stem cells. Subsequently, we conducted a pre-clinical trial involving a mouse model subjected to SCI compression, evaluating recovery across motor, sensory, autonomic, and histological functions. Furthermore, a proteomic analysis was performed to elucidate mechanistic insights into our proposed therapy, providing a deeper understanding of the molecular underpinnings behind the observed therapeutic effects.

Chapter 3 - Presentation of a general discussion of the study and future perspectives.

Chapter 1: Introduction

1.1 Nervous system and Spinal Cord

The nervous system is a complex network that enables an organism to interact with its environment [1]. In vertebrates, the nervous system subdivides into the central nervous system (CNS) and the peripheral nervous system (PNS) [2]. The CNS is composed of the brain [3], including cerebrum, cerebellum and brainstem [4], the olfactory nerve (cranial nerve I), olfactory epithelium [5], optic nerve (cranial nerve II) [6], retina [7], and the spinal cord [1]. The central nervous system functions include receiving, processing, and responding to sensory information [2]. The PNS is divided into the cranial nerves III to XII and spinal nerves [3], including their roots, and distal branches with receptor endings and ganglia [8]. The PNS has several functions, such as providing communication between the body and the brain, controlling development, stem cell niches and regenerative processes [9].

1.1.1 Spinal Cord

Spinal cord function and gross anatomy

The Spinal Cord is the part of the central nervous system that conducts sensory information from the peripheral nervous system to the brain and conveys motor information from the brain to muscular or glandular tissues [10]. Besides controlling voluntary muscles of the trunk and upper and lower extremities [11], the spinal cord is also able to produce reflexes, called the spinal reflexes [12].

The human and mouse spinal cord is a generally cylindrical, white structure slightly flattened dorsoventrally [10,13] that is protected by the vertebral column, and it extends from the base of the brain (in *medulla oblongata*) through the *foramen magnum* of the skull to the first lumbar vertebras [12,14,15]. The most distal part of the spinal cord is called the *conus medullaris*. The tapering end of the *conus medullaris* continues as a slender filament; the *filum terminale* that connects the lower end of the spinal cord to the vertebral column. Below the *conus medullaris*, the bundle of nerve roots resembles to a horse's tail and due to this is named the *cauda equina* [10].

Spinal Meninges

Like the brain, spinal cord is also protected by the meninges [14,15]. The meninges covering the spinal cord are arranged in three layers from the most superficial layer to that closest to the spinal cord, and are respectively [11], *dura mater*, *arachnoid mater*, and *pia mater* [10,11] (Figure 1.1).

The epidural space lies between the spinal *dura mater* and the periosteum of the vertebral canal [10], the spinal subdural space is a potential space between the *dura* and *arachnoid mater* [16,17], and the subarachnoid space (Figure 1.1), extends as an opening between the *arachnoid* and the *pia mater* ,

and it is filled with cerebrospinal fluid separating the *arachnoid* from the *pia mater* surrounding the spinal cord [10,11].

Spinal Cord Segments and Nerves

The human spinal cord has 31 segments: 8 cervical (C1 to C8), 12 thoracic or dorsal (T1 to T12), 5 lumbar (L1-L5), 5 sacral (S1 to S5), and 1 coccygeal (Co1) and comprises 31 pairs of spinal nerves [11,12], where each segment has a pair of posterior [11] (dorsal) [10] and anterior [11] (ventral) [10] roots (except the first cervical segment, which as only a ventral root) [11] (Figure 1.1) , that near the cord combine to form a spinal nerve [12], (one nerve from each side) (Figure 1.2). The mouse spinal cord has 34 segments: 8 cervical (C1 to C8), 13 thoracic (T1 to T13), 6 lumbar (L1 to L6), 4 sacral (S1 to S4), and 3 coccygeal (Co1 to Co3), and respectively, 34 pairs of spinal nerves [10] . The dorsal roots carry information from muscle and tendon organs, conveys impulses from skin, joints, deep tissues, viscera [10,11] and noxious and thermal sensation [11]. Outside the spinal cord and just proximal to its junction with the ventral root, the dorsal root has a ganglionic swelling or enlargement, the dorsal root ganglion (DRG) (Figure 1.1), which contains sensory neurons [10,11]. DRG neurons are functionally signaling receptor-transduced stimuli of diverse sensory modalities, including pain, temperature touch, and proprioception [10]. The ventral roots constitute the motor output from the spinal cord [11].

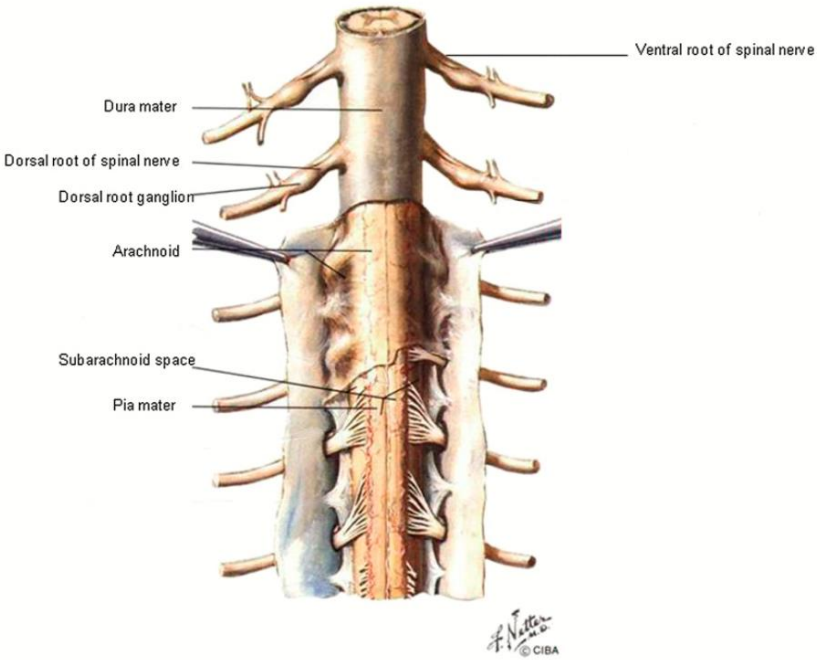

Figure 1.1: Posterior view of the spinal cord indicating the meningeal layers, dorsal and ventral roots of spinal nerves, DRG and subarachnoid space. Drawing by Frank Netter. Adapted from Bican, Minagar and Pruitt [11].

Internal anatomy of the Spinal Cord

- Spinal Cord Gray Matter

In transverse section of the spinal cord, the gray matter of the spinal cord is an H-shaped structure [11] that resembles a butterfly [10], with 2 symmetric halves connected by a bridge or commissure composed of gray matter through which runs the central canal, which is filled with cerebrospinal fluid [11] . This matter is located centrally, surrounded by white matter, except when the dorsal horns touch the margins of the spinal cord. The gray matter is made up of entering fibers of afferent neurons, interneurons, the cell bodies and dendrites of efferent neurons, and glial cells [12].

The gray matter is divided into posterior (dorsal) lateral and anterior (ventral) "horns." The neurons of the dorsal horns receive sensory information that enters the spinal cord via the dorsal roots of the spinal nerves. The lateral horns are present primarily in the thoracic region, and contain the preganglionic visceral motor neurons that project to the sympathetic ganglia [10,18]. Parasympathetic preganglionic visceral motor neurons are located in the sacral parasympathetic nucleus in sacral segments [10,19]. The ventral horns contain the cell bodies of motor neurons, which send axons via the ventral roots of the spinal nerves to end on striated muscles [18]. The gray matter of the spinal cord can also be divided into 9 distinct cellular layers, or *laminae*, organized from dorsal to ventral, with the remaining *lamina* (*lamina* 10) surrounding the central canal. *Laminae* 1-6 constitute the dorsal horn, *lamina* 7 is the intermediate gray matter, and *laminae* 8-9 constitute the ventral horn [10,20–23].

- Spinal Cord White Matter

The white matter is composed mostly of groups of myelinated axons. These groups of axons, are called fiber tracts or pathways, and run longitudinally through the cord, some ascending to convey information to the brain and others descending to relay information from the brain to the periphery [12]. The white matter of the spinal cord is divided by columns or funiculi, which are groups of tracts [10,11]. In the spinal cord there are 3 pairs of columns: the posterior/dorsal, the lateral that lies between the dorsal and ventral roots and the anterior/ventral columns [10,11].

The tracts are generally named according to their origin and destination [10]. The names of the ascending tracts usually start with the prefix spino- and end with the name of the brain region where the spinal cord fibers first synapse [13]. For instance, the Spinocerebellar tract (SCT) (Figure 1.2) is an ascending tract that travels a path from the spinal cord to the cerebellum [24]. The names of descending motor tracts, conversely, begin with a prefix of the brain region that gives rise to the fibbers and end with the suffix spinal [13]. For instance, the Corticospinal tract (CST) [13] (Figure 1.2), and Rubrospinal tract

(RST) [25] (Figure 1.2), begin in the cerebral cortex [13] and in the red nucleus of the midbrain tegmentum [25], respectively, and terminate in the spinal cord [13,25].

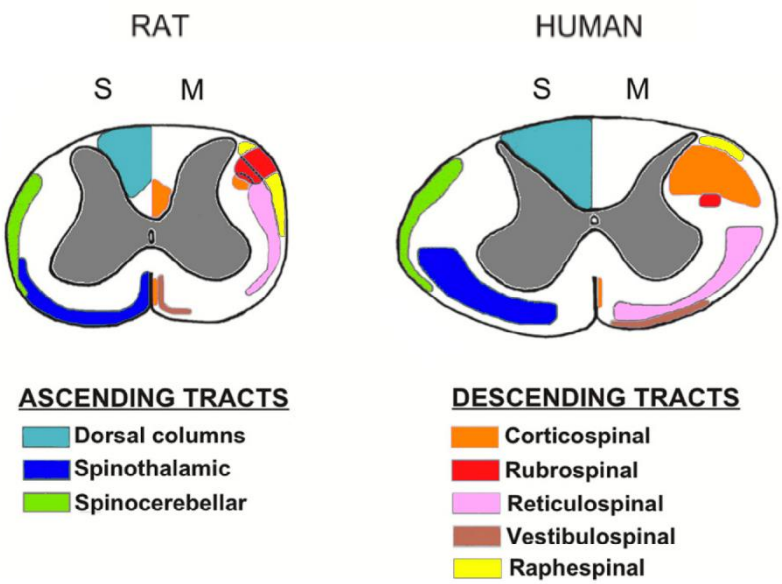

Figure 1.2: Approximated location of some ascending and descending tracts in cross-sections of cervical spinal cord in rat (which is quite similar to that of the mouse) and in human. Abbreviations: S - Sensory tracts; M - Motor tracts. Figure adapted from Watson et al. [13].

1.2. Spinal Cord Injury

The spinal cord is a vital part of the central nervous system that serves as a conduit for transmitting sensory and motor signals between the brain and all the others parts of the body. An injury in this organ has devastating consequences and affects thousands of individuals each year [12]. Spinal cord injury (SCI) leads to severe and sustained impairments in sensory, motor and autonomic functions, and may lead to multiple organ dysfunction, with currently no effective clinical treatment [12,26,27].

1.2.1 Epidemiology of Spinal Cord Injury

Incidence and prevalence, of Spinal Cord Injury

It was estimated that there are almost one million new cases of SCI each year, globally. The incidence numbers for SCI are highest in South Asia (~0.18 million), Western Europe (~0.12 million) and East Asia (~0.10 million). At a country level, India had the highest incidence of SCI (~0.14 million), followed by China (~0.10 million) and USA (~0.09 million) [28]. In the year of 2016, the global number of prevalent cases of SCI was estimated to be 27.04 million. Similarly to incidence, the same regions had

the highest prevalence numbers, but here, the leader was Western Europe (~4.30 million), followed by South Asia (~4.13 million) and East Asia (~3.85 million). Regarding the number of prevalent cases of SCI by country and in comparison with incidence, China switched places with India, being China the country with most prevalent cases of SCI (~3.74 million), India being in second place (~3.25 million), and USA maintaining the third place (~2.63 million) [28]. Specifically, in Portugal, it was estimated, that there are 2425 new cases annually and 92 650 prevalent cases of SCI [28].

Economic Impact of Spinal Cord Injury

The economic burden of SCI has become an increasingly concern for individuals and for society at large [26]. Costs associated with spinal cord injury are greatly influenced by the patient's severity of injury and resultant degree of disability [29]. In 2011, in USA, average per-person yearly expenses ranged from $334,170 in the first year and $40,589 in each following year for patients with incomplete injury, versus $1,023,924 in the first year and $177,808 in each subsequent year for patients with C1-4 tetraplegia [30]. Also In USA, the total annual cost attributed to spinal cord injury was approximately $21.5 billion in 2013 [31]. Estimates for direct costs ranged from $14.0 billion [32] to 18.1 billion dollars [31], while estimates for indirect costs ranged from $3.83 billion [31] to 7.0 billion in dollars [29].

Etiology and risk factors of Spinal cord Injury

In 2016, an epidemiologic study estimated that falls and road injuries were the leading causes of new cases of SCI in most regions of the world [28]. For instance, it was reported that in USA, the commonest cause of SCI is motor vehicle crashes (47.7%) followed by falls (20.8%), acts of violence—gun-shot wounds and stabbings (14.6%) and sporting related activities (14.2%) [33].

Young males comprise the majority of SCI cases, peaking, in most countries in the third and fourth decades [33–35]. Over time, significant trends have been observed in the distribution of SCI cases, for instance, between 1973 and 1979, 76.8% were Caucasian, 14.2% were African American, and 0.9% were Asian. Since 2005, there was a change to 66.1% that were Caucasian, 27.1% were African American, and 2.0% were Asian. At the same time, new cases in the Hispanic population had increased from 6.0 to 8.1% [36]. Moreover, in the USA, since 2010, about 22% of injuries have occurred among non-Hispanic blacks [37].

Co-morbidities and causes of death after Spinal Cord Injury

Several co-morbidities haven been associated with SCI, including high blood pressure, high cholesterol, diabetes, obesity and infection [36,38,39]. Individuals with SCI also have increased risk of bladder cancer [40–42]. Renal failure was the reported cause of death in 49% of patients with SCI from a prospective follow-up of 270 SCI patients in the 1970s [43]. A decade later as a consequence of improved urological care the leading causes of death switched to pneumonia, accidents and mental health related causes such suicides [36].

1.2.2 Clinical presentation of Spinal Cord Injury

Types of Injury

Patients with traumatic spinal cord injury can present with either complete or incomplete injury. An injury is only classified as complete if there is no motor or sensory function in the anal and perineal region representing the lowest sacral segments (S4-5) [44]. The American Spinal Injury Association (ASIA) scoring system (ASIA Impairment Scale (AIS)) [45] is used to universally describe the severity of a patient's spinal cord injury [46].

Examination in a complete injury (ASIA grade A), reveals no motor function, no sensory function below neurological level of injury, and no sacral sparing. In the acute setting, reflexes are absent and male patients may have priapism. Urinary retention and bladder distension may also occur. Patients with cervical or high thoracic complete cord injuries can suffer sympathetic dysfunction including bradycardia and hypotension [44].

Incomplete injuries (ASIA grades B - D) have preservation of voluntary anal contraction, non-zero perineal sensory scores and often preserved bulbocavernosus reflex. Furthermore, there are various degrees of motor function and sensation caudal to the level of injury. Sensation is often preserved to a greater extent than motor function [44]. There are some syndromes or patterns of incomplete SCI, like for instance, the central, anterior and hemicord syndromes that we will briefly describe:

- Central cord syndrome is a pattern of incomplete SCI to the cervical region characterized by disproportionately greater motor impairment in upper compared with lower extremities, bladder dysfunction, and a variable degree of sensory loss below the level of injury, and is described after relatively mild trauma in the setting of preexisting cervical spondylosis and/or central canal stenosis [44,47,48].
- Anterior cord syndrome is another incomplete pattern of SCI pattern that is characterized by damage to the anterior two thirds of the spinal cord, often secondary to anterior spinal artery

injury from either vascular occlusion (embolic stroke) or ligation. The direct mechanical injury to the anterior cord can also occur from bone fragment/disc retropulsion, often with flexion as the causative mechanism. This region includes the ventral corticospinal tract, spinothalamic tracts and descending autonomic tracts, while preserving the posterior column. As a result, patients experience complete motor paralysis and loss of pain and temperature, though have preservation of tactile position and vibration [44].

- The lateral hemisection or hemicord syndrome, also known as Brown-Sequard injuries, involve unilateral damage to the dorsal column, the corticospinal tract and the spinothalamic tract. Patients experience ipsilateral weakness, contralateral loss of pain and temperature sensation, and loss of vibration and proprioception, beginning approximately two spinal levels below the injured level. Common causes of this syndrome include penetrating injuries and ballistic [44].

Spinal Shock

Immediately after a spinal cord injury, may be a physiologic transient loss of all spinal cord function caudal to the level of the injury, with anesthesia, flaccid paralysis, absent bladder and bowel control, and loss of reflex activity. This altered physiologic state may last several hours to several weeks and is referred to as spinal shock [44,49,50]. However, it is important to distinguish between spinal shock and neurogenic shock. Whereas, spinal shock can occur from damage to any region of the spinal cord, neurogenic shock typically occurs with cervical and high thoracic (i.e., above T6) vertebral levels. Consequently, the symptoms associated with neurogenic shock such as hypothermia, hypotension and bradycardia, reflect sympathetic dysfunction. The occurrence of the two shocks is not mutually exclusive of one another [44].

1.2.3 Spinal cord injury management

Medical care and health complications after Spinal Cord Injury

Patients with traumatic SCI require intensive medical care and continuous monitoring of vital signs, cardiac rhythm, arterial oxygenation, and neurologic signs in the intensive care unit [51,52].

A number of complications are common after SCI, and are potentially avoidable or ameliorated with early intervention [52]. After SCI, the health complications will vary depending on the severity and location of the damage, like for instance, as we have already mentioned, persons living with SCI may

present hypotension, usually with bradycardia, due to neurogenic shock [53]. Patients with traumatic spinal cord injury may also suffer from hemodynamic shock related to blood loss [53].

In persons with SCI, respiratory dysfunction leads to an increased risk for pulmonary infection [54], like pneumonia [55], and death [54]. Additionally, they may present other pulmonary complications including respiratory failure, edema, and pulmonary embolism. These complications are most frequent during acute hospitalization after traumatic SCI and contribute substantively to early morbidity and mortality [52,55–59]. Weakness of the diaphragm and chest wall muscles leads to impaired clearance of secretions, ineffective cough, atelectasis, and hypoventilation [53]. Since SCI patients are vulnerable to pulmonary infections, and in light of the Coronavirus Disease (Covid-19) pandemic, there is a need to prepare to detect and treat this virus in vulnerable populations [60]. Care providers must be aware that individuals with SCI may not present with the typical Covid-19 symptoms of fever, cough and shortness of breath [60–62], and that as a result, their diagnosis may be delayed [60]. First, thermoregulatory dysfunction is a well-known sequela after spinal cord injury, due to disruption of neurologic signals to and from the hypothalamic temperature regulation center. Consequently, this disruption results in subnormal (<35.7 °C) resting core body temperature, poikilothermia, and absence of the typical fever response to infectious or inflammatory processes >38°C as defined by the CDC and WHO [60,61,63]. However, in a study conducted by Rodriguez -Cola et al. [64], in a cohort of patients with SCI and Covid-19 infection, fever was the most frequent symptom. The second most common symptom was asthenia, followed by dyspnea, cough, and expectoration, Despite of this, the patients exhibit fewer symptoms than the general population, but the clinical severity was similar or greater [64].

SCI frequently causes neuropathic pain that is associated with chronic inflammation in both the dorsal horn and in spinothalamic projection sites in the thalamus [65–73]. Felix et al. [74] reported increased inflammation in the brain after rat cervical SCI. Damage to the spinal cord can cause chronic neuroinflammation in the cortex, hippocampus and thalamus at delayed time points post-injury [75]. In the brain, the up-regulation of CCL21 expression is associated with increased microglial activation and neurodegeneration, which can cause long-term neurological impairments following SCI [75–77]. These studies indicate that isolated SCI can cause chronic brain inflammation that is notably similar to that observed after Traumatic Brain Injury, resulting in progressive delayed neurodegeneration and functional deficits that include cognitive deficit and depressive-like behaviour [76,77].

Other medical complications experienced by persons with SCI includes venous thromboembolism, pain, pressure sores, bladder infections, gastrointestinal stress ulceration, paralytic

ileus [52,53,55,78,79]. Moreover, persons with a cervical injuries may lack vasomotor control and cannot sweat below the lesion [53]. On table 1.1 are represented several health complications following SCI.

Table 1.1: Organ system complications following spinal cord injury. Table adapted from Eckert and Martin [55], and Hansebout and Kachur [53], Stevens et al. [56], Jia et al.[52], DeVivo et al. [57], Wuermser et al. [58], Ball [59], Wu et al. [76,77], Simons et al. [78] and Karlsson [79].

Organ System	Complications
Cardiovascular	Hypotension Bradycardia/dysrhythmia Hemodynamic shock Cardiac arrest Cardiogenic pulmonary edema
Pulmonary	Hypoventilation/respiratory failure Pneumonia Pulmonary edema Pulmonary embolism Poor secretion control Atelectasis Acute respiratory distress syndrome Aspiration
Gastrointestinal	Gastric dysmotility Gastritis Gastrointestinal stress ulceration Paralytic ileus Pancreatitis
Hematologic	Venous thromboembolism
Neurologic	Neurogenic shock Depression Posttraumatic stress disorder Anxiety Autonomic dysreflexia Pain Cognitive deficit
Genitourinary	Bladder dysfunction Urinary tract infection Priapism
Integument	Pressure sores Inability to sweat (below the cervical lesion)

Surgery

The usual surgical interventions performed by physicians are stabilization and decompression of spinal cord combined with the administration of a high dose of methylprednisolone [80]. However, surgical and methylprednisolone approaches are highly contentious since there is lack of consensus about their true beneficial effects [12]. The issue of optimal timing for surgical interventions (or even the intervention itself) has created considerable debate and remains unresolved. Nevertheless, the number of studies indicating that early decompression has a neuroprotective effect in humans is much larger compared to the studies that show no effects or negative impact [81].

Pharmacological interventions

The administration of steroids in the treatment of acute SCI continues controversial. Initially, the interest in the use of steroids was based on a rationale of increasing anti-inflammatory mechanisms and thereby promoting cell survival by restraining inflammation-mediated secondary injury [82]. Methylprednisolone is a corticosteroid that acts as a free radical scavenger thereby inhibiting the lipid peroxidation, and being able of maintaining the blood-spinal cord barrier, improving spinal cord blood flow, inhibiting endorphin release and restraining the inflammatory response [83–85]. However, for some authors [44], there is no consistent or compelling evidence to suggest high-dose methylprednisolone administration improves outcomes in SCI. Indeed, there is evidence suggesting that it is associated with increased complications including infection, respiratory compromise, gastrointestinal hemorrhage and death [44].

Other pharmacological agents, such as monosialotetrahexosylganglioside (GM-1), thyrotropin-releasing hormone (TRH) and naloxone, have been subjected to investigation in large multicenter prospective randomized controlled clinical trials [86]. However, none of the tested agents have demonstrated strong clinical benefits in SCI patients [12].

1.2.4 Neuronal plasticity after spinal cord injury

Derived from the Greek word "*plassein*", plasticity means the ability of being altered or molded. The CNS exhibits significant malleability, experiencing plasticity over its lifetime. The process of learning, skill acquisition and particularly the response to an injury leads to neuronal reorganization, synaptic rearrangements, alterations in the neuronal activation pattern and the collateral sprouting of intact or lesioned axons [12]. Using functional magnetic resonance imaging (fMRI), it was described that the volume of activation of the sensorimotor cortex of chronic SCI patients was strongly reduced compared

to controls [87]. However, to note that the cortex is not the only region in the brain affected by a SCI [12], subcortical structures like the red nucleus and the cuneate nuclei of the brainstem also undergo plasticity [88–90]. The discovery of the plastic properties of the spinal cord led to novel rehabilitation approaches for SCI in humans. For instance, patients with incomplete SCI achieved significant functional improvements trough daily training on a moving treadmill [91]. Nonetheless, not all plasticity is beneficial, because it is well documented that following SCI, maladaptive plasticity conducts to the appearance of autonomic dysreflexia, spasticity and central pain [92,93].

1.2.5 Spinal Cord Injury Pathophysiology

Traumatic SCI results from either exogenous or endogenous trauma, but regardless of the cause, the resultant pathology is caused by two mechanisms: primary injury mechanisms (the initial mechanical damage), and secondary injury mechanisms (secondary change due to vascular and biochemical effects) [94,95].

When the spinal cord is macerated or lacerated by a sharp penetrating force, contused or compressed by a blunt force (most common) [96], it begins a neurological damage in the spinal cord that is called ''primary injury'' [12]. The mechanical injury then leads to a cascade of biological events, named as ''secondary injury'', leading to further neurological damage [12].

The primary injury initiates a cascade of secondary injury events, including the following [97]:

- Vascular changes [12], including breakdown of blood–spinal cord barrier [98], ischemia, neurogenic shock, hemorrhage, edema, microcirculatory derangements, vasospasm, and thrombosis [99–102];
- Programmed cell death or apoptosis [103–105];
- Neurotransmitter accumulation, including serotonin or catecholamines [106] and extracellular glutamate [107], the latter causing excitotoxic cell injury [108];
- Loss of adenosine triphosphate (ATP)-dependent cellular processes [109];
- Ionic derangements, including increased extracellular potassium, and increased sodium permeability, increased intracellular calcium [110,111], calcium dependent nitric oxide production [101,112,113];
- Immune and inflammatory changes [81,97];
- Release of DNA by necrotic neurons and glia [114];
- Arachidonic acid release, free radical production [115] and oxidative damage [101,112,113];
- Eicosanoid production, and lipid peroxidation [116,117];

- Demyelination of surviving axons [118];
- Formation of cystic cavities [119];
- Release of neurite growth-inhibitory factors e.g., Nogo-A, myelin- associated glycoprotein (MAG), and chondroitin sulfate proteoglycans (CSPGS) [95,120];
- Astroglial scar formation [121–123].

Temporal division of secondary injury

The secondary injury can temporally divided [124] into the acute, subacute, intermediate and chronic phases [114], which we will describe below.

- Acute injury phase (<48 hours)

The initial traumatic event (primary injury) produces immediate mechanical disruption and dislocation of the vertebral column, which can compress or transect of the spinal cord, which immediately initiate a sustained secondary injury cascade, that leads to further damage to the spinal cord and neurological dysfunction .The focal region of damage disrupts the vasculature, compromises the blood–spinal cord barrier and injures neurons and oligodendrocytes (the myelinating cell type of the CNS) [114]. Cell permeabilization, pro-apoptotic signalling, and ischaemic injury, due to the destruction of the micro-vascular supply of the spinal cord, cause secondary cellular changes, such as cell dysfunction and death [125,126]. Elevated levels of the glutamate are released from dying neurons and astrocytes and are poorly re-uptaked by surviving astrocytes [127,128]. This triggers overactivation of NMDA, kainate and AMPA and receptors, which, when combined with impairment of ATP-dependent ion pump functions and ensuing resultant sodium dysregulation, can lead to excitotoxic cell death [129,130]. Excitotoxicity contributes to the loss of intracellular and extracellular ionic homeostasis, with intracellular calcium dysregulation being a critical mediator of cell death in both neurons and glia. High intracellular calcium concentration activates calpains, which can cause mitochondrial dysfunction and cell death [131,132].

Additionally, blood vessel injury can cause severe haemorrhages, which can expose the cord to an influx of inflammatory cells, cytokines and vasoactive peptides. Inflammatory cells arrive into the spinal cord, leading to an exacerbated inflammatory response during the acute and subacute phases of injury. This coupled with the compromised blood–spinal cord barrier, contributes to progressive swelling of the spinal cord. Swelling may result in additional mechanical compression of the cord, potentially spanning across multiple spinal segments and exacerbating the injury [114].

- Subacute injury phase (48 hours to 14 days)

In this phase, continuous necrosis of neurons and glia leads to the release ATP, DNA and potassium, which can trigger the activation of microglial cells. The activated microglia, along with infiltrating inflammatory cells such as macrophages, polymorphonuclear cells and lymphocytes, propagate the inflammatory response contributing to ongoing apoptosis of neurons and oligodendrocytes [114].

Phagocytic inflammatory cells play a dual role by clearing myelin debris at the site of injury, but also causing additional damage to the spinal cord through the release of cytotoxic by-products, including free radicals (for example, superoxide (O_2^-) hydrogen peroxide (H_2O_2) and peroxynitrite ($ONOO^-$). The reactive oxygen species cause lipid peroxidation, DNA oxidative damage and protein oxidation, which induce further necrotic and delayed apoptotic cell death, consequently contributing to the harsh post-injury microenvironment [133–135].

The compromised autoregulatory capacity of the injured spinal cord vasculature, along with systemic effects like hypotension and respiratory failure resulting from SCI, can contribute to ongoing ischaemia that persists for days to weeks after injury. Prolonged ischaemia contributes to extra neuronal and glial (predominantly oligodendrocyte) cell death and the progression of the injury [114].

During this phase, as cells and the extracellular architecture of the cord are damaged, cystic microcavities form [114]. In humans, the cystic cavities, contain extracellular fluid, thin bands of connective tissue and macrophages [119]. Furthermore, astrocytes proliferate and deposit extracellular matrix molecules into the perilesional area [114].

- Intermediate (14 days to 6 months) – Chronic injury phases (>6 months)

In the intermediate and chronic phases axonal degeneration continues, the astroglial scar matures to become a potent inhibitor of regeneration and cystic cavities merge to further restrict axon regrowth and cell migration [114]. However, as the inflammatory response diminishes, the spinal cord lesion evolves by attempts at vascular reorganization, alterations in the composition of the extracellular matrix, remyelination, and remodelling of neural circuits [132].

1.2.6 Immune responses after Spinal Cord Injury

Of all secondary injury mechanisms, inflammatory responses endure the longest and play a direct or indirect role in regulating the healing process following SCI, a topic that has recently garnered significant attention [136]. Inflammation subsequent to SCI is a complex process characterized by the release of damage-associated molecular patterns (DAMPs) from injured cells, including, for instance, ATP, high mobility group box 1 (HMGB1), interleukin-33 (IL-33), triggering an inflammatory response. These substances activate pattern recognition receptors (PRRs) also inducing immune responses [137].

The CNS has been considered an immune privileged site, because of its inability to mount an immune response and process antigens [138], due to the highly controlled adaptive immunity and inflammation [139]. This feature served to protect post-mitotic neural cells from potential immune response-mediated injury and death [139]. However, its now known, when the CNS is challenged by injury and systemic infections, it has the ability to mount an organized immune response [140], thus redefining the CNS from 'immunologically privileged' to an 'immunologically quiescent' site [141]. This quiescent state is significantly altered in the injured spinal cord where there is the activation of resident microglia and astrocytes and a coordinated invasion of circulating immune cells, [142]. Moreover, the immune response in the CNS varies according to location, with differences between the injured spinal cord and the brain [143–145]. Injury to the spinal cord results in a stronger inflammatory response than seen in the brain. For instance, after a mechanical injury or injection of proinflammatory cytokines, there is a significantly higher neutrophil recruitment in the spinal cord as well as more widespread within the cord parenchyma relative to the adult brain, which is almost refractory to leukocyte infiltration [143–145].

<u>Microglia</u>

Microglia, an essential component of the long-term multiphase response after SCI, undergo immediate activation following injury [136]. Microglia participate in clearing myelin debris and production of growth factors such as glial cell line derived neurotrophic factor, which favor neurite growth and regeneration. Additionally, they express transforming growth factor-beta1 (TGF-β1), a cytokine/growth factor that inhibits the release of cytotoxic molecules, reduces astrocyte proliferation, and promotes neuronal survival [146]. Moreover, Popovich lab demonstrated that microglia are vital for SCI recovery and coordinate injury responses in CNS-resident glia and infiltrating leukocytes. Microglia depletion exacerbates tissue damage and worsens functional recovery [147]. Nevertheless, microglia also act as the primary source of inflammation after SCI, producing and pro-inflammatory and toxic mediators that initiate signaling cascades and neurotoxic responses, that lead to neuronal death and neurite damage

[136,148,149]. Activated microglia have the capacity to release cytokines such as Interleukin-1 alpha (IL-1α) and Tumour Necrosis Factor α (TNF-α), which can activate neurotoxic reactive astrocytes and contribute to neuronal death [150]. In addition, Microglia can also produce free radicals, nitric oxide and keratan sulfate proteoglycans, which form inhibitory boundaries to extending neurites [151]. It should also be noted that, in the injured cord, microglia and macrophages also function as antigen presenting cells [140].

Neutrophils

Neutrophils represent the initial wave of infiltrating immune cells in response to SCI, and start appearing 4–6 h after injury [152] and reach their peak according to some authors at 24 h post injury [153] or at 3 days according to others, followed by a second peak several weeks later [154]. Neutrophils help in recovery processes by phagocyting cellular debris, and they summon macrophages into the damaged tissue [154]. These macrophages function not only as phagocytes [155], but also act as a reservoir of cholesterol derived from ingested myelin. The cholesterol can then be utilized during remyelination of regenerating axons [156]. The early recruitment of neutrophils is also essential for initiating subsequent leukocyte-mediated tissue repair processes like revascularization and epithelialization [157]. Depletion of neutrophils that arrive early at the injury site post-SCI reduces the number of white blood cells adhering to endothelial cells, delays wound healing, resulting in less preservation of axons and white matter, and hampers functional recovery [158]. While early neutrophil recruitment is crucial for wound healing, an excessive number of neutrophils can be detrimental to the tissue [159,160]. Neutrophils also play a pivotal role in secondary tissue damage by releasing reactive oxygen and nitrosyl radicals, along with cytokines, chemokines, and various proteases, including metalloproteinases and neutrophil elastase [161–164]. Inhibition of neutrophil elastase can decrease the expression of inflammatory factors after SCI, alleviate secondary injury and prevent glial scar formation [165].

Monocytes and macrophages

About 2–3 days post-injury (dpi), a first wave of blood monocytes migrate to the injury site where they differentiate into macrophages [166,167] and reaches peak around 7 days [167,168] and then this wave declines [167]. Blomster at al. showed that the majority of infiltrating monocytes at 7 days post-SCI originate from the spleen [168]. The second wave begins around 14 days, peaks again at 60 days, and maintains this level until at least 180 days after injury [167,169,170]. This second wave could be from

either the bone marrow or from a self-renewing source at the injury site [167]. Therefore, monocytes/macrophages can be present in the injured cord for weeks to months [171,172], or even years thereafter [167]. Macrophages contribute to several wound healing processes [173], however, they also serve as sources of pro-inflammatory cytokines such as IL-1, IL-33, and TNF- α post-injury [136,174], as well as neurotoxins like reactive oxygen species [175–177] and inducible nitric oxide synthase (iNOS) [178], implicating them in cellular injury [173]. The presence of monocytes and macrophages in SCI will be described with more detail later.

B-Lymphocytes

B-lymphocytes numbers decline in the peripheral lymph nodes and spleen following SCI [179], and they appear near the lesion site within hours and remain present for up to 1 week, after the injury [179,180]. B-lymphocytes produce antibodies in response to injury and thereby are responsible for memory in adaptive immunity [173]. Ankeny et al. [181] showed that mice lacking B cells exhibited improved locomotor recovery and reduced lesion pathology following SCI. Antibody-secreting B cells and immunoglobulins were present in the cerebrospinal fluid and in the injured spinal cord of wild-type mice. Moreover, large deposits of antibody and complement component 1q (C1q) accumulated at sites of axon pathology and demyelination in mice with normal B cell function. Antibodies produced after SCI cause pathology, in part by activating intraspinal complement and cells bearing Fc receptors [181].

T- Lymphocytes

T-lymphocytes are present in low numbers in the uninjured spinal cord [182] and progressively increase, within the first week post injury in parallel with the activation of microglia and influx of peripheral macrophages [183]. In mice, there is a biphasic peak of infiltration, with the first peak occurring between 7–14 days and a second at 42 days. Both CD4+ and CD8+ cells follow similar kinetics, although CD4+ cells occur in higher numbers and typically localize in a centralized fibrotic zone [154]. Rats exhibit a biphasic T cell influx similar to that observed in mice [182], but with the first of peak T cell infiltration in SCI occurring between 3–7 dpi [171,182,184].

T-lymphocytes likely play complex roles in both injury and repair mechanisms. After their activation, T-lymphocytes may kill target cells and produce cytokines [184,185]. Moreover, chronic T-cell activation can lead to pathological fibrosis and scarring [186]. T-lymphocytes can potentially promote greater tissue damage than macrophages and activated microglia, by recognizing specific antigens, like myelin basic protein, and proliferating in response to those antigens [187]. However, other studies

counter such detrimental interactions by supporting a neuroprotective role in models of CNS injury and neurodegeneration [188,189].

Dendritic cells

Dendritic cells (DC) are antigen presenting cells [190], that the injured spinal cord, function by signaling through Toll-like receptors (TLRs) [140]. These receptors bind to specific components of the pathogen, the pathogen-associated molecular patterns (PAMPs), leading to activation of antigen presenting cells [140]. Upon activation, antigen presenting cells phagocytose debris, express MHC-II on their surface, and present degraded peptides to helper T-lymphocytes [173]. In addition to expressing high levels of MHC II, dendritic cells all express pro-inflammatory cytokines [190], and consequently, they contribute to the ongoing inflammatory response, which may aggravate the secondary injury [173,191–193]. The debate regarding their influence on wound healing and recovery [173,191–193] arises from their capacity to produce growth factors, such as neurotrophin-3, and promote neurogenesis [194]. Mikami and colleagues [194] reported a treatment for spinal cord injury involving implantation of DCs. They found that DCs implanted into the injured adult mouse spinal cord activated the proliferation of endogenous neural stem/progenitor cells (NSPCs) *in vivo* and induced *de novo* neurogenesis. These DCs produced neurotrophin-3 and activated endogenous microglia in the injured spinal cord. Behavioral analysis showed the locomotor functions of DC-implanted mice to have recovered significantly as compared to those of control mice. Such pleiotropic functions of DCs, may be involved in regeneration of injured axons and recovery of locomotor functions, and these results suggested that DC-implantation exerted trophic effects, leading to repair of the injured adult spinal cord [194].

1.3 Monocytes

1.3.1 Monocyte development, proliferation, recruitment and migration

In mice, hematopoiesis emerges in three embryonic sequential waves or programs, the first, the primitive wave, the second, the transient definitive wave and the third, the definitive wave [195]. Initially, in mice, monocytes arise in the fetal liver from late yolk sac (YS)-derived erythromyeloid progenitors during the transient definitive wave of hematopoiesis, which starts around embryonic day 8.25 (E8.25) (it starts at 3.25 weeks of gestation in humans) [195–197]. These erythromyeloid progenitors are generated in the hemogenic endothelium of the YS developing vasculature [195]. At E10.5 (definitive wave beginning) [195], immature hematopoietic stem cells (HSCs), originating from hemogenic endothelium of the aorta-

gonad-mesonephros (AGM) region of the embryo [195,198], colonize, and establish definitive hematopoiesis in the fetal liver, which serves as the major hematopoietic organ for the developing immune system [198]. Beyond E10.5, HSCs are also produced in hemogenic endothelium situated in umbilical and vitelline arteries, as well as in the placenta and YS [195,199,200]. After colonization and establishment of definitive hematopoiesis in fetal liver, HSCs seed the spleen [201] and the bone marrow [198]. However, in the bone marrow, HSCs are not fully functional until several days after birth [198] and during the perinatal window, the bone marrow niche the still maturing and recruiting HSCs present in the liver and spleen [195,198,202]. Therefore, liver and spleen HSCs continue supplying monocytes during the peri-natal period until the establishment of nascent adult-like HSCs [198].

Monocytes arise in the bone marrow from HSCs that, following asymmetric division, give rise to the common myeloid progenitors (CMPs) [203,204]. In the adult mouse, according to the classical model, monopoiesis presents as linear hierarchy [205] (Figure 1.4A), with CMPs differentiating into myeloid-lineage-dedicated granulocyte and macrophage progenitors (GMPs) [203,204] as well as macrophage and DC progenitors (MDPs) [206,207] . MDP give rise to common monocyte progenitor (cMoP) [208,209] which were originally defined as the sole monocyte-committed precursors [209,210]. This linear hierarchy presents branching occurring at the levels of the GMP and MDP that give rise to neutrophils and classical DC, respectively [205] (Fig 1.4A).

However, in accordance with the revised model of myelopoiesis, monocyte development undergoes a major bifurcation at the level of the CMP. This revised model suggests the emergence of monocytes with distinct flavors, such as neutrophil-like (NeuMo) and DC-like (DCMo) monocytes, downstream of the GMP and MDP, respectively [205]. Furthermore, deviations of this respective monocyte program have been reported, including segregated-nucleus-containing atypical monocytes (SatM) proposed to arise from dedicated progenitors (SMP) [210], and atypical progenitors at the level of the MDP and downstream, that might give rise to unusual DC-like CX3CR1^{-} monocytes after exposure to IFN-γ [211] (Fig 1.4B). Alternatively, GMP and MDP could give rise to a single, highly plastic monocyte [205] (Fig 1.4B). The study by Chong and colleagues raised the possibility that neutrophil-like NeuMo and DCMo monocytes reflect different monocyte maturation states [212] or it could be a re-routing of monopoiesis or the omission of certain intermediates under conditions of pathology [205].

In humans, like in the revised model of myelopoiesis of adult mouse, there is a major bifurcation giving rise to revised GMPs (rGMPs) and MDPs [213]. rGMPs give rise to cMoPs [213,214], unlike the

mouse, in which cMoPs arise from MDPs [205], CMoPs sequentially differentiate in humans into pre-monocytes and then into monocytes [213].

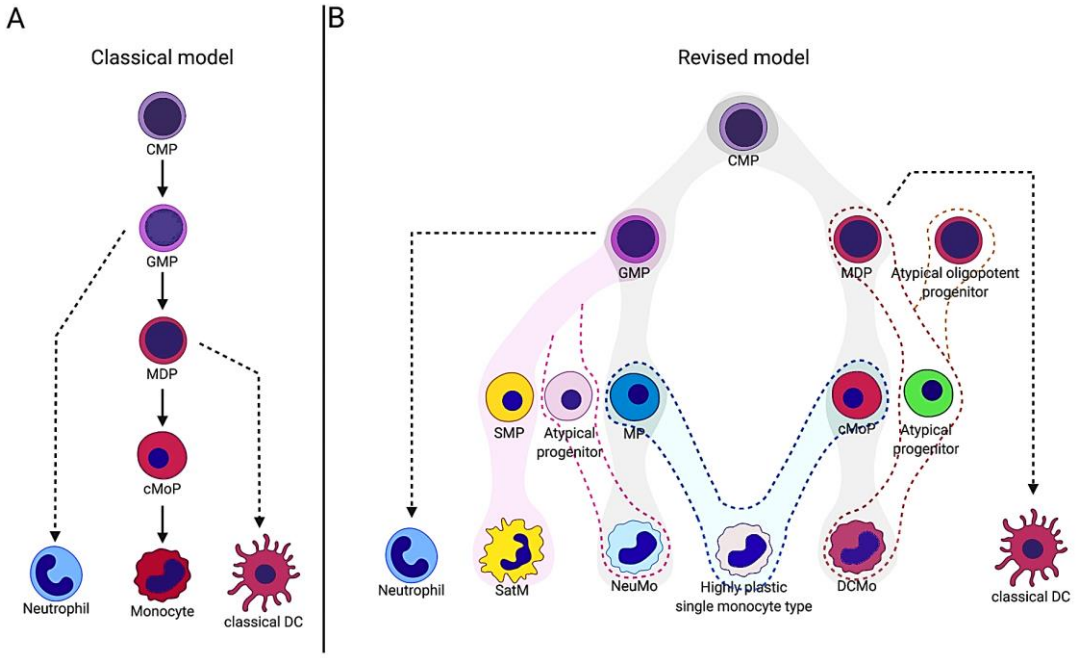

Figure 1.3: Scheme of Monopoiesis in the adult mouse. **(A)** The classical model of monopoiesis. **(B)** Revised model of monopoieses. Abbreviations: cMoP - Common monocyte progenitor; CMP - Common myeloid progenitor; DC - Dendritic cell; DCMo – Dendritic cell-like monocyte; GMP - Granulocyte and Macrophage progenitor; MDP - Macrophage and dendritic cell progenitor; MP - Monocyte progenitor; NeuMo - Neutrophil-like monocyte; SatM - Segregated-nucleus-containing atypical monocyte; SMP - Segregated-nucleus-containing atypical monocyte precursor. Figure adapted from Trzebanski and Jung [205].

Colony stimulating factor-1 (CSF-1; also known as macrophage CSF (M-CSF)) [215], is constitutively produced by mesenchymal cells [216] and is detectable in the circulation under resting conditions [217]. M-CSF is capable to promote monocyte development [218], and in adult mice, monocyte development is dependent on M-CSF [215]. However, as opposed to adult monocytes, fetal liver monocytes were shown to proliferate and to be independent of M-CSF [219]. M-CSF is also capable to differentiate monocytes into macrophages [220–222]. M-CSF is a homeostatic cytokine that, in addition to exerting effects on monocytes, it also exerts effects on other cells such as macrophages and bone marrow progenitor cells [223]. Through the MEK, PI3K, and PLC-γ2 pathways signaling [223], the M-CSF receptor (CSF1R; CD115) [223,224] is capable of affecting the proliferation, differentiation, and survival of these cells via its intrinsic tyrosine kinase activity [223]. Besides M-CSF, Granulocyte-macrophage colony-stimulating factor (GM-CSF) also affects monocyte survival and differentiation [225].

After maturation, monocytes enter the blood stream, a process that in depends on expression of the chemokine receptor CCR2 [209,226]. During homeostasis, inflammation, infection and tissue damage or injury, circulating monocytes leave the bloodstream and migrate into tissues [227–229].

During homeostasis, monocytes are recruited to continuously replenish tissue-resident macrophages [230], through chemokines like CCl2 and CCL3 [229,231,232]. Monocytes can also be recruited into normal tissue and become DCs [229]. However, monocytes can also retain their monocyte-like state and act as a local monocyte reservoir [233]. During inflammation, monocytes also differentiate into macrophages [229,234], and in aseptic inflammatory conditions, like atherosclerosis, monocytes are recruited to the lesions in a CCR2-, CCR5- and CX3CR1-dependent manner [235–237], and can exhibit phagocytic and pro-angiogenic functions, and also might differentiate into DCs in the lesion [238]. Upon infection or tissue damage [229], monocytes are rapidly recruited and migrate to affected sites and tissues [227–229], in a process that is mainly initiated by PAMPs and DAMPs [228,239]. Chemokines are directly involved in monocyte migration through the endothelium [240]. Abundant experimental evidence indicates that recruited monocytes serve as innate effectors of the inflammatory response to microbes and kill pathogens through phagocytosis, production of reactive oxygen species (ROS), nitric oxide (NO) and inflammatory cytokines [241]. They are involved in initiation and also in resolution of inflammation [198], and have the capability to trigger and polarize T cell responses [241,242]. After infection or tissue damage [229], following conditioning by local growth factors, cytokines and microbial products [227], monocytes can also differentiate into tissue macrophages or dendritic cells [227,229]. Besides regulating immune response, monocytes can also maintain vascular homeostasis, and participate in tissue remodeling [198].

1.3.2 Monocyte subsets

In humans there are 3 subsets of monocytes: $CD14^{++}CD16^{-}$ classical (cMo), $CD14^{++}CD16^{+}$ intermediate (intMo), and $CD14^{+}CD16^{++}$ non-classical (ncMo) monocytes [243,244]. In mice, two main monocyte subsets have been described, $Ly6C^{high}$ monocytes, which resemble $CD14^{++}CD16^{-}$ cMo, and $Ly6C^{low}$ monocytes, which represent the murine counterpart to $CD14^{+}CD16^{++}$ ncMo [245,246]. However, in mice, a heterogeneous monocyte subset expressing intermediate levels of Ly6C ($Ly6C^{middle/int}$) has also been described [235,247] and according with some authors, $Ly6C^{+}Treml4^{+}$ monocytes are considered intermediate [248]. In humans, the expression of M-CSF receptor CD115 (CSF1R) was high on ncMo [224], and blocking M-CSF receptor signalling reduced ncMo but not cMo numbers [249]. In contrast, GM-CSF receptor CD116 (CSF2R) was found to be expressed on all monocyte subsets, with highest

expression in cMo [225]. Some monocyte surface markers as well as their chemokine receptors are indicated in Table 1.2.

Table 1.2: Surface markers and chemokine receptors in human and mouse monocyte subsets. Table adapted from Yang et al. [229], and Tacke et al. [235].

Species	Subsets	% in MNC	Surface markers	Chemokine receptors
Human	Classical	80-95	$CD14^{++}CD16^{-}$	$CCR2^{high}CX3CR1^{low}$
	Intermediate	2-11	$CD14^{++}CD16^{+}$	$CCR2^{mid}CX3CR^{high}CCR5^{+}$
	Non-classical	2-8	$CD14^{+}CD16^{++}$	$CCR2^{low}CX3CR1^{high}$
Mouse	$Ly6C^{high}$ ($Ly6C^{+}$)	40-45	$CD11b^{+}CD115^{+}Ly6C^{high}$	$CCR2^{high}CX3CR1^{low}$
	$Ly6C^{middle/int}$ ($Ly6C^{+}$)	5-32	$CD11b^{+}CD115^{+}Ly6C^{middle}$	$CCR2^{high}CX3CR1^{low}$
	$Ly6C^{low}$ ($Ly6C^{-}$)	26-50	$CD11b^{+}CD115^{+}Ly6C^{low}$	$CCR2^{low}CX3CR1^{high}$

Abbreviations: int – intermediate; MNC – Mononuclear cells;

Monocyte subsets differentiation

In human monocyte differentiation, $CD14^{++}CD16^{-}$ cMo leave the bone marrow in a CC-chemokine receptor 2 (CCR2)-dependent manner, and in the steady state, they differentiate into $CD14^{++}CD16^{+}$ intMo and sequentially to $CD14^{+}CD16^{++}$ ncMo in peripheral blood circulation [229,250].

Mouse $Ly6C^{+}$ ($Ly6C^{high}$ + $Ly6C^{middle/int}$) monocytes leave the bone marrow, like in humans, in a CCR2-dependent manner [229,235]. The $Ly6C^{middle\ (int)}$ monocyte subset is believed to be differentiated from $Ly6C^{high}$ monocytes [235], and a monocyte fate mapping study strongly supported that in the steady state $Ly6C^{High}$ and $Ly6C^{middle/int}$ monocytes are the obligatory precursors for generation of $Ly6C^{Low}$ monocyte in the peripheral blood, bone marrow (returned), and spleen [210,229,235,251–253]. The conversion to $Ly6C^{low}$ was found to be dependent on CCR2 [251]. $Ly6C^{low}$ ncMo showed higher expression of Nr4a1 than $Ly6C^{high}$ [254, 255] and Nr4a1 knockout led to partial depletion of the $Ly6C^{low}$ ncMo pool, indicating its crucial role for the generation of $Ly6C^{low}$ monocytes [254]. The regulation of the Nr4a1 gene was studied by Thomas et al. [255], who elucidated the mechanism underlying the conversion of $Ly6C^{high}$ to $Ly6C^{low}$. These authors found Nr4a1 to be regulated by the interaction of KLF2 with the Nr4a1 super-enhancer domain E2 [255]. In vascular niches of mouse bone marrow and the marginal

zone of spleen, Ly6C^{high} monocytes bind to endothelial cell ligand DLL1 trough the Notch2 receptor, inducing conversion to Ly6C^{low} monocytes [256]. During bacterial infections, the conversion of cMo to Ly6C^{low} patrolling monocytes can be induced by NOD2 receptors [257]. These receptors bind to fragments of bacterial peptidoglycans, which can then increase intMo and ncMo populations for both human and mouse monocyte cultures, albeit the mechanism was not clear [248].

Monocyte subsets functions

- Classical monocytes functions

cMo are involved in various immune responses such as inflammation and tissue repair [258]. cMo sense cues from sites of inflammation and injury and are released into circulation through CCL2-CCR2 signalling, and extravasate into affected tissues [259–261]. During inflammation, human CD14^{++}CD16^{-} cMo and also CD14^{++}CD16^{+} intMos are tethered and invade tissue trough the interaction of complementary pair CCR2/CCL2(MCP1) or/and CCR5/CCL5(RANTES) in a VLA1/VCAM1 dependent manner [229]. They can be highly active in production of reactive oxygen species (ROS) and phagocytosis [245,262,263], overexpressing genes related to last process, such as CD64, CD93, CD36, CD32, CD11B, CD14, ficolin-1 (FCN1), and signal regulatory protein alpha (SIRPA) [264,265]. cMo are also equipped with TLRs and scavenger receptors, recognizing PAMPs and removing microorganisms, lipids, and dying cells via phagocytosis [266]. In response to bacterial signals, cMo can secrete inflammatory cytokines such as IL-6, IL-8, and IL-1β [267,268]. They can also produce other citokines, such as IL-1, IL-10, IL-12, TNF-α [269,270]. Although they are able to clear debris [260], this capacity is less developed than in ncMo [271].

Mouse Ly6C^{+} (Ly6C^{High} + Ly6C$^{middle/int}$) monocytes are described as pro-inflammatory [229,235] and in vascular inflammation, Ly6C^{+} monocytes are tethered and invade tissue by interaction complimentary pair of CCR2/CCL2(MPC-1) via a VLA-1/VCAM1-dependent manner [229]. These monocytes have a high antimicrobial capability due to their potent capacity for phagocytosis, secrete ROS, nitric oxide, TNF-α, IL-1β, little IL-10 upon bacterial infection [241] and large amount of type 1 IFN in response to viral ligands [272].

- Intermediate monocytes functions

Compared to cMo and ncMo, the knowledge about the functions of intMo in homeostasis and inflammation is sparse. This is partly due to the low and variable numbers of this subset in circulation [243]. Moreover, because of their scarcity, intMo were often examined after pooling with ncMo, which

complicates the interpretation of findings [243]. intMo exhibit the highest expression of TLR4, TLR2, CD40 and MHC-class II molecules (HLA-DR), and also possess the greatest ability to present antigens [265]. IntMo were found to produce both pro-inflammatory (TNF-α, IL-1β, and IL-6) and anti-inflammatory cytokines upon TLR stimulation [245,264,265,273–275], and like cMo, they show phagocytic activity [262]. Zawada et al. [264] suggested that intMo produce the most ROS and cMo produce the lowest ROS, while Cros et al. [245], also suggested that intMo do not produce ROS and cMo produce large amounts of ROS. These last authors also reported highest secretion of TNF-α and IL-1β by intMo compared to cMo and cMo, and found intMo to secrete IL-8, although at lower levels than cMos [245]. On the contrary, Wong et al. [265] reported that ncMo secrete the highest levels of TNF-α and IL-1β and similar levels of IL-8 secreted by all subsets. intMo are also involved in diseases, for instance, the Prospective Halle Monocyte Study showed a shift from cMo to intMo in patients with coronary artery disease [276]. Functional mapping of intMo and elucidation of their differentiation kinetics is essential to clarify their role in both homeostasis and disease, and to address whether the observed association with disease signifies adverse functions or is a bystander effect of a failure to mature into ncMo [243].

- Non-classical monocytes functions

ncMo perform endothelial cell patrolling, which helps in cellular integrity maintenance, removing dead endothelial cells, repairing the vasculature in atherosclerotic diseases, and removing lipids from the blood [261]. $CD14^{+}CD16^{++}$ncMo patrol the vessel wall and invade by interaction of complementary pair of CX3CR1/CCL3 via LAF/ICAM1-dependent manner [229]. *In vitro* studies revealed that ncMos exhibit the strongest response to lipopolysaccharide (LPS), and possess the ability to secrete proinflammatory cytokines like TNF-α and IL-1β [277]. Unlike cMo, ncMo produce anti-inflammatory cytokines like IL-10 when exposed to bacterial stimuli [245]. However, this characteristic does not turn ncMo the anti-inflammatory counterpart of cMo, since they produce elevated levels of inflammatory cytokines in a TLR7-mediated response to viruses and nucleic acids [261,268,278]. Additionally, ncMo were capable to initiate recruitment and activation of other innate immune cells, such as NK cells and neutrophils through TNF-α-induced upregulation of E-selectin on endothelial cells [279,280]. Chimen et al. [280] reported that pooled ncMo and intMo transmigrate faster through unstimulated endothelial cell monolayers *in vitro*, despite fewer ncMo/intMo adhere compared to cMo. Furthermore, the former did not re-enter the blood stream, while cMo did, consistent with findings on the regress of $Ly6C^{high}$ but not $Ly6C^{low}$ to the bone marrow in mice [210,229,281]. Apparently, ncMo are either not equipped to respond to signals for reverse transmigration or are retained more firmly in the subendothelial space [280]. NcMo are thought to play a

role in the resolution of inflammation, as they differentiate into wound-healing macrophages [282]. Studies have reported both elevated levels of ROS production at baseline [283] as well as low ROS levels in response to IgG-opsonized bovine serum albumin [245].

Mouse Ly6C^{low} monocytes perform patrolling and surveillance of the luminal surface of the vascular endothelium [271,284,285]. This patrolling behavior, along with the ability to phagocytose endothelial-associated particles, suggests that a primary role of these monocytes is sensing (for instance, viral nucleic acids) and scanning the endothelial surface for damage and/or the presence of pathogens [271,285]. Ly6C^{low} monocytes are recruited into normal tissue by interaction of complementary pair CX3CR1/CCL3 via a LAF/ICAM1-dependent manner [229]. These monocytes respond mainly via TLR7 to the local danger signs (although they respond poorly to bacterial products as LPS) producing inflammatory mediators [271]. Ly6C^{low} monocytes can be recruited to sites of infection even earlier than Ly6C^{high} monocytes, and can participate in the initial inflammatory response by releasing tumour necrosis factor (TNF) and chemokines [284]. However, in most cases of infection, the ensuing recruitment of Ly6C^{high} monocytes is more prominent and robust [227].

However, Ly6C^{low}can also secrete anti-inflammatory cytokine IL-10 upon *in vivo* bacterial infection [229]. They are also capable of inducing intravascular recruitment of neutrophils, that trigger endothelial necrosis and subsequently they eliminate the resulting debris [271].

1.3.3 Monocyte to macrophage differentiation

After being released into the circulation from the bone marrow under healthy homeostasis, classical monocytes remain in the circulation for approximately a day, before they traffic to repopulate a proportion of tissue-resident macrophages in the dermis, heart, lung, pancreas, testis and intestine [231,286–294]. For example, the recruitment of Ly6C^{high} monocytes to the adult intestinal mucosa is dependent on CCR2, as mice lacking either CCR2 or its ligand CCL2 have markedly reduced intestinal macrophage pools [231,232]. Interestingly, migrated Ly6C^{high} monocytes can also retain their monocyte-like state and act as a local monocyte reservoir showing minimal transcriptional changes [233]. In steady state, the patrolling anti-inflammatory monocytes patrol the vasculature to monitor PAMPs and become tissue resident macrophages or dendritic cells [229,234]. Remarkable exceptions in which little or no monocyte engraftment include the epidermis and the central nervous system [295–299]. These organs are probably spared from adult monocyte infiltrates due to the combination of two factors, the high self-

renewal potential of the tissue-resident macrophages, and by the limited access for monocytes to reach these sites due to existing epithelial and blood-brain barriers [279].

During inflammation, human cMos and intMos are tethered and invade tissue [229], and then, monocytes mature to pro-inflammatory M1 macrophages in tissue and present self-antigen via MHC-I/II to T cell receptor leading to T cell activation [229]. During inflammation, patrolling anti-inflammatory monocytes differentiate into anti-inflammatory (M2) macrophages, which repair damaged tissues [234].

Ly6C^{+}CCR2^{hi} inflammatory and Ly6C^{-} (Ly6C^{low})CCR2^{low} monocytes are generally thought to preferentially differentiate into M1 inflammatory and M2 anti-inflammatory macrophages [284]. In the early phase of myocardial infarction [229] (which is associated with an inflammatory reaction) [300–303], Ly6C^{+} monocytes dominate and exhibit phagocytic, proteolytic, inflammatory function and digest damaged tissue [229]. In vascular inflammation, Ly6C^{+} monocytes are tethered and invade tissue, then also mature to inflammatory M1 macrophages [229]. On the other hand, Ly6C^{low} monocytes, recruited at later phase of inflammation, attenuate inflammatory properties and differentiate toward M2 macrophages, contributing to angiogenesis, genesis of myofibroblasts, and collagen deposition [229].

However, several studies also revealed "unusual" cascades of monocytes to macrophage transition. Specifically, it was a shown that in steady state, Ly6C^{+} monocytes are recruited to healthy lamina propria and differentiate into tissue resident CX3CR1^{high} macrophages [304] and that Ly6C$^{middle/int}$ monocytes emigrate to lymph nodes via CCR7 and CCR8 and differentiate into dendritic cells [294,305]. Moreover, it was demonstrated that Infiltrated Ly6C^{+} monocytes in inflamed skeletal muscle or brain tissues acquire phenotypic features of anti-inflammatory monocytes by down-regulating Ly6C expression, thus exhibiting anti-inflammatory M2 macrophages function [306,307].

Monocytes recruited from the blood during the post-inflammatory phase can lose the expression of Ly6C and become Ly6C^{-} cells, subsequently differentiating in M2 macrophages. They may also become memory macrophages. Memory macrophages that are present in the tissue, reminiscent of previous inflammatory events, would probably behave like naïve macrophages upon a new inflammatory challenge, except for a much quicker reaction, and will, therefore, mostly die or generate M2-like macrophages or again memory macrophages [285].

1.3.4 Monocytes in Spinal Cord Injury

SCI studies on *Cx3Cr1*^{GFP} mice have demonstrated the presence of both Cx_3Cr1^{low} and Cx_3Cr1^{high} macrophages at the injury site, indicating that both pro-inflammatory Ly6C^{high}, and anti-inflammatory Ly6C^{low} monocytes contribute to the macrophage population after SCI [308,309].

Blomster et al. [168] showed an increased early presence of infiltrating monocytes/macrophages, as a result of CX3CR1 deficiency within the peripheral immune compartment, correlated with worsened the outcome of SCI, both at a functional and histological level. Adoptive transfer of identified *Cx$_3$cr1*$^{gfp/+}$ monocytes revealed a peak of infiltration at 7 days post-injury, with Ly6C^{high} inflammatory monocytes being most efficiently recruited. The composition of the two major monocyte subsets in the blood was also changed by focal SCI, with more Ly6C^{high} cells present during peak recruitment [168]. The adoptive transfer experiments further suggested high turnover of inflammatory monocytes in the spinal cord at 7 days post-injury, and only a small proportion of infiltrating cells unequivocally expressed polarization markers for pro-inflammatory (M1) or alternatively activated (M2) macrophages at that time point [168].

Spleen Monocytes and Spinal Cord Injury

In the human spleen, monocytes are present in an area called the 'perifollicular zone', together with granulocytes and accumulations of erythrocytes [310–313]. In humans, it was reported that spleen monocytes expressed low levels of CD163 [314].

Observations in rats argue for a generalizable existence of a splenic monocyte reservoir [233], and in mouse this reservoir of monocytes resides in the splenic subcapsular red pulp, clustered in red pulp cords [233], providing an emergency monocyte reservoir that is rapidly deployed during inflammation [233,315]. However, and despite of the existence of the reservoir of monocytes in red pulp, some authors also pointed to the existence, in mice, of monocytes in marginal zone of the spleen [256]. Extramedullary monopoiesis was also reported in the adult mouse spleen under inflammatory conditions, including in the presence of tumors, in models of psychosocial stress, and upon aging [316–319].

Although bone marrow was previously believed to be the exclusively origin of Ly6C^{high} and Ly6C^{low} monocytes, the spleen is now recognized as a major monocyte reservoir during the acute injury phase in many organ systems [167]. Using a mouse model of myocardial infarction, Swirski et al. [233] demonstrated that a population of monocytes reside within the subcapsular red pulp of the spleen, and had both Ly6C^{high} and Ly6C^{low} subtypes. Following splenectomy, the number of pro-inflammatory

Ly6C^{high} monocytes decreased by about 75% within 1 day after injury, at the site of myocardium infarct, whereas the number of anti-inflammatory Ly6C^{low} monocytes remained unchanged, implicating the spleen as the major source of the pro-inflammatory subtype [233]. These results give the impression that the pro-inflammatory characteristic is intrinsic to splenic macrophages [167] suggesting that splenic reservoir monocytes can exacerbate inflammation and impair wound resolution [320], however, it should be noted that tumor associated macrophages, which are pro-regenerative, also arise from the spleen [317]. Swirski and colleagues [233] also observed that splenic monocytes exhibited morphological similarities to their blood counterparts, with Ly6C^{high} monocytes appearing larger than Ly6C^{low} monocytes, and both subsets featuring kidney- or horseshoe-shaped nuclei. Ly6C^{high} monocytes in spleen and blood had essentially indistinguishable transcriptomes, and this similarity was validated by refined mRNA and protein analysis [233], although, as expected, Ly6C^{high} monocytes differed from their Ly6C^{low} counterparts [321]. Moreover, splenic Ly6C^{high} and Ly6C^{low} monocytes had phagocytic functions akin to those of their blood counterparts and differentiated into macrophages or DCs *in vitro* [233]. Thus, these authors [233] concluded that the spleen contains a population of monocytes that outnumbers blood monocytes and that coexists with, but is different from, macrophages and DCs.

One of the factors controlling rapid monocyte deployment from the spleen, is for instance, the activation of autonomic responses [322]. Shortly after an ischemic insult, there is an increase in norepinephrine and epinephrine in the systemic circulation, which can activate adrenergic receptors in the spleen to trigger release of monocytes [323].

Although resident microglia can act as macrophage-like cells, most of macrophages seen at the injury site are immature monocytes that infiltrate the parenchyma from the blood [154,169,324]. Reports indicated that the spleen is the primary depot and origin of inflammatory monocyte-derived macrophages that infiltrate the injured spinal cord [168]. Blomster et al. [168], showed that the majority of infiltrating monocytes at 7 days post-injury originate from the spleen and only to a lesser extent from the bone marrow. Removal of the spleen, at the time of SCI, resulted in a dramatic decline in the number of blood monocyte-derived macrophages present at the injury site 7 days later. Moreover, prevention of early monocyte infiltration through splenectomy was also associated with improved recovery at 42 days post-injury [168]. The benefits of splenectomy may be partly explained by reduced entry of inflammatory Ly6C^{high}CX$_3$CR1^{low} monocytes, which are more efficiently recruited to the injured spinal cord than wound-resolving Ly6C^{low}CX$_3$CR1^{high} monocyte-derived macrophages [168,320]. An interesting and potentially important observation is that even after a splenectomy, macrophages started to reappear at the injury

site, and over time the number of macrophages was similar to non-splenectomized animals [168], which confirmed another source of macrophages, such as the bone marrow [167,168].

1.4 Macrophages

1.4.1 Macrophage ontogeny, survival and proliferation

As mentioned before, in mouse, hematopoiesis emerges in three sequential waves. The first wave, the primitive, starts at E7.0 (in humans this wave starts between 2.5 - 3 weeks of gestation) [197,325–328], in the YS blood islands and give rise to erythroid, megakaryocytes and macrophage progenitors [195,325,329]. Macrophage progenitors will subsequently give rise to pre-macrophages and then YS or "primitive" macrophages at the origin of microglia in the brain [195,298,330,331] (Figure 1.4). The second wave occurs at E8.25 in mouse (3.25 weeks of gestation in humans), in hemogenic endothelium of the YS and give rise to erythromyeloid progenitors (EMPs) that will generate notably the first fetal monocytes [195–197,325,332]. In turn, fetal monocytes will infiltrate every tissue, with the exception of the brain, and differentiate into most adult resident macrophage populations [195,219,333]. This second wave is also generating lymphomyeloid progenitors (LMPs) that will provide B and T lymphoid precursors [195,334] (Figure 1.4). The third wave is starting at E10.5 (5 weeks of gestation in humans) [327,335], with the emergence of the first HSC in the aorta-gonads-mesonephros region [195] (Figure 1.4). Over E10.5, HSCs are also produced in umbilical and vitelline arteries, placenta and YS [195,200,334]. EMPs, LMPs and HSCs rapidly seed the fetal liver that will become the main hematopoietic organ until late gestation [195,326,336–339]. Fetal HSC will also migrate and seed the spleen and finally the bone marrow, which will eventually lead to the generation of adult HSCs in the bone marrow [201,340]. However, and despite the bone marrow niche take several days to become functional after birth, during the perinatal window, the hematopoiesis is still functional in the newborn liver and can generate fetal HSC-derived "liver" monocytes able to spread in tissues of the neonate and generate additional tissue-resident macrophages, until adult monopoiesis starts [195].

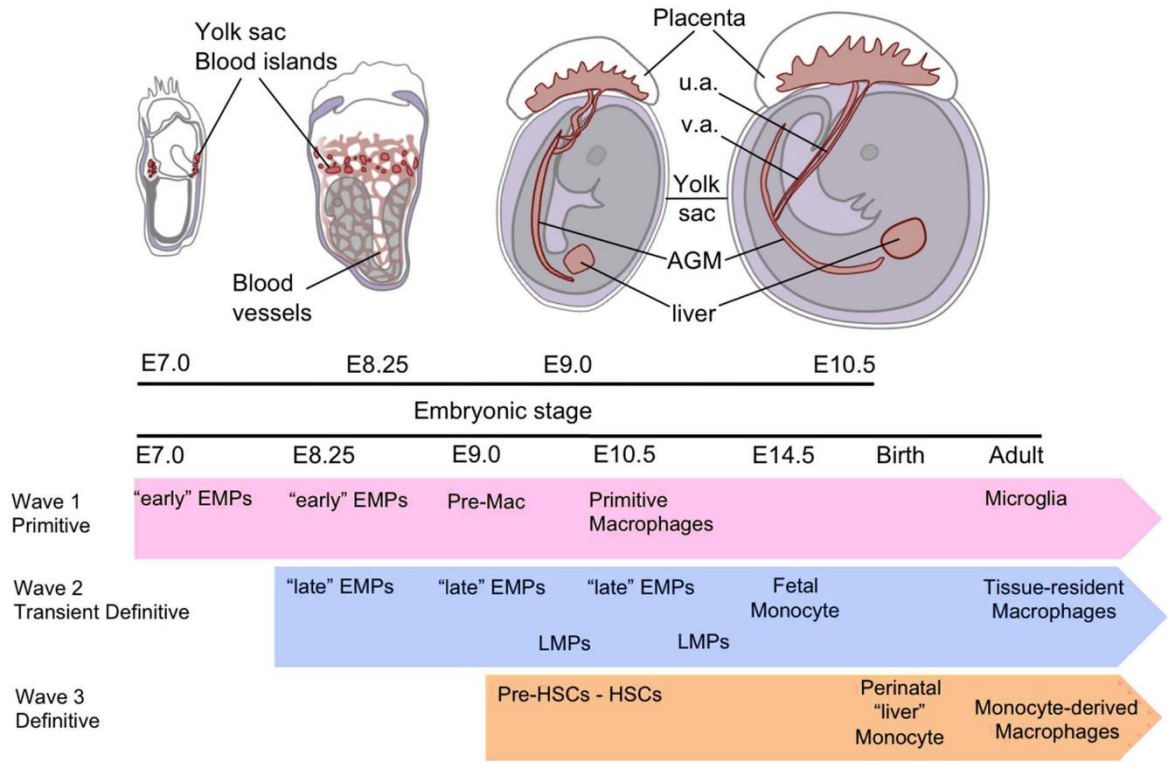

Figure 1.4: The three embryonic hematopoietic programs or waves in mice. Abbreviations: AGM - Aorta-gonads-mesonephros; EMPs - Erythromyeloid progenitors; HSCs - Hematopoietic stem cells; LMPs - Lymphomyeloid progenitors; u.a. - Umbilical artery; v.a. - Vitelline artery. Figure adapted from Hoefflel and Ginhoux [195].

M-CSF and GM-CSF are the apex macrophage survival cytokines, and although mice lacking M-CSF or GM-CSF have macrophages, both cytokines are essential for the maintenance of macrophage numbers, even in inflammation [341]. It is crucial to emphasize that while GM-CSF and M-CSF (or IL-34, a second ligand of the CSF-1 receptor that is important for microglia and Langerhans cell survival and proliferation) are necessary for macrophage proliferation, their equally important role lies in enforcing survival by blocking apoptosis [341].

M-CSF promotes macrophage proliferation [218], and it is also typically used to differentiate human monocytes found in circulation into macrophages *in vitro*, as well as murine bone marrow or spleen cells into macrophages [220–222]. While M-CSF has the capacity to influence a variety of cells, it can also be used as a to generate M2 macrophages *in vitro* [342,343]. Nonetheless, there is some debate as to the status of these MCSF derived cells being truly M2, with data in human cells showing that M-CSF

treated macrophages can still polarize towards an M1 phenotype upon stimulation with IFN-γ and LPS [344]. Consequently, it has been proposed that a "pro-M2" status is a more appropriate term for macrophages treated with M-CSF. When considering the *in vivo* context, M-CSF has been proposed as a promoter of M2 polarization due to its homeostatic expression coupled with the general M2-like phenotype of resident macrophage populations under normal conditions [345,346].

1.4.2 Tissue Resident Macrophages

Although fetal macrophages populate all tissues at birth, gradual replacement of these cells to a greater or lesser extent by HSC-derived progenitors can occur with time at specific sites [340]. Fate mapping model of HSCs or their immediate progeny have revealed that the contribution of adult HSCs to tissue-resident macrophages differs among organs and increases with age. Further evidence for the contribution of adult precursors to some tissue-resident macrophages and continuous turnover in adulthood revealed the recruitment of circulating Ly6C^{high} monocytes and their differentiation into tissue macrophages [340,347]. However, Ly6C^{low} can also become tissue resident macrophages [229].

Tissue macrophages that are maintained by adult circulating precursors include dermis, heart, pancreas and intestine macrophages [286–288,290,292]. Other tissue-resident macrophage populations such as epidermal Langerhans and liver Kupffer cells, and microglia, exhibit negligible need for replacement in adulthood [340]. For example, in brain, tissue-resident macrophages are maintained locally by proliferative self-renewal and retain an M2-like phenotype [348–351].

Table 1.3 summarizes the subpopulations of tissue-resident macrophages present in selected individual organs and their functions. These representative tissues were chosen to illustrate the complex heterogeneity and functions of resident macrophages, rather than an exhaustive description in all tissues [352]. Resident macrophages in nervous system and bordering compartments, and in the spleen will be described with more detail later.

Table 1.3: Microheterogeneity of selected tissue-resident macrophages: subpopulations and functions. Table adapted from Gordon and Plüddermann [352].

Source	Macrophage subpopulation	Functions
Lymph nodes	Subcapsular macrophages	Subcapsular sinus macrophages capture antigens for delivery to DC, for activation of B and T lymphocytes
	Medulla	Activation of T and B cells
Gut	Lamina propria macrophages	Modulation of inflammation and immune activation
	Submucosal macrophages	Interactions with smooth muscle cells, myenteric and autonomic nervous system
Peritoneal cavity	Large and small resident macrophages	Interactions with B lymphocytes, inflammation stimulates migration to draining lymph nodes and abdominal organs, such as liver, upon injury
Liver	Kupffer cells	Clearance, phagocytosis and receptor-mediated endocytosis, interactions with hepatocytes, metabolism of iron, lipids, and micronutrients
Lung	Alveolar macrophages	Particle clearance, surfactant metabolism
	Bronchial macrophages	Antigen capture and presentation
Heart	Resident cardiac macrophages in AV node	Regulate cardiomyocyte electrical activity through macrophage Connexin43- mediated adhesion

Nervous system macrophages

- Central nervous system macrophages

The CNS consists of not only billions of cells such as neurons, astrocytes, and oligodendrocytes but also resident immune cells [353]. The immune system of the CNS consists primarily of innate immune cells, and these are the parenchymal macrophages are known as microglia [353] (Figure 1.3), while the extraparenchymal macrophages in the CNS border structures are collectively termed CNS- or border-associated macrophages (CAMs or BAMs, respectively; the BAM terminology is used herein) [354,355] (Figure 1.3). Macrophages are also present within the cerebrospinal fluid system [356] (Figure. 1.3).

Specifically, BAMs are divided into perivascular macrophages, stromal choroid plexus macrophages, dural macrophages, subdural macrophages (these last two, classified as meningeal macrophages) [357] (Figure 1.3). Cerebrospinal fluid macrophages can be subcategorized as either surface-attached or freely floating [356]. Surface-attached macrophages are divided into subarachnoid space macrophages, choroid epiplexus macrophages, also known as Kolmer's cells, and supraependymal macrophages [357,358] (Figure 1.3). Freely floating macrophages are present throughout much of the cerebrospinal fluid system, possibly excepting the uninjured central canal of the spinal cord [359]. The locations and markers of these macrophages can be seen in the Figure 1.3.

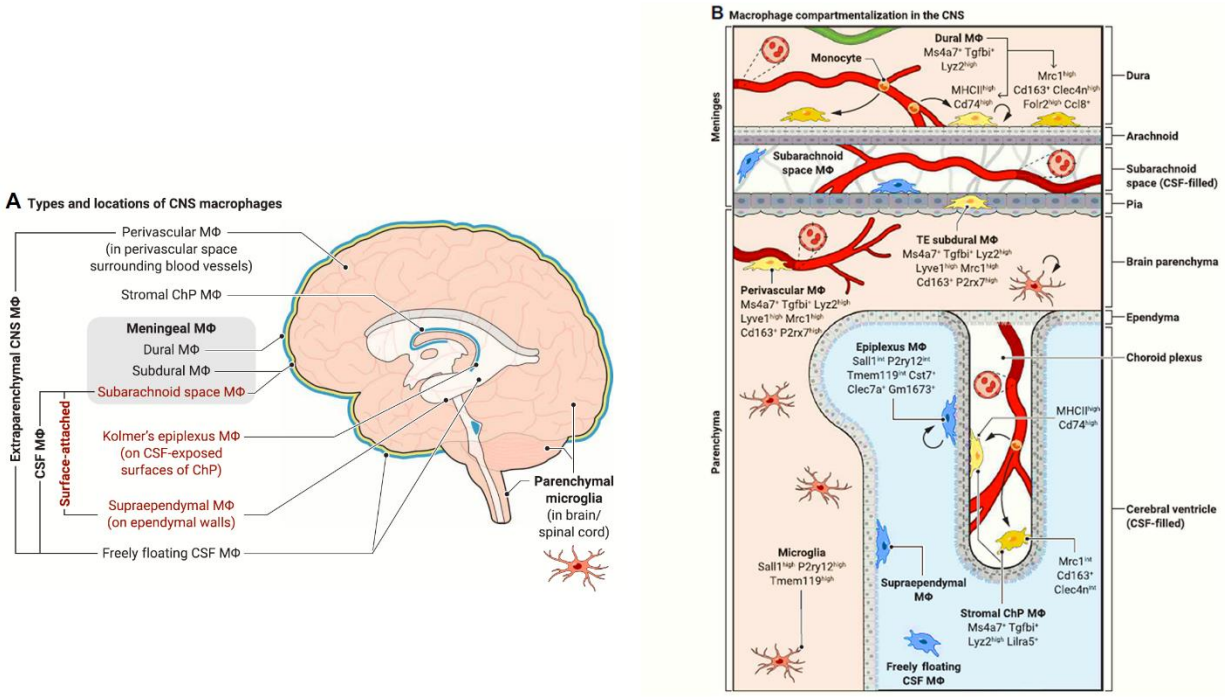

Figure 1.5: CNS macrophage locations, terminologies, and compartment-specific identities. **(A)** The types and locations of parenchymal and extraparenchymal CNS macrophages. **(B)** Macrophage compartmentalization in the CNS. Example key markers are shown to demonstrate the compartment-specific identities of homeostatic CNS macrophages. Blood-derived and self-renewal arrows are based on Munro, Movahedi and Priller [357] understanding of CNS macrophage turnover. The green vessel in the dura represents lymphatics. Abbreviations: ChP - Choroid plexus CNS – Central nervous system; CSF - Cerebrospinal fluid; MΦ - Macrophage; TE - Tissue-embedded. Figure adapted from Munro, Movahedi and Priller [357].

Origins of Central Nervous System macrophages

Microglia were initially believed to originate from the neuroectoderm, but this view was later replaced by the idea of a blood monocytic origin, a concept that has prevailed for the last decades [330,360]. However, it has already been convincingly shown that microglia arise from embryonic YS precursors [298,326,340]. Microglia maintain their CNS population by self-renewal, with little contribution from blood cells [297,298,348,357,361] (Figure1.3). Recent data showed that BAMs also originate from YS progenitors (early EMPs) instead of bone marrow-derived monocytes [362,363], although specific BAMs, such as dural and choroid plexus macrophages, can be replenished by blood-circulating bone marrow-derived monocytes [357,364] (Figure 1.3).

Functions of Central Nervous System macrophages

Microglia has several roles, and here we will just describe few of them, such as, the phagocytosis of dead cells, the trophic support of developing neurons in the CNS, the guidance of developing vasculature in the CNS, the support and refinement of developing neural circuits by synaptic pruning [365]. In the adult brain, microglia act as modulators of synaptic plasticity and regulate neurogenesis [365].

In contrast to the roles of microglia, the functions of BAMs are less understood [354]. This lack of knowledge is mostly due to low numbers of BAMs in the CNS compared to microglia [353]. BAMs found in the leptomeninges (subdural macrophages), choroid plexus, and perivascular space are thought to be important effectors and regulators of the immune response at CNS borders, due to their ability to phagocytose and migrate [353,366]. In zebrafish brains, perivascular macrophages promote vessel repair after microlesions [367].

- Peripheral Nervous System macrophages

Sensory neurons situated in DRG transmit sensory information from peripheral tissue to the brain. Following peripheral nerve injury, sensory neurons switch to a regenerative state to allow axon regeneration and functional recovery [368]. Macrophages present in the DRG (DRGMacs) contribute to the regenerative capabilities of sensory neurons [369–373], however, DRGMacs also contribute to the initiation and persistence of neuropathic pain following nerve injury [374] and chemotherapy-induced neuropathy [375–377]. Feng et al. [368] identified three subtypes of DRGMacs after nerve injury in addition to a small population of circulating bone-marrow–derived precursors. Self-renewing

macrophages, which proliferated from local resident macrophages, represented the largest population of DRGMacs. The other two subtypes included microglia-like cells and macrophage-like satellite glial cells (Imoonglia) [368]. They also showed that self-renewing DRGMacs contributed to promote axon regeneration, and revealed that macrophages expressed the neuroprotective and glioprotective ligand prosaposin and communicated with satellite glial cells via the prosaposin receptor GPR37L1 [368].

In the PNS, tissue-resident macrophages are also located in the endoneurium as well as the epineurium of healthy nerves [378]. In addition, from PNS macrophages within peripheral nerves, there are also 'nerve-associated macrophages' and these encompass macrophages in close proximity to sympathetic neurons in white and brown adipose tissue [379,380], macrophages in the intestinal muscularis externa and lamina propria that are closely associated with the enteric nervous system [381,382] or macrophages in contact with dermal sensory nerves [383].

The macrophages of the PNS have been described as a local surveillance system due to their ability to take up proteins in the endoneurial space and display antigen via MHC class II molecules to T cells during inflammation [384]. Only a small portion of tissue-resident macrophages within PNS is YS-derived. Instead, macrophages begin to populate the PNS during late embryonic development. Nevertheless, a considerable number of these fetus-derived PNS macrophages is subsequently replaced during the first weeks after birth. During adolescence and adulthood, the integration of bone marrow-derived cells into the PNS parenchyma is dramatically reduced [385]. Wang et al. [386], revealed a surprisingly unique transcriptional profile for PNS macrophages when compared with brain microglia and macrophages from lung, liver, spleen or the peritoneum . It was found that genes such as *Foxred2*, *Cd209d*, *Mgl2*, *Il1rl1*, *Cbr2*, *Adam19*, *Mmp9*, *Fxyd2*, *Kmo* or *Tslp* were typically present in PNS macrophages [385].

Acute injury of the PNS conducts to a rapid infiltration of circulating monocytes and, to a much minor extent, other hematopoietic cells like neutrophils, eosinophils and some T cells [387–389]. This recruitment is mediated by the release of cytokines and chemokines by local tissue-resident macrophages and Schwann cells [390,391]. Data showed that recruited monocyte-derived macrophages and not resident macrophages, are the source of VEGF-A [388], and VEGF-A produced by macrophages is required for efficient regeneration of peripheral nerves following injury [392]. Therefore, it was suggested that recruited macrophages are the main drivers of nerve regeneration in a model of Wallerian degeneration [385,388]. Several studies have reported the role of M2 macrophages in peripheral nerve regeneration [393,394], however, other studies have also shown that M1 macrophages are indispensable for peripheral nerve repair and facilitate many critical processes in axonal regeneration [395–398]. It was

also shown that after functional recovery of the sciatic nerve, the recruited macrophages persist within the nerve and acquire a PNS macrophage signature [388]. This stands in contrast to what is observed in the CNS, where monocyte-derived cells are unable to adopt a microglia signature and are entirely absent after recovery from injury [297,349,399–402].

Spleen macrophages

Splenic macrophages are heterogeneous, with different types occupying the red pulp, the B cell area of the white pulp, the interface between these zones, the marginal zone (in rats and mice) [403–405], and in the T cell area of the white pulp [406]. Data suggested that yolk sac-derived macrophages are the sole origin of spleen macrophages of adult mice [407]. Next, we will briefly describe the different types of spleen macrophages.

- Red pulp Macrophages

Splenic macrophages were originally located in the cords of Billroth in red pulp and termed red pulp macrophages [408–412] (Figure 1.4). Red pulp macrophages filter the blood of bacteria, apoptotic or fragmented cells, and other debris, as well as "groom" red blood cells of inappropriate inclusions such as denatured hemoglobin [413]. Red pulp macrophages also perform erythrophagocytosis which is important for the turnover of red blood cells, recycling of iron to feed erythropoiesis [406,414] and promote extramedullary hematopoiesis [415]. Although the coordination of innate and adaptive immune responses is classically attributed to white pulp zones, the red pulp also performs important roles in host defense [320]. Red pulp macrophages produce and secrete type I interferons during the parasite *Plasmodium chabaudi* infection [416,417], and also recycle erythrocyte iron to defend against bacteria [416]. These cells are also able to produce proinflammatory cytokines besides type 1 interferons, such as TNF-α [418]. Red pulp macrophages can induce the generation of regulatory T (Treg) cells [419] and promote their differentiation via expression of transforming growth factor-β [416,420]. Red pulp macrophages can also prevent autoimmunity by producing anti-inflammatory cytokines such as IL-10 [419].

- Macrophages in the Marginal Zone and in the B cell area of the White Pulp

In rats and mice, two special macrophage populations are associated with the marginal zone, the Marginal zone macrophages (MZMs) and the marginal metallophilic macrophages (MMMs) [320,421] (Figure 1.4). In humans, the perifollicular zone is the border between the white pulp and red pulp [312] and the existence of MMMs in this zone was not clearly elucidated [413,422]. Within the germinal centers

of B cell area, macrophages containing phagocytosed apoptotic cells are called tingible body macrophages [423] (Fig. 1.4).

Marginal zone macrophages

MZMs (Fig. 1.4) present processed antigens to Marginal Zone B cells [424–426], and also interact with B cells promoting their maintenance and correct positioning in the marginal zone [427]. This crosstalk between the MZMs and marginal zone B cells is crucial to ensure the correct immune responses against T cell independent antigens, contributing to maintain central tolerance [423]. MZMs are also implicated in central tolerance through phagocytosis of blood-borne apoptotic cells [423]. MZMs are involved in clearance of bacteria and virus [406,428,429], and can recognize non-opsonized molecules [430], mainly blood-borne antigens, and bind to yeasts and the yeast-derived particle zymosan [431].

Metallophilic zone macrophages

MMMs (Figure 1.4), like MZM can clear bacteria [406] and have been implicated in the degradation and clearance of viruses [428,429,432]. They can specifically take up antigens, transfer them to CD8+ dendritic cells, ultimately activating T cells [406,433], and also perform trophic functions by actively interacting with their neighboring cells [423]. Follicular B cells are crucial to the maintenance of MMMs via release of LTαβ [434]. The close association of MMMs with MadCAM1^{+} endothelial sinus lining cells suggests a cooperative role for these macrophages in the organizing functions of the sinus lining cells in the maintenance of the splenic structure [423,435].

Tingible body macrophages

Inside the germinal centers, macrophages containing phagocytosed apoptotic cells are often found. These macrophages display visible condensed chromatin fragments inside of them, which appear as a dark blue staining pattern when stained with hematoxylin and eosin. As a result, these macrophages were originally called tingible body macrophages (tingible meaning stainable) [423] (Figure 1.4). Their main function, in the spleen, is the phagocytosis of apoptotic B cells produced in the germinal centers during antigenic responses, where hyper proliferation and somatic hypermutation of these cells take place [436].

- Macrophages in the T cell area of the white pulp

In the mouse, the macrophages located in the T cell area of the white pulp could be descendants of patrolling monocytes that have entered the white pulp from the blood. Their position among T cells suggests a role in antigen presentation or clearance of dying lymphocytes [406].

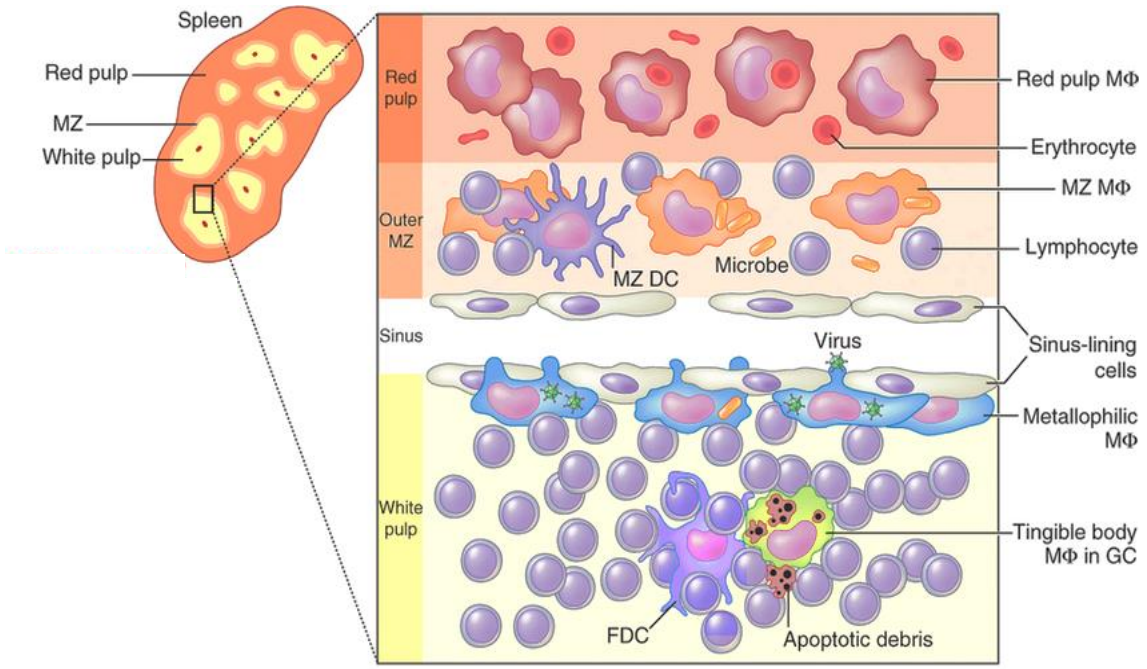

Figure 1.6: Microanatomy of the murine spleen showing localization of splenic macrophage populations. Abbreviations: DC - Dendritic cell; FDC - Follicular dendritic cell; GC - Germinal center; MΦ - Macrophage; MZ - Marginal zone. Figure adapted from Davies et al. [345].

- Spleen macrophages in Spinal Cord Injury and other diseases

After high level SCI, supraphysiological levels of norepinephrine are produced, activating β2-ARs on splenic lymphocytes and macrophages. This signaling pathway is amplified by serum glucocorticoids, which upregulate expression of β_2ARs to increase lymphocyte sensitivity to norepinephrine [437,438]. Convergent signaling via β_2ARs causes the transcription of genes including the cell cycle inhibitor p21waf1/cip1 and the pro-apoptotic factors Bim and caspase-3 [438–440]. This ultimately drives apoptosis of multiple splenic leukocyte populations, and splenic atrophy after SCI [437], and this pathway

was identified as the major driver of leukocyte death after SCI [437]. Clinical and experimental high level SCI caused a dramatic reduction in splenic cell populations and immune competence. Specifically, numbers of splenic $CD11b^+$ macrophages and major histocompatibility complex class II (MHCII)-positive antigen presenting cells are reduced following chronic SCI [179,441]. In chronic experimental and human SCI, circulating monocytes are also reduced [442–444].

In experimental ischemia/reperfusion kidney injury, it was reported that phenotypic switch of macrophages can occur *in vivo*, from M1 macrophages during the phase of kidney injury to M2 macrophages during kidney repair [445]. M2 macrophages have been shown to promote kidney repair by induction of tubule cell proliferation [445]. Alternatively activated macrophages M2 can further be classified into four subsets based on their *in vitro* response to stimuli [445]: M2a, M2b, M2c and M2d [446,447] (Table 1.4) . M2a can be induced by IL-4, Il-13 [446–448] or both (IL-4+IL-13) [445] and M2c by IL-10, TGF-β [447–449] or both (IL-10+TGF-β) [445], or glucocorticoids [447–449]. Specifically, M2a macrophages induced by IL-4+IL-13 and M2c by IL-10+TGF-β exhibit anti-inflammatory functions *in vitro* and protect against renal injury *in vivo* [445]. However, and since their relative therapeutic efficacy was unclear, Lu and colleagues [445], compared the effects of these two macrophage subsets in murine adriamycin-induced nephrosis. BALB/c mouse splenocytes were harvested and the adherent spleen derived macrophages were cultured with IL-4 and IL-13 (IL-4+IL-13) to become M2a and with IL-10 and TGF-β (IL-10+TGF-β) to become M2c macrophages [445]. The results revealed that compared with M2a, M2c expressed IL-10 and TGF-β highly. M2c did not express surface FIZZ-1, but expressed B7-H4, a regulatory surface molecule. They found that M2c expressed transcription factor hypoxia-inducible factor-1α (HIF-1α) and signal transducer and activator of transcription 3 (STAT3) however, M2a expressed high levels of early growth response 2 (EGR2) and interferon regulatory factor 4 (IRF4). Regarding the function, both cells inhibited T-cell proliferation, however, M2c were able to induce regulatory T cells (Tregs) from $CD4^+CD25^-$ T cells *in vitro*, and M2a did not [445]. Mice with adriamycin-induced nephrosis showed severe structural injury including glomerular sclerosis, tubular atrophy, and interstitial expansion, and severe functional injury including increase in serum creatinine and proteinuria and reduction of creatinine clearance. M2a and M2c macrophages reduced significantly glomerular sclerosis, tubular atrophy, and interstitial expansion as well as improved serum creatinine, creatinine clearance, and proteinuria [445]. However, glomerulosclerosis was more effectively reduced with M2c macrophages than with M2a. Tubular cell height was significantly better in mice treated with M2c than with M2a, and urine protein was significantly lower in mice treated with M2c than in mice treated with M2a [445]. CD4+ and CD8+ T cells

were significantly reduced in renal cortex of mice treated with both M2a or M2c. Nevertheless, M2c macrophages were also more effective than M2a in reduction of CD4+ T-cell infiltration in kidney [445]. Moreover, nephrotic mice treated with M2c had a greater reduction in renal fibrosis than those treated with M2a [445]. M2c macrophages, but not M2a, significantly increased the percentage of Foxp3^{+} T cells (Tregs) in renal draining lymph nodes [445]. To determine whether the greater protection with M2c was due to their capability to induce Tregs, the Tregs were depleted by PC61 antibody in nephrotic mice treated with M2a or M2c. Treg depletion reduced the superior effects of M2c compared to M2a in protection against renal injury, inflammatory infiltrates, and renal fibrosis. Thus, M2c were more potent than M2a macrophages in protecting against renal injury due to their ability to induce Tregs, namely due to their B7-H4-dependent ability to induce naïve T cells into Tregs [445].

1.4.3 Macrophage polarization

Macrophages are remarkable plastic cells which can switch from one phenotype to another [240,450]. Macrophage polarization is a process whereby macrophages mount a specific phenotype and a functional response to the micro-environmental stimuli and signals that encounter in each specific tissue [450]. Several classes of macrophages have been described in human and mice based on the expression of their cell surface markers, production of specific factors, and biological activities [448]. Two major macrophage sub-populations are the classically activated or inflammatory (M1) and alternatively activated or anti-inflammatory (M2) macrophages have been recognized [448] and some of their characteristics are presented in Table 1.4.

<u>M1 macrophages</u>

M1 macrophages are typically induced by IFN-γ, LPS [448] or both (IFN-γ+LPS) [166] or TNF-α [448]. These macrophages produce and secrete higher levels of proinflammatory cytokines TNF-α, IL-1α, IL-1β, IL-6, IL-12, IL-23, low levels of anti-inflammatory cytokine IL-10, and cyclooxygenase-2 (COX-2). M1 macrophages participate in the removal of pathogens during infection via activation of the nicotinamide adenine dinucleotide phosphate (NADPH) oxidase system, and subsequent generation of reactive oxygen species (ROS). Therefore, M1 macrophage has robust antimicrobial and anti-tumoral activity and mediates ROS-induced tissue damage. However, M1 can impair tissue regeneration and wound healing, if for instance, they persist too long at wound site [166,240,341,450–458].

M2 macrophages

M2 macrophages have been classified into subdivisions or subsets, based on the applied stimuli and the achieved transcriptional changes [342,455]. These subdivisions are M2a, M2b, M2c, and according to some authors, also M2d [459–461].

The M2a subset of macrophages could be induced by IL-4, Il-13 [446–448] or both (IL-4+IL-13) [445] and produces high levels of CD206, decoy receptor IL-1 receptor II (IL-RII), and IL-1 receptor antagonist (IL1Ra) [446,447].

The M2b subset could be induced by stimulation with immune complexes, TLR agonists [446–448] or both [166] or IL-1 receptor ligands, like IL-1β [446–448]. These macrophages produce both anti- and pro-inflammatory cytokines like IL-10, IL-1β, IL-6, and TNF-α [447].

M2c subset is induced by IL-10, TGF-β [447–449] or both (IL-10+TGF-β) [445] or glucocorticoids [447–449] and exhibit strongly anti-inflammatory activities against apoptotic cells by releasing high amounts of IL-10 and TGF-β [447,449]. M2c macrophages are also able to up-regulate genes involved in sequestering iron acquired from erythrocyte phagocytosis [98]. Lurier et al. [462] performed next generation sequencing (RNA-seq) to identify biological functions and gene expression signatures of macrophages polarized *in vitro* with IL-10 to the M2c phenotype, in comparison to M1 and M2a macrophages and an unactivated control (M0). For RNA-seq analysis, human blood-derived monocytes were isolated from peripheral blood mononuclear cells. Next, monocytes were cultured and differentiated to unactivated macrophages (M0) using M-CSF, and then, M0 macrophages were stimulated with IFN-γ and LPS (IFN-γ+LPS) for M1, IL-4 and IL-13 (IL-4+IL-13) for M2a, and IL-10 for M2c [462]. Then, they explored the expression of these gene signatures in a publicly available dataset of human wound healing. RNA-seq analysis showed that hundreds of genes were upregulated in M2c macrophages compared to the M0 control, with thousands of alternative splicing events. Following validation by Nanostring, 39 genes were found to be upregulated by M2c macrophages compared to the M0 control, and of these genes only 17 genes were significantly upregulated relative M1, and M2a phenotypes [462]. Many of the identified M2c-specific genes are associated with angiogenesis, matrix remodeling, and phagocytosis, including *CD163, MMP8, TIMP1, VCAN, SERPINA1, MARCO, PLOD2, PCOCLE2* and *F5*. The analysis of the macrophage-conditioned media for secretion of matrix-remodeling proteins revealed that M2c macrophages secreted higher levels of MMP7, MMP8, and TIMP1 compared to the other phenotypes [462].

Finally, a fourth type of M2 macrophage, the M2d [446], are considered tumor-associated macrophages (TAMs) [463]. M2d is induced by IL-6 [464,465], TLR agonists through the adenosine receptor [446], or adenosine receptor ligands [448]. Upon M2d activation, there is suppression of the production of pro-inflammatory cytokines and induction of secretion of anti-inflammatory cytokines (IL-10^{high} IL-12^{low}) and vascular endothelial growth factor (VEGF), thus providing proangiogenic properties [446,465–467]. Heterogeneous M2d populations were found to coexist in the tumour microenvironment. For instance, MHC-II^{low} M2d macrophages promote tumour growth, while MHC-II^{high} M2d macrophages promote tumor inhibition [463,464].

The exposure of M2 macrophages to M1 signals, or vice versa, which induce "re-polarization" or "re-programing" of differentiated macrophages is another evidence of their high functional plasticity which can be potentially pursued for therapeutic goals [448].

Table 1.4: Characteristics of the M1 and M2 macrophage subtypes. Table adapted from Kong and Gao [98], Gensel and Zhang [166], and Lu et al. [445], Shapouri-Moghaddam et al. [448] and Röszer [459].

Classification	M1 (classical)	M2 (alternatively-activated)			
		M2a	M2b	M2c	M2d
Phenotypes	Classical/Pro-inflammatory activation	Alternative activation, anti-inflammatory	Wound healing	Repair and remodelling of damaged tissues	Tumour-associated macrophages
Signalling factors	INF-γ, LPS, or both, TNF-α	IL-4, IL-13 or both	Immune complexes, TLR agonists, or both, IL-1R ligands	IL-10, TGF-β or both, glucocorticoids	IL-6, TLR agonists, adenosine receptor ligands
Cytokines	TNF-α, IL-1α, IL-1β, IL-6, IL-12, IL-15, IL-23, IL-10 (low levels)	IL-RII, IL-1Ra, TGF-β, IL-10, fibronectin 1, IGF1, PDGF	IL-10, IL-1β, IL-6, TNF-α	IL-10, IL-1β	IL-10, IL-12, TNF-α, TGF-β
Chemokines	CCL8, CCL15, CCL19, CCL20, CXCL9, CXCL 10, CXCL11, CXCL13	CCL13, CCL14, CCL17, CCL18, CCL22, CCL23, CCL24, CCL26	CCL1, CCL 20, CXCL1, CXCL2, CXCL3	CCL16, CCL18, CXCL13	CCL5, CXCL10, CXCL16
Markers	iNOS, CD16, CD32, CCL2, CD86, MARCO	EGR2, IRF4, Arginase-1 (ARG1), IL1Ra CD206, CD209, FIZZ1, YM1, IGF-1	SOCS3, CD206, CD86, TNF-α, CD64	Arginase-1 (ARG1), HIF-1α, CD163, SLAM, Sphk-1, THBS1, HMOX-1	IL-10^{high}, IL-12^{low}, VEGF
Functions in normal healing	Pro-inflammatory Boost inflammation, debris removal, sterilization, apoptotic cell removal	Wound healing Anti-inflammatory, cell proliferation, cell migration, growth factors, apoptotic cell removal	Immunoregulatory Cell maturation, tissue stabilization, angiogenesis, ECM synthesis	Immunosuppressive Inflammatory resolution, tissue repair, ECM synthesis, growth factors	—
Additional functions in SCI	Causes axon dieback	Remyelination, axon regeneration/reduces dieback	Axon regeneration/reduces dieback???	Remyelination???	—

M3 macrophages

Interestingly, a definition of the M3 phenotype was provided by Jackaman et al. [468]. These authors defined this phenotype as a phenotype with "incomplete polarization into an M1/M2-like phenotype"[468].

Many tumors produce anti-inflammatory cytokines, such as TGF-β, IL-10, and IL-13 [469,470], which reprogram the anti-tumor M1 phenotype into the pro-tumor M2 phenotype [471] and Kalish et al. [472] hypothesized that the problem of pro-tumor macrophage reprogramming could be solved by using a special M3 switch phenotype. In contrast to the M1 macrophages, M3 macrophages should respond to anti-inflammatory cytokines by increasing production of pro-inflammatory cytokines to retain its anti-tumor properties [472]. Thus, they conducted a study to form an M3 switch phenotype *in vitro* and to evaluate the effect of M3 macrophages on growth of Ehrlich ascites carcinoma *in vitro* and *in vivo* [472]. First native peritoneal macrophages (M0 phenotype) were isolated and cultured, and then they were reprogramed towards the M1 phenotype using 20 ng/ml IFN-γ in the absence of serum [447,472,473]. For reprogramming towards the M3 phenotype, IFN-γ was supplemented with: 1) STAT3 and STAT6 inhibitors; 2) SMAD3 inhibitor; or 3) STAT3, STAT6, and SMAD3 inhibitors [472]. The tumor microenvironment was created by addition of ascitic fluid from mice with Ehrlich ascites carcinoma to cultured macrophages. In mice, the tumor growth was initiated by an intraperitoneal injection of Ehrlich ascites carcinoma cells [472,474]. The results showed that the M3 switch phenotype can be programed by activation of M1-reprogramming pathways with simultaneous inhibition of the M2 phenotype transcription factors, STAT3, STAT6, and/or SMAD3. M3 macrophages showed an anti-tumor effect both *in vitro* and *in vivo*, which surpassed the anti-tumor effects of cisplatin or M1 macrophages, and the anti-tumoral effect of M3 macrophages was attributed to their anti-proliferative effect [472].

M(Hb), Mhem, Mox, and M4 macrophages

In atherosclerotic plaques, macrophages are simultaneously stimulated by a variety of signals and accordingly polarize into different subtypes, including in M(Hb), Mhem, Mox, and M4 [450,475].

M(Hb) macrophages are produced by hemoglobin stimulation, and typically express high levels of mannose and CD163 receptors, and participate in the clearance of hemoglobin/haptoglobin complex after plaque hemorrhage [476].

Following endocytosis of the hemoglobin/haptoglobin complex and erythrocytes, the liberated heme has the potential to prime macrophages toward a Mhem macrophage phenotype. In intraplaque hemorrhages, they engage the engulfment and recycling of erythrocyte remnants and hemoglobin, and

may be induced by hemoglobin, albumin and CD163 [477]. This subtype can prevent foam cell formation and provide certain protective effects against atherosclerosis [476,477].

Likewise, Mox macrophages are induced by oxidized phospholipids, distinguished by reduced phagocytic activity and chemotaxis. The expression of antioxidant enzymes such as heme oxygenase-1, thioredoxin reductase-1, and sulfiredoxin-1 are significantly upregulated by nuclear factor erythroid 2-related factor 2. This suggests that Mox macrophages might also possess anti-atherosclerotic properties and display resistance against oxidative stress [478].

M4 macrophages are induced by CXCL-4 and primarily exhibit the expression of CD68, calcium-binding protein S100A8, and MMP7 in the arterial adventitia and intima. They are accompanied by the expression of pro-inflammatory factors such as MMP-12, IL-6, and TNF-α [479]. Furthermore, CXCL-4 induces inflammation and exacerbates atherosclerosis by suppressing CD163 [480], suggesting the pro-atherogenic nature of this subtype [479,481]. De Sousa et al. [482] conducted an analysis on the presence of M4 macrophage markers (CD68, MRP8, MMP7, IL-6, and TNF-α) in 33 leprosy skin lesion samples from 18 patients with tuberculoid leprosy and 15 with lepromatous leprosy by immunohistochemistry. The results revealed that the M4 phenotype was more strongly expressed in patients with the lepromatous form of the disease [482]. This indicates that this subpopulation is less effective in the elimination of the bacillus and consequently is associated with the evolution to one of the multibacillary clinical forms of infection [482]. They concluded that M4 macrophages are one of the cell types involved in the microbial response to *M. leprae* and probably are less effective in controlling bacillus replication, fostering the evolution towards the lepromatous form of the disease [482].

Pathways of macrophage polarization

The main regulatory pathways of macrophage M1 – M2 polarization will be briefly described.

The predominance of activation of IRF3 and NF-kB signaling pathways by LPS, via TLR4 signaling will direct macrophage function toward the M1 phenotype [457], and the predominance of STAT1 activation by IFN-γ, via IFN-γR also promotes polarization of M1 macrophages, resulting in cytotoxic and tissue damage pro-inflammatory functions [457]. Conversely, a predominance activation of STAT6 and STAT3 and by IL-4/13 and IL-10, via IL-4Rα and IL-10R, respectively, promote M2 macrophage polarization, associated with immunotolerance and tissue repairing [450,457]. Activation of PPARδ through IL-4Rα, and of PPARγ, regulate distinct aspects of the M2 macrophage activation and oxidative metabolism [457]. Downstream of STAT6, KLF-4, participates in promoting the functions of M2 macrophages by suppressing NF-kB/HIF-1α-dependent transcription. IL-4 not only induces c-Myc, which

controls the expression of a subset of genes but also the IRF4 axis of M2 polarization to inhibit IRF5-mediated M1 polarization [457]. IL-10 promotes M2 polarization through induction of c-Maf, STAT3 and p50 NF-kB homodimer activities [457]. However, STAT3 is also activated by the pro-inflammatory cytokine IL-6. A potential explanation for this paradox is that IL-6 results in a more transient STAT3 activation, whereas IL-10 results in a more sustained activation [483], perhaps due to negative feedback from SOCS family members after IL-6 activation but not IL-10 [484]. TGF-β is a cytokine [1], with three isoforms (TGFβ-1, β2 and β3) that have been identified in mammals, and TGF-β1 is the predominant isoform expressed in immune cells, [485–488]. TGF-β signals are transmitted via a cell surface receptor complex consisting of the TGF-β type I receptor (TβRI) and TGF-β type II receptor (TβRII), and through Smad2 and Smad3 activation, and then formation of the Smad2/3/4 complex that translocates to nucleus to regulate gene expression [489].

Another signaling pathways, like Notch pathway are required for macrophage polarization [136]. The Notch pathway consists of ligands (Delta-like ligands Dll1, Dll3, Dll4, Jagged1, and Jagged2) and cell surface receptors (Notch1-4) that are primarily responsible for the pro-inflammatory polarization of macrophages *in vitro* and *in vivo* [136]. Dll4 triggers Notch1 [490] signaling to mediate proinflammatory responses in M1 macrophages, and at the same time, it hindered the differentiation of M2 macrophages and promoted their apoptosis [491,492]. Dll4 also activates the NF-κB pathway, which is involved in the M1 proinflammatory response [136]. The main sensor of Notch signaling is the recombining binding protein for immunoglobulin Jκ region (RBP-J), and RBP-J promotes the synthesis of the transcription factor interferon regulatory factor 8 (IRF8) protein via TLR4, thus promoting M1 macrophage polarization [493].

Macrophage polarization in inflammation, injury and normal wound healing

- Inflammation

Macrophages respond to inflammation or injury by migrating to affected sites to eliminate primary inflammatory signals, ultimately aiding in wound healing and tissue repair [227,228]. This process is also mainly initiated by PAMPs and DAMPs [228,239]. Moreover, activation of tissue-resident memory T cells by antigens can trigger the recruitment of macrophages through secretion of various inflammatory cytokines and chemokines [228].

The effective resolution of infection and inflammation requires the switch of the effector functions of macrophages from proinflammatory to anti-inflammatory. This kind of switch between states of macrophage polarization is necessary to terminate the inflammatory response and reestablish homeostasis, and is observed in the course of many inflammatory diseases [494,495]. The release of

anti-inflammatory and reparative mediators such as IL-4, IL-13, glucocorticoids, IL-10 or TGFβ, as well as lipid mediators such as lipoxins, resolvins or protectins promotes the shift of the macrophage phenotype towards anti-inflammatory and pro-resolution properties [496–498].

Under normal circumstances the activity of macrophages switches in the course of inflammation from proinflammatory to anti-inflammatory to restore homeostasis, and the inflammatory response resolves once the threat has passed. However, when the inflammation persists and incomplete resolution is incomplete, it often leads to chronic inflammation [499]. The impaired phenotype transition of proinflammatory activated to anti-inflammatory monocytes and macrophages is a characteristic feature of chronic inflammatory disorders [499]. Macrophages are key cellular components involved in the development and regulation of numerous chronic inflammatory conditions, including cancer and autoimmune diseases such as rheumatoid arthritis, therefore contributing to the pathogenesis of these disorders [500].

- Injury and normal wound healing

In cases of normal tissue repair, after skin or muscle repair injury, macrophages with specific phenotypes and functions are present in different phases of repair and contribute to processes and transitions within the wound repair program [501,502] (Fig.1.7).

The inflammatory phase consists of macrophages with both phenotypes M1 and M2a [503]. Evidence of M1 macrophages comes from the secretion of the pro-inflammatory cytokines IL-1, TNF-α and IL-6 [502]. M1 macrophages have enhanced phagocytic capabilities that facilitate debris removal, bacterial removal and sterilization and elimination of spent neutrophils [166]. On the other hand, M2a macrophages, initiate the proliferative phase of repair through the release of anti-inflammatory cytokines, increase cell proliferation and migration through release of arginase and Ym1, and promote the initiation of tissue formation through the secretion of growth factors [502,504,505]. During the early proliferative phase, macrophages continue to secrete pro-inflammatory cytokines, but transition toward release of IL-10 and some anti-inflammatory markers [502]. Interestingly, macrophages at this stage do not signal STAT6, a traditional M2a activation pathway, instead, adopt they a different M2 phenotype [506]. Given the mixed pro- and anti-inflammatory cytokines released and increased expression of IL-10, macrophages in the proliferative phase, most easily map onto M2b phenotype [240,447,503]. During later proliferative stages, M2b-mediated IL-10 release stimulates the activation of M2c cells, evidenced by increased expression of the M2c marker, TGF-β [240,502]. The remodeling phase is mainly dominated by M2c macrophages, as indicated by elevated TGF-β and CD206 (mannose receptor) with simultaneous

reductions in arginase-1 [502,503]. Interestingly, in burn wound healing it was suggested that M2c macrophages may act at early stages, in contrast to M2a macrophages, which act at later stages [462].

In successful wound repair, macrophage numbers return to normal levels within weeks of injury in parallel with the time of wound closure and healing [507]. However, wounds that fail to heal within 3 months are considered chronic [508] and persistent macrophage activation is a hallmark of this chronic condition [507]. Prolonged, improper macrophage activation disrupts transitions between different repair phases. For instance, chronic venous ulcers are the most common type of chronic wound and in this condition, macrophages fail to switch from M1 to M2 phenotype [507,508].

1.4.4 Macrophages in the context of Spinal Cord Injury

Macrophage polarization in Spinal Cord Injury

- Spinal Cord Injury healing

In the inflammation phase of SCI healing (Figure 1.7), a similar mixed response of M1 and M2 macrophages, like normal wound healing occurs shortly after SCI [509]. Expression of pro-inflammatory markers IL-6, TNF-α, IL-1β and IL-12 increase acutely in response to SCI [510,511]. Macrophage arginase expression peaks within 1–3 dpi along with other markers of M2a activation, IL-4, CD206 and Fizz-1 [509,512–515]. In the proliferation phase, the key macrophage phenotype that regulates the proliferative phase of repair, the M2b macrophage phenotype, is incorrectly activated after SCI. It is likely, therefore, that the SCI macrophages do not facilitate adequate transitions within the proliferative phase of repair [502,516,517]. In remodeling phase, little is known about the role of macrophages. This is partly because remodeling events that occur endogenously after SCI do not lead for successful healing and therefore the remodeling phase is not appropriately executed [518]. Furthermore, to the best of our knowledge, phenotypic characterization of M2c macrophages was not performed after SCI, with the exception of the preliminary short-term classification done by Gensel and Zhang [166] (Figure 1.7).

Globally, the phases of normal wound healing are orchestrated through the sequential activation of M1 to M2c macrophages, however, a different pattern of macrophage activation and wound healing occurs after spinal cord injury compared to the skin and muscle injury, in which potentially reparative and immunosuppressive M2b and M2c macrophages are unable to populate the lesion site, while pathological M1 macrophages remain elevated [166]. Therefore, the enduring presence of M1 macrophages after SCI stands in contrast to what happens in typical wound healing process, where M2 macrophages predominate [519]. Therefore, the persistence of M1 macrophages after SCI possibly contributes to a chronic inflammatory state that impedes cellular regeneration [167].

Kigerl et al. [509] reported that, other than the temporary presence of M2 macrophages during the first 7 days, the SCI site is comprised predominantly of M1 macrophages. M2 macrophages are induced at 3–7 days after SCI, however, M2 markers were reduced or eliminated after 1 week. In contrast, M1 macrophage response is also rapidly induced and then sustained at injured spinal cord [509,520]. According to Kigerl et al. [509], microglia and newly recruited monocytes differentiate into proinflammatory M1 macrophages at sites of SCI, and it is likely for this that acute depletion or functional inhibition of macrophages is neuroprotective and promotes recovery of function after SCI [176,521–523].

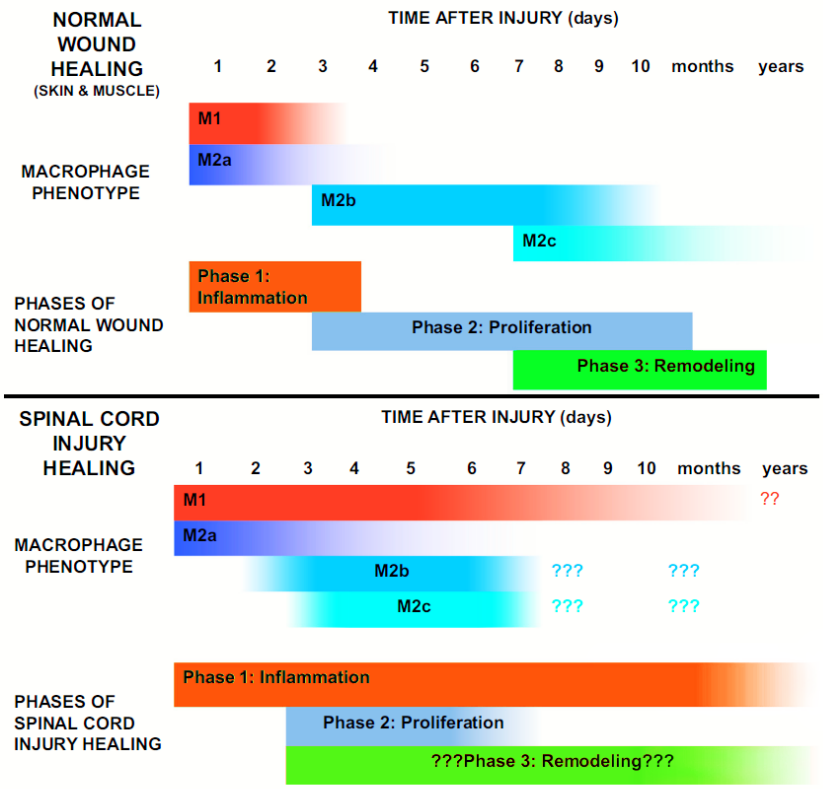

Figure 1.7: Phases and existence of distinct macrophages subsets in normal wound healing and after spinal cord injury. Figure adapted from Gensel and Zhang [166].

- Transcriptional regulation and signaling pathways of polarization in Spinal Cord Injury

Transcription factors that influence macrophage polarization have been an intense area of investigation in various disorders [457,524,525]. Herein, we will focus just in the context of SCI.

IFN-γ and LPS are the classical activating ligands to induce M1 polarization. IFN-γ binds to the IFN-γR, which signals primarily via STAT1 activation. However, since IFN-γ is not highly expressed at the SCI site [513], it remains uncertain whether this signaling pathway plays a major role in macrophage polarization following SCI [167]. Although LPS stimulation is not very representative of sterile inflammatory mechanisms that occur post SCI, its receptor, TLR4, is one of the major receptors for DAMPs, such as HMGB1, that are widespread at the injury site [526] and present in higher levels in plasma samples from humans with SCI [527]. TLR4 receptors signal via activation of NF-κB, which is a classic transcription factor for many pro-inflammatory cytokines, including TNF, IL-1β, COX-2, and IL-6, and a potent inducer of M1-like polarization [528]. TNF and IL-1β are often used to model sterile inflammation that induces M1 polarization *in vitro*, and both cytokines are expressed highly after SCI [529].

The majority of inflammatory effects attributed to TNF are via the activation of TNFR1 by the soluble form of TNF (solTNF), which eventually leads to NF-κB activation and polarization of M1 macrophage [167,530]. Notably the pharmacological inhibition of solTNF signaling has been reported to enhance function after SCI, although it is not clear whether the effects were mediated by macrophage polarization [531,532]. IL-1β also activates NF-κB by binding to the Type I IL-1 receptor (IL-1RI), consequently promoting M1 polarization. Administration of recombinant IL-1β exacerbates histopathology and function loss, whereas genetic deletion of IL-1β has a beneficial effect on these outcome measures [533]. Nonetheless, like TNF, it remains unclear whether either the detrimental or the beneficial effects are mediated by changes in macrophage polarization [167].

IL-4 and IL-10 are the classic M2 polarizing ligands. IL-4, as mentioned before, ultimately leads to activation of PPARγ, which leads to expression of classical M2 associated genes such as Arg1 and MMR (CD206) [525,534,535]. IL-10 binds to IL-10R, which activates the JAK1/STAT3 pathway, indirectly suppressing the expression of pro-inflammatory cytokines through expression of several effector genes [536]. Interestingly, expression of IL-4 and IL-10, along with most other anti-inflammatory cytokines, exhibit transient and acute expression after SCI [537–539], which may contribute to the prevalence of M1-like macrophages that persist chronically at the injury site. Consequently, the exogenous administration of IL-4 can promote M2 polarization associated with improved histopathology and behavioral outcomes [537].

- Polarization switch in Spinal cord Injury

Macrophages have extensive functional plasticity, which allows them to switch from one phenotype to another in the presence of various factors in the inflammatory microenvironment after SCI [98]. Myelin debris at lesion site, can cause bone marrow-derived macrophages polarization switch, from M2 towards M1 [520]. Iron accumulated in macrophages in SCI can prevent conversion from M1 to M2 [540]. In Yao et al.'s study [541], programmed cell death 1 (PD-1), a critical immune inhibitory receptor involved in innate and adaptive immune responses, is implicated in the modulation of macrophage/microglial polarization. In their study, M1-type macrophages/microglia accumulated in greater numbers in the injured spinal cord of PD-1 knockout mice. In PD-1 knockout mice, the M1 response was enhanced via the activation of STAT1 and NF-kB. Moreover, PD-1 suppressed M1 polarization and promoted M2 polarization [541].

Origin of Macrophages and replenishment in Spinal cord Injury

Macrophages are the most prevalent immune cell type in the injured spinal cord [154,324], and persist chronically at the injury site in both humans and rodents [324]. This prolonged presence raises the question of their turnover rate and origin at various stages of injury progression [167]. Resident microglia contribute to the intraspinal macrophage pool, however according to some authors most macrophages seed the injury site as immature monocytes that infiltrate the parenchyma from the blood [154,169,324]. Circulating monocytes have a lifespan of 1–3 days, and monocyte-derived macrophages typically have a lifespan of several weeks [542], which means that macrophages must be replenished in disorders like SCI, in which macrophages can persist for years [167]. The traditional view holds that since circulating monocytes terminally differentiate into macrophages, turnover of macrophages must rely on new monocyte influx [167]. However, accumulating evidence indicates that local proliferation of macrophages at the injury site may also significantly contribute to the total population, like for instance, in a model of peritonitis, proliferation of both resident and monocyte-derived macrophages contributed to the macrophage expansion [167,351], whereas in a mouse model of spontaneous mammary carcinogenesis, local proliferation, instead of monocyte recruitment, appeared to be the major mechanism of accumulation of tumor-associated macrophages [543]. Also in a mouse model of atherosclerosis, the turnover kinetics of almost macrophages is not changed following monocyte depletion or parabiosis, suggesting that monocyte recruitment cannot fully account for the number of macrophages in an atherosclerotic lesion [544].

Distribution of macrophages in SCI

Understanding the spatiotemporal dynamics of macrophage infiltration is complicated by the presence of microglia. Due to the phenotypic and antigenic similarities between microglia and macrophages, it is difficult to differentiate between these two populations [167]. However, Shechter et al. [545] showed that bone marrow monocyte-derived macrophages are often localized mainly in the margins of the lesion site following SCI, while microglia were located in the lesion margins and in its core. According to Hines et al. [546], after injury, infiltrating bone marrow derived macrophages (CX_3CR1^{low}/Mac-2 ^{high}) migrate to the epicentre of injury, while microglia (CX_3CR1^{high}/ Mac-2 ^{low}) localize to the edges of lesion. Therefore, it means that the majority of macrophages in the lesion site are bone marrow-derived macrophages rather than locally activated microglia [98]. These two populations of macrophages with different locations have different functions. Residential microglia form a border that seems to seal the lesion and block the spread of damage, while bone marrow-derived macrophages enter the epicentre of injured spinal cord and phagocytize apoptotic and necrotic cells and clear tissue debris such as myelin debris [98].

Roles of macrophages in pathological, regenerative and recovery processes during Spinal Cord Injury

- Phagocytosis

Greenhalgh and David [547] showed that microglia-derived macrophages contact with damaged axons early (24 hrs) after SCI and are the main type of macrophage to contain phagocytic material at day 3. Then, infiltrating macrophages become the predominant cells in contact with degenerating axons and contain more phagocytic materials that persist for up to 42 days, which is different from microglia [547]. Moreover, after phagocytosis of myelin *in vitro*, macrophages are much more susceptible to apoptotic and necrotic cell death than microglia [547].

Upon monocyte infiltration into the injury site, the injured milieu may favor an M1-like polarization. The fact that most macrophages persist chronically in this state rather than an M2-like state associated with wound resolution indicates that the injured spinal cord environment is unique compared to other injured tissues [167]. For instance, Myelin debris at the lesion site switches bone marrow derived macrophages from M2 phenotype towards M1-like phenotype. The abundance of myelin debris in the injured spinal cord leads macrophages to become lipid-laden foam cells that are characterized as proinflammatory M1-like cells [520]. Foamy macrophages are neurotoxic and showed delayed wound healing and their persistence at lesion site, signifies a pro-inflammatory environment, associated with enhanced neurotoxicity and impaired wound healing [520]. These foamy macrophages also have poor

capacity to phagocytose apoptotic neutrophils resulting in uningested neutrophils releasing their toxic contents and promoting further tissue damage [520]. Myelin debris also significantly enhanced the expression of M1 cytokines [520]. However, previous works has shown that myelin phagocytosis *in vitro* induces a shift in expression from proinflammatory to anti-inflammatory cytokines [548,549]. Nonetheless, and despite Kroner et al. [540] showed that despite the myelin phagocytosis *in vitro* induced M1-polarized macrophages and microglia to switch to a M2 state, this does not happen *in vivo*, and macrophage/ microglia in the injured spinal cord retain a predominantly M1 state that is detrimental to recovery. .

Tissue damage and hemorrhage that results from SCI leads to phagocytosis of the damaged myelin and red blood cells, which are a rich source of iron [540]. Phagocytosis of erythrocytes or myelin, *in vitro*, by activated macrophages resulted in reduced expressions of proinflammatory cytokines such as IL-12 and TNF-α [548,550]. However, transplantation experiments showed that increased loading of M2 macrophages with iron induces a rapid switch from M2 to M1 phenotype [540]. This combined effect promoted predominant and sustained M1 macrophage polarization that is detrimental to recovery after SCI [540].

After a peripheral nerve lesion, clearance of the distal nerve stump during Wallerian degeneration is primarily done by neutrophils rather than macrophages [551], and as neutrophils begin to undergo apoptosis, monocytes are subsequently recruited to the site [167]. Once at the SCI injury site, monocytes can also differentiate into macrophages in response to cytokines and chemokines present in the lesion environment and start to remove dying neutrophils through a process called efferocytosis [322,509]. *In vitro* work has shown a dependence of macrophage phagocytosis of apoptotic neutrophils on the interaction between the scavenger receptor CD36 with the vitronectin receptor and thrombospondin [552].

- Glial scar

During the acute phase of SCI, signalling from activated microglia, macrophages and astrocytes causes the secretion of ECM proteins that are inhibitory to axonal growth, such as CSPGs like NG2 proteoglycan, and tenascin, which condense with astrocytes to form the glial scar [114]. The glial scar potently restricts axon regeneration and anatomical plasticity by neurite outgrowth inhibition [553,554]. Furthermore, other studies revealed that CSPG, a potential inhibitor of axon growth, is substantially more abundant in M1 compared to M2, suggesting that M1 may also impede the neural regeneration after SCI [555,556]. The formation of the glial scar by reactive astrocytes is a key factor in the potential long-term recovery of functionality [98]. The infiltration of macrophages to glial scars contributes to axonal dieback

and soluble factors from M1 macrophages are able to induce a reactive astrocyte gene expression pattern, while M2 macrophages factors inhibit expression of these genes [98]. In addition, astrocytes previously stimulated by M2 macrophages can decrease macrophage proliferation and activity, and decrease TNF-α production in M1 macrophages, pointing an important role of the astrocyte–macrophage axis in SCI [98].

- Neuronal death, axonal dieback, demyelination and sensory anomalies

In SCI, pathophysiological processes such as neuronal cell death, axonal dieback and demyelination, are linked to macrophages. Neuronal loss can be directly mediated by M1 *in vitro* [509,557], and these macrophages can also cause axon dieback (retraction from a spinal lesion) [98,166,558]. Depletion of M1s from the injured spinal cord tissue could preclude the neural retraction and loss induced by repulsive guidance molecule A (RGMA) [559], which is a potent inhibitor of axon regeneration in the adult CNS [560]. As we have mentioned, macrophages also contributes to axonal diebacks when they infiltrate glial scars [98], and a study utilizing a model of glial scar revealed that macrophages are associated with unhealth axons and directly lead to long-distance retraction of axons [559,561].

Activated and resting macrophages and microglia secrete molecules such as glutamate, NOS, IL-1β, and TNF-α which all contribute to death of oligodendrocyte cells [562–564]. Oligodendrocytes are injured by macrophages activity at the lesion epicenter and continue to undergo apoptosis in the spinal parenchyma for many weeks after SCI [565,566]. Consequently, the results of the loss of oligodendrocytes are the demyelination of many spared axons and the loss of conduction of action potential by ascending and descending axons [66]. In spinal lesions during secondary injury, the activities of microglia and macrophages were significantly higher within regions of immunological demyelination [567]. Immunological demyelination creates a unique environment in which astrocytes do not form a glial scar. During the process of demyelination, axons are directly exposed to damaging effects such as inflammatory cytokines and free radicals, leading to neuronal loss, and thus to conduction delays and block [568,569].

It was also revealed that M1 macrophages express higher levels of leukotriene B4 (LTB4) than M2 [570]. Leukotrienes are not only potent mediators of inflammation and secondary injury within the injured spinal cord [571], but also contribute to pathological sensory abnormalities [572,573].

- Regeneration and recovery

In SCI, M2 macrophages, serve as anti-inflammatory cells that play a critical role in reducing pro-inflammatory environments induced by resident astrocytes, microglia and M1 macrophages, thus promoting neuroprotection and regeneration of injured spinal cord tissues and foment the renewal of damaged cells from progenitors [98]. M2 macrophages also release neurotrophic factors such as insulin-like growth factor (IGF) that stimulate axonal and neural regeneration after SCI [136]. However, the low numbers of such anti-inflammatory M2 macrophages after SCI prolong the pro-inflammatory process, thereby exerting destructive effects on neural regeneration and neuron viability [509]. Nevertheless, in the late stages of the lesion, M2 macrophages secrete large amounts of pro-fibrotic factors, which helps form scarring. The glial scar is known to block axonal growth, however, on the other hand, it also serve to prevent the spread of the lesion to the peri-spinal region [136,574]. Regarding specific roles of M2 macrophages subsets in SCI, M2a are able to promote remyelination and axon regeneration/dieback reduction, although it has been also speculated about a possible involvement of M2b and M2c macrophages in axon regeneration/dieback reduction and remyelination [98,166].

Notably, it has also been demonstrated that M1 plays an essential role in pathogens' defense as well [136], most notably in Fujiyoshi's [575] work , in which IFN-γ reduced the accumulation of axonal growth inhibitor CSPGs and improved functional recovery after SCI. Yaguchi et al. [576] discovered that administration of IL-12, at the site of injury, increased macrophage activation and facilitated functional recovery. So, it seems that more important than shutting down the M1 response, what is actually fundamental to repair is to have a balance, moderated and resolved pro-inflammatory response in the acute phase of the injury.

1.5 Therapeutic strategies involving monocytes and macrophages for Spinal Cord Injury repair

As previously referred a combination of factors is responsible for the lack of axonal regeneration and minimal functional recovery usually observed after SCI. Given the multifaceted nature of SCI, many conceptually different paths to facilitate recovery have been investigated [12]. In this section we discuss the diverse therapeutic approaches involving monocytes and macrophages to treat SCI.

1.5.1 Pharmacological therapies

Bethea and colleagues [577] proposed the use of IL-10, an anti-inflammatory cytokine capable of inhibiting the inflammatory reactions of monocytes and macrophages in the PNS. They observed that acute administration of IL-10 after SCI reduces TNF-α synthesis in the spinal cord by activated macrophages, and moreover, it leads to neuroprotection, and promotes functional recovery following SCI [577]. Another immunomodulatory strategy is related to IL-4 therapy [578]. A delayed administration of IL-4 48 hours after injury was able to skew macrophages/microglia to a M2 phenotype contrasting with the acute administration that has no immunomodulatory effect [537]. However, in another study conducted by Lima et al. [579] systemic administration of IL-4 was able to reduce the number of macrophages/microglia at the spinal cord tissue but did not promote functional benefits.

Blocking MCSF-MCSFR signaling stops macrophage proliferation [580]. IL-10, IL-4 and liverXreceptor (LXR) agonists block M-CSF-induced macrophage proliferation, but also participate in activation of M2 macrophage phenotype [581,582]. However, blocking M-CSF signaling may also have an adverse effect on neuron protection, because M-CSF promotes neuroprotection in mouse models from nerve injury, stroke, and Alzheimer's disease [583–585].

Higenamine administration increased the expression of IL-4 and IL-10 and promoted M2 macrophage activation [586]. Higenamine treatment also displayed increased myelin sparring and enhanced spinal cord repair process, and promoted locomotor function after SCI. Significantly reduced HMGB1 expression was also observed in Higenamine-treated mice with SCI. Beyond that, Higenamine treatment also promoted HO-1 (Heme Oxigenase-1) production. In conclusion, Higenamine promoted M2 macrophage activation and reduced HMGB1 expression dependent on HO-1 induction and then promoted locomotor function after SCI [586].

In Zhang et al. [587] study, SCI mice showed significantly increased anti-inflammatory and decreased pro-inflammatory macrophage activation in response to Azithromycin treatment. Additionally, Azithromycin treatment led to improved tissue sparing and recovery of gross and coordinated locomotor function. Moreover, Azithromycin treatment altered macrophage phenotype *in vitro* and reduced the neurotoxic potential of pro-inflammatory M1 macrophages [587]. Taken together, these data suggest that Azithromycin intervention can alter SCI macrophage polarization toward a beneficial phenotype that, in turn, may potentially limit secondary injury processes [587].

A study was designed by Ji et al. [588] to investigate the effects of BDNF (neurotrophic factor) [589], with a special focus on their effect on macrophage polarization after SCI. Adult C57 mice underwent T10 spinal cord clip compression injury and received Lentiviral vector injections (lenti-BDNF

(BDNF+EGFP) and lenti-EGFP (EGFP only)) at the epicenter of the lesion site. More than 80% of the lentivirus infected cells were CD11b-positive macrophages. In addition, the expression of arginase-1 and CD206 (associated with M2 macrophages) significantly increased in the animals that received lenti-BDNF injections compared with those that received lenti-EGFP injections [588]. By the contrary, the expression of CD16/32 and inducible nitric oxide synthase (M1 phenotype marker) was down-regulated. The production of interleukin 1β and TNF-α was significantly reduced while the levels of IL-10 and IL-13 were elevated in subjects that received lenti-BDNF vector injections. Moreover, at functional recovery level, gradual recovery was observed in the subacute phase in lenti-BDNF group, and little improvement was observed in lenti-EGFP group. At the axonal level, significant retraction of the CST axons was observed in lenti-EGFP injected animals relative to lenti-BDNF group. Additionally, compared to lenti-BDNF group, markedly demyelination was observed in the lenti-EGFP group [588]. Concluding, these authors [588] found that BDNF could promote the shift of M1 to M2 phenotype and ameliorate the inflammatory microenvironment. Moreover, the roles of BDNF in immunity modulation may enhance neuroprotective effects and partially contribute to the locomotor functional recovery after SCI [588].

Zhang and colleagues [590], performed a study in which, wild-type (WT) or aldose reductase (AR)-knockout (KO) mice were subjected to SCI by a spinal crush injury model, and found that the expression of AR is upregulated in microglia/macrophages after SCI in WT mice. In AR KO mice, SCI led to smaller injury lesion areas compared to WT, and AR deficiency-induced microglia/macrophages induced the M2 rather than the M1 response and promoted locomotion recovery after SCI in mice [590]. In *in vitro* experiments, when N9 cells (microglia cell line) were treated with LPS (to polarize to M1 phenotype) and with AR inhibitor (ARI) fidarestat (LPS+ARI), ARG1 expression increased. These results suggested that AR works as a switch which can regulate microglia by polarizing cells to either the M1 or the M2 phenotype under M1 stimulation, and the authors also proposed that inhibiting AR may be a promising therapeutic method for SCI [590].

1.5.2 Activation and transplantation of macrophages

Activation of intrinsic macrophages at the spinal contusion site with micro-injections of a proinflammatory agent had detrimental effects on hindlimb functional recovery and tissue survival [591]. However, depletion of macrophages has also led to significantly better hindlimb usage during overground locomotion, more extensive white matter sparing and decreased tissue cavitation [522].

Some researchers have proposed that M2 macrophages could be effective candidates for cell transplantation therapy following SCI [136]. Kobashi et al. [592] used GM-CSF and IL-4 induced as M1

and M2 microglia and transplanted into the spinal cord of injured mice, and the results showed that the M2 group recovered more motor function than M1, and recovery of retrograde axonal transport from the neuromuscular junction to upstream of the injured spinal cord only in M2 group [592]. Han et al. [593] demonstrated that the transplantation of tauroursodeoxycholic acid (TUDCA)-induced M2 macrophages promoted an anti-neuroinflammatory effect and motor function recovery in SCI.

In a study led by Ma et al. [594], it was observed that transfer of M2 macrophages led to a reduction in spinal cord lesion volume and in an increase in myelination of axons and preservation of neurons. These beneficial effects were accompanied by significant locomotor improvement. The results indicate that as compared to vehicle treatment or M1 macrophage transfer, M2 transfer had beneficial effects for the injured spinal cord, in which the increased number of M2 macrophages induced a shift in the immunological response from Th1 to Th2 dominated through the production of anti-inflammatory cytokines, which in turn induced the polarization of local microglia and/or macrophages to the M2 phenotype, creating a local microenvironment that is conducive to the rescue of residual myelin and neurons and preservation of neuronal function [594].

The co-incubation of monocytes with excised skin (an injured tissue with regenerative capacity) has been shown to generate macrophages with an 'alternatively activated' wound-healing phenotype. This beneficial phenotype not only aids in removal of growth-inhibitory myelin components from the cellular environment and the potential secretion of trophic factors, but also provides benefits through cytokine signaling and activation of the local adaptive immune response [595]. Based on these pre-clinical findings, an open-label phase 1 clinical trial was initiated, using autologous incubated macrophages for treatment of patients with acute complete C5-T11 SCI, [45]. That trial enrolled 8 participants with complete SCI who were treated with autologous macrophages prepared by co-incubating peripheral blood monocytes with harvested autologous skin. The participants were followed for 12 months and during the study period, 3 of 8 subjects (37.5%) exhibited improvement in their AIS grade from A (complete injury) to C (sensory and motor incomplete) [45]. With these results showing a higher recovery rate than that commonly reported in the literature and an adverse events experience that did not suggest significant safety concerns, in 2003, a study was initiated as a phase 2 multicenter randomized controlled trial of autologous incubated macrophage therapy for acute complete SCI. This project studied the hypothesis that treatment with autologous incubated macrophages introduced into the spinal cord within 14 days of SCI would be associated with improved neurological outcomes and reasonable safety [596]. Lammertse et al. [596] reported the efficacy and safety findings of the phase 2 multicenter trial. Of 43 participants (17 control and 26 treatment), AIS A to B or better conversion was experienced by 7 treatment and 10

control participants; AIS A to C conversion was experienced by 2 treatment and 2 control participants. The primary outcome analysis for subjects with at least 6 months follow-up showed a trend favoring the control group that did not achieve statistical significance and the mean number of adverse events reported per participant was not significantly different between the groups. Thus, the analysis failed to show a significant difference in primary outcome between the two groups and the results did not supported treatment of acute complete SCI with autologous incubated macrophage therapy as specified in that protocol [596].

1.5.3 Transplantation of mesenchymal stem cells

Nakajima et al. [514] found that mesenchymal stem cells (MSC) transplantation led to preferential development of M2 macrophages, while preventing the development of M1 macrophages, which was accompanied with a decrease in TNF-α and IL-6, and an increase in IL-4 and IL-13. Consequently, MSC transplantation resulted in reduction in the size of the SCI site, less scar tissue formation and increased myelin sparing, correlating with increased axonal growth and improved locomotor function [514]. MSCs are also able to express or secreting a set of inducers for anti-inflammatory M2 macrophages, specifically, monocyte chemoattractant protein-1 (MCP-1) and the ectodomain of sialic acid-binding Ig-like lectin-9 (ED-Siglec-9) [597]. Peripheral blood mesenchymal stem cells (PB-MSCs) were transplanted into rat SCI contusion models, and it was found that the function of posterior limb locomotion was significantly improved in the PB-MSCs transplantation group, which correlated with a significant increase in the ratio of M2/M1 macrophages and higher levels of the anti-inflammatory cytokines (IL-10 and TGF-β1), as well as decreased levels of the pro-inflammatory cytokines (IL-6 and TNF-α). Furthermore, similar molecular expression patterns and macrophages polarization were found while macrophages co-cultured with PB-MSCs *in vitro* [598].

1.5.4 miRNA-induced macrophage polarization

MiRNAs are short endogenous single-stranded RNA molecules of approximately 22 nucleotides in length that target mRNAs and reduce their expression to regulate gene expression in plants and animals, and they can control more than half of all human genes [136,599,600]. A large number of studies have been conducted over the last decade on the effects of miRNA on macrophage polarization [136], and we will just mention and describe a few of them.

For instance, MiR-155, miR-9, miR-127, and miR26a promote M1 polarization [601]. MiR-155 was the most extensively researched pro-inflammatory miRNA [136] and MiR-155KO suppressed the expression of associated genes in M1 macrophages but not in M2 macrophages, showing that miR-155 is important in driving the M1 phenotype [602]. MiR-155 blockade reduces the inflammatory response of type M1 macrophages and no other miRNA has the same potent pro-inflammatory effect as miR-155 [136,603]. MiR-155 deletion attenuated inflammatory signaling in macrophages, reduced macrophage-mediated neuron toxicity, and increased macrophage-elicited axon growth by ~40% relative to control conditions [604]. Moreover, miR-155 deletion increased spontaneous axon growth from neuron, and adult miR-155 KO DRG neurons extended 44% longer neurites than WT neurons. After dorsal column SCI, miR-155 KO mouse spinal cord has reduced neuroinflammation and increased peripheral conditioning-lesion-enhanced axon regeneration beyond the epicenter. Lastly, in a model of spinal contusion injury, miR-155 deletion improved locomotor function at post-injury times (4, 7, 10 and 14 dpi) [604]. In miR-155KO mice, improved locomotor function was associated with smaller contusion lesions and decreased accumulation of inflammatory macrophages. Collectively, these data indicate that miR-155 is a therapeutic target capable of simultaneously overcoming neuron-intrinsic and neuron-extrinsic barriers to repair following SCI [604].

On the other hand, for instance, miR-124, miR-150, miR-21, and miR-132 promote M2 polarization [601]. Taking miR-124 as example, this miRNA polarizes macrophages from M1 to M2 phenotype, and at the same time, polarization of M2-type macrophages enhanced miR-124 expression, which aided in the formation and maintenance of the M2 phenotype. This miRNA is an essential regulator of microglia/macrophages in the CNS [605,606]. Willemen et al. proposed that intravenous injection of miR-124 could restore the M1:M2 ratio to normal levels following injury and alleviate chronic pain caused by microglia activation [607]. MiR-124 is more than 100 times more abundant in the mouse CNS than in other organs [608], and microarray analysis has revealed that miR-124 is also one of the most strongly expressed miRNA groups in the spinal cord [609]. Studies have shown that MiR-124 plays a crucial role in neural regeneration and may one day be used to treat SCI. MiR-124 can regulate the differentiation of neural stem cells into neurons via the Neat1-Wnt/-catenin signaling axis, which assisting in neural regeneration and promoting the restoration of motor function [136,610]. Furthermore, Song et al. [611] investigated how miR-124 affected the transplantation of bone marrow-derived stem cells (BMSCs) for the treatment of SCI in a rat SCI model and showed that miR-124 promotes the differentiation of BMSCs into neuronal cells for SCI repair. Using miRNA microarray hybridization, a study discovered that miR-124-3p,

(a mature miRNA processed from the 3′ end of miR-124 pre-miRNA, essential for neuron growth and function), was substantially expressed in released neuronal exosomes [612,613]. Furthermore, Jiang et al. found through miRNA array, that miR-124-3p, was the most enriched in neuron-derived exosomes, and suppressed M1 microglia activation, via the MYH9/PI3K/AKT/NF-κB signaling pathway, hence promoting functional recovery after SCI [614].

1.5.5 Secretome

For almost three decades, cell-based therapies have been tested in modern regenerative medicine to either replace or regenerate human cells, tissues, or organs and restore normal function. Nonetheless, secreted paracrine factors are increasingly accepted to exert beneficial biological effects that promote tissue regeneration [615].

Secretome was defined by the factors that are secreted by a cell, tissue, or organism to the extracellular space under a defined time and conditions [616,617]. Beyond soluble factors, such citokines and proteins, the secretome also has the presence of lipids, microRNAs and extracellular vesicles carrying important molecules, such as exosomes and microparticles [615,618–620]. This new concept of cell-free-based therapies focused on the cells' secretome gained momentum with the work of Gnecchi and colleagues [621]. These authors demonstrated the regenerative potential of MSC secretome in a model of heart infarct [621] and inspired secretome application in the most diverse areas of regenerative medicine including the CNS [622].

Martins et al. [623] demonstrated that the application of MSCs secretome to both rat cortical and hippocampal neurons induces an increase in axonal length and that this growth effect is axonal intrinsic with no contribution from the cell body. To further understand which are the molecules required for secretome-induced axonal outgrowth effect, they depleted BDNF from the secretome. Their findings showed that in the absence of BDNF, secretome-induced axonal elongation effect is lost and that axons present a reduced axonal growth rate. Collectively, their results demonstrated that MSCs secretome has the capacity to promote axonal outgrowth in CNS neurons and this effect is mediated by BDNF [623].

Subsequently, MSCs secretome was injected in a compression SCI mice model [624]. Results revealed that when injected intravenously the secretome of adipose-derived MSCs has a beneficial effect on motor recovery of SCI animals compared with a single local injection and respective controls. *In vitro* results also demonstrated that the whole secretome performed better than the fractions (proteic and vesicular fraction) individually [624].

Semita et al. [589] conducted a study in which they evaluated how the mechanism of human neural stem cell (HNSC)-secretome improves neuropathic pain and locomotor function in SCI rat models through antioxidant, anti-inflammatory, anti-matrix degradation, and neurotrophic activities. They showed that HNSC-secretome could improve locomotor recovery and neuropathic pain, decrease F2 Isoprostane (antioxidant role), decrease matrix metalloproteinase-9 (MMP-9) and TNF-α (anti-inflammatory role), as well as modulate TGF-β and BDNF. Moreover, HNSC-secretome maintained the extracellular matrix of SCI by reducing the matrix degradation effect of MMP-9 and increasing the collagen formation effect of TGF-β as a resistor of glial scar formation [589].

Haider et al. [625] investigated the role of the apoptotic peripheral blood mononuclear cells (PBMCs) secretome, termed MNC-secretome, in a rodent SCI model. Rats treated with paracrine factors from irradiated PBMCs had significantly improved neurological function compared to the control group. Histological evaluation of spine sections revealed a smaller spinal cord cavity, reduced axonal damage, and improved vascularity index around the lesion. The MNC-secretome enhanced angiogenesis in aortic ring assays and spinal cord tissue [625]. Moreover, experiments showed that the angiogenic potential of MNC-secretome may be regulated by CXCL-1 upregulation *in vivo.* Systemic application of MNC-secretome also activated the ERK1/2 pathway in the spinal cord. These authors [625] tested whether an immunological mechanism may be involved in neuroprotection. The secretome-treated animals exhibited enhanced recruitment of CD68-positive cells with parallel reduction in the levels of iNOS 3 days after injury. These data indicated that the MNC-secretome increases the presence of cells with beneficial anti-inflammatory effects that accelerate the clearance of immunological disturbances, attenuating the secondary damage after SCI [625].

Since peripheral macrophages (PMs) and microglia are involved in SCI, Zhang et al. [626] hypothesized the PM-derived exosomes (PM-Exos) play an important role in signal transmission with local microglia and can be used therapeutic agents for SCI in a series of *in vivo* and *in vitro* studies. In these studies, they used PM from the peritoneal fluid of Sprague-Dawley rats. For the *in vivo* experiment, three groups of Sprague-Dawley rats subjected to spinal cord contusion injury were injected with 200 μg/ml PM-Exos, 20μg/ml PM-Exos or PBS via the tail vein [626]. They observed significantly motor recovery in both 200 μg/ml or 20μg/ml PM-Exos treatment. In the *in vitro* study, microglial autophagy levels and the expression of anti-inflammatory type microglia were higher in the experimental groups than the control group. In addition, the expression of proteins related to the PI3K/AKT/mTOR autophagic signaling pathway was suppressed in the PM-Exo groups. Therefore, PM-Exos have a beneficial effect in SCI, and activation of microglial autophagy through inhibition of the PI3K/AKT/mTOR signaling pathway,

enhancing the polarization of anti-inflammatory type microglia, that may play a major role in the anti-inflammatory process [626].

Kigerl at al. [509] showed that M1 but not M2 macrophage conditioned media (secretome) was toxic to cortical neurons. Then they evaluated the potential of M1 and M2 macrophages to influence axon growth/sprouting, and to this end M1 or M2 secretome was overlaid onto adult DRG neurons. Although both M1 and M2 secretome promoted axon growth relative to control media, their growth-promoting effects were distinct. Specifically, they showed that neurons stimulated with M1 secretome extended short, highly branched neurites, whereas those stimulated with M2 secretome exhibited a unipolar or bipolar phenotype with their axons projecting over long distances, some >1200 μm or more than two times the distance covered by DRGs stimulated with M1 secretome [509]. CSPG and MAG are potent inhibitors of axon growth [627,628] and when M1 or M2 secretome was combined with chondroitinase ABC (chABC) (enzyme acts by degrading the glycosaminoglycan side chains of CSPGs [629], and can be used *in vivo* and *in vitro* to degrade inhibitory proteoglycan substrates and promote axon sprouting and regeneration [630,631]), axon growth across the CSPGs gradient was increased threefold to fivefold relative to that achieved by M1 or M2 secretome alone [509]. Importantly, M2 secretome was more effective at synergizing with chABC to promote axon growth. A qualitative inspection of the laminin enriched core of the spot assays showed that the overall density of axonal projections was consistently greater when cultures were exposed to M2 secretome, which is consistent with the effects of M2 secretome on cortical neurons and further supports the notion that M2 macrophages promote axon growth without causing concurrent neurotoxicity [509]. Then, they evaluated the relative capacity of M1 and M2 secreted molecules to influence axon growth on an inhibitory myelin substrate. Specifically, they grew DRG neurons on a live cell monolayer engineered to express MAG [628] in the presence of M1 or M2 secretome [509]. In general, very few neurons in either culture extended neurites on the MAG substrate. However, the number of neurites extending from a given cell as well as the overall length of the neurite was consistently enhanced in response to M2 relative to M1 secretome [509].

1.6 References

1. Ludwig PE, Reddy V, Varacallo M. "Neuroanatomy, Central Nervous System (CNS)," in *StatPearls* (Treasure Island (FL): StatPearls Publishing). Available at: http://www.ncbi.nlm.nih.gov/books/NBK442010/ [Accessed February 19, 2024]
2. Thau L, Reddy V, Singh P. "Anatomy, Central Nervous System," in *StatPearls* (Treasure Island (FL): StatPearls Publishing). Available at: http://www.ncbi.nlm.nih.gov/books/NBK542179/ [Accessed February 18, 2024]
3. Catala M, Kubis N. Gross anatomy and development of the peripheral nervous system. *Handb Clin Neurol* (2013) 115:29–41. doi:10.1016/B978-0-444-52902-2.00003-5
4. Bui T, M Das J. "Neuroanatomy, Cerebral Hemisphere," in *StatPearls* (Treasure Island (FL): StatPearls Publishing). Available at: http://www.ncbi.nlm.nih.gov/books/NBK549789/ [Accessed March 29, 2024]
5. Helwany M, Bordoni B. "Neuroanatomy, Cranial Nerve 1 (Olfactory)," in *StatPearls* (Treasure Island (FL): StatPearls Publishing). Available at: http://www.ncbi.nlm.nih.gov/books/NBK556051/ [Accessed February 19, 2024]
6. Smith AM, Czyz CN. "Neuroanatomy, Cranial Nerve 2 (Optic)," in *StatPearls* (Treasure Island (FL): StatPearls Publishing). Available at: http://www.ncbi.nlm.nih.gov/books/NBK507907/ [Accessed February 19, 2024]
7. Purves D, Augustine GJ, Fitzpatrick D, Katz LC, LaMantia A-S, McNamara JO, Williams SM. "The Retina," in *Neuroscience. 2nd edition* (Sinauer Associates). Available at: https://www.ncbi.nlm.nih.gov/books/NBK10885/ [Accessed February 19, 2024]
8. Martinez-Pereira MA, Zancan DM. "Comparative Anatomy of the Peripheral Nerves," in *Nerves and Nerve Injuries* (Elsevier), 55–77. doi:10.1016/B978-0-12-410390-0.00005-6
9. Murtazina A, Adameyko I. The peripheral nervous system. *Development* (2023) 150:dev201164. doi:10.1242/dev.201164
10. Sengul G, Watson C. "Spinal Cord," in *The Mouse Nervous System* (Elsevier), 424–458. doi:10.1016/B978-0-12-369497-3.10013-5
11. Bican O, Minagar A, Pruitt AA. The Spinal Cord. *Neurologic Clinics* (2013) 31:1–18. doi:10.1016/j.ncl.2012.09.009
12. Silva NA, Sousa N, Reis RL, Salgado AJ. From basics to clinical: A comprehensive review on spinal cord injury. *Progress in Neurobiology* (2014) 114:25–57. doi:10.1016/j.pneurobio.2013.11.002

13. Watson C, Kayalioglu G. “Chapter 1 - The Organization of the Spinal Cord,” in *The Spinal Cord*, eds. C. Watson, G. Paxinos, G. Kayalioglu (San Diego: Academic Press), 1–7. doi:10.1016/B978-0-12-374247-6.50005-5
14. Van De Graaff KM. *Human Anatomy 6th*. 6th Edition. Boston, MA: McGraw-Hill (2001). Available at: https://www.biblio.com/book/human-anatomy-6th-van-graaff-kent/d/382143297 [Accessed March 18, 2024]
15. Vander AJ, Sherman J, Luciano DS. *Human Physiology: The Mechanisms of Body Function*. 8Rev Ed edition. McGraw-Hill (2001).
16. Atlas of Image-Guided Spinal Procedures: 9780323401531: Medicine & Health Science Books @ Amazon.com. Available at: https://www.amazon.com/Image-Guided-Spinal-Procedures-Michael-Furman/dp/0323401538 [Accessed March 18, 2024]
17. Manchikanti L, Kaye AD, Falco FJE, Hirsch JA eds. *Essentials of Interventional Techniques in Managing Chronic Pain*. Cham: Springer International Publishing (2018). doi:10.1007/978-3-319-60361-2
18. Purves D, Augustine GJ, Fitzpatrick D, Katz LC, LaMantia A-S, McNamara JO, Williams SM. “The Internal Anatomy of the Spinal Cord,” in *Neuroscience. 2nd edition* (Sinauer Associates). Available at: https://www.ncbi.nlm.nih.gov/books/NBK11008/ [Accessed February 19, 2024]
19. McCorry LK. Physiology of the Autonomic Nervous System. *Am J Pharm Educ* (2007) 71:78.
20. Rexed B. The cytoarchitectonic organization of the spinal cord in the cat. *J Comp Neurol* (1952) 96:414–495. doi:10.1002/cne.900960303
21. Rexed B. A cytoarchitectonic atlas of the spinal cord in the cat. *J Comp Neurol* (1954) 100:297–379. doi:10.1002/cne.901000205
22. Sidman RL. *Atlas of the mouse brain and spinal cord / Richard L. Sidman, Jay B. Angevine, Jr., Elizabeth Taber Pierce.* Cambridge, Mass: Harvard University Press (1971).
23. Paxinos G, Mai JK. *The Human Nervous System*. Elsevier (2004).
24. Vartak A, Goyal D, Kumar H. Role of Axon Guidance Molecules in Ascending and Descending Paths in Spinal Cord Regeneration. *Neuroscience* (2023) 533:36–52. doi:10.1016/j.neuroscience.2023.08.034
25. Lee J, Muzio MR. “Neuroanatomy, Extrapyramidal System,” in *StatPearls* (Treasure Island (FL): StatPearls Publishing). Available at: http://www.ncbi.nlm.nih.gov/books/NBK554542/ [Accessed February 19, 2024]

26. Kang Y, Ding H, Zhou H, Wei Z, Liu L, Pan D, Feng S. Epidemiology of worldwide spinal cord injury: a literature review. *JN* (2017) Volume 6:1–9. doi:10.2147/JN.S143236
27. Krenz NR, Weaver LC. Sprouting of primary afferent fibers after spinal cord transection in the rat. *Neuroscience* (1998) 85:443–458. doi:10.1016/s0306-4522(97)00622-2
28. James SL, Theadom A, Ellenbogen RG, Bannick MS, Montjoy-Venning W, Lucchesi LR, Abbasi N, Abdulkader R, Abraha HN, Adsuar JC, et al. Global, regional, and national burden of traumatic brain injury and spinal cord injury, 1990–2016: a systematic analysis for the Global Burden of Disease Study 2016. *The Lancet Neurology* (2019) 18:56–87. doi:10.1016/S1474-4422(18)30415-0
29. National Spinal Cord Injury Statistical Center. Spinal cord injury facts and figures at a glance. *J Spinal Cord Med* (2013) 36:1–2. doi:10.1179/1079026813Z.000000000136
30. DeVivo M, Chen Y, Mennemeyer S, Deutsch A. Costs of Care Following Spinal Cord Injury. *Topics in Spinal Cord Injury Rehabilitation* (2011) 16:1–9. doi:10.1310/sci1604-1
31. Berkowitz M. *Spinal Cord Injury: An Analysis of Medical and Social Costs*. Demos Medical Publishing (1998).
32. DeVivo MJ. Causes and costs of spinal cord injury in the United States. *Spinal Cord* (1997) 35:809–813. doi:10.1038/sj.sc.3100501
33. Stover SL, Fine PR. The epidemiology and economics of spinal cord injury. *Spinal Cord* (1987) 25:225–228. doi:10.1038/sc.1987.40
34. Kraus JF, Franti CE, Riggins RS, Richards D, Borhani NO. Incidence of traumatic spinal cord lesions. *J Chronic Dis* (1975) 28:471–492. doi:10.1016/0021-9681(75)90057-0
35. Griffin MR, O'Fallon WM, Opitz JL, Kurland LT. Mortality, survival and prevalence: traumatic spinal cord injury in Olmsted County, Minnesota, 1935-1981. *J Chronic Dis* (1985) 38:643–653. doi:10.1016/0021-9681(85)90018-9
36. Hamid R, Averbeck MA, Chiang H, Garcia A, Al Mousa RT, Oh S-J, Patel A, Plata M, Del Popolo G. Epidemiology and pathophysiology of neurogenic bladder after spinal cord injury. *World J Urol* (2018) 36:1517–1527. doi:10.1007/s00345-018-2301-z
37. Center NSCIS. Spinal cord injury: facts and figures at a glance. 2016. https://www.nscisc.uab.edu/Public/Facts%202016.pdf. [Accessed March 21, 2024]
38. Meyers AR, Branch LG, Cupples LA, Lederman RI, Feltin M, Master RJ. Predictors of medical care utilization by independently living adults with spinal cord injuries. *Arch Phys Med Rehabil* (1989) 70:471–476. doi:10.1016/0003-9993(89)90010-5

39. Stover SL, DeLisa JA, Whiteneck GG. *Spinal Cord Injury: Clinical Outcomes from the Model Systems*. Aspen Publications (1995).
40. Kaufman JM, Fam B, Jacobs SC, Gabilondo F, Yalla S, Kane JP, Rossier AB. Bladder cancer and squamous metaplasia in spinal cord injury patients. *J Urol* (1977) 118:967–971. doi:10.1016/s0022-5347(17)58266-x
41. El-Masri WS, Fellows G. Bladder cancer after spinal cord injury. *Paraplegia* (1981) 19:265–270. doi:10.1038/sc.1981.52
42. Broecker BH, Klein FA, Hackler RH. Cancer of the bladder in spinal cord injury patients. *J Urol* (1981) 125:196–197. doi:10.1016/s0022-5347(17)54963-0
43. Hackler RH. A 25-year prospective mortality study in the spinal cord injured patient: comparison with the long-term living paraplegic. *J Urol* (1977) 117:486–488. doi:10.1016/s0022-5347(17)58506-7
44. Wang TY, Park C, Zhang H, Rahimpour S, Murphy KR, Goodwin CR, Karikari IO, Than KD, Shaffrey CI, Foster N, et al. Management of Acute Traumatic Spinal Cord Injury: A Review of the Literature. *Front Surg* (2021) 8:698736. doi:10.3389/fsurg.2021.698736
45. Knoller N, Auerbach G, Fulga V, Zelig G, Attias J, Bakimer R, Marder JB, Yoles E, Belkin M, Schwartz M, et al. Clinical experience using incubated autologous macrophages as a treatment for complete spinal cord injury: phase I study results. *J Neurosurg Spine* (2005) 3:173–181. doi:10.3171/spi.2005.3.3.0173
46. Kirshblum SC, Burns SP, Biering-Sorensen F, Donovan W, Graves DE, Jha A, Johansen M, Jones L, Krassioukov A, Mulcahey MJ, et al. International standards for neurological classification of spinal cord injury (revised 2011). *J Spinal Cord Med* (2011) 34:535–546. doi:10.1179/204577211X13207446293695
47. Morse SD. Acute central cervical spinal cord syndrome. *Annals of Emergency Medicine* (1982) 11:436–439. doi:10.1016/S0196-0644(82)80042-5
48. Ishida Y, Tominaga T. Predictors of neurologic recovery in acute central cervical cord injury with only upper extremity impairment. *Spine (Phila Pa 1976)* (2002) 27:1652–1658; discussion 1658. doi:10.1097/00007632-200208010-00011
49. Ditunno JF, Little JW, Tessler A, Burns AS. Spinal shock revisited: a four-phase model. *Spinal Cord* (2004) 42:383–395. doi:10.1038/sj.sc.3101603
50. Nanković V, Snur I, Nanković S, Sokolović-Matejcić B, Kvesić D. [Spinal shock. Diagnosis and therapy. Problems and dilemmas]. *Lijec Vjesn* (1995) 117 Suppl 2:30–32.

51. Management of acute spinal cord injuries in an intensive care unit or other monitored setting. *Neurosurgery* (2002) 50:S51-57. doi:10.1097/00006123-200203001-00011
52. Jia X, Kowalski RG, Sciubba DM, Geocadin RG. Critical care of traumatic spinal cord injury. *J Intensive Care Med* (2013) 28:12–23. doi:10.1177/0885066611403270
53. Hansebout RR, Kachur E. Acute traumatic spinal cord injury - UpToDate. Available at: https://www.uptodate.com/contents/acute-traumatic-spinal-cord-injury [Accessed February 9, 2024]
54. Schmidt KD, Chan CW. Thermoregulation and fever in normal persons and in those with spinal cord injuries. *Mayo Clin Proc* (1992) 67:469–475. doi:10.1016/s0025-6196(12)60394-2
55. Eckert MJ, Martin MJ. Trauma. *Surgical Clinics of North America* (2017) 97:1031–1045. doi:10.1016/j.suc.2017.06.008
56. Stevens RD, Bhardwaj A, Kirsch JR, Mirski MA. Critical care and perioperative management in traumatic spinal cord injury. *J Neurosurg Anesthesiol* (2003) 15:215–229. doi:10.1097/00008506-200307000-00009
57. DeVivo MJ, Kartus PL, Stover SL, Rutt RD, Fine PR. Cause of death for patients with spinal cord injuries. *Arch Intern Med* (1989) 149:1761–1766.
58. Wuermser L-A, Ho CH, Chiodo AE, Priebe MM, Kirshblum SC, Scelza WM. Spinal cord injury medicine. 2. Acute care management of traumatic and nontraumatic injury. *Arch Phys Med Rehabil* (2007) 88:S55-61. doi:10.1016/j.apmr.2006.12.002
59. Ball PA. Critical care of spinal cord injury. *Spine (Phila Pa 1976)* (2001) 26:S27-30. doi:10.1097/00007632-200112151-00006
60. Dicks MA, Clements ND, Gibbons CR, Verduzco-Gutierrez M, Trbovich M. Atypical presentation of Covid-19 in persons with spinal cord injury. *Spinal Cord Ser Cases* (2020) 6:38. doi:10.1038/s41394-020-0289-2
61. Livingston E, Bucher K, Rekito A. Coronavirus Disease 2019 and Influenza 2019-2020. *JAMA* (2020) 323:1122. doi:10.1001/jama.2020.2633
62. Interim clinical guidance for management of patients with confirmed coronavirus disease (COVID-19). Available at: https://stacks.cdc.gov/view/cdc/89980 [Accessed March 22, 2024]
63. Trbovich M, Li C, Lee S. Does the CDC Definition of Fever Accurately Predict Inflammation and Infection in Persons With SCI? *Top Spinal Cord Inj Rehabil* (2016) 22:260–268. doi:10.1310/sci2016-00049

64. Rodríguez-Cola M, Jiménez-Velasco I, Gutiérrez-Henares F, López-Dolado E, Gambarrutta-Malfatti C, Vargas-Baquero E, Gil-Agudo Á. Clinical features of coronavirus disease 2019 (COVID-19) in a cohort of patients with disability due to spinal cord injury. *Spinal Cord Ser Cases* (2020) 6:39. doi:10.1038/s41394-020-0288-3
65. Schmitt AB, Buss A, Breuer S, Brook GA, Pech K, Martin D, Schoenen J, Noth J, Love S, Schröder JM, et al. Major histocompatibility complex class II expression by activated microglia caudal to lesions of descending tracts in the human spinal cord is not associated with a T cell response. *Acta Neuropathol* (2000) 100:528–536. doi:10.1007/s004010000221
66. Hains BC, Klein JP, Saab CY, Craner MJ, Black JA, Waxman SG. Upregulation of sodium channel Nav1.3 and functional involvement in neuronal hyperexcitability associated with central neuropathic pain after spinal cord injury. *J Neurosci* (2003) 23:8881–8892. doi:10.1523/JNEUROSCI.23-26-08881.2003
67. Hains BC, Waxman SG. Activated microglia contribute to the maintenance of chronic pain after spinal cord injury. *J Neurosci* (2006) 26:4308–4317. doi:10.1523/JNEUROSCI.0003-06.2006
68. Zhao P, Waxman SG, Hains BC. Extracellular signal-regulated kinase-regulated microglia-neuron signaling by prostaglandin E2 contributes to pain after spinal cord injury. *J Neurosci* (2007) 27:2357–2368. doi:10.1523/JNEUROSCI.0138-07.2007
69. Zhao P, Waxman SG, Hains BC. Modulation of Thalamic Nociceptive Processing after Spinal Cord Injury through Remote Activation of Thalamic Microglia by Cysteine–Cysteine Chemokine Ligand 21. *J Neurosci* (2007) 27:8893–8902. doi:10.1523/JNEUROSCI.2209-07.2007
70. Hulsebosch CE. Gliopathy Ensures Persistent Inflammation and Chronic Pain after Spinal Cord Injury. *Exp Neurol* (2008) 214:6–9. doi:10.1016/j.expneurol.2008.07.016
71. Gwak YS, Hassler SE, Hulsebosch CE. Reactive oxygen species contribute to neuropathic pain and locomotor dysfunction via activation of CamKII in remote segments following spinal cord contusion injury in rats. *Pain* (2013) 154:1699–1708. doi:10.1016/j.pain.2013.05.018
72. Wu J, Renn CL, Faden AI, Dorsey SG. TrkB.T1 contributes to neuropathic pain after spinal cord injury through regulation of cell cycle pathways. *J Neurosci* (2013) 33:12447–12463. doi:10.1523/JNEUROSCI.0846-13.2013
73. Wu J, Raver C, Piao C, Keller A, Faden AI. Cell cycle activation contributes to increased neuronal activity in the posterior thalamic nucleus and associated chronic hyperesthesia after rat spinal cord contusion. *Neurotherapeutics* (2013) 10:520–538. doi:10.1007/s13311-013-0198-1

74. Felix M-S, Popa N, Djelloul M, Boucraut J, Gauthier P, Bauer S, Matarazzo VA. Alteration of Forebrain Neurogenesis after Cervical Spinal Cord Injury in the Adult Rat. *Front Neurosci* (2012) 6:45. doi:10.3389/fnins.2012.00045
75. Faden AI, Wu J, Stoica BA, Loane DJ. Progressive inflammation-mediated neurodegeneration after traumatic brain or spinal cord injury. *British J Pharmacology* (2016) 173:681–691. doi:10.1111/bph.13179
76. Wu J, Zhao Z, Sabirzhanov B, Stoica BA, Kumar A, Luo T, Skovira J, Faden AI. Spinal cord injury causes brain inflammation associated with cognitive and affective changes: role of cell cycle pathways. *J Neurosci* (2014) 34:10989–11006. doi:10.1523/JNEUROSCI.5110-13.2014
77. Wu J, Stoica BA, Luo T, Sabirzhanov B, Zhao Z, Guanciale K, Nayar SK, Foss CA, Pomper MG, Faden AI. Isolated spinal cord contusion in rats induces chronic brain neuroinflammation, neurodegeneration, and cognitive impairment. *Cell Cycle* (2014) 13:2446–2458. doi:10.4161/cc.29420
78. Simons RK, Hoyt DB, Winchell RJ, Holbrook T, Eastman AB. A risk analysis of stress ulceration after trauma. *J Trauma* (1995) 39:289–293; discussion 293-294. doi:10.1097/00005373-199508000-00017
79. Karlsson A-K. Autonomic dysfunction in spinal cord injury: clinical presentation of symptoms and signs. *Prog Brain Res* (2006) 152:1–8. doi:10.1016/S0079-6123(05)52034-X
80. Bracken MB, Holford TR. Neurological and functional status 1 year after acute spinal cord injury: estimates of functional recovery in National Acute Spinal Cord Injury Study II from results modeled in National Acute Spinal Cord Injury Study III. *J Neurosurg* (2002) 96:259–266. doi:10.3171/spi.2002.96.3.0259
81. Fehlings MG, Perrin RG. The role and timing of early decompression for cervical spinal cord injury: update with a review of recent clinical evidence. *Injury* (2005) 36 Suppl 2:B13-26. doi:10.1016/j.injury.2005.06.011
82. Eli I, Lerner DP, Ghogawala Z. Acute Traumatic Spinal Cord Injury. *Neurologic Clinics* (2021) 39:471–488. doi:10.1016/j.ncl.2021.02.004
83. Hall ED, Braughler JM. Acute effects of intravenous glucocorticoid pretreatment on the in vitro peroxidation of cat spinal cord tissue. *Exp Neurol* (1981) 73:321–324. doi:10.1016/0014-4886(81)90067-4

84. Hall ED, Braughler JM. Effects of intravenous methylprednisolone on spinal cord lipid peroxidation and Na+ + K+)-ATPase activity. Dose-response analysis during 1st hour after contusion injury in the cat. *J Neurosurg* (1982) 57:247–253. doi:10.3171/jns.1982.57.2.0247
85. Tator CH. Biology of neurological recovery and functional restoration after spinal cord injury. *Neurosurgery* (1998) 42:696–707; discussion 707-708. doi:10.1097/00006123-199804000-00007
86. Hawryluk GWJ, Rowland J, Kwon BK, Fehlings MG. Protection and repair of the injured spinal cord: a review of completed, ongoing, and planned clinical trials for acute spinal cord injury. *Neurosurg Focus* (2008) 25:E14. doi:10.3171/FOC.2008.25.11.E14
87. Cramer SC, Lastra L, Lacourse MG, Cohen MJ. Brain motor system function after chronic, complete spinal cord injury. *Brain* (2005) 128:2941–2950. doi:10.1093/brain/awh648
88. Lawrence DG, Kuypers HG. The functional organization of the motor system in the monkey. II. The effects of lesions of the descending brain-stem pathways. *Brain* (1968) 91:15–36. doi:10.1093/brain/91.1.15
89. Jain N, Catania KC, Kaas JH. Deactivation and reactivation of somatosensory cortex after dorsal spinal cord injury. *Nature* (1997) 386:495–498. doi:10.1038/386495a0
90. Kaas JH, Qi H-X, Burish MJ, Gharbawie OA, Onifer SM, Massey JM. Cortical and subcortical plasticity in the brains of humans, primates, and rats after damage to sensory afferents in the dorsal columns of the spinal cord. *Exp Neurol* (2008) 209:407–416. doi:10.1016/j.expneurol.2007.06.014
91. Wernig A, Müller S, Nanassy A, Cagol E. Laufband therapy based on “rules of spinal locomotion” is effective in spinal cord injured persons. *Eur J Neurosci* (1995) 7:823–829. doi:10.1111/j.1460-9568.1995.tb00686.x
92. Christensen MD, Hulsebosch CE. Chronic central pain after spinal cord injury. *J Neurotrauma* (1997) 14:517–537. doi:10.1089/neu.1997.14.517
93. Rabchevsky AG, Kitzman PH. Latest approaches for the treatment of spasticity and autonomic dysreflexia in chronic spinal cord injury. *Neurotherapeutics* (2011) 8:274–282. doi:10.1007/s13311-011-0025-5
94. Ray SK, Dixon CE, Banik NL. Molecular mechanisms in the pathogenesis of traumatic brain injury. *Histol Histopathol* (2002) 17:1137–1152. doi:10.14670/HH-17.1137
95. Rossignol S, Schwab M, Schwartz M, Fehlings MG. Spinal cord injury: time to move? *J Neurosci* (2007) 27:11782–11792. doi:10.1523/JNEUROSCI.3444-07.2007

96. DeVivo MJ, Go BK, Jackson AB. Overview of the national spinal cord injury statistical center database. *J Spinal Cord Med* (2002) 25:335–338. doi:10.1080/10790268.2002.11753637
97. Sekhon LHS, Fehlings MG. Epidemiology, Demographics, and Pathophysiology of Acute Spinal Cord Injury: *Spine* (2001) 26:S2–S12. doi:10.1097/00007632-200112151-00002
98. Kong X, Gao J. Macrophage polarization: a key event in the secondary phase of acute spinal cord injury. *J Cellular Molecular Medi* (2017) 21:941–954. doi:10.1111/jcmm.13034
99. Bareyre FM, Schwab ME. Inflammation, degeneration and regeneration in the injured spinal cord: insights from DNA microarrays. *Trends Neurosci* (2003) 26:555–563. doi:10.1016/j.tins.2003.08.004
100. Tator CH. Review of experimental spinal cord injury with emphasis on the local and systemic circulatory effects. *Neurochirurgie* (1991) 37:291–302.
101. Tator CH, Fehlings MG. Review of the secondary injury theory of acute spinal cord trauma with emphasis on vascular mechanisms. *J Neurosurg* (1991) 75:15–26. doi:10.3171/jns.1991.75.1.0015
102. Tator CH, Koyanagi I. Vascular mechanisms in the pathophysiology of human spinal cord injury. *J Neurosurg* (1997) 86:483–492. doi:10.3171/jns.1997.86.3.0483
103. Casha S, Yu WR, Fehlings MG. Oligodendroglial apoptosis occurs along degenerating axons and is associated with FAS and p75 expression following spinal cord injury in the rat. *Neuroscience* (2001) 103:203–218. doi:10.1016/s0306-4522(00)00538-8
104. de la Torre JC. Spinal cord injury. Review of basic and applied research. *Spine (Phila Pa 1976)* (1981) 6:315–335.
105. Lou J, Lenke LG, Ludwig FJ, O'Brien MF. Apoptosis as a mechanism of neuronal cell death following acute experimental spinal cord injury. *Spinal Cord* (1998) 36:683–690. doi:10.1038/sj.sc.3100632
106. Osterholm JL, Mathews GJ. Altered norepinephrine metabolism, following experimental spinal cord injury. 2. Protection against traumatic spinal cord hemorrhagic necrosis by norepinephrine synthesis blockade with alpha methyl tyrosine. *J Neurosurg* (1972) 36:395–401. doi:10.3171/jns.1972.36.4.0395
107. Agrawal SK, Fehlings MG. Role of NMDA and non-NMDA ionotropic glutamate receptors in traumatic spinal cord axonal injury. *J Neurosci* (1997) 17:1055–1063. doi:10.1523/JNEUROSCI.17-03-01055.1997

108. Faden AI, Simon RP. A potential role for excitotoxins in the pathophysiology of spinal cord injury. *Ann Neurol* (1988) 23:623–626. doi:10.1002/ana.410230618

109. Anderson DK, Means ED, Waters TR, Spears CJ. Spinal cord energy metabolism following compression trauma to the feline spinal cord. *J Neurosurg* (1980) 53:375–380. doi:10.3171/jns.1980.53.3.0375

110. Agrawal SK, Fehlings MG. Mechanisms of secondary injury to spinal cord axons in vitro: role of Na+, Na(+)-K(+)-ATPase, the Na(+)-H+ exchanger, and the Na(+)-Ca2+ exchanger. *J Neurosci* (1996) 16:545–552. doi:10.1523/JNEUROSCI.16-02-00545.1996

111. Young W, Koreh I. Potassium and calcium changes in injured spinal cords. *Brain Res* (1986) 365:42–53. doi:10.1016/0006-8993(86)90720-1

112. Choi WS, Lee EH, Chung CW, Jung YK, Jin BK, Kim SU, Oh TH, Saido TC, Oh YJ. Cleavage of Bax is mediated by caspase-dependent or -independent calpain activation in dopaminergic neuronal cells: protective role of Bcl-2. *J Neurochem* (2001) 77:1531–1541. doi:10.1046/j.1471-4159.2001.00368.x

113. Eaton MJ. Cell and molecular approaches to the attenuation of pain after spinal cord injury. *J Neurotrauma* (2006) 23:549–559. doi:10.1089/neu.2006.23.549

114. Ahuja CS, Wilson JR, Nori S, Kotter MRN, Druschel C, Curt A, Fehlings MG. Traumatic spinal cord injury. *Nat Rev Dis Primers* (2017) 3:17018. doi:10.1038/nrdp.2017.18

115. Demopoulos HB, Flamm ES, Pietronigro DD, Seligman ML. The free radical pathology and the microcirculation in the major central nervous system disorders. *Acta Physiol Scand Suppl* (1980) 492:91–119.

116. Hall ED, Yonkers PA, Horan KL, Braughler JM. Correlation between attenuation of posttraumatic spinal cord ischemia and preservation of tissue vitamin E by the 21-aminosteroid U74006F: evidence for an in vivo antioxidant mechanism. *J Neurotrauma* (1989) 6:169–176. doi:10.1089/neu.1989.6.169

117. Hung TK, Albin MS, Brown TD, Bunegin L, Albin R, Jannetta PJ. Biomechanical responses to open experimental spinal cord injury. *Surg Neurol* (1975) 4:271–276.

118. Oyinbo C. Secondary injury mechanisms in traumatic spinal cord injury: a nugget of this multiply cascade. *Acta Neurobiol Exp* (2011) 71:281–299. doi:10.55782/ane-2011-1848

119. Norenberg MD, Smith J, Marcillo A. The pathology of human spinal cord injury: defining the problems. *J Neurotrauma* (2004) 21:429–440. doi:10.1089/089771504323004575

120. Liverman CT, Altevogt B, Joy JE, Johnson R. *Spinal Cord Injury: Progress, Promise, and Priorities*. (2005). doi:10.17226/11253

121. Allan SM, Rothwell NJ. Inflammation in central nervous system injury. *Philos Trans R Soc Lond B Biol Sci* (2003) 358:1669–1677. doi:10.1098/rstb.2003.1358

122. Herrmann JE, Imura T, Song B, Qi J, Ao Y, Nguyen TK, Korsak RA, Takeda K, Akira S, Sofroniew MV. STAT3 is a critical regulator of astrogliosis and scar formation after spinal cord injury. *J Neurosci* (2008) 28:7231–7243. doi:10.1523/JNEUROSCI.1709-08.2008

123. Buss A, Pech K, Kakulas BA, Martin D, Schoenen J, Noth J, Brook GA. NG2 and phosphacan are present in the astroglial scar after human traumatic spinal cord injury. *BMC Neurol* (2009) 9:32. doi:10.1186/1471-2377-9-32

124. Alizadeh A, Dyck SM, Karimi-Abdolrezaee S. Traumatic Spinal Cord Injury: An Overview of Pathophysiology, Models and Acute Injury Mechanisms. *Front Neurol* (2019) 10:282. doi:10.3389/fneur.2019.00282

125. LaPlaca MC, Simon CM, Prado GR, Cullen DK. CNS injury biomechanics and experimental models. *Prog Brain Res* (2007) 161:13–26. doi:10.1016/S0079-6123(06)61002-9

126. Choo AM, Liu J, Lam CK, Dvorak M, Tetzlaff W, Oxland TR. Contusion, dislocation, and distraction: primary hemorrhage and membrane permeability in distinct mechanisms of spinal cord injury. *J Neurosurg Spine* (2007) 6:255–266. doi:10.3171/spi.2007.6.3.255

127. Liu M, Wu W, Li H, Li S, Huang L, Yang Y, Sun Q, Wang C, Yu Z, Hang C. Necroptosis, a novel type of programmed cell death, contributes to early neural cells damage after spinal cord injury in adult mice. *J Spinal Cord Med* (2015) 38:745–753. doi:10.1179/2045772314Y.0000000224

128. Wang Y, Wang H, Tao Y, Zhang S, Wang J, Feng X. Necroptosis inhibitor necrostatin-1 promotes cell protection and physiological function in traumatic spinal cord injury. *Neuroscience* (2014) 266:91–101. doi:10.1016/j.neuroscience.2014.02.007

129. Li S, Mealing GA, Morley P, Stys PK. Novel injury mechanism in anoxia and trauma of spinal cord white matter: glutamate release via reverse Na+-dependent glutamate transport. *J Neurosci* (1999) 19:RC16. doi:10.1523/JNEUROSCI.19-14-j0002.1999

130. Li S, Stys PK. Mechanisms of ionotropic glutamate receptor-mediated excitotoxicity in isolated spinal cord white matter. *J Neurosci* (2000) 20:1190–1198. doi:10.1523/JNEUROSCI.20-03-01190.2000

131. Schanne FA, Kane AB, Young EE, Farber JL. Calcium dependence of toxic cell death: a final common pathway. *Science* (1979) 206:700–702. doi:10.1126/science.386513

132. Kwon BK, Tetzlaff W, Grauer JN, Beiner J, Vaccaro AR. Pathophysiology and pharmacologic treatment of acute spinal cord injury. *Spine J* (2004) 4:451–464. doi:10.1016/j.spinee.2003.07.007

133. Dizdaroglu M, Jaruga P, Birincioglu M, Rodriguez H. Free radical-induced damage to DNA: mechanisms and measurement. *Free Radic Biol Med* (2002) 32:1102–1115. doi:10.1016/s0891-5849(02)00826-2

134. Hausmann ON. Post-traumatic inflammation following spinal cord injury. *Spinal Cord* (2003) 41:369–378. doi:10.1038/sj.sc.3101483

135. Hall ED. Antioxidant Therapies for Acute Spinal Cord Injury. *Neurotherapeutics* (2011) 8:152–167. doi:10.1007/s13311-011-0026-4

136. Wang J, Tian F, Cao L, Du R, Tong J, Ding X, Yuan Y, Wang C. Macrophage polarization in spinal cord injury repair and the possible role of microRNAs: A review. *Heliyon* (2023) 9:e22914. doi:10.1016/j.heliyon.2023.e22914

137. Rhodes J, Zipfel C, Jones JDG, Ngou BPM. Concerted actions of PRR- and NLR-mediated immunity. *Essays Biochem* (2022) 66:501–511. doi:10.1042/EBC20220067

138. Cserr HF, Knopf PM. Cervical lymphatics, the blood-brain barrier and the immunoreactivity of the brain: a new view. *Immunol Today* (1992) 13:507–512. doi:10.1016/0167-5699(92)90027-5

139. Harris MG, Hulseberg P, Ling C, Karman J, Clarkson BD, Harding JS, Zhang M, Sandor A, Christensen K, Nagy A, et al. Immune privilege of the CNS is not the consequence of limited antigen sampling. *Sci Rep* (2014) 4:4422. doi:10.1038/srep04422

140. Nguyen MD, Julien J-P, Rivest S. Innate immunity: the missing link in neuroprotection and neurodegeneration? *Nat Rev Neurosci* (2002) 3:216–227. doi:10.1038/nrn752

141. Prins RM, Liau LM. Immunology and immunotherapy in neurosurgical disease. *Neurosurgery* (2003) 53:144–152; discussion 152-153. doi:10.1227/01.neu.0000068865.34216.3a

142. Stoll G, Jander S, Schroeter M. Detrimental and beneficial effects of injury-induced inflammation and cytokine expression in the nervous system. *Adv Exp Med Biol* (2002) 513:87–113. doi:10.1007/978-1-4615-0123-7_3

143. Schnell L, Fearn S, Klassen H, Schwab ME, Perry VH. Acute inflammatory responses to mechanical lesions in the CNS: differences between brain and spinal cord. *Eur J Neurosci* (1999) 11:3648–3658. doi:10.1046/j.1460-9568.1999.00792.x

144. Schnell L, Fearn S, Schwab ME, Perry VH, Anthony DC. Cytokine-induced acute inflammation in the brain and spinal cord. *J Neuropathol Exp Neurol* (1999) 58:245–254. doi:10.1097/00005072-199903000-00004

145. Campbell SJ, Wilcockson DC, Butchart AG, Perry VH, Anthony DC. Altered chemokine expression in the spinal cord and brain contributes to differential interleukin-1beta-induced neutrophil recruitment. *J Neurochem* (2002) 83:432–441. doi:10.1046/j.1471-4159.2002.01166.x

146. McTigue DM, Popovich PG, Jakeman LB, Stokes BT. Strategies for spinal cord injury repair. *Prog Brain Res* (2000) 128:3–8. doi:10.1016/S0079-6123(00)28002-3

147. Brennan FH, Li Y, Wang C, Ma A, Guo Q, Li Y, Pukos N, Campbell WA, Witcher KG, Guan Z, et al. Microglia coordinate cellular interactions during spinal cord repair in mice. *Nat Commun* (2022) 13:4096. doi:10.1038/s41467-022-31797-0

148. Guadagno J, Xu X, Karajgikar M, Brown A, Cregan SP. Microglia-derived TNFα induces apoptosis in neural precursor cells via transcriptional activation of the Bcl-2 family member Puma. *Cell Death Dis* (2013) 4:e538. doi:10.1038/cddis.2013.59

149. Teeling JL, Perry VH. Systemic infection and inflammation in acute CNS injury and chronic neurodegeneration: underlying mechanisms. *Neuroscience* (2009) 158:1062–1073. doi:10.1016/j.neuroscience.2008.07.031

150. Liddelow SA, Guttenplan KA, Clarke LE, Bennett FC, Bohlen CJ, Schirmer L, Bennett ML, Münch AE, Chung W-S, Peterson TC, et al. Neurotoxic reactive astrocytes are induced by activated microglia. *Nature* (2017) 541:481–487. doi:10.1038/nature21029

151. Jones LL, Tuszynski MH. Spinal cord injury elicits expression of keratan sulfate proteoglycans by macrophages, reactive microglia, and oligodendrocyte progenitors. *J Neurosci* (2002) 22:4611–4624. doi:10.1523/JNEUROSCI.22-11-04611.2002

152. Taoka Y, Okajima K, Uchiba M, Murakami K, Kushimoto S, Johno M, Naruo M, Okabe H, Takatsuki K. Role of neutrophils in spinal cord injury in the rat. *Neuroscience* (1997) 79:1177–1182. doi:10.1016/s0306-4522(97)00011-0

153. Hellenbrand DJ, Quinn CM, Piper ZJ, Morehouse CN, Fixel JA, Hanna AS. Inflammation after spinal cord injury: a review of the critical timeline of signaling cues and cellular infiltration. *Journal of Neuroinflammation* (2021) 18:284. doi:10.1186/s12974-021-02337-2

154. Kigerl KA, McGaughy VM, Popovich PG. Comparative analysis of lesion development and intraspinal inflammation in four strains of mice following spinal contusion injury. *J of Comparative Neurology* (2006) 494:578–594. doi:10.1002/cne.20827

155. Blight AR. Delayed demyelination and macrophage invasion: a candidate for secondary cell damage in spinal cord injury. *Cent Nerv Syst Trauma* (1985) 2:299–315. doi:10.1089/cns.1985.2.299

156. Boyles JK, Zoellner CD, Anderson LJ, Kosik LM, Pitas RE, Weisgraber KH, Hui DY, Mahley RW, Gebicke-Haerter PJ, Ignatius MJ. A role for apolipoprotein E, apolipoprotein A-I, and low density lipoprotein receptors in cholesterol transport during regeneration and remyelination of the rat sciatic nerve. *J Clin Invest* (1989) 83:1015–1031. doi:10.1172/JCI113943

157. Dorschner RA, Lee J, Cohen O, Costantini T, Baird A, Eliceiri BP. ECRG4 regulates neutrophil recruitment and CD44 expression during the inflammatory response to injury. *Sci Adv* (2020) 6:eaay0518. doi:10.1126/sciadv.aay0518

158. Stirling DP, Liu S, Kubes P, Yong VW. Depletion of Ly6G/Gr-1 leukocytes after spinal cord injury in mice alters wound healing and worsens neurological outcome. *J Neurosci* (2009) 29:753–764. doi:10.1523/JNEUROSCI.4918-08.2009

159. Ley K, Hoffman HM, Kubes P, Cassatella MA, Zychlinsky A, Hedrick CC, Catz SD. Neutrophils: New insights and open questions. *Sci Immunol* (2018) 3:eaat4579. doi:10.1126/sciimmunol.aat4579

160. Zivkovic S, Ayazi M, Hammel G, Ren Y. For Better or for Worse: A Look Into Neutrophils in Traumatic Spinal Cord Injury. *Front Cell Neurosci* (2021) 15:648076. doi:10.3389/fncel.2021.648076

161. Weiss SJ. Tissue destruction by neutrophils. *N Engl J Med* (1989) 320:365–376. doi:10.1056/NEJM198902093200606

162. Noble LJ, Donovan F, Igarashi T, Goussev S, Werb Z. Matrix metalloproteinases limit functional recovery after spinal cord injury by modulation of early vascular events. *J Neurosci* (2002) 22:7526–7535. doi:10.1523/JNEUROSCI.22-17-07526.2002

163. Bethea JR, Castro M, Keane RW, Lee TT, Dietrich WD, Yezierski RP. Traumatic spinal cord injury induces nuclear factor-kappaB activation. *J Neurosci* (1998) 18:3251–3260. doi:10.1523/JNEUROSCI.18-09-03251.1998

164. Dusart I, Schwab ME. Secondary cell death and the inflammatory reaction after dorsal hemisection of the rat spinal cord. *Eur J Neurosci* (1994) 6:712–724. doi:10.1111/j.1460-9568.1994.tb00983.x

165. Kumar H, Choi H, Jo M-J, Joshi HP, Muttigi M, Bonanomi D, Kim SB, Ban E, Kim A, Lee S-H, et al. Neutrophil elastase inhibition effectively rescued angiopoietin-1 decrease and inhibits glial scar after spinal cord injury. *Acta Neuropathol Commun* (2018) 6:73. doi:10.1186/s40478-018-0576-3

166. Gensel JC, Zhang B. Macrophage activation and its role in repair and pathology after spinal cord injury. *Brain Research* (2015) 1619:1–11. doi:10.1016/j.brainres.2014.12.045

167. Milich LM, Ryan CB, Lee JK. The origin, fate, and contribution of macrophages to spinal cord injury pathology. *Acta Neuropathol* (2019) 137:785–797. doi:10.1007/s00401-019-01992-3

168. Blomster LV, Brennan FH, Lao HW, Harle DW, Harvey AR, Ruitenberg MJ. Mobilisation of the splenic monocyte reservoir and peripheral CX3CR1 deficiency adversely affects recovery from spinal cord injury. *Experimental Neurology* (2013) 247:226–240. doi:10.1016/j.expneurol.2013.05.002

169. Beck KD, Nguyen HX, Galvan MD, Salazar DL, Woodruff TM, Anderson AJ. Quantitative analysis of cellular inflammation after traumatic spinal cord injury: evidence for a multiphasic inflammatory response in the acute to chronic environment. *Brain* (2010) 133:433–447. doi:10.1093/brain/awp322

170. Donnelly DJ, Popovich PG. Inflammation and its role in neuroprotection, axonal regeneration and functional recovery after spinal cord injury. *Experimental Neurology* (2008) 209:378–388. doi:10.1016/j.expneurol.2007.06.009

171. Popovich PG, Wei P, Stokes BT. Cellular inflammatory response after spinal cord injury in Sprague-Dawley and Lewis rats. *J Comp Neurol* (1997) 377:443–464. doi:10.1002/(sici)1096-9861(19970120)377:3<443::aid-cne10>3.0.co;2-s

172. Carlson SL, Parrish ME, Springer JE, Doty K, Dossett L. Acute inflammatory response in spinal cord following impact injury. *Exp Neurol* (1998) 151:77–88. doi:10.1006/exnr.1998.6785

173. Trivedi A, Olivas AD, Noble-Haeusslein LJ. Inflammation and spinal cord injury: Infiltrating leukocytes as determinants of injury and repair processes. *Clinical Neuroscience Research* (2006) 6:283–292. doi:10.1016/j.cnr.2006.09.007

174. Hellenbrand DJ, Reichl KA, Travis BJ, Filipp ME, Khalil AS, Pulito DJ, Gavigan AV, Maginot ER, Arnold MT, Adler AG, et al. Sustained interleukin-10 delivery reduces inflammation and improves motor function after spinal cord injury. *J Neuroinflammation* (2019) 16:93. doi:10.1186/s12974-019-1479-3

175. Blight AR. Macrophages and inflammatory damage in spinal cord injury. *J Neurotrauma* (1992) 9 Suppl 1:S83-91.

176. Blight AR. Effects of silica on the outcome from experimental spinal cord injury: implication of macrophages in secondary tissue damage. *Neuroscience* (1994) 60:263–273. doi:10.1016/0306-4522(94)90220-8

177. Popovich PG, Reinhard JF, Flanagan EM, Stokes BT. Elevation of the neurotoxin quinolinic acid occurs following spinal cord trauma. *Brain Res* (1994) 633:348–352. doi:10.1016/0006-8993(94)91560-1

178. Minc-Golomb D, Yadid G, Tsarfaty I, Resau JH, Schwartz JP. In vivo expression of inducible nitric oxide synthase in cerebellar neurons. *J Neurochem* (1996) 66:1504–1509. doi:10.1046/j.1471-4159.1996.66041504.x

179. Popovich PG, Stuckman S, Gienapp IE, Whitacre CC. Alterations in immune cell phenotype and function after experimental spinal cord injury. *J Neurotrauma* (2001) 18:957–966. doi:10.1089/089771501750451866

180. Schnell L, Schneider R, Berman MA, Perry VH, Schwab ME. Lymphocyte recruitment following spinal cord injury in mice is altered by prior viral exposure. *Eur J Neurosci* (1997) 9:1000–1007. doi:10.1111/j.1460-9568.1997.tb01450.x

181. Ankeny DP, Guan Z, Popovich PG. B cells produce pathogenic antibodies and impair recovery after spinal cord injury in mice. *J Clin Invest* (2009) 119:2990–2999. doi:10.1172/JCI39780

182. Sroga JM, Jones TB, Kigerl KA, McGaughy VM, Popovich PG. Rats and mice exhibit distinct inflammatory reactions after spinal cord injury. *J Comp Neurol* (2003) 462:223–240. doi:10.1002/cne.10736

183. Popovich PG. Immunological regulation of neuronal degeneration and regeneration in the injured spinal cord. *Prog Brain Res* (2000) 128:43–58. doi:10.1016/S0079-6123(00)28006-0

184. Jones TB, Hart RP, Popovich PG. Molecular control of physiological and pathological T-cell recruitment after mouse spinal cord injury. *J Neurosci* (2005) 25:6576–6583. doi:10.1523/JNEUROSCI.0305-05.2005

185. Gonzalez R, Glaser J, Liu MT, Lane TE, Keirstead HS. Reducing inflammation decreases secondary degeneration and functional deficit after spinal cord injury. *Exp Neurol* (2003) 184:456–463. doi:10.1016/s0014-4886(03)00257-7

186. Wynn TA. Fibrotic disease and the T(H)1/T(H)2 paradigm. *Nat Rev Immunol* (2004) 4:583–594. doi:10.1038/nri1412

187. Popovich PG, Stokes BT, Whitacre CC. Concept of autoimmunity following spinal cord injury: possible roles for T lymphocytes in the traumatized central nervous system. *J Neurosci Res* (1996) 45:349–363. doi:10.1002/(SICI)1097-4547(19960815)45:4<349::AID-JNR4>3.0.CO;2-9

188. Schwartz M, Kipnis J. Protective autoimmunity: regulation and prospects for vaccination after brain and spinal cord injuries. *Trends Mol Med* (2001) 7:252–258. doi:10.1016/s1471-4914(01)01993-1

189. Kipnis J, Mizrahi T, Hauben E, Shaked I, Shevach E, Schwartz M. Neuroprotective autoimmunity: naturally occurring CD4+CD25+ regulatory T cells suppress the ability to withstand injury to the central nervous system. *Proc Natl Acad Sci U S A* (2002) 99:15620–15625. doi:10.1073/pnas.232565399

190. Town T, Nikolic V, Tan J. The microglial "activation" continuum: from innate to adaptive responses. *J Neuroinflammation* (2005) 2:24. doi:10.1186/1742-2094-2-24

191. David S, Bouchard C, Tsatas O, Giftochristos N. Macrophages can modify the nonpermissive nature of the adult mammalian central nervous system. *Neuron* (1990) 5:463–469. doi:10.1016/0896-6273(90)90085-t

192. Streit WJ. Microglial-neuronal interactions. *J Chem Neuroanat* (1993) 6:261–266. doi:10.1016/0891-0618(93)90047-8

193. Schwartz M, Lazarov-Spiegler O, Rapalino O, Agranov I, Velan G, Hadani M. Potential repair of rat spinal cord injuries using stimulated homologous macrophages. *Neurosurgery* (1999) 44:1041–1045; discussion 1045-1046. doi:10.1097/00006123-199905000-00057

194. Mikami Y, Okano H, Sakaguchi M, Nakamura M, Shimazaki T, Okano HJ, Kawakami Y, Toyama Y, Toda M. Implantation of dendritic cells in injured adult spinal cord results in activation of endogenous neural stem/progenitor cells leading to de novo neurogenesis and functional recovery. *J Neurosci Res* (2004) 76:453–465. doi:10.1002/jnr.20086

195. Hoeffel G, Ginhoux F. Fetal monocytes and the origins of tissue-resident macrophages. *Cellular Immunology* (2018) 330:5–15. doi:10.1016/j.cellimm.2018.01.001

196. Naito M, Takahashi K, Nishikawa S. Development, Differentiation, and Maturation of Macrophages in the Fetal Mouse Liver. *Journal of Leukocyte Biology* (1990) 48:27–37. doi:10.1002/jlb.48.1.27

197. Calvanese V, Mikkola HKA. The genesis of human hematopoietic stem cells. *Blood* (2023) 142:519–532. doi:10.1182/blood.2022017934

198. Wolf AA, Yáñez A, Barman PK, Goodridge HS. The Ontogeny of Monocyte Subsets. *Front Immunol* (2019) 10:1642. doi:10.3389/fimmu.2019.01642

199. Lin Y, Yoder MC, Yoshimoto M. Lymphoid progenitor emergence in the murine embryo and yolk sac precedes stem cell detection. *Stem Cells Dev* (2014) 23:1168–1177. doi:10.1089/scd.2013.0536

200. Mikkola HKA, Gekas C, Orkin SH, Dieterlen-Lievre F. Placenta as a site for hematopoietic stem cell development. *Exp Hematol* (2005) 33:1048–1054. doi:10.1016/j.exphem.2005.06.011

201. Christensen JL, Wright DE, Wagers AJ, Weissman IL. Circulation and chemotaxis of fetal hematopoietic stem cells. *PLoS Biol* (2004) 2:E75. doi:10.1371/journal.pbio.0020075

202. Khan JA, Mendelson A, Kunisaki Y, Birbrair A, Kou Y, Arnal-Estapé A, Pinho S, Ciero P, Nakahara F, Ma'ayan A, et al. Fetal liver hematopoietic stem cell niches associate with portal vessels. *Science* (2016) 351:176–180. doi:10.1126/science.aad0084

203. Akashi K, Traver D, Miyamoto T, Weissman IL. A clonogenic common myeloid progenitor that gives rise to all myeloid lineages. *Nature* (2000) 404:193–197. doi:10.1038/35004599

204. Traver D, Akashi K, Manz M, Merad M, Miyamoto T, Engleman EG, Weissman IL. Development of CD8alpha-positive dendritic cells from a common myeloid progenitor. *Science* (2000) 290:2152–2154. doi:10.1126/science.290.5499.2152

205. Trzebanski S, Jung S. Plasticity of monocyte development and monocyte fates. *Immunology Letters* (2020) 227:66–78. doi:10.1016/j.imlet.2020.07.007

206. Liu Z, Gu Y, Chakarov S, Bleriot C, Kwok I, Chen X, Shin A, Huang W, Dress RJ, Dutertre C-A, et al. Fate Mapping via Ms4a3-Expression History Traces Monocyte-Derived Cells. *Cell* (2019) 178:1509-1525.e19. doi:10.1016/j.cell.2019.08.009

207. Fogg DK, Sibon C, Miled C, Jung S, Aucouturier P, Littman DR, Cumano A, Geissmann F. A clonogenic bone marrow progenitor specific for macrophages and dendritic cells. *Science* (2006) 311:83–87. doi:10.1126/science.1117729

208. Yáñez A, Coetzee SG, Olsson A, Muench DE, Berman BP, Hazelett DJ, Salomonis N, Grimes HL, Goodridge HS. Granulocyte-Monocyte Progenitors and Monocyte-Dendritic Cell Progenitors Independently Produce Functionally Distinct Monocytes. *Immunity* (2017) 47:890-902.e4. doi:10.1016/j.immuni.2017.10.021

209. Hettinger J, Richards DM, Hansson J, Barra MM, Joschko A-C, Krijgsveld J, Feuerer M. Origin of monocytes and macrophages in a committed progenitor. *Nat Immunol* (2013) 14:821–830. doi:10.1038/ni.2638

210. Varol C, Landsman L, Fogg DK, Greenshtein L, Gildor B, Margalit R, Kalchenko V, Geissmann F, Jung S. Monocytes give rise to mucosal, but not splenic, conventional dendritic cells. *J Exp Med* (2007) 204:171–180. doi:10.1084/jem.20061011

211. Giladi A, Paul F, Herzog Y, Lubling Y, Weiner A, Yofe I, Jaitin D, Cabezas-Wallscheid N, Dress R, Ginhoux F, et al. Single-cell characterization of haematopoietic progenitors and their trajectories in homeostasis and perturbed haematopoiesis. *Nat Cell Biol* (2018) 20:836–846. doi:10.1038/s41556-018-0121-4

212. Chong SZ, Evrard M, Devi S, Chen J, Lim JY, See P, Zhang Y, Adrover JM, Lee B, Tan L, et al. CXCR4 identifies transitional bone marrow premonocytes that replenish the mature monocyte pool for peripheral responses. *Journal of Experimental Medicine* (2016) 213:2293–2314. doi:10.1084/jem.20160800

213. Kawamura S, Ohteki T. Monopoiesis in humans and mice. *Int Immunol* (2018) 30:503–509. doi:10.1093/intimm/dxy063

214. Kawamura S, Onai N, Miya F, Sato T, Tsunoda T, Kurabayashi K, Yotsumoto S, Kuroda S, Takenaka K, Akashi K, et al. Identification of a Human Clonogenic Progenitor with Strict Monocyte Differentiation Potential: A Counterpart of Mouse cMoPs. *Immunity* (2017) 46:835-848.e4. doi:10.1016/j.immuni.2017.04.019

215. Jung S, Aliberti J, Graemmel P, Sunshine MJ, Kreutzberg GW, Sher A, Littman DR. Analysis of fractalkine receptor CX(3)CR1 function by targeted deletion and green fluorescent protein reporter gene insertion. *Mol Cell Biol* (2000) 20:4106–4114. doi:10.1128/MCB.20.11.4106-4114.2000

216. Chitu V, Stanley ER. Colony-stimulating factor-1 in immunity and inflammation. *Curr Opin Immunol* (2006) 18:39–48. doi:10.1016/j.coi.2005.11.006

217. Hamilton JA. Colony-stimulating factors in inflammation and autoimmunity. *Nat Rev Immunol* (2008) 8:533–544. doi:10.1038/nri2356

218. Hume DA. Differentiation and heterogeneity in the mononuclear phagocyte system. *Mucosal Immunol* (2008) 1:432–441. doi:10.1038/mi.2008.36

219. Hoeffel G, Chen J, Lavin Y, Low D, Almeida FF, See P, Beaudin AE, Lum J, Low I, Forsberg EC, et al. C-Myb(+) erythro-myeloid progenitor-derived fetal monocytes give rise to adult tissue-resident macrophages. *Immunity* (2015) 42:665–678. doi:10.1016/j.immuni.2015.03.011

220. Akagawa KS. Functional heterogeneity of colony-stimulating factor-induced human monocyte-derived macrophages. *Int J Hematol* (2002) 76:27–34. doi:10.1007/BF02982715

221. Cunnick J, Kaur P, Cho Y, Groffen J, Heisterkamp N. Use of bone marrow-derived macrophages to model murine innate immune responses. *J Immunol Methods* (2006) 311:96–105. doi:10.1016/j.jim.2006.01.017

222. Mulder R, Banete A, Basta S. Spleen-derived macrophages are readily polarized into classically activated (M1) or alternatively activated (M2) states. *Immunobiology* (2014) 219:737–745. doi:10.1016/j.imbio.2014.05.005

223. Stanley ER, Chitu V. CSF-1 receptor signaling in myeloid cells. *Cold Spring Harb Perspect Biol* (2014) 6:a021857. doi:10.1101/cshperspect.a021857

224. Ożańska A, Szymczak D, Rybka J. Pattern of human monocyte subpopulations in health and disease. *Scand J Immunol* (2020) 92:e12883. doi:10.1111/sji.12883

225. Evren E, Ringqvist E, Tripathi KP, Sleiers N, Rives IC, Alisjahbana A, Gao Y, Sarhan D, Halle T, Sorini C, et al. Distinct developmental pathways from blood monocytes generate human lung macrophage diversity. *Immunity* (2021) 54:259-275.e7. doi:10.1016/j.immuni.2020.12.003

226. Serbina NV, Pamer EG. Monocyte emigration from bone marrow during bacterial infection requires signals mediated by chemokine receptor CCR2. *Nat Immunol* (2006) 7:311–317. doi:10.1038/ni1309

227. Shi C, Pamer EG. Monocyte recruitment during infection and inflammation. *Nat Rev Immunol* (2011) 11:762–774. doi:10.1038/nri3070

228. Nourshargh S, Alon R. Leukocyte migration into inflamed tissues. *Immunity* (2014) 41:694–707. doi:10.1016/j.immuni.2014.10.008

229. Yang J, Zhang L, Yu C, Yang X-F, Wang H. Monocyte and macrophage differentiation: circulation inflammatory monocyte as biomarker for inflammatory diseases. *Biomark Res* (2014) 2:1. doi:10.1186/2050-7771-2-1

230. Robinson A, Han CZ, Glass CK, Pollard JW. Monocyte Regulation in Homeostasis and Malignancy. *Trends in Immunology* (2021) 42:104–119. doi:10.1016/j.it.2020.12.001

231. Bain CC, Scott CL, Uronen-Hansson H, Gudjonsson S, Jansson O, Grip O, Guilliams M, Malissen B, Agace WW, Mowat AM. Resident and pro-inflammatory macrophages in the colon represent alternative context-dependent fates of the same Ly6Chi monocyte precursors. *Mucosal Immunol* (2013) 6:498–510. doi:10.1038/mi.2012.89

232. Takada Y, Hisamatsu T, Kamada N, Kitazume MT, Honda H, Oshima Y, Saito R, Takayama T, Kobayashi T, Chinen H, et al. Monocyte chemoattractant protein-1 contributes to gut homeostasis

and intestinal inflammation by composition of IL-10-producing regulatory macrophage subset. *J Immunol* (2010) 184:2671–2676. doi:10.4049/jimmunol.0804012

233. Swirski FK, Nahrendorf M, Etzrodt M, Wildgruber M, Cortez-Retamozo V, Panizzi P, Figueiredo J-L, Kohler RH, Chudnovskiy A, Waterman P, et al. Identification of Splenic Reservoir Monocytes and Their Deployment to Inflammatory Sites. *Science* (2009) 325:612–616. doi:10.1126/science.1175202

234. Nahrendorf M, Swirski FK, Aikawa E, Stangenberg L, Wurdinger T, Figueiredo J-L, Libby P, Weissleder R, Pittet MJ. The healing myocardium sequentially mobilizes two monocyte subsets with divergent and complementary functions. *J Exp Med* (2007) 204:3037–3047. doi:10.1084/jem.20070885

235. Tacke F, Alvarez D, Kaplan TJ, Jakubzick C, Spanbroek R, Llodra J, Garin A, Liu J, Mack M, van Rooijen N, et al. Monocyte subsets differentially employ CCR2, CCR5, and CX3CR1 to accumulate within atherosclerotic plaques. *J Clin Invest* (2007) 117:185–194. doi:10.1172/JCI28549

236. Saederup N, Chan L, Lira SA, Charo IF. Fractalkine deficiency markedly reduces macrophage accumulation and atherosclerotic lesion formation in CCR2-/- mice: evidence for independent chemokine functions in atherogenesis. *Circulation* (2008) 117:1642–1648. doi:10.1161/CIRCULATIONAHA.107.743872

237. Lesnik P, Haskell CA, Charo IF. Decreased atherosclerosis in CX3CR1-/- mice reveals a role for fractalkine in atherogenesis. *J Clin Invest* (2003) 111:333–340. doi:10.1172/JCI15555

238. Swirski FK, Weissleder R, Pittet MJ. Heterogeneous in vivo behavior of monocyte subsets in atherosclerosis. *Arterioscler Thromb Vasc Biol* (2009) 29:1424–1432. doi:10.1161/ATVBAHA.108.180521

239. Martinez FO, Helming L, Gordon S. Alternative activation of macrophages: an immunologic functional perspective. *Annu Rev Immunol* (2009) 27:451–483. doi:10.1146/annurev.immunol.021908.132532

240. Mantovani A, Sica A, Sozzani S, Allavena P, Vecchi A, Locati M. The chemokine system in diverse forms of macrophage activation and polarization. *Trends Immunol* (2004) 25:677–686. doi:10.1016/j.it.2004.09.015

241. Serbina NV, Jia T, Hohl TM, Pamer EG. Monocyte-mediated defense against microbial pathogens. *Annu Rev Immunol* (2008) 26:421–452. doi:10.1146/annurev.immunol.26.021607.090326

242. Evans HG, Gullick NJ, Kelly S, Pitzalis C, Lord GM, Kirkham BW, Taams LS. In vivo activated monocytes from the site of inflammation in humans specifically promote Th17 responses.

Proceedings of the National Academy of Sciences (2009) 106:6232–6237. doi:10.1073/pnas.0808144106

243. Ruder AV, Wetzels SMW, Temmerman L, Biessen EAL, Goossens P. Monocyte heterogeneity in cardiovascular disease. *Cardiovasc Res* (2023) 119:2033–2045. doi:10.1093/cvr/cvad069

244. Ziegler-Heitbrock L, Ancuta P, Crowe S, Dalod M, Grau V, Hart DN, Leenen PJM, Liu Y-J, MacPherson G, Randolph GJ, et al. Nomenclature of monocytes and dendritic cells in blood. *Blood* (2010) 116:e74-80. doi:10.1182/blood-2010-02-258558

245. Cros J, Cagnard N, Woollard K, Patey N, Zhang S-Y, Senechal B, Puel A, Biswas SK, Moshous D, Picard C, et al. Human CD14dim monocytes patrol and sense nucleic acids and viruses via TLR7 and TLR8 receptors. *Immunity* (2010) 33:375–386. doi:10.1016/j.immuni.2010.08.012

246. Ingersoll MA, Spanbroek R, Lottaz C, Gautier EL, Frankenberger M, Hoffmann R, Lang R, Haniffa M, Collin M, Tacke F, et al. Comparison of gene expression profiles between human and mouse monocyte subsets. *Blood* (2010) 115:e10-19. doi:10.1182/blood-2009-07-235028

247. Garré JM, Yang G. Contributions of monocytes to nervous system disorders. *J Mol Med* (2018) 96:873–883. doi:10.1007/s00109-018-1672-3

248. Narasimhan PB, Marcovecchio P, Hamers AAJ, Hedrick CC. Nonclassical Monocytes in Health and Disease. *Annu Rev Immunol* (2019) 37:439–456. doi:10.1146/annurev-immunol-042617-053119

249. Kerkhofs D, van Hagen BT, Milanova IV, Schell KJ, van Essen H, Wijnands E, Goossens P, Blankesteijn WM, Unger T, Prickaerts J, et al. Pharmacological depletion of microglia and perivascular macrophages prevents Vascular Cognitive Impairment in Ang II-induced hypertension. *Theranostics* (2020) 10:9512–9527. doi:10.7150/thno.44394

250. Zawada AM, Rogacev KS, Schirmer SH, Sester M, Böhm M, Fliser D, Heine GH. Monocyte heterogeneity in human cardiovascular disease. *Immunobiology* (2012) 217:1273–1284. doi:10.1016/j.imbio.2012.07.001

251. Yona S, Kim K-W, Wolf Y, Mildner A, Varol D, Breker M, Strauss-Ayali D, Viukov S, Guilliams M, Misharin A, et al. Fate mapping reveals origins and dynamics of monocytes and tissue macrophages under homeostasis. *Immunity* (2013) 38:79–91. doi:10.1016/j.immuni.2012.12.001

252. Patel AA, Zhang Y, Fullerton JN, Boelen L, Rongvaux A, Maini AA, Bigley V, Flavell RA, Gilroy DW, Asquith B, et al. The fate and lifespan of human monocyte subsets in steady state and systemic inflammation. *J Exp Med* (2017) 214:1913–1923. doi:10.1084/jem.20170355

253. Sunderkötter C, Nikolic T, Dillon MJ, Van Rooijen N, Stehling M, Drevets DA, Leenen PJM. Subpopulations of mouse blood monocytes differ in maturation stage and inflammatory response. *J Immunol* (2004) 172:4410–4417. doi:10.4049/jimmunol.172.7.4410

254. Hanna RN, Carlin LM, Hubbeling HG, Nackiewicz D, Green AM, Punt JA, Geissmann F, Hedrick CC. The transcription factor NR4A1 (Nur77) controls bone marrow differentiation and the survival of Ly6C- monocytes. *Nat Immunol* (2011) 12:778–785. doi:10.1038/ni.2063

255. Thomas GD, Hanna RN, Vasudevan NT, Hamers AA, Romanoski CE, McArdale S, Ross K, Blatchley A, Yoakum D, Hamilton BA, et al. Deleting an Nr4a1 super-enhancer subdomain ablates Ly6Clow monocytes while preserving macrophage gene function. *Immunity* (2016) 45:975–987. doi:10.1016/j.immuni.2016.10.011

256. Gamrekelashvili J, Giagnorio R, Jussofie J, Soehnlein O, Duchene J, Briseño CG, Ramasamy SK, Krishnasamy K, Limbourg A, Kapanadze T, et al. Regulation of monocyte cell fate by blood vessels mediated by Notch signalling. *Nat Commun* (2016) 7:12597. doi:10.1038/ncomms12597

257. Lessard A-J, LeBel M, Egarnes B, Préfontaine P, Thériault P, Droit A, Brunet A, Rivest S, Gosselin J. Triggering of NOD2 Receptor Converts Inflammatory Ly6Chigh into Ly6Clow Monocytes with Patrolling Properties. *Cell Rep* (2017) 20:1830–1843. doi:10.1016/j.celrep.2017.08.009

258. Das A, Sinha M, Datta S, Abas M, Chaffee S, Sen CK, Roy S. Monocyte and macrophage plasticity in tissue repair and regeneration. *Am J Pathol* (2015) 185:2596–2606. doi:10.1016/j.ajpath.2015.06.001

259. França CN, Izar MCO, Hortêncio MNS, do Amaral JB, Ferreira CES, Tuleta ID, Fonseca FAH. Monocyte subtypes and the CCR2 chemokine receptor in cardiovascular disease. *Clin Sci (Lond)* (2017) 131:1215–1224. doi:10.1042/CS20170009

260. Kapellos TS, Bonaguro L, Gemünd I, Reusch N, Saglam A, Hinkley ER, Schultze JL. Human Monocyte Subsets and Phenotypes in Major Chronic Inflammatory Diseases. *Front Immunol* (2019) 10:2035. doi:10.3389/fimmu.2019.02035

261. Thomas G, Tacke R, Hedrick CC, Hanna RN. Nonclassical Patrolling Monocyte Function in the Vasculature. *ATVB* (2015) 35:1306–1316. doi:10.1161/ATVBAHA.114.304650

262. Sampath P, Moideen K, Ranganathan UD, Bethunaickan R. Monocyte Subsets: Phenotypes and Function in Tuberculosis Infection. *Front Immunol* (2018) 9:1726. doi:10.3389/fimmu.2018.01726

263. Sprangers S, de Vries TJ, Everts V. Monocyte Heterogeneity: Consequences for Monocyte-Derived Immune Cells. *J Immunol Res* (2016) 2016:1475435. doi:10.1155/2016/1475435

264. Zawada AM, Rogacev KS, Rotter B, Winter P, Marell R-R, Fliser D, Heine GH. SuperSAGE evidence for CD14++CD16+ monocytes as a third monocyte subset. *Blood* (2011) 118:e50-61. doi:10.1182/blood-2011-01-326827

265. Wong KL, Tai JJ-Y, Wong W-C, Han H, Sem X, Yeap W-H, Kourilsky P, Wong S-C. Gene expression profiling reveals the defining features of the classical, intermediate, and nonclassical human monocyte subsets. *Blood* (2011) 118:e16–e31. doi:10.1182/blood-2010-12-326355

266. Yasaka T, Mantich NM, Boxer LA, Baehner RL. Functions of human monocyte and lymphocyte subsets obtained by countercurrent centrifugal elutriation: differing functional capacities of human monocyte subsets. *J Immunol* (1981) 127:1515–1518.

267. Boyette LB, Macedo C, Hadi K, Elinoff BD, Walters JT, Ramaswami B, Chalasani G, Taboas JM, Lakkis FG, Metes DM. Phenotype, function, and differentiation potential of human monocyte subsets. *PLoS ONE* (2017) 12:e0176460. doi:10.1371/journal.pone.0176460

268. Villani A-C, Satija R, Reynolds G, Sarkizova S, Shekhar K, Fletcher J, Griesbeck M, Butler A, Zheng S, Lazo S, et al. Single-cell RNA-seq reveals new types of human blood dendritic cells, monocytes, and progenitors. *Science* (2017) 356:eaah4573. doi:10.1126/science.aah4573

269. Swirski FK. The spatial and developmental relationships in the macrophage family. *Arterioscler Thromb Vasc Biol* (2011) 31:1517–1522. doi:10.1161/ATVBAHA.110.221150

270. Han Z, Liu Q, Li H, Zhang M, You L, Lin Y, Wang K, Gou Q, Wang Z, Zhou S, et al. The role of monocytes in thrombotic diseases: a review. *Front Cardiovasc Med* (2023) 10:1113827. doi:10.3389/fcvm.2023.1113827

271. Carlin LM, Stamatiades EG, Auffray C, Hanna RN, Glover L, Vizcay-Barrena G, Hedrick CC, Cook HT, Diebold S, Geissmann F. Nr4a1-dependent Ly6C(low) monocytes monitor endothelial cells and orchestrate their disposal. *Cell* (2013) 153:362–375. doi:10.1016/j.cell.2013.03.010

272. Barbalat R, Lau L, Locksley RM, Barton GM. Toll-like receptor 2 on inflammatory monocytes induces type I interferon in response to viral but not bacterial ligands. *Nat Immunol* (2009) 10:1200–1207. doi:10.1038/ni.1792

273. Merino A, Buendia P, Martin-Malo A, Aljama P, Ramirez R, Carracedo J. Senescent CD14+CD16+ monocytes exhibit proinflammatory and proatherosclerotic activity. *J Immunol* (2011) 186:1809–1815. doi:10.4049/jimmunol.1001866

274. Belge K-U, Dayyani F, Horelt A, Siedlar M, Frankenberger M, Frankenberger B, Espevik T, Ziegler-Heitbrock L. The proinflammatory CD14+CD16+DR++ monocytes are a major source of TNF. *J Immunol* (2002) 168:3536–3542. doi:10.4049/jimmunol.168.7.3536

275. Skrzeczyńska-Moncznik J, Bzowska M, Loseke S, Grage-Griebenow E, Zembala M, Pryjma J. Peripheral blood CD14high CD16+ monocytes are main producers of IL-10. *Scand J Immunol* (2008) 67:152–159. doi:10.1111/j.1365-3083.2007.02051.x

276. Höpfner F, Jacob M, Ulrich C, Russ M, Simm A, Silber RE, Girndt M, Noutsias M, Werdan K, Schlitt A. Subgroups of monocytes predict cardiovascular events in patients with coronary heart disease. The PHAMOS trial (Prospective Halle Monocytes Study). *Hellenic J Cardiol* (2019) 60:311–321. doi:10.1016/j.hjc.2019.04.012

277. Ong S-M, Hadadi E, Dang T-M, Yeap W-H, Tan CT-Y, Ng T-P, Larbi A, Wong S-C. The pro-inflammatory phenotype of the human non-classical monocyte subset is attributed to senescence. *Cell Death Dis* (2018) 9:266. doi:10.1038/s41419-018-0327-1

278. Duroux-Richard I, Robin M, Peillex C, Apparailly F. MicroRNAs: Fine Tuners of Monocyte Heterogeneity. *Front Immunol* (2019) 10:2145. doi:10.3389/fimmu.2019.02145

279. Guilliams M, Mildner A, Yona S. Developmental and Functional Heterogeneity of Monocytes. *Immunity* (2018) 49:595–613. doi:10.1016/j.immuni.2018.10.005

280. Chimen M, Yates CM, McGettrick HM, Ward LSC, Harrison MJ, Apta B, Dib LH, Imhof BA, Harrison P, Nash GB, et al. Monocyte Subsets Coregulate Inflammatory Responses by Integrated Signaling through TNF and IL-6 at the Endothelial Cell Interface. *J Immunol* (2017) 198:2834–2843. doi:10.4049/jimmunol.1601281

281. Tak T, Drylewicz J, Conemans L, de Boer RJ, Koenderman L, Borghans JAM, Tesselaar K. Circulatory and maturation kinetics of human monocyte subsets in vivo. *Blood* (2017) 130:1474–1477. doi:10.1182/blood-2017-03-771261

282. Olingy CE, San Emeterio CL, Ogle ME, Krieger JR, Bruce AC, Pfau DD, Jordan BT, Peirce SM, Botchwey EA. Non-classical monocytes are biased progenitors of wound healing macrophages during soft tissue injury. *Sci Rep* (2017) 7:447. doi:10.1038/s41598-017-00477-1

283. Ong S-M, Teng K, Newell E, Chen H, Chen J, Loy T, Yeo T-W, Fink K, Wong S-C. A Novel, Five-Marker Alternative to CD16-CD14 Gating to Identify the Three Human Monocyte Subsets. *Front Immunol* (2019) 10:1761. doi:10.3389/fimmu.2019.01761

284. Auffray C, Fogg D, Garfa M, Elain G, Join-Lambert O, Kayal S, Sarnacki S, Cumano A, Lauvau G, Geissmann F. Monitoring of blood vessels and tissues by a population of monocytes with patrolling behavior. *Science* (2007) 317:666–670. doi:10.1126/science.1142883

285. Italiani P, Boraschi D. From Monocytes to M1/M2 Macrophages: Phenotypical vs. Functional Differentiation. *Front Immunol* (2014) 5: doi:10.3389/fimmu.2014.00514

286. Tamoutounour S, Guilliams M, Montanana Sanchis F, Liu H, Terhorst D, Malosse C, Pollet E, Ardouin L, Luche H, Sanchez C, et al. Origins and functional specialization of macrophages and of conventional and monocyte-derived dendritic cells in mouse skin. *Immunity* (2013) 39:925–938. doi:10.1016/j.immuni.2013.10.004

287. Epelman S, Lavine KJ, Beaudin AE, Sojka DK, Carrero JA, Calderon B, Brija T, Gautier EL, Ivanov S, Satpathy AT, et al. Embryonic and adult-derived resident cardiac macrophages are maintained through distinct mechanisms at steady state and during inflammation. *Immunity* (2014) 40:91–104. doi:10.1016/j.immuni.2013.11.019

288. Molawi K, Wolf Y, Kandalla PK, Favret J, Hagemeyer N, Frenzel K, Pinto AR, Klapproth K, Henri S, Malissen B, et al. Progressive replacement of embryo-derived cardiac macrophages with age. *J Exp Med* (2014) 211:2151–2158. doi:10.1084/jem.20140639

289. Jakubzick C, Gautier EL, Gibbings SL, Sojka DK, Schlitzer A, Johnson TE, Ivanov S, Duan Q, Bala S, Condon T, et al. Minimal differentiation of classical monocytes as they survey steady-state tissues and transport antigen to lymph nodes. *Immunity* (2013) 39:599–610. doi:10.1016/j.immuni.2013.08.007

290. Calderon B, Carrero JA, Ferris ST, Sojka DK, Moore L, Epelman S, Murphy KM, Yokoyama WM, Randolph GJ, Unanue ER. The pancreas anatomy conditions the origin and properties of resident macrophages. *J Exp Med* (2015) 212:1497–1512. doi:10.1084/jem.20150496

291. Mossadegh-Keller N, Gentek R, Gimenez G, Bigot S, Mailfert S, Sieweke MH. Developmental origin and maintenance of distinct testicular macrophage populations. *J Exp Med* (2017) 214:2829–2841. doi:10.1084/jem.20170829

292. Bain CC, Bravo-Blas A, Scott CL, Perdiguero EG, Geissmann F, Henri S, Malissen B, Osborne LC, Artis D, Mowat AM. Constant replenishment from circulating monocytes maintains the macrophage pool in the intestine of adult mice. *Nat Immunol* (2014) 15:929–937. doi:10.1038/ni.2967

293. Tamoutounour S, Henri S, Lelouard H, de Bovis B, de Haar C, van der Woude CJ, Woltman AM, Reyal Y, Bonnet D, Sichien D, et al. CD64 distinguishes macrophages from dendritic cells in the gut and reveals the Th1-inducing role of mesenteric lymph node macrophages during colitis. *Eur J Immunol* (2012) 42:3150–3166. doi:10.1002/eji.201242847

294. Zigmond E, Varol C, Farache J, Elmaliah E, Satpathy AT, Friedlander G, Mack M, Shpigel N, Boneca IG, Murphy KM, et al. Ly6C hi monocytes in the inflamed colon give rise to proinflammatory effector cells and migratory antigen-presenting cells. *Immunity* (2012) 37:1076–1090. doi:10.1016/j.immuni.2012.08.026

295. Chorro L, Sarde A, Li M, Woollard KJ, Chambon P, Malissen B, Kissenpfennig A, Barbaroux J-B, Groves R, Geissmann F. Langerhans cell (LC) proliferation mediates neonatal development, homeostasis, and inflammation-associated expansion of the epidermal LC network. *J Exp Med* (2009) 206:3089–3100. doi:10.1084/jem.20091586

296. Merad M, Manz MG, Karsunky H, Wagers A, Peters W, Charo I, Weissman IL, Cyster JG, Engleman EG. Langerhans cells renew in the skin throughout life under steady-state conditions. *Nat Immunol* (2002) 3:1135–1141. doi:10.1038/ni852

297. Ajami B, Bennett JL, Krieger C, Tetzlaff W, Rossi FMV. Local self-renewal can sustain CNS microglia maintenance and function throughout adult life. *Nat Neurosci* (2007) 10:1538–1543. doi:10.1038/nn2014

298. Ginhoux F, Greter M, Leboeuf M, Nandi S, See P, Gokhan S, Mehler MF, Conway SJ, Ng LG, Stanley ER, et al. Fate mapping analysis reveals that adult microglia derive from primitive macrophages. *Science* (2010) 330:841–845. doi:10.1126/science.1194637

299. Mildner A, Schmidt H, Nitsche M, Merkler D, Hanisch U-K, Mack M, Heikenwalder M, Brück W, Priller J, Prinz M. Microglia in the adult brain arise from Ly-6ChiCCR2+ monocytes only under defined host conditions. *Nat Neurosci* (2007) 10:1544–1553. doi:10.1038/nn2015

300. Entman ML, Smith CW. Postreperfusion inflammation: a model for reaction to injury in cardiovascular disease. *Cardiovasc Res* (1994) 28:1301–1311. doi:10.1093/cvr/28.9.1301

301. Frangogiannis NG, Youker KA, Rossen RD, Gwechenberger M, Lindsey MH, Mendoza LH, Michael LH, Ballantyne CM, Smith CW, Entman ML. Cytokines and the microcirculation in ischemia and reperfusion. *J Mol Cell Cardiol* (1998) 30:2567–2576. doi:10.1006/jmcc.1998.0829

302. Frangogiannis NG, Entman ML. "Role of Inflammation Following Myocardial Ischemia and Reperfusion," in *Textbook of Coronary Thrombosis and Thrombolysis*, ed. R. C. Becker (Boston, MA: Springer US), 569–584. doi:10.1007/978-0-585-33754-8_42

303. Mehta JL, Li DY. Inflammation in ischemic heart disease: response to tissue injury or a pathogenetic villain? *Cardiovasc Res* (1999) 43:291–299. doi:10.1016/s0008-6363(99)00132-7

304. Rivollier A, He J, Kole A, Valatas V, Kelsall BL. Inflammation switches the differentiation program of Ly6Chi monocytes from antiinflammatory macrophages to inflammatory dendritic cells in the colon. *J Exp Med* (2012) 209:139–155. doi:10.1084/jem.20101387

305. Qu C, Edwards EW, Tacke F, Angeli V, Llodrá J, Sanchez-Schmitz G, Garin A, Haque NS, Peters W, van Rooijen N, et al. Role of CCR8 and other chemokine pathways in the migration of monocyte-

derived dendritic cells to lymph nodes. *J Exp Med* (2004) 200:1231–1241. doi:10.1084/jem.20032152

306. Arnold L, Henry A, Poron F, Baba-Amer Y, van Rooijen N, Plonquet A, Gherardi RK, Chazaud B. Inflammatory monocytes recruited after skeletal muscle injury switch into antiinflammatory macrophages to support myogenesis. *J Exp Med* (2007) 204:1057–1069. doi:10.1084/jem.20070075

307. Saederup N, Cardona AE, Croft K, Mizutani M, Cotleur AC, Tsou C-L, Ransohoff RM, Charo IF. Selective chemokine receptor usage by central nervous system myeloid cells in CCR2-red fluorescent protein knock-in mice. *PLoS One* (2010) 5:e13693. doi:10.1371/journal.pone.0013693

308. Donnelly DJ, Longbrake EE, Shawler TM, Kigerl KA, Lai W, Tovar CA, Ransohoff RM, Popovich PG. Deficient CX3CR1 signaling promotes recovery after mouse spinal cord injury by limiting the recruitment and activation of Ly6Clo/iNOS+ macrophages. *J Neurosci* (2011) 31:9910–9922. doi:10.1523/JNEUROSCI.2114-11.2011

309. Zhu Y, Soderblom C, Krishnan V, Ashbaugh J, Bethea JR, Lee JK. Hematogenous macrophage depletion reduces the fibrotic scar and increases axonal growth after spinal cord injury. *Neurobiol Dis* (2015) 74:114–125. doi:10.1016/j.nbd.2014.10.024

310. Steiniger B, Barth P, Hellinger A. The perifollicular and marginal zones of the human splenic white pulp : do fibroblasts guide lymphocyte immigration? *Am J Pathol* (2001) 159:501–512. doi:10.1016/S0002-9440(10)61722-1

311. van Krieken JH, te Velde J. Immunohistology of the human spleen: an inventory of the localization of lymphocyte subpopulations. *Histopathology* (1986) 10:285–294. doi:10.1111/j.1365-2559.1986.tb02482.x

312. van Krieken JH, te Velde J. Normal histology of the human spleen. *Am J Surg Pathol* (1988) 12:777–785. doi:10.1097/00000478-198810000-00007

313. Puga I, Cols M, Barra CM, He B, Cassis L, Gentile M, Comerma L, Chorny A, Shan M, Xu W, et al. B–helper neutrophils stimulate immunoglobulin diversification and production in the marginal zone of the spleen. *Nat Immunol* (2011) 13:170–180. doi:10.1038/ni.2194

314. Nagelkerke SQ, Bruggeman CW, Den Haan JMM, Mul EPJ, Van Den Berg TK, Van Bruggen R, Kuijpers TW. Red pulp macrophages in the human spleen are a distinct cell population with a unique expression of Fc-γ receptors. *Blood Advances* (2018) 2:941–953. doi:10.1182/bloodadvances.2017015008

315. Bronte V, Pittet MJ. The spleen in local and systemic regulation of immunity. *Immunity* (2013) 39:806–818. doi:10.1016/j.immuni.2013.10.010

316. McKim DB, Yin W, Wang Y, Cole SW, Godbout JP, Sheridan JF. Social Stress Mobilizes Hematopoietic Stem Cells to Establish Persistent Splenic Myelopoiesis. *Cell Rep* (2018) 25:2552-2562.e3. doi:10.1016/j.celrep.2018.10.102

317. Cortez-Retamozo V, Etzrodt M, Newton A, Rauch PJ, Chudnovskiy A, Berger C, Ryan RJH, Iwamoto Y, Marinelli B, Gorbatov R, et al. Origins of tumor-associated macrophages and neutrophils. *Proc Natl Acad Sci U S A* (2012) 109:2491–2496. doi:10.1073/pnas.1113744109

318. Loukov D, Naidoo A, Puchta A, Marin JLA, Bowdish DME. Tumor necrosis factor drives increased splenic monopoiesis in old mice. *J Leukoc Biol* (2016) 100:121–129. doi:10.1189/jlb.3MA0915-433RR

319. Wu C, Ning H, Liu M, Lin J, Luo S, Zhu W, Xu J, Wu W-C, Liang J, Shao C-K, et al. Spleen mediates a distinct hematopoietic progenitor response supporting tumor-promoting myelopoiesis. *J Clin Invest* (2018) 128:3425–3438. doi:10.1172/JCI97973

320. Noble BT, Brennan FH, Popovich PG. The spleen as a neuroimmune interface after spinal cord injury. *Journal of Neuroimmunology* (2018) 321:1–11. doi:10.1016/j.jneuroim.2018.05.007

321. Gordon S, Taylor PR. Monocyte and macrophage heterogeneity. *Nat Rev Immunol* (2005) 5:953–964. doi:10.1038/nri1733

322. Hawthorne AL, Popovich PG. Emerging concepts in myeloid cell biology after spinal cord injury. *Neurotherapeutics* (2011) 8:252–261. doi:10.1007/s13311-011-0032-6

323. Liu Z-J, Chen C, Li F-W, Shen J-M, Yang Y-Y, Leak RK, Ji X-M, Du H-S, Hu X-M. Splenic responses in ischemic stroke: new insights into stroke pathology. *CNS Neurosci Ther* (2015) 21:320–326. doi:10.1111/cns.12361

324. Fleming JC, Norenberg MD, Ramsay DA, Dekaban GA, Marcillo AE, Saenz AD, Pasquale-Styles M, Dietrich WD, Weaver LC. The cellular inflammatory response in human spinal cords after injury. *Brain* (2006) 129:3249–3269. doi:10.1093/brain/awl296

325. Palis J, Robertson S, Kennedy M, Wall C, Keller G. Development of erythroid and myeloid progenitors in the yolk sac and embryo proper of the mouse. *Development* (1999) 126:5073–5084. doi:10.1242/dev.126.22.5073

326. Hoeffel G, Ginhoux F. Ontogeny of Tissue-Resident Macrophages. *Front Immunol* (2015) 6:486. doi:10.3389/fimmu.2015.00486

327. Tavian M, Péault B. Embryonic development of the human hematopoietic system. *Int J Dev Biol* (2005) 49:243–250. doi:10.1387/ijdb.041957mt

328. Ditadi A, Sturgeon CM, Keller G. A view of human haematopoietic development from the Petri dish. *Nat Rev Mol Cell Biol* (2017) 18:56–67. doi:10.1038/nrm.2016.127

329. Tober J, Koniski A, McGrath KE, Vemishetti R, Emerson R, de Mesy-Bentley KKL, Waugh R, Palis J. The megakaryocyte lineage originates from hemangioblast precursors and is an integral component both of primitive and of definitive hematopoiesis. *Blood* (2007) 109:1433–1441. doi:10.1182/blood-2006-06-031898

330. Ginhoux F, Lim S, Hoeffel G, Low D, Huber T. Origin and differentiation of microglia. *Front Cell Neurosci* (2013) 7:45. doi:10.3389/fncel.2013.00045

331. Hoeffel G, Squarzoni P, Garel S, Ginhoux F. "Microglial Ontogeny and Functions in Shaping Brain Circuits," in *Macrophages : Biology and Role in the Pathology of Diseases*, eds.Biswas, S. K, Mantovani, Alberto (Springer), 183–215. Available at: https://hal.science/hal-03657190 [Accessed April 8, 2024]

332. Frame JM, McGrath KE, Palis J. Erythro-myeloid progenitors: "definitive" hematopoiesis in the conceptus prior to the emergence of hematopoietic stem cells. *Blood Cells Mol Dis* (2013) 51:220–225. doi:10.1016/j.bcmd.2013.09.006

333. Hoeffel G, Wang Y, Greter M, See P, Teo P, Malleret B, Leboeuf M, Low D, Oller G, Almeida F, et al. Adult Langerhans cells derive predominantly from embryonic fetal liver monocytes with a minor contribution of yolk sac-derived macrophages. *J Exp Med* (2012) 209:1167–1181. doi:10.1084/jem.20120340

334. Lin Y, Yoder MC, Yoshimoto M. Lymphoid progenitor emergence in the murine embryo and yolk sac precedes stem cell detection. *Stem Cells Dev* (2014) 23:1168–1177. doi:10.1089/scd.2013.0536

335. Clements WK, Traver D. Signalling pathways that control vertebrate haematopoietic stem cell specification. *Nat Rev Immunol* (2013) 13:336–348. doi:10.1038/nri3443

336. Orkin SH, Zon LI. Hematopoiesis: an evolving paradigm for stem cell biology. *Cell* (2008) 132:631–644. doi:10.1016/j.cell.2008.01.025

337. Medvinsky A, Rybtsov S, Taoudi S. Embryonic origin of the adult hematopoietic system: advances and questions. *Development* (2011) 138:1017–1031. doi:10.1242/dev.040998

338. Golub R, Cumano A. Embryonic hematopoiesis. *Blood Cells Mol Dis* (2013) 51:226–231. doi:10.1016/j.bcmd.2013.08.004

339. Swiers G, Rode C, Azzoni E, de Bruijn MFTR. A short history of hemogenic endothelium. *Blood Cells Mol Dis* (2013) 51:206–212. doi:10.1016/j.bcmd.2013.09.005

340. Ginhoux F, Guilliams M. Tissue-Resident Macrophage Ontogeny and Homeostasis. *Immunity* (2016) 44:439–449. doi:10.1016/j.immuni.2016.02.024

341. Murray PJ. Macrophage Polarization. *Annu Rev Physiol* (2017) 79:541–566. doi:10.1146/annurev-physiol-022516-034339

342. Martinez FO, Gordon S. The M1 and M2 paradigm of macrophage activation: time for reassessment. *F1000Prime Rep* (2014) 6:13. doi:10.12703/P6-13

343. Martinez FO, Gordon S, Locati M, Mantovani A. Transcriptional profiling of the human monocyte-to-macrophage differentiation and polarization: new molecules and patterns of gene expression. *J Immunol* (2006) 177:7303–7311. doi:10.4049/jimmunol.177.10.7303

344. Jaguin M, Houlbert N, Fardel O, Lecureur V. Polarization profiles of human M-CSF-generated macrophages and comparison of M1-markers in classically activated macrophages from GM-CSF and M-CSF origin. *Cell Immunol* (2013) 281:51–61. doi:10.1016/j.cellimm.2013.01.010

345. Davies LC, Jenkins SJ, Allen JE, Taylor PR. Tissue-resident macrophages. *Nat Immunol* (2013) 14:986–995. doi:10.1038/ni.2705

346. Hamilton TA, Zhao C, Pavicic PG, Datta S. Myeloid colony-stimulating factors as regulators of macrophage polarization. *Front Immunol* (2014) 5:554. doi:10.3389/fimmu.2014.00554

347. Scott CL, Henri S, Guilliams M. Mononuclear phagocytes of the intestine, the skin, and the lung. *Immunol Rev* (2014) 262:9–24. doi:10.1111/imr.12220

348. Hashimoto D, Chow A, Noizat C, Teo P, Beasley MB, Leboeuf M, Becker CD, See P, Price J, Lucas D, et al. Tissue-resident macrophages self-maintain locally throughout adult life with minimal contribution from circulating monocytes. *Immunity* (2013) 38:792–804. doi:10.1016/j.immuni.2013.04.004

349. Ajami B, Bennett JL, Krieger C, McNagny KM, Rossi FMV. Infiltrating monocytes trigger EAE progression, but do not contribute to the resident microglia pool. *Nat Neurosci* (2011) 14:1142–1149. doi:10.1038/nn.2887

350. Davies LC, Rosas M, Smith PJ, Fraser DJ, Jones SA, Taylor PR. A quantifiable proliferative burst of tissue macrophages restores homeostatic macrophage populations after acute inflammation. *Eur J Immunol* (2011) 41:2155–2164. doi:10.1002/eji.201141817

351. Davies LC, Rosas M, Jenkins SJ, Liao C-T, Scurr MJ, Brombacher F, Fraser DJ, Allen JE, Jones SA, Taylor PR. Distinct bone marrow-derived and tissue-resident macrophage lineages proliferate at key stages during inflammation. *Nat Commun* (2013) 4:1886. doi:10.1038/ncomms2877

352. Gordon S, Plüddemann A. Tissue macrophages: heterogeneity and functions. *BMC Biol* (2017) 15:53. doi:10.1186/s12915-017-0392-4

353. Prinz M, Masuda T, Wheeler MA, Quintana FJ. Microglia and Central Nervous System–Associated Macrophages—From Origin to Disease Modulation. *Annu Rev Immunol* (2021) 39:251–277. doi:10.1146/annurev-immunol-093019-110159

354. Kierdorf K, Masuda T, Jordão MJC, Prinz M. Macrophages at CNS interfaces: ontogeny and function in health and disease. *Nat Rev Neurosci* (2019) 20:547–562. doi:10.1038/s41583-019-0201-x

355. Mrdjen D, Pavlovic A, Hartmann FJ, Schreiner B, Utz SG, Leung BP, Lelios I, Heppner FL, Kipnis J, Merkler D, et al. High-Dimensional Single-Cell Mapping of Central Nervous System Immune Cells Reveals Distinct Myeloid Subsets in Health, Aging, and Disease. *Immunity* (2018) 48:380-395.e6. doi:10.1016/j.immuni.2018.01.011

356. Ling EA, Kaur C, Lu J. Origin, nature, and some functional considerations of intraventricular macrophages, with special reference to the epiplexus cells. *Microsc Res Tech* (1998) 41:43–56. doi:10.1002/(SICI)1097-0029(19980401)41:1<43::AID-JEMT5>3.0.CO;2-V

357. Munro DAD, Movahedi K, Priller J. Macrophage compartmentalization in the brain and cerebrospinal fluid system. *Sci Immunol* (2022) 7:eabk0391. doi:10.1126/sciimmunol.abk0391

358. Kappers JA. [Experimental study of the function and origin of Kolmer's cells of plexus chorioideus in axolotl and guinea pig]. *Z Anat Entwicklungsgesch* (1953) 117:1–19.

359. Shechter R, Miller O, Yovel G, Rosenzweig N, London A, Ruckh J, Kim K-W, Klein E, Kalchenko V, Bendel P, et al. Recruitment of beneficial M2 macrophages to injured spinal cord is orchestrated by remote brain choroid plexus. *Immunity* (2013) 38:555–569. doi:10.1016/j.immuni.2013.02.012

360. Li Q, Barres BA. Microglia and macrophages in brain homeostasis and disease. *Nat Rev Immunol* (2018) 18:225–242. doi:10.1038/nri.2017.125

361. Sheng J, Ruedl C, Karjalainen K. Most Tissue-Resident Macrophages Except Microglia Are Derived from Fetal Hematopoietic Stem Cells. *Immunity* (2015) 43:382–393. doi:10.1016/j.immuni.2015.07.016

362. Goldmann T, Wieghofer P, Jordão MJC, Prutek F, Hagemeyer N, Frenzel K, Amann L, Staszewski O, Kierdorf K, Krueger M, et al. Origin, fate and dynamics of macrophages at central nervous system interfaces. *Nat Immunol* (2016) 17:797–805. doi:10.1038/ni.3423

363. Dermitzakis I, Theotokis P, Evangelidis P, Delilampou E, Evangelidis N, Chatzisavvidou A, Avramidou E, Manthou ME. CNS Border-Associated Macrophages: Ontogeny and Potential Implication in Disease. *CIMB* (2023) 45:4285–4300. doi:10.3390/cimb45050272

364. Van Hove H, Martens L, Scheyltjens I, De Vlaminck K, Pombo Antunes AR, De Prijck S, Vandamme N, De Schepper S, Van Isterdael G, Scott CL, et al. A single-cell atlas of mouse brain macrophages reveals unique transcriptional identities shaped by ontogeny and tissue environment. *Nat Neurosci* (2019) 22:1021–1035. doi:10.1038/s41593-019-0393-4

365. Kierdorf K, Prinz M. Microglia in steady state. *Journal of Clinical Investigation* (2017) 127:3201–3209. doi:10.1172/JCI90602

366. Taketomi T, Tsuruta F. Towards an Understanding of Microglia and Border-Associated Macrophages. *Biology (Basel)* (2023) 12:1091. doi:10.3390/biology12081091

367. Liu C, Wu C, Yang Q, Gao J, Li L, Yang D, Luo L. Macrophages Mediate the Repair of Brain Vascular Rupture through Direct Physical Adhesion and Mechanical Traction. *Immunity* (2016) 44:1162–1176. doi:10.1016/j.immuni.2016.03.008

368. Feng R, Muraleedharan Saraswathy V, Mokalled MH, Cavalli V. Self-renewing macrophages in dorsal root ganglia contribute to promote nerve regeneration. *Proc Natl Acad Sci USA* (2023) 120:e2215906120. doi:10.1073/pnas.2215906120

369. Lu X, Richardson PM. Responses of macrophages in rat dorsal root ganglia following peripheral nerve injury. *J Neurocytol* (1993) 22:334–341. doi:10.1007/BF01195557

370. Kwon MJ, Kim J, Shin H, Jeong SR, Kang YM, Choi JY, Hwang DH, Kim BG. Contribution of macrophages to enhanced regenerative capacity of dorsal root ganglia sensory neurons by conditioning injury. *J Neurosci* (2013) 33:15095–15108. doi:10.1523/JNEUROSCI.0278-13.2013

371. Niemi JP, DeFrancesco-Lisowitz A, Roldán-Hernández L, Lindborg JA, Mandell D, Zigmond RE. A critical role for macrophages near axotomized neuronal cell bodies in stimulating nerve regeneration. *J Neurosci* (2013) 33:16236–16248. doi:10.1523/JNEUROSCI.3319-12.2013

372. Niemi JP, DeFrancesco-Lisowitz A, Cregg JM, Howarth M, Zigmond RE. Overexpression of the monocyte chemokine CCL2 in dorsal root ganglion neurons causes a conditioning-like increase in neurite outgrowth and does so via a STAT3 dependent mechanism. *Exp Neurol* (2016) 275 Pt 1:25–37. doi:10.1016/j.expneurol.2015.09.018

373. Zigmond RE, Echevarria FD. Macrophage biology in the peripheral nervous system after injury. *Prog Neurobiol* (2019) 173:102–121. doi:10.1016/j.pneurobio.2018.12.001

374. Yu X, Liu H, Hamel KA, Morvan MG, Yu S, Leff J, Guan Z, Braz JM, Basbaum AI. Dorsal root ganglion macrophages contribute to both the initiation and persistence of neuropathic pain. *Nat Commun* (2020) 11:264. doi:10.1038/s41467-019-13839-2

375. Addington J, Freimer M. Chemotherapy-induced peripheral neuropathy: an update on the current understanding. *F1000Res* (2016) 5:F1000 Faculty Rev-1466. doi:10.12688/f1000research.8053.1

376. Kallenborn-Gerhardt W, Hohmann SW, Syhr KMJ, Schröder K, Sisignano M, Weigert A, Lorenz JE, Lu R, Brüne B, Brandes RP, et al. Nox2-dependent signaling between macrophages and sensory neurons contributes to neuropathic pain hypersensitivity. *Pain* (2014) 155:2161–2170. doi:10.1016/j.pain.2014.08.013

377. Zhang H, Li Y, de Carvalho-Barbosa M, Kavelaars A, Heijnen CJ, Albrecht PJ, Dougherty PM. Dorsal Root Ganglion Infiltration by Macrophages Contributes to Paclitaxel Chemotherapy-Induced Peripheral Neuropathy. *J Pain* (2016) 17:775–786. doi:10.1016/j.jpain.2016.02.011

378. Arvidson B. Cellular uptake of exogenous horseradish peroxidase in mouse peripheral nerve. *Acta Neuropathol* (1977) 37:35–41. doi:10.1007/BF00684538

379. Pirzgalska RM, Seixas E, Seidman JS, Link VM, Sánchez NM, Mahú I, Mendes R, Gres V, Kubasova N, Morris I, et al. Sympathetic neuron-associated macrophages contribute to obesity by importing and metabolizing norepinephrine. *Nat Med* (2017) 23:1309–1318. doi:10.1038/nm.4422

380. Wolf Y, Boura-Halfon S, Cortese N, Haimon Z, Sar Shalom H, Kuperman Y, Kalchenko V, Brandis A, David E, Segal-Hayoun Y, et al. Brown-adipose-tissue macrophages control tissue innervation and homeostatic energy expenditure. *Nat Immunol* (2017) 18:665–674. doi:10.1038/ni.3746

381. Gabanyi I, Muller PA, Feighery L, Oliveira TY, Costa-Pinto FA, Mucida D. Neuro-immune Interactions Drive Tissue Programming in Intestinal Macrophages. *Cell* (2016) 164:378–391. doi:10.1016/j.cell.2015.12.023

382. De Schepper S, Verheijden S, Aguilera-Lizarraga J, Viola MF, Boesmans W, Stakenborg N, Voytyuk I, Schmidt I, Boeckx B, Dierckx de Casterlé I, et al. Self-Maintaining Gut Macrophages Are Essential for Intestinal Homeostasis. *Cell* (2018) 175:400-415.e13. doi:10.1016/j.cell.2018.07.048

383. Kolter J, Feuerstein R, Zeis P, Hagemeyer N, Paterson N, d'Errico P, Baasch S, Amann L, Masuda T, Lösslein A, et al. A Subset of Skin Macrophages Contributes to the Surveillance and Regeneration of Local Nerves. *Immunity* (2019) 50:1482-1497.e7. doi:10.1016/j.immuni.2019.05.009

384. Griffin JW, George R, Ho T. Macrophage systems in peripheral nerves. A review. *J Neuropathol Exp Neurol* (1993) 52:553–560. doi:10.1097/00005072-199311000-00001

385. Amann L, Prinz M. The origin, fate and function of macrophages in the peripheral nervous system—an update. *International Immunology* (2020) 32:709–717. doi:10.1093/intimm/dxaa030

386. Wang PL, Yim AK, Kim K, Avey D, Czepielewski RS, Colonna M, Milbrandt J, Randolph GJ, Project TIG. Peripheral nerve resident macrophages are microglia-like cells with tissue-specific programming. *bioRxiv* (2019)2019.12.19.883546. doi:10.1101/2019.12.19.883546

387. Gaudet AD, Popovich PG, Ramer MS. Wallerian degeneration: gaining perspective on inflammatory events after peripheral nerve injury. *J Neuroinflammation* (2011) 8:110. doi:10.1186/1742-2094-8-110

388. Ydens E, Amann L, Asselbergh B, Scott CL, Martens L, Sichien D, Mossad O, Blank T, De Prijck S, Low D, et al. Profiling peripheral nerve macrophages reveals two macrophage subsets with distinct localization, transcriptome and response to injury. *Nat Neurosci* (2020) 23:676–689. doi:10.1038/s41593-020-0618-6

389. Perkins NM, Tracey DJ. Hyperalgesia due to nerve injury: role of neutrophils. *Neuroscience* (2000) 101:745–757. doi:10.1016/s0306-4522(00)00396-1

390. Siebert H, Sachse A, Kuziel WA, Maeda N, Brück W. The chemokine receptor CCR2 is involved in macrophage recruitment to the injured peripheral nervous system. *J Neuroimmunol* (2000) 110:177–185. doi:10.1016/s0165-5728(00)00343-x

391. Tofaris GK, Patterson PH, Jessen KR, Mirsky R. Denervated Schwann cells attract macrophages by secretion of leukemia inhibitory factor (LIF) and monocyte chemoattractant protein-1 in a process regulated by interleukin-6 and LIF. *J Neurosci* (2002) 22:6696–6703. doi:10.1523/JNEUROSCI.22-15-06696.2002

392. Cattin A-L, Burden JJ, Van Emmenis L, Mackenzie FE, Hoving JJA, Garcia Calavia N, Guo Y, McLaughlin M, Rosenberg LH, Quereda V, et al. Macrophage-Induced Blood Vessels Guide Schwann Cell-Mediated Regeneration of Peripheral Nerves. *Cell* (2015) 162:1127–1139. doi:10.1016/j.cell.2015.07.021

393. Huang T-C, Wu H-L, Chen S-H, Wang Y-T, Wu C-C. Thrombomodulin facilitates peripheral nerve regeneration through regulating M1/M2 switching. *J Neuroinflammation* (2020) 17:240. doi:10.1186/s12974-020-01897-z

394. Yu J, Lin Y, Wang G, Song J, Hayat U, Liu C, Raza A, Huang X, Lin H, Wang J-Y. Zein-induced immune response and modulation by size, pore structure and drug-loading: Application for sciatic nerve regeneration. *Acta Biomater* (2022) 140:289–301. doi:10.1016/j.actbio.2021.11.035

395. Feng R, Zhang P. The significance of M1 macrophage should be highlighted in peripheral nerve regeneration. *Histol Histopathol* (2023) 38:975–987. doi:10.14670/HH-18-591

396. Hervera A, De Virgiliis F, Palmisano I, Zhou L, Tantardini E, Kong G, Hutson T, Danzi MC, Perry RB-T, Santos CXC, et al. Reactive oxygen species regulate axonal regeneration through the release of exosomal NADPH oxidase 2 complexes into injured axons. *Nat Cell Biol* (2018) 20:307–319. doi:10.1038/s41556-018-0039-x

397. Tomlinson JE, Žygelytė E, Grenier JK, Edwards MG, Cheetham J. Temporal changes in macrophage phenotype after peripheral nerve injury. *J Neuroinflammation* (2018) 15:185. doi:10.1186/s12974-018-1219-0

398. Vereyken EJF, Heijnen PDAM, Baron W, de Vries EHE, Dijkstra CD, Teunissen CE. Classically and alternatively activated bone marrow derived macrophages differ in cytoskeletal functions and migration towards specific CNS cell types. *J Neuroinflammation* (2011) 8:58. doi:10.1186/1742-2094-8-58

399. Jordão MJC, Sankowski R, Brendecke SM, Sagar null, Locatelli G, Tai Y-H, Tay TL, Schramm E, Armbruster S, Hagemeyer N, et al. Single-cell profiling identifies myeloid cell subsets with distinct fates during neuroinflammation. *Science* (2019) 363:eaat7554. doi:10.1126/science.aat7554

400. Bennett FC, Bennett ML, Yaqoob F, Mulinyawe SB, Grant GA, Hayden Gephart M, Plowey ED, Barres BA. A Combination of Ontogeny and CNS Environment Establishes Microglial Identity. *Neuron* (2018) 98:1170-1183.e8. doi:10.1016/j.neuron.2018.05.014

401. Shemer A, Grozovski J, Tay TL, Tao J, Volaski A, Süß P, Ardura-Fabregat A, Gross-Vered M, Kim J-S, David E, et al. Engrafted parenchymal brain macrophages differ from microglia in transcriptome, chromatin landscape and response to challenge. *Nat Commun* (2018) 9:5206. doi:10.1038/s41467-018-07548-5

402. Cronk JC, Filiano AJ, Louveau A, Marin I, Marsh R, Ji E, Goldman DH, Smirnov I, Geraci N, Acton S, et al. Peripherally derived macrophages can engraft the brain independent of irradiation and maintain an identity distinct from microglia. *J Exp Med* (2018) 215:1627–1647. doi:10.1084/jem.20180247

403. Noel G, Guo X, Wang Q, Schwemberger S, Byrum D, Ogle C. POSTBURN MONOCYTES ARE THE MAJOR PRODUCERS OF TNF-α IN THE HETEROGENEOUS SPLENIC MACROPHAGE POPULATION*. *Shock* (2007) 27:312–319. doi:10.1097/01.shk.0000239753.75088.5e

404. Martinez-Pomares L, Platt N, McKnight AJ, da Silva RP, Gordon S. Macrophage membrane molecules: markers of tissue differentiation and heterogeneity. *Immunobiology* (1996) 195:407–416. doi:10.1016/S0171-2985(96)80012-X

405. Witmer MD, Steinman RM. The anatomy of peripheral lymphoid organs with emphasis on accessory cells: light-microscopic immunocytochemical studies of mouse spleen, lymph node, and Peyer's patch. *Am J Anat* (1984) 170:465–481. doi:10.1002/aja.1001700318

406. Den Haan JMM, Kraal G. Innate Immune Functions of Macrophage Subpopulations in the Spleen. *J Innate Immun* (2012) 4:437–445. doi:10.1159/000335216

407. Schulz C, Gomez Perdiguero E, Chorro L, Szabo-Rogers H, Cagnard N, Kierdorf K, Prinz M, Wu B, Jacobsen SEW, Pollard JW, et al. A lineage of myeloid cells independent of Myb and hematopoietic stem cells. *Science* (2012) 336:86–90. doi:10.1126/science.1219179

408. Wang C, Yu X, Cao Q, Wang Y, Zheng G, Tan TK, Zhao H, Zhao Y, Wang Y, Harris DC. Characterization of murine macrophages from bone marrow, spleen and peritoneum. *BMC Immunol* (2013) 14:6. doi:10.1186/1471-2172-14-6

409. Springer T, Galfré G, Secher DS, Milstein C. Mac-1: a macrophage differentiation antigen identified by monoclonal antibody. *Eur J Immunol* (1979) 9:301–306. doi:10.1002/eji.1830090410

410. Austyn JM, Gordon S. F4/80, a monoclonal antibody directed specifically against the mouse macrophage. *Eur J Immunol* (1981) 11:805–815. doi:10.1002/eji.1830111013

411. Hume DA, Robinson AP, MacPherson GG, Gordon S. The mononuclear phagocyte system of the mouse defined by immunohistochemical localization of antigen F4/80. Relationship between macrophages, Langerhans cells, reticular cells, and dendritic cells in lymphoid and hematopoietic organs. *J Exp Med* (1983) 158:1522–1536. doi:10.1084/jem.158.5.1522

412. Kraal G, Rep M, Janse M. Macrophages in T and B cell compartments and other tissue macrophages recognized by monoclonal antibody MOMA-2. An immunohistochemical study. *Scand J Immunol* (1987) 26:653–661. doi:10.1111/j.1365-3083.1987.tb02301.x

413. Lewis SM, Williams A, Eisenbarth SC. Structure and function of the immune system in the spleen. *Sci Immunol* (2019) 4:eaau6085. doi:10.1126/sciimmunol.aau6085

414. Lévesque J-P, Summers KM, Bisht K, Millard SM, Winkler IG, Pettit AR. Macrophages form erythropoietic niches and regulate iron homeostasis to adapt erythropoiesis in response to infections

and inflammation. *Experimental Hematology* (2021) 103:1–14. doi:10.1016/j.exphem.2021.08.011

415. Dutta P, Hoyer FF, Grigoryeva LS, Sager HB, Leuschner F, Courties G, Borodovsky A, Novobrantseva T, Ruda VM, Fitzgerald K, et al. Macrophages retain hematopoietic stem cells in the spleen via VCAM-1. *J Exp Med* (2015) 212:497–512. doi:10.1084/jem.20141642

416. Kurotaki D, Uede T, Tamura T. Functions and development of red pulp macrophages. *Microbiology and Immunology* (2015) 59:55–62. doi:10.1111/1348-0421.12228

417. Kim CC, Nelson CS, Wilson EB, Hou B, DeFranco AL, DeRisi JL. Splenic red pulp macrophages produce type I interferons as early sentinels of malaria infection but are dispensable for control. *PLoS One* (2012) 7:e48126. doi:10.1371/journal.pone.0048126

418. Borges Da Silva H, Fonseca R, Pereira RM, Cassado ADA, Álvarez JM, D'Império Lima MR. Splenic Macrophage Subsets and Their Function during Blood-Borne Infections. *Front Immunol* (2015) 6: doi:10.3389/fimmu.2015.00480

419. Kurotaki D, Kon S, Bae K, Ito K, Matsui Y, Nakayama Y, Kanayama M, Kimura C, Narita Y, Nishimura T, et al. CSF-1-dependent red pulp macrophages regulate CD4 T cell responses. *J Immunol* (2011) 186:2229–2237. doi:10.4049/jimmunol.1001345

420. Chen W, Jin W, Hardegen N, Lei K-J, Li L, Marinos N, McGrady G, Wahl SM. Conversion of peripheral CD4+CD25- naive T cells to CD4+CD25+ regulatory T cells by TGF-beta induction of transcription factor Foxp3. *J Exp Med* (2003) 198:1875–1886. doi:10.1084/jem.20030152

421. Steiniger BS. Human spleen microanatomy: why mice do not suffice. *Immunology* (2015) 145:334–346. doi:10.1111/imm.12469

422. Steiniger B, Barth P, Herbst B, Hartnell A, Crocker PR. The species-specific structure of microanatomical compartments in the human spleen: strongly sialoadhesin-positive macrophages occur in the perifollicular zone, but not in the marginal zone. *Immunology* (1997) 92:307–316. doi:10.1046/j.1365-2567.1997.00328.x

423. A-Gonzalez N, Castrillo A. Origin and specialization of splenic macrophages. *Cellular Immunology* (2018) 330:151–158. doi:10.1016/j.cellimm.2018.05.005

424. Aichele P, Zinke J, Grode L, Schwendener RA, Kaufmann SHE, Seiler P. Macrophages of the splenic marginal zone are essential for trapping of blood-borne particulate antigen but dispensable for induction of specific T cell responses. *J Immunol* (2003) 171:1148–1155. doi:10.4049/jimmunol.171.3.1148

425. Mebius RE, Kraal G. Structure and function of the spleen. *Nat Rev Immunol* (2005) 5:606–616. doi:10.1038/nri1669

426. MacLennan IC, Gray D, Kumararatne DS, Bazin H. The lymphocytes of splenic marginal zones: a distinct B-cell lineage. *Immunol Today* (1982) 3:305–307. doi:10.1016/0167-5699(82)90032-9

427. Karlsson MCI, Guinamard R, Bolland S, Sankala M, Steinman RM, Ravetch JV. Macrophages control the retention and trafficking of B lymphocytes in the splenic marginal zone. *J Exp Med* (2003) 198:333–340. doi:10.1084/jem.20030684

428. Di Paolo NC, Miao EA, Iwakura Y, Murali-Krishna K, Aderem A, Flavell RA, Papayannopoulou T, Shayakhmetov DM. Virus binding to a plasma membrane receptor triggers interleukin-1 alpha-mediated proinflammatory macrophage response in vivo. *Immunity* (2009) 31:110–121. doi:10.1016/j.immuni.2009.04.015

429. Hsu KM, Pratt JR, Akers WJ, Achilefu SI, Yokoyama WM. Murine cytomegalovirus displays selective infection of cells within hours after systemic administration. *J Gen Virol* (2009) 90:33–43. doi:10.1099/vir.0.006668-0

430. Elomaa O, Kangas M, Sahlberg C, Tuukkanen J, Sormunen R, Liakka A, Thesleff I, Kraal G, Tryggvason K. Cloning of a novel bacteria-binding receptor structurally related to scavenger receptors and expressed in a subset of macrophages. *Cell* (1995) 80:603–609. doi:10.1016/0092-8674(95)90514-6

431. Geijtenbeek TBH, Groot PC, Nolte MA, van Vliet SJ, Gangaram-Panday ST, van Duijnhoven GCF, Kraal G, van Oosterhout AJM, van Kooyk Y. Marginal zone macrophages express a murine homologue of DC-SIGN that captures blood-borne antigens in vivo. *Blood* (2002) 100:2908–2916. doi:10.1182/blood-2002-04-1044

432. Vanderheijden N, Delputte PL, Favoreel HW, Vandekerckhove J, Van Damme J, van Woensel PA, Nauwynck HJ. Involvement of sialoadhesin in entry of porcine reproductive and respiratory syndrome virus into porcine alveolar macrophages. *J Virol* (2003) 77:8207–8215. doi:10.1128/jvi.77.15.8207-8215.2003

433. Backer R, Schwandt T, Greuter M, Oosting M, Jüngerkes F, Tüting T, Boon L, O'Toole T, Kraal G, Limmer A, et al. Effective collaboration between marginal metallophilic macrophages and CD8+ dendritic cells in the generation of cytotoxic T cells. *Proc Natl Acad Sci U S A* (2010) 107:216–221. doi:10.1073/pnas.0909541107

434. Nolte MA, Arens R, Kraus M, van Oers MHJ, Kraal G, van Lier RAW, Mebius RE. B cells are crucial for both development and maintenance of the splenic marginal zone. *J Immunol* (2004) 172:3620–3627. doi:10.4049/jimmunol.172.6.3620

435. Tumanov AV, Grivennikov SI, Shakhov AN, Rybtsov SA, Koroleva EP, Takeda J, Nedospasov SA, Kuprash DV. Dissecting the role of lymphotoxin in lymphoid organs by conditional targeting. *Immunol Rev* (2003) 195:106–116. doi:10.1034/j.1600-065x.2003.00071.x

436. De Silva NS, Klein U. Dynamics of B cells in germinal centres. *Nat Rev Immunol* (2015) 15:137–148. doi:10.1038/nri3804

437. Lucin KM, Sanders VM, Popovich PG. Stress hormones collaborate to induce lymphocyte apoptosis after high level spinal cord injury. *J Neurochem* (2009) 110:1409–1421. doi:10.1111/j.1471-4159.2009.06232.x

438. Kohm AP, Sanders VM. Norepinephrine: a messenger from the brain to the immune system. *Immunol Today* (2000) 21:539–542. doi:10.1016/s0167-5699(00)01747-3

439. Lucin KM, Sanders VM, Jones TB, Malarkey WB, Popovich PG. Impaired antibody synthesis after spinal cord injury is level dependent and is due to sympathetic nervous system dysregulation. *Exp Neurol* (2007) 207:75–84. doi:10.1016/j.expneurol.2007.05.019

440. Zha J, Smith A, Andreansky S, Bracchi-Ricard V, Bethea JR. Chronic thoracic spinal cord injury impairs CD8+ T-cell function by up-regulating programmed cell death-1 expression. *J Neuroinflammation* (2014) 11:65. doi:10.1186/1742-2094-11-65

441. Zhang B-J, Men X-J, Lu Z-Q, Li H-Y, Qiu W, Hu X-Q. Splenectomy protects experimental rats from cerebral damage after stroke due to anti-inflammatory effects. *Chin Med J (Engl)* (2013) 126:2354–2360.

442. Riegger T, Conrad S, Schluesener HJ, Kaps H-P, Badke A, Baron C, Gerstein J, Dietz K, Abdizahdeh M, Schwab JM. Immune depression syndrome following human spinal cord injury (SCI): a pilot study. *Neuroscience* (2009) 158:1194–1199. doi:10.1016/j.neuroscience.2008.08.021

443. Campagnolo DI, Dixon D, Schwartz J, Bartlett JA, Keller SE. Altered innate immunity following spinal cord injury. *Spinal Cord* (2008) 46:477–481. doi:10.1038/sc.2008.4

444. Riegger T, Conrad S, Liu K, Schluesener HJ, Adibzahdeh M, Schwab JM. Spinal cord injury-induced immune depression syndrome (SCI-IDS). *Eur J Neurosci* (2007) 25:1743–1747. doi:10.1111/j.1460-9568.2007.05447.x

445. Lu J, Cao Q, Zheng D, Sun Y, Wang C, Yu X, Wang Y, Lee VWS, Zheng G, Tan TK, et al. Discrete functions of M 2a and M 2c macrophage subsets determine their relative efficacy in treating chronic kidney disease. *Kidney International* (2013) 84:745–755. doi:10.1038/ki.2013.135

446. Chistiakov DA, Bobryshev YV, Nikiforov NG, Elizova NV, Sobenin IA, Orekhov AN. Macrophage phenotypic plasticity in atherosclerosis: The associated features and the peculiarities of the expression of inflammatory genes. *Int J Cardiol* (2015) 184:436–445. doi:10.1016/j.ijcard.2015.03.055

447. Martinez FO, Sica A, Mantovani A, Locati M. Macrophage activation and polarization. *Front Biosci* (2008) 13:453–461. doi:10.2741/2692

448. Shapouri-Moghaddam A, Mohammadian S, Vazini H, Taghadosi M, Esmaeili S, Mardani F, Seifi B, Mohammadi A, Afshari JT, Sahebkar A. Macrophage plasticity, polarization, and function in health and disease. *Journal Cellular Physiology* (2018) 233:6425–6440. doi:10.1002/jcp.26429

449. Zizzo G, Hilliard BA, Monestier M, Cohen PL. Efficient clearance of early apoptotic cells by human macrophages requires M2c polarization and MerTK induction. *J Immunol* (2012) 189:3508–3520. doi:10.4049/jimmunol.1200662

450. Sica A, Mantovani A. Macrophage plasticity and polarization: in vivo veritas. *J Clin Invest* (2012) 122:787–795. doi:10.1172/JCI59643

451. Bashir S, Sharma Y, Elahi A, Khan F. Macrophage polarization: the link between inflammation and related diseases. *Inflamm Res* (2016) 65:1–11. doi:10.1007/s00011-015-0874-1

452. Biswas SK, Chittezhath M, Shalova IN, Lim J-Y. Macrophage polarization and plasticity in health and disease. *Immunol Res* (2012) 53:11–24. doi:10.1007/s12026-012-8291-9

453. Cassetta L, Cassol E, Poli G. Macrophage polarization in health and disease. *ScientificWorldJournal* (2011) 11:2391–2402. doi:10.1100/2011/213962

454. Locati M, Mantovani A, Sica A. Macrophage activation and polarization as an adaptive component of innate immunity. *Adv Immunol* (2013) 120:163–184. doi:10.1016/B978-0-12-417028-5.00006-5

455. Murray PJ, Allen JE, Biswas SK, Fisher EA, Gilroy DW, Goerdt S, Gordon S, Hamilton JA, Ivashkiv LB, Lawrence T, et al. Macrophage activation and polarization: nomenclature and experimental guidelines. *Immunity* (2014) 41:14–20. doi:10.1016/j.immuni.2014.06.008

456. Murray PJ, Wynn TA. Obstacles and opportunities for understanding macrophage polarization. *J Leukoc Biol* (2011) 89:557–563. doi:10.1189/jlb.0710409

457. Wang N, Liang H, Zen K. Molecular mechanisms that influence the macrophage m1-m2 polarization balance. *Front Immunol* (2014) 5:614. doi:10.3389/fimmu.2014.00614

458. Sica A, Erreni M, Allavena P, Porta C. Macrophage polarization in pathology. *Cell Mol Life Sci* (2015) 72:4111–4126. doi:10.1007/s00018-015-1995-y

459. Rőszer T. Understanding the Mysterious M2 Macrophage through Activation Markers and Effector Mechanisms. *Mediators of Inflammation* (2015) 2015:1–16. doi:10.1155/2015/816460

460. Colin S, Chinetti-Gbaguidi G, Staels B. Macrophage phenotypes in atherosclerosis. *Immunol Rev* (2014) 262:153–166. doi:10.1111/imr.12218

461. Ferrante CJ, Leibovich SJ. Regulation of Macrophage Polarization and Wound Healing. *Adv Wound Care (New Rochelle)* (2012) 1:10–16. doi:10.1089/wound.2011.0307

462. Lurier EB, Dalton D, Dampier W, Raman P, Nassiri S, Ferraro NM, Rajagopalan R, Sarmady M, Spiller KL. Transcriptome analysis of IL-10-stimulated (M2c) macrophages by next-generation sequencing. *Immunobiology* (2017) 222:847–856. doi:10.1016/j.imbio.2017.02.006

463. Duluc D, Corvaisier M, Blanchard S, Catala L, Descamps P, Gamelin E, Ponsoda S, Delneste Y, Hebbar M, Jeannin P. Interferon-gamma reverses the immunosuppressive and protumoral properties and prevents the generation of human tumor-associated macrophages. *Int J Cancer* (2009) 125:367–373. doi:10.1002/ijc.24401

464. Wang Q, Ni H, Lan L, Wei X, Xiang R, Wang Y. Fra-1 protooncogene regulates IL-6 expression in macrophages and promotes the generation of M2d macrophages. *Cell Res* (2010) 20:701–712. doi:10.1038/cr.2010.52

465. Ferrante CJ, Pinhal-Enfield G, Elson G, Cronstein BN, Hasko G, Outram S, Leibovich SJ. The adenosine-dependent angiogenic switch of macrophages to an M2-like phenotype is independent of interleukin-4 receptor alpha (IL-4Rα) signaling. *Inflammation* (2013) 36:921–931. doi:10.1007/s10753-013-9621-3

466. Haskó G, Pacher P, Deitch EA, Vizi ES. Shaping of monocyte and macrophage function by adenosine receptors. *Pharmacol Ther* (2007) 113:264–275. doi:10.1016/j.pharmthera.2006.08.003

467. Pinhal-Enfield G, Ramanathan M, Hasko G, Vogel SN, Salzman AL, Boons G-J, Leibovich SJ. An angiogenic switch in macrophages involving synergy between Toll-like receptors 2, 4, 7, and 9 and adenosine A(2A) receptors. *Am J Pathol* (2003) 163:711–721. doi:10.1016/S0002-9440(10)63698-X

468. Jackaman C, Yeoh TL, Acuil ML, Gardner JK, Nelson DJ. Murine mesothelioma induces locally-proliferating IL-10 + TNF-α + CD206 - CX3CR1 + M3 macrophages that can be selectively depleted by chemotherapy or immunotherapy. *OncoImmunology* (2016) 5:e1173299. doi:10.1080/2162402X.2016.1173299

469. Khong HT, Restifo NP. Natural selection of tumor variants in the generation of "tumor escape" phenotypes. *Nat Immunol* (2002) 3:999–1005. doi:10.1038/ni1102-999

470. Zou W. Regulatory T cells, tumour immunity and immunotherapy. *Nat Rev Immunol* (2006) 6:295–307. doi:10.1038/nri1806

471. Stout RD, Watkins SK, Suttles J. Functional plasticity of macrophages: in situ reprogramming of tumor-associated macrophages. *J Leukoc Biol* (2009) 86:1105–1109. doi:10.1189/jlb.0209073

472. Kalish S, Lyamina S, Manukhina E, Malyshev Y, Raetskaya A, Malyshev I. M3 Macrophages Stop Division of Tumor Cells In Vitro and Extend Survival of Mice with Ehrlich Ascites Carcinoma. *Med Sci Monit Basic Res* (2017) 23:8–19. doi:10.12659/MSMBR.902285

473. Mills CD, Kincaid K, Alt JM, Heilman MJ, Hill AM. M-1/M-2 Macrophages and the Th1/Th2 Paradigm1. *The Journal of Immunology* (2000) 164:6166–6173. doi:10.4049/jimmunol.164.12.6166

474. Ostrovskaia LA, Skibida IP, Krugliak SA, Emanuél' NM. [Kinetic peculiarities of the development of Ehrlich ascites tumor in linear and non-linear mice]. *Izv Akad Nauk SSSR Biol* (1966) 5:734–738.

475. Wu J, He S, Song Z, Chen S, Lin X, Sun H, Zhou P, Peng Q, Du S, Zheng S, et al. Macrophage polarization states in atherosclerosis. *Front Immunol* (2023) 14:1185587. doi:10.3389/fimmu.2023.1185587

476. Finn AV, Nakano M, Polavarapu R, Karmali V, Saeed O, Zhao X, Yazdani S, Otsuka F, Davis T, Habib A, et al. Hemoglobin directs macrophage differentiation and prevents foam cell formation in human atherosclerotic plaques. *J Am Coll Cardiol* (2012) 59:166–177. doi:10.1016/j.jacc.2011.10.852

477. Boyle JJ, Johns M, Kampfer T, Nguyen AT, Game L, Schaer DJ, Mason JC, Haskard DO. Activating Transcription Factor 1 Directs Mhem Atheroprotective Macrophages Through Coordinated Iron Handling and Foam Cell Protection. *Circ Res* (2012) 110:20–33. doi:10.1161/CIRCRESAHA.111.247577

478. Kadl A, Meher AK, Sharma PR, Lee MY, Doran AC, Johnstone SR, Elliott MR, Gruber F, Han J, Chen W, et al. Identification of a novel macrophage phenotype that develops in response to

atherogenic phospholipids via Nrf2. *Circ Res* (2010) 107:737–746. doi:10.1161/CIRCRESAHA.109.215715

479. Erbel C, Tyka M, Helmes CM, Akhavanpoor M, Rupp G, Domschke G, Linden F, Wolf A, Doesch A, Lasitschka F, et al. CXCL4-induced plaque macrophages can be specifically identified by co-expression of MMP7+S100A8+ in vitro and in vivo. *Innate Immun* (2015) 21:255–265. doi:10.1177/1753425914526461

480. Gleissner CA, Shaked I, Erbel C, Böckler D, Katus HA, Ley K. CXCL4 downregulates the atheroprotective hemoglobin receptor CD163 in human macrophages. *Circ Res* (2010) 106:203–211. doi:10.1161/CIRCRESAHA.109.199505

481. Domschke G, Gleissner CA. CXCL4-induced macrophages in human atherosclerosis. *Cytokine* (2019) 122:154141. doi:10.1016/j.cyto.2017.08.021

482. De Sousa JR, Lucena Neto FD, Sotto MN, Quaresma JAS. Immunohistochemical characterization of the M4 macrophage population in leprosy skin lesions. *BMC Infect Dis* (2018) 18:576. doi:10.1186/s12879-018-3478-x

483. Braun DA, Fribourg M, Sealfon SC. Cytokine response is determined by duration of receptor and signal transducers and activators of transcription 3 (STAT3) activation. *J Biol Chem* (2013) 288:2986–2993. doi:10.1074/jbc.M112.386573

484. Yasukawa H, Ohishi M, Mori H, Murakami M, Chinen T, Aki D, Hanada T, Takeda K, Akira S, Hoshijima M, et al. IL-6 induces an anti-inflammatory response in the absence of SOCS3 in macrophages. *Nat Immunol* (2003) 4:551–556. doi:10.1038/ni938

485. Gong D, Shi W, Yi S, Chen H, Groffen J, Heisterkamp N. TGFβ signaling plays a critical role in promoting alternative macrophage activation. *BMC Immunology* (2012) 13:31. doi:10.1186/1471-2172-13-31

486. Iseki S, Osumi-Yamashita N, Miyazono K, Franzén P, Ichijo H, Ohtani H, Hayashi Y, Eto K. Localization of transforming growth factor-beta type I and type II receptors in mouse development. *Exp Cell Res* (1995) 219:339–347. doi:10.1006/excr.1995.1237

487. Millan FA, Denhez F, Kondaiah P, Akhurst RJ. Embryonic gene expression patterns of TGF beta 1, beta 2 and beta 3 suggest different developmental functions in vivo. *Development* (1991) 111:131–143. doi:10.1242/dev.111.1.131

488. Roberts AB, Sporn MB. Differential expression of the TGF-beta isoforms in embryogenesis suggests specific roles in developing and adult tissues. *Mol Reprod Dev* (1992) 32:91–98. doi:10.1002/mrd.1080320203

489. Li MO, Wan YY, Sanjabi S, Robertson A-KL, Flavell RA. Transforming growth factor-beta regulation of immune responses. *Annu Rev Immunol* (2006) 24:99–146. doi:10.1146/annurev.immunol.24.021605.090737

490. Yuwen Y, Wang X, Liu J, Liu Z, Zhu H. Delta- like ligand 4- expressing macrophages and human diseases: Insights into pathophysiology and therapeutic opportunities. *Heliyon* (2023) 9:e20777. doi:10.1016/j.heliyon.2023.e20777

491. Covarrubias AJ, Aksoylar HI, Horng T. Control of macrophage metabolism and activation by mTOR and Akt signaling. *Semin Immunol* (2015) 27:286–296. doi:10.1016/j.smim.2015.08.001

492. Fung E, Tang S-MT, Canner JP, Morishige K, Arboleda-Velasquez JF, Cardoso AA, Carlesso N, Aster JC, Aikawa M. Delta-like 4 induces notch signaling in macrophages: implications for inflammation. *Circulation* (2007) 115:2948–2956. doi:10.1161/CIRCULATIONAHA.106.675462

493. Xu H, Zhu J, Smith S, Foldi J, Zhao B, Chung AY, Outtz H, Kitajewski J, Shi C, Weber S, et al. Notch-RBP-J signaling regulates the transcription factor IRF8 to promote inflammatory macrophage polarization. *Nat Immunol* (2012) 13:642–650. doi:10.1038/ni.2304

494. Shirey KA, Pletneva LM, Puche AC, Keegan AD, Prince GA, Blanco JCG, Vogel SN. Control of RSV-induced lung injury by alternatively activated macrophages is IL-4R alpha-, TLR4-, and IFN-beta-dependent. *Mucosal Immunol* (2010) 3:291–300. doi:10.1038/mi.2010.6

495. Porta C, Rimoldi M, Raes G, Brys L, Ghezzi P, Di Liberto D, Dieli F, Ghisletti S, Natoli G, De Baetselier P, et al. Tolerance and M2 (alternative) macrophage polarization are related processes orchestrated by p50 nuclear factor kappaB. *Proc Natl Acad Sci U S A* (2009) 106:14978–14983. doi:10.1073/pnas.0809784106

496. Ehrchen J, Steinmüller L, Barczyk K, Tenbrock K, Nacken W, Eisenacher M, Nordhues U, Sorg C, Sunderkötter C, Roth J. Glucocorticoids induce differentiation of a specifically activated, anti-inflammatory subtype of human monocytes. *Blood* (2007) 109:1265–1274. doi:10.1182/blood-2006-02-001115

497. Doyle AG, Herbein G, Montaner LJ, Minty AJ, Caput D, Ferrara P, Gordon S. Interleukin-13 alters the activation state of murine macrophages in vitro: comparison with interleukin-4 and interferon-gamma. *Eur J Immunol* (1994) 24:1441–1445. doi:10.1002/eji.1830240630

498. Stein M, Keshav S, Harris N, Gordon S. Interleukin 4 potently enhances murine macrophage mannose receptor activity: a marker of alternative immunologic macrophage activation. *J Exp Med* (1992) 176:287–292. doi:10.1084/jem.176.1.287

499. Austermann J, Roth J, Barczyk-Kahlert K. The Good and the Bad: Monocytes' and Macrophages' Diverse Functions in Inflammation. *Cells* (2022) 11:1979. doi:10.3390/cells11121979

500. Laria A, Lurati A, Marrazza M, Mazzocchi D, Re KA, Scarpellini M. The macrophages in rheumatic diseases. *J Inflamm Res* (2016) 9:1–11. doi:10.2147/JIR.S82320

501. Gurtner GC, Werner S, Barrandon Y, Longaker MT. Wound repair and regeneration. *Nature* (2008) 453:314–321. doi:10.1038/nature07039

502. Novak ML, Koh TJ. Phenotypic transitions of macrophages orchestrate tissue repair. *Am J Pathol* (2013) 183:1352–1363. doi:10.1016/j.ajpath.2013.06.034

503. Lech M, Anders H-J. Macrophages and fibrosis: How resident and infiltrating mononuclear phagocytes orchestrate all phases of tissue injury and repair. *Biochim Biophys Acta* (2013) 1832:989–997. doi:10.1016/j.bbadis.2012.12.001

504. Sindrilaru A, Scharffetter-Kochanek K. Disclosure of the Culprits: Macrophages-Versatile Regulators of Wound Healing. *Adv Wound Care (New Rochelle)* (2013) 2:357–368. doi:10.1089/wound.2012.0407

505. Novak ML, Koh TJ. Macrophage phenotypes during tissue repair. *J Leukoc Biol* (2013) 93:875–881. doi:10.1189/jlb.1012512

506. Daley JM, Brancato SK, Thomay AA, Reichner JS, Albina JE. The phenotype of murine wound macrophages. *J Leukoc Biol* (2010) 87:59–67. doi:10.1189/jlb.0409236

507. Sindrilaru A, Peters T, Wieschalka S, Baican C, Baican A, Peter H, Hainzl A, Schatz S, Qi Y, Schlecht A, et al. An unrestrained proinflammatory M1 macrophage population induced by iron impairs wound healing in humans and mice. *J Clin Invest* (2011) 121:985–997. doi:10.1172/JCI44490

508. Werdin F, Tennenhaus M, Schaller H-E, Rennekampff H-O. Evidence-based management strategies for treatment of chronic wounds. *Eplasty* (2009) 9:e19.

509. Kigerl KA, Gensel JC, Ankeny DP, Alexander JK, Donnelly DJ, Popovich PG. Identification of Two Distinct Macrophage Subsets with Divergent Effects Causing either Neurotoxicity or Regeneration in the Injured Mouse Spinal Cord. *J Neurosci* (2009) 29:13435–13444. doi:10.1523/JNEUROSCI.3257-09.2009

510. Nocentini G, Cuzzocrea S, Genovese T, Bianchini R, Mazzon E, Ronchetti S, Esposito E, Rosanna DP, Bramanti P, Riccardi C. Glucocorticoid-induced tumor necrosis factor receptor-related (GITR)-Fc fusion protein inhibits GITR triggering and protects from the inflammatory response after spinal cord injury. *Mol Pharmacol* (2008) 73:1610–1621. doi:10.1124/mol.107.044354

511. Sato A, Ohtaki H, Tsumuraya T, Song D, Ohara K, Asano M, Iwakura Y, Atsumi T, Shioda S. Interleukin-1 participates in the classical and alternative activation of microglia/macrophages after spinal cord injury. *J Neuroinflammation* (2012) 9:65. doi:10.1186/1742-2094-9-65

512. Kuo H-S, Tsai M-J, Huang M-C, Chiu C-W, Tsai C-Y, Lee M-J, Huang W-C, Lin Y-L, Kuo W-C, Cheng H. Acid fibroblast growth factor and peripheral nerve grafts regulate Th2 cytokine expression, macrophage activation, polyamine synthesis, and neurotrophin expression in transected rat spinal cords. *J Neurosci* (2011) 31:4137–4147. doi:10.1523/JNEUROSCI.2592-10.2011

513. Guerrero AR, Uchida K, Nakajima H, Watanabe S, Nakamura M, Johnson WE, Baba H. Blockade of interleukin-6 signaling inhibits the classic pathway and promotes an alternative pathway of macrophage activation after spinal cord injury in mice. *J Neuroinflammation* (2012) 9:40. doi:10.1186/1742-2094-9-40

514. Nakajima H, Uchida K, Guerrero AR, Watanabe S, Sugita D, Takeura N, Yoshida A, Long G, Wright KT, Johnson WEB, et al. Transplantation of mesenchymal stem cells promotes an alternative pathway of macrophage activation and functional recovery after spinal cord injury. *J Neurotrauma* (2012) 29:1614–1625. doi:10.1089/neu.2011.2109

515. Thawer SG, Mawhinney L, Chadwick K, de Chickera SN, Weaver LC, Brown A, Dekaban GA. Temporal changes in monocyte and macrophage subsets and microglial macrophages following spinal cord injury in the Lys-Egfp-ki mouse model. *J Neuroimmunol* (2013) 261:7–20. doi:10.1016/j.jneuroim.2013.04.008

516. Shechter R, Schwartz M. CNS sterile injury: just another wound healing? *Trends Mol Med* (2013) 19:135–143. doi:10.1016/j.molmed.2012.11.007

517. Burda JE, Sofroniew MV. Reactive gliosis and the multicellular response to CNS damage and disease. *Neuron* (2014) 81:229–248. doi:10.1016/j.neuron.2013.12.034

518. Beattie MS, Bresnahan JC, Komon J, Tovar CA, Van Meter M, Anderson DK, Faden AI, Hsu CY, Noble LJ, Salzman S, et al. Endogenous repair after spinal cord contusion injuries in the rat. *Exp Neurol* (1997) 148:453–463. doi:10.1006/exnr.1997.6695

519. Krzyszczyk P, Schloss R, Palmer A, Berthiaume F. The Role of Macrophages in Acute and Chronic Wound Healing and Interventions to Promote Pro-wound Healing Phenotypes. *Front Physiol* (2018) 9:419. doi:10.3389/fphys.2018.00419

520. Wang X, Cao K, Sun X, Chen Y, Duan Z, Sun L, Guo L, Bai P, Sun D, Fan J, et al. Macrophages in spinal cord injury: Phenotypic and functional change from exposure to myelin debris. *Glia* (2015) 63:635–651. doi:10.1002/glia.22774

521. Giulian D, Robertson C. Inhibition of mononuclear phagocytes reduces ischemic injury in the spinal cord. *Ann Neurol* (1990) 27:33–42. doi:10.1002/ana.410270107

522. Popovich PG, Guan Z, Wei P, Huitinga I, van Rooijen N, Stokes BT. Depletion of hematogenous macrophages promotes partial hindlimb recovery and neuroanatomical repair after experimental spinal cord injury. *Exp Neurol* (1999) 158:351–365. doi:10.1006/exnr.1999.7118

523. Gris D, Marsh DR, Oatway MA, Chen Y, Hamilton EF, Dekaban GA, Weaver LC. Transient blockade of the CD11d/CD18 integrin reduces secondary damage after spinal cord injury, improving sensory, autonomic, and motor function. *J Neurosci* (2004) 24:4043–4051. doi:10.1523/JNEUROSCI.5343-03.2004

524. Fang P, Li X, Dai J, Cole L, Camacho JA, Zhang Y, Ji Y, Wang J, Yang X-F, Wang H. Immune cell subset differentiation and tissue inflammation. *J Hematol Oncol* (2018) 11:97. doi:10.1186/s13045-018-0637-x

525. Porta C, Riboldi E, Ippolito A, Sica A. Molecular and epigenetic basis of macrophage polarized activation. *Semin Immunol* (2015) 27:237–248. doi:10.1016/j.smim.2015.10.003

526. Didangelos A, Puglia M, Iberl M, Sanchez-Bellot C, Roschitzki B, Bradbury EJ. High-throughput proteomics reveal alarmins as amplifiers of tissue pathology and inflammation after spinal cord injury. *Sci Rep* (2016) 6:21607. doi:10.1038/srep21607

527. Papatheodorou A, Stein A, Bank M, Sison CP, Gibbs K, Davies P, Bloom O. High-Mobility Group Box 1 (HMGB1) Is Elevated Systemically in Persons with Acute or Chronic Traumatic Spinal Cord Injury. *J Neurotrauma* (2017) 34:746–754. doi:10.1089/neu.2016.4596

528. Liu T, Zhang L, Joo D, Sun S-C. NF-κB signaling in inflammation. *Signal Transduct Target Ther* (2017) 2:17023-. doi:10.1038/sigtrans.2017.23

529. Pineau I, Lacroix S. Proinflammatory cytokine synthesis in the injured mouse spinal cord: multiphasic expression pattern and identification of the cell types involved. *J Comp Neurol* (2007) 500:267–285. doi:10.1002/cne.21149

530. Grell M, Douni E, Wajant H, Löhden M, Clauss M, Maxeiner B, Georgopoulos S, Lesslauer W, Kollias G, Pfizenmaier K, et al. The transmembrane form of tumor necrosis factor is the prime activating ligand of the 80 kDa tumor necrosis factor receptor. *Cell* (1995) 83:793–802. doi:10.1016/0092-8674(95)90192-2

531. Mironets E, Osei-Owusu P, Bracchi-Ricard V, Fischer R, Owens EA, Ricard J, Wu D, Saltos T, Collyer E, Hou S, et al. Soluble TNFα Signaling within the Spinal Cord Contributes to the Development

of Autonomic Dysreflexia and Ensuing Vascular and Immune Dysfunction after Spinal Cord Injury. *J Neurosci* (2018) 38:4146–4162. doi:10.1523/JNEUROSCI.2376-17.2018

532. Novrup HG, Bracchi-Ricard V, Ellman DG, Ricard J, Jain A, Runko E, Lyck L, Yli-Karjanmaa M, Szymkowski DE, Pearse DD, et al. Central but not systemic administration of XPro1595 is therapeutic following moderate spinal cord injury in mice. *J Neuroinflammation* (2014) 11:159. doi:10.1186/s12974-014-0159-6

533. Boato F, Rosenberger K, Nelissen S, Geboes L, Peters EM, Nitsch R, Hendrix S. Absence of IL-1β positively affects neurological outcome, lesion development and axonal plasticity after spinal cord injury. *Journal of Neuroinflammation* (2013) 10:792. doi:10.1186/1742-2094-10-6

534. Coste A, Dubourdeau M, Linas MD, Cassaing S, Lepert J-C, Balard P, Chalmeton S, Bernad J, Orfila C, Séguéla J-P, et al. PPARgamma promotes mannose receptor gene expression in murine macrophages and contributes to the induction of this receptor by IL-13. *Immunity* (2003) 19:329–339. doi:10.1016/s1074-7613(03)00229-2

535. Odegaard JI, Ricardo-Gonzalez RR, Red Eagle A, Vats D, Morel CR, Goforth MH, Subramanian V, Mukundan L, Ferrante AW, Chawla A. Alternative M2 activation of Kupffer cells by PPARdelta ameliorates obesity-induced insulin resistance. *Cell Metab* (2008) 7:496–507. doi:10.1016/j.cmet.2008.04.003

536. Murray PJ. Understanding and exploiting the endogenous interleukin-10/STAT3-mediated anti-inflammatory response. *Curr Opin Pharmacol* (2006) 6:379–386. doi:10.1016/j.coph.2006.01.010

537. Francos-Quijorna I, Amo-Aparicio J, Martinez-Muriana A, López-Vales R. IL-4 drives microglia and macrophages toward a phenotype conducive for tissue repair and functional recovery after spinal cord injury. *Glia* (2016) 64:2079–2092. doi:10.1002/glia.23041

538. Lee SI, Jeong SR, Kang YM, Han DH, Jin BK, Namgung U, Kim BG. Endogenous expression of interleukin-4 regulates macrophage activation and confines cavity formation after traumatic spinal cord injury. *J Neurosci Res* (2010) 88:2409–2419. doi:10.1002/jnr.22411

539. Mukhamedshina YO, Akhmetzyanova ER, Martynova EV, Khaiboullina SF, Galieva LR, Rizvanov AA. Systemic and Local Cytokine Profile following Spinal Cord Injury in Rats: A Multiplex Analysis. *Front Neurol* (2017) 8:581. doi:10.3389/fneur.2017.00581

540. Kroner A, Greenhalgh AD, Zarruk JG, Passos dos Santos R, Gaestel M, David S. TNF and Increased Intracellular Iron Alter Macrophage Polarization to a Detrimental M1 Phenotype in the Injured Spinal Cord. *Neuron* (2014) 83:1098–1116. doi:10.1016/j.neuron.2014.07.027

541. Yao A, Liu F, Chen K, Tang L, Liu L, Zhang K, Yu C, Bian G, Guo H, Zheng J, et al. Programmed death 1 deficiency induces the polarization of macrophages/microglia to the M1 phenotype after spinal cord injury in mice. *Neurotherapeutics* (2014) 11:636–650. doi:10.1007/s13311-013-0254-x

542. Kezic J, McMenamin PG. Differential turnover rates of monocyte-derived cells in varied ocular tissue microenvironments. *J Leukoc Biol* (2008) 84:721–729. doi:10.1189/jlb.0308166

543. Tymoszuk P, Evens H, Marzola V, Wachowicz K, Wasmer M-H, Datta S, Müller-Holzner E, Fiegl H, Böck G, van Rooijen N, et al. In situ proliferation contributes to accumulation of tumor-associated macrophages in spontaneous mammary tumors. *Eur J Immunol* (2014) 44:2247–2262. doi:10.1002/eji.201344304

544. Robbins CS, Hilgendorf I, Weber GF, Theurl I, Iwamoto Y, Figueiredo J-L, Gorbatov R, Sukhova GK, Gerhardt LMS, Smyth D, et al. Local proliferation dominates lesional macrophage accumulation in atherosclerosis. *Nat Med* (2013) 19:1166–1172. doi:10.1038/nm.3258

545. Shechter R, London A, Varol C, Raposo C, Cusimano M, Yovel G, Rolls A, Mack M, Pluchino S, Martino G, et al. Infiltrating Blood-Derived Macrophages Are Vital Cells Playing an Anti-inflammatory Role in Recovery from Spinal Cord Injury in Mice. *PLoS Med* (2009) 6:e1000113. doi:10.1371/journal.pmed.1000113

546. Hines DJ, Hines RM, Mulligan SJ, Macvicar BA. Microglia processes block the spread of damage in the brain and require functional chloride channels. *Glia* (2009) 57:1610–1618. doi:10.1002/glia.20874

547. Greenhalgh AD, David S. Differences in the Phagocytic Response of Microglia and Peripheral Macrophages after Spinal Cord Injury and Its Effects on Cell Death. *J Neurosci* (2014) 34:6316–6322. doi:10.1523/JNEUROSCI.4912-13.2014

548. Boven LA, Van Meurs M, Van Zwam M, Wierenga-Wolf A, Hintzen RQ, Boot RG, Aerts JM, Amor S, Nieuwenhuis EE, Laman JD. Myelin-laden macrophages are anti-inflammatory, consistent with foam cells in multiple sclerosis. *Brain* (2006) 129:517–526. doi:10.1093/brain/awh707

549. Liu Y, Hao W, Letiembre M, Walter S, Kulanga M, Neumann H, Fassbender K. Suppression of Microglial Inflammatory Activity by Myelin Phagocytosis: Role of p47-PHOX-Mediated Generation of Reactive Oxygen Species. *J Neurosci* (2006) 26:12904–12913. doi:10.1523/JNEUROSCI.2531-06.2006

550. van Rossum D, Hilbert S, Strassenburg S, Hanisch U-K, Brück W. Myelin-phagocytosing macrophages in isolated sciatic and optic nerves reveal a unique reactive phenotype. *Glia* (2008) 56:271–283. doi:10.1002/glia.20611

551. Lindborg JA, Mack M, Zigmond RE. Neutrophils Are Critical for Myelin Removal in a Peripheral Nerve Injury Model of Wallerian Degeneration. *J Neurosci* (2017) 37:10258–10277. doi:10.1523/JNEUROSCI.2085-17.2017

552. Savill J, Hogg N, Ren Y, Haslett C. Thrombospondin cooperates with CD36 and the vitronectin receptor in macrophage recognition of neutrophils undergoing apoptosis. *J Clin Invest* (1992) 90:1513–1522. doi:10.1172/JCI116019

553. McKeon RJ, Schreiber RC, Rudge JS, Silver J. Reduction of neurite outgrowth in a model of glial scarring following CNS injury is correlated with the expression of inhibitory molecules on reactive astrocytes. *J Neurosci* (1991) 11:3398–3411. doi:10.1523/JNEUROSCI.11-11-03398.1991

554. Ahuja CS, Martin AR, Fehlings M. Recent advances in managing a spinal cord injury secondary to trauma. *F1000Res* (2016) 5:F1000 Faculty Rev-1017. doi:10.12688/f1000research.7586.1

555. Busch SA, Silver J. The role of extracellular matrix in CNS regeneration. *Curr Opin Neurobiol* (2007) 17:120–127. doi:10.1016/j.conb.2006.09.004

556. Galtrey CM, Fawcett JW. The role of chondroitin sulfate proteoglycans in regeneration and plasticity in the central nervous system. *Brain Res Rev* (2007) 54:1–18. doi:10.1016/j.brainresrev.2006.09.006

557. Kaushal V, Koeberle PD, Wang Y, Schlichter LC. The Ca2+-activated K+ channel KCNN4/KCa3.1 contributes to microglia activation and nitric oxide-dependent neurodegeneration. *J Neurosci* (2007) 27:234–244. doi:10.1523/JNEUROSCI.3593-06.2007

558. Zhou X, He X, Ren Y. Function of microglia and macrophages in secondary damage after spinal cord injury. *Neural Regen Res* (2014) 9:1787. doi:10.4103/1673-5374.143423

559. Horn KP, Busch SA, Hawthorne AL, van Rooijen N, Silver J. Another barrier to regeneration in the CNS: activated macrophages induce extensive retraction of dystrophic axons through direct physical interactions. *J Neurosci* (2008) 28:9330–9341. doi:10.1523/JNEUROSCI.2488-08.2008

560. Hata K, Fujitani M, Yasuda Y, Doya H, Saito T, Yamagishi S, Mueller BK, Yamashita T. RGMa inhibition promotes axonal growth and recovery after spinal cord injury. *The Journal of Cell Biology* (2006) 173:47–58. doi:10.1083/jcb.200508143

561. Busch SA, Horn KP, Silver DJ, Silver J. Overcoming macrophage-mediated axonal dieback following CNS injury. *J Neurosci* (2009) 29:9967–9976. doi:10.1523/JNEUROSCI.1151-09.2009

562. Streit WJ, Semple-Rowland SL, Hurley SD, Miller RC, Popovich PG, Stokes BT. Cytokine mRNA profiles in contused spinal cord and axotomized facial nucleus suggest a beneficial role for inflammation and gliosis. *Exp Neurol* (1998) 152:74–87. doi:10.1006/exnr.1998.6835

563. Merrill JE, Scolding NJ. Mechanisms of damage to myelin and oligodendrocytes and their relevance to disease. *Neuropathol Appl Neurobiol* (1999) 25:435–458. doi:10.1046/j.1365-2990.1999.00200.x

564. Rosenberg LJ, Teng YD, Wrathall JR. 2,3-Dihydroxy-6-nitro-7-sulfamoyl-benzo(f)quinoxaline reduces glial loss and acute white matter pathology after experimental spinal cord contusion. *J Neurosci* (1999) 19:464–475. doi:10.1523/JNEUROSCI.19-01-00464.1999

565. Classen A, Lloberas J, Celada A. Macrophage activation: classical versus alternative. *Methods Mol Biol* (2009) 531:29–43. doi:10.1007/978-1-59745-396-7_3

566. Comalada M, Yeramian A, Modolell M, Lloberas J, Celada A. Arginine and macrophage activation. *Methods Mol Biol* (2012) 844:223–235. doi:10.1007/978-1-61779-527-5_16

567. Cloutier F, Sears-Kraxberger I, Keachie K, Keirstead HS. Immunological demyelination triggers macrophage/microglial cells activation without inducing astrogliosis. *Clin Dev Immunol* (2013) 2013:812456. doi:10.1155/2013/812456

568. McTigue DM. Potential Therapeutic Targets for PPARgamma after Spinal Cord Injury. *PPAR Res* (2008) 2008:517162. doi:10.1155/2008/517162

569. Hall ED, Traystman RJ. Role of animal studies in the design of clinical trials. *Front Neurol Neurosci* (2009) 25:10–33. doi:10.1159/000209470

570. Dalli J, Serhan CN. Specific lipid mediator signatures of human phagocytes: microparticles stimulate macrophage efferocytosis and pro-resolving mediators. *Blood* (2012) 120:e60-72. doi:10.1182/blood-2012-04-423525

571. Liu N-K, Xu X-M. Phospholipase A2 and its molecular mechanism after spinal cord injury. *Mol Neurobiol* (2010) 41:197–205. doi:10.1007/s12035-010-8101-0

572. Buczynski MW, Svensson CI, Dumlao DS, Fitzsimmons BL, Shim J-H, Scherbart TJ, Jacobsen FE, Hua X-Y, Yaksh TL, Dennis EA. Inflammatory hyperalgesia induces essential bioactive lipid production in the spinal cord. *J Neurochem* (2010) 114:981–993. doi:10.1111/j.1471-4159.2010.06815.x

573. Noguchi K, Okubo M. Leukotrienes in nociceptive pathway and neuropathic/inflammatory pain. *Biol Pharm Bull* (2011) 34:1163–1169. doi:10.1248/bpb.34.1163

574. Song G, Yang R, Zhang Q, Chen L, Huang D, Zeng J, Yang C, Zhang T. TGF-β Secretion by M2 Macrophages Induces Glial Scar Formation by Activating Astrocytes In Vitro. *J Mol Neurosci* (2019) 69:324–332. doi:10.1007/s12031-019-01361-5

575. Fujiyoshi T, Kubo T, Chan CCM, Koda M, Okawa A, Takahashi K, Yamazaki M. Interferon-γ Decreases Chondroitin Sulfate Proteoglycan Expression and Enhances Hindlimb Function after Spinal Cord Injury in Mice. *Journal of Neurotrauma* (2010) 27:2283–2294. doi:10.1089/neu.2009.1144

576. Yaguchi M, Ohta S, Toyama Y, Kawakami Y, Toda M. Functional recovery after spinal cord injury in mice through activation of microglia and dendritic cells after IL-12 administration. *Journal of Neuroscience Research* (2008) 86:1972–1980. doi:10.1002/jnr.21658

577. Bethea JR, Nagashima H, Acosta MC, Briceno C, Gomez F, Marcillo AE, Loor K, Green J, Dietrich WD. Systemically administered interleukin-10 reduces tumor necrosis factor-alpha production and significantly improves functional recovery following traumatic spinal cord injury in rats. *J Neurotrauma* (1999) 16:851–863. doi:10.1089/neu.1999.16.851

578. Monteiro S, Salgado AJ, Silva NA. Immunomodulation as a neuroprotective strategy after spinal cord injury. *Neural Regen Res* (2018) 13:423–424. doi:10.4103/1673-5374.228722

579. Lima R, Monteiro S, Lopes J, Barradas P, Vasconcelos N, Gomes E, Assunção-Silva R, Teixeira F, Morais M, Sousa N, et al. Systemic Interleukin-4 Administration after Spinal Cord Injury Modulates Inflammation and Promotes Neuroprotection. *Pharmaceuticals* (2017) 10:83. doi:10.3390/ph10040083

580. Hume DA, MacDonald KPA. Therapeutic applications of macrophage colony-stimulating factor-1 (CSF-1) and antagonists of CSF-1 receptor (CSF-1R) signaling. *Blood* (2012) 119:1810–1820. doi:10.1182/blood-2011-09-379214

581. Hong C, Tontonoz P. Coordination of inflammation and metabolism by PPAR and LXR nuclear receptors. *Curr Opin Genet Dev* (2008) 18:461–467. doi:10.1016/j.gde.2008.07.016

582. Wynn TA, Chawla A, Pollard JW. Macrophage biology in development, homeostasis and disease. *Nature* (2013) 496:445–455. doi:10.1038/nature12034

583. Boissonneault V, Filali M, Lessard M, Relton J, Wong G, Rivest S. Powerful beneficial effects of macrophage colony-stimulating factor on beta-amyloid deposition and cognitive impairment in Alzheimer's disease. *Brain* (2009) 132:1078–1092. doi:10.1093/brain/awn331

584. Yagihashi A, Sekiya T, Suzuki S. Macrophage colony stimulating factor (M-CSF) protects spiral ganglion neurons following auditory nerve injury: morphological and functional evidence. *Exp Neurol* (2005) 192:167–177. doi:10.1016/j.expneurol.2004.10.020

585. Berezovskaya O, Maysinger D, Fedoroff S. Colony stimulating factor-1 potentiates neuronal survival in cerebral cortex ischemic lesion. *Acta Neuropathol* (1996) 92:479–486. doi:10.1007/s004010050550

586. Zhang Z, Li M, Wang Y, Wu J, Li J. Higenamine promotes M2 macrophage activation and reduces Hmgb1 production through HO-1 induction in a murine model of spinal cord injury. *Int Immunopharmacol* (2014) 23:681–687. doi:10.1016/j.intimp.2014.10.022

587. Zhang B, Bailey WM, Kopper TJ, Orr MB, Feola DJ, Gensel JC. Azithromycin drives alternative macrophage activation and improves recovery and tissue sparing in contusion spinal cord injury. *J Neuroinflammation* (2015) 12:218. doi:10.1186/s12974-015-0440-3

588. Ji X-C, Dang Y-Y, Gao H-Y, Wang Z-T, Gao M, Yang Y, Zhang H-T, Xu R-X. Local Injection of Lenti-BDNF at the Lesion Site Promotes M2 Macrophage Polarization and Inhibits Inflammatory Response After Spinal Cord Injury in Mice. *Cell Mol Neurobiol* (2015) 35:881–890. doi:10.1007/s10571-015-0182-x

589. Semita IN, Utomo DN, Suroto H, Sudiana IK, Gandi P. The mechanism of human neural stem cell secretomes improves neuropathic pain and locomotor function in spinal cord injury rat models: through antioxidant, anti-inflammatory, anti-matrix degradation, and neurotrophic activities. *Korean J Pain* (2023) 36:72–83. doi:10.3344/kjp.22279

590. Zhang Q, Bian G, Chen P, Liu L, Yu C, Liu F, Xue Q, Chung SK, Song B, Ju G, et al. Aldose Reductase Regulates Microglia/Macrophages Polarization Through the cAMP Response Element-Binding Protein After Spinal Cord Injury in Mice. *Mol Neurobiol* (2016) 53:662–676. doi:10.1007/s12035-014-9035-8

591. Popovich PG, Guan Z, McGaughy V, Fisher L, Hickey WF, Basso DM. The neuropathological and behavioral consequences of intraspinal microglial/macrophage activation. *J Neuropathol Exp Neurol* (2002) 61:623–633. doi:10.1093/jnen/61.7.623

592. Kobashi S, Terashima T, Katagi M, Nakae Y, Okano J, Suzuki Y, Urushitani M, Kojima H. Transplantation of M2-Deviated Microglia Promotes Recovery of Motor Function after Spinal Cord Injury in Mice. *Molecular Therapy* (2020) 28:254–265. doi:10.1016/j.ymthe.2019.09.004

593. Han GH, Kim SJ, Ko W-K, Lee D, Han I-B, Sheen SH, Hong JB, Sohn S. Transplantation of tauroursodeoxycholic acid–inducing M2-phenotype macrophages promotes an anti-neuroinflammatory effect and functional recovery after spinal cord injury in rats. *Cell Proliferation* (2021) 54:e13050. doi:10.1111/cpr.13050

594. Ma S-F, Chen Y-J, Zhang J-X, Shen L, Wang R, Zhou J-S, Hu J-G, Lü H-Z. Adoptive transfer of M2 macrophages promotes locomotor recovery in adult rats after spinal cord injury. *Brain Behav Immun* (2015) 45:157–170. doi:10.1016/j.bbi.2014.11.007

595. Bomstein Y, Marder JB, Vitner K, Smirnov I, Lisaey G, Butovsky O, Fulga V, Yoles E. Features of skin-coincubated macrophages that promote recovery from spinal cord injury. *J Neuroimmunol* (2003) 142:10–16. doi:10.1016/s0165-5728(03)00260-1

596. Lammertse DP, Jones LAT, Charlifue SB, Kirshblum SC, Apple DF, Ragnarsson KT, Falci SP, Heary RF, Choudhri TF, Jenkins AL, et al. Autologous incubated macrophage therapy in acute, complete spinal cord injury: results of the phase 2 randomized controlled multicenter trial. *Spinal Cord* (2012) 50:661–671. doi:10.1038/sc.2012.39

597. Matsubara K, Matsushita Y, Sakai K, Kano F, Kondo M, Noda M, Hashimoto N, Imagama S, Ishiguro N, Suzumura A, et al. Secreted ectodomain of sialic acid-binding Ig-like lectin-9 and monocyte chemoattractant protein-1 promote recovery after rat spinal cord injury by altering macrophage polarity. *J Neurosci* (2015) 35:2452–2464. doi:10.1523/JNEUROSCI.4088-14.2015

598. Yang R, Gao H, Chen L, Fang N, Chen H, Song G, Yu L, Zhang Q, Zhang T. Effect of peripheral blood-derived mesenchymal stem cells on macrophage polarization and Th17/Treg balance in vitro. *Regen Ther* (2020) 14:275–283. doi:10.1016/j.reth.2020.03.008

599. Bartel DP. Metazoan MicroRNAs. *Cell* (2018) 173:20–51. doi:10.1016/j.cell.2018.03.006

600. Ha M, Kim VN. Regulation of microRNA biogenesis. *Nat Rev Mol Cell Biol* (2014) 15:509–524. doi:10.1038/nrm3838

601. Khayati S, Dehnavi S, Sadeghi M, Tavakol Afshari J, Esmaeili S-A, Mohammadi M. The potential role of miRNA in regulating macrophage polarization. *Heliyon* (2023) 9:e21615. doi:10.1016/j.heliyon.2023.e21615

602. Jablonski KA, Gaudet AD, Amici SA, Popovich PG, Guerau-de-Arellano M. Control of the Inflammatory Macrophage Transcriptional Signature by miR-155. *PLoS One* (2016) 11:e0159724. doi:10.1371/journal.pone.0159724

603. Pasca S, Jurj A, Petrushev B, Tomuleasa C, Matei D. MicroRNA-155 Implication in M1 Polarization and the Impact in Inflammatory Diseases. *Front Immunol* (2020) 11:625. doi:10.3389/fimmu.2020.00625

604. Gaudet AD, Mandrekar-Colucci S, Hall JCE, Sweet DR, Schmitt PJ, Xu X, Guan Z, Mo X, Guerau-de-Arellano M, Popovich PG. miR-155 Deletion in Mice Overcomes Neuron-Intrinsic and Neuron-

Extrinsic Barriers to Spinal Cord Repair. *J Neurosci* (2016) 36:8516–8532. doi:10.1523/JNEUROSCI.0735-16.2016

605. Ponomarev ED, Veremeyko T, Barteneva N, Krichevsky AM, Weiner HL. MicroRNA-124 promotes microglia quiescence and suppresses EAE by deactivating macrophages via the C/EBP-α-PU.1 pathway. *Nat Med* (2011) 17:64–70. doi:10.1038/nm.2266

606. Veremeyko T, Siddiqui S, Sotnikov I, Yung A, Ponomarev ED. IL-4/IL-13-dependent and independent expression of miR-124 and its contribution to M2 phenotype of monocytic cells in normal conditions and during allergic inflammation. *PLoS One* (2013) 8:e81774. doi:10.1371/journal.pone.0081774

607. Willemen HLDM, Huo X-J, Mao-Ying Q-L, Zijlstra J, Heijnen CJ, Kavelaars A. MicroRNA-124 as a novel treatment for persistent hyperalgesia. *J Neuroinflammation* (2012) 9:143. doi:10.1186/1742-2094-9-143

608. Mishima T, Mizuguchi Y, Kawahigashi Y, Takizawa T, Takizawa T. RT-PCR-based analysis of microRNA (miR-1 and -124) expression in mouse CNS. *Brain Res* (2007) 1131:37–43. doi:10.1016/j.brainres.2006.11.035

609. Hohjoh H, Fukushima T. Expression profile analysis of microRNA (miRNA) in mouse central nervous system using a new miRNA detection system that examines hybridization signals at every step of washing. *Gene* (2007) 391:39–44. doi:10.1016/j.gene.2006.11.018

610. Cui Y, Yin Y, Xiao Z, Zhao Y, Chen B, Yang B, Xu B, Song H, Zou Y, Ma X, et al. LncRNA Neat1 mediates miR-124-induced activation of Wnt/β-catenin signaling in spinal cord neural progenitor cells. *Stem Cell Res Ther* (2019) 10:400. doi:10.1186/s13287-019-1487-3

611. Song J-L, Zheng W, Chen W, Qian Y, Ouyang Y-M, Fan C-Y. Lentivirus-mediated microRNA-124 gene-modified bone marrow mesenchymal stem cell transplantation promotes the repair of spinal cord injury in rats. *Exp Mol Med* (2017) 49:e332. doi:10.1038/emm.2017.48

612. Men Y, Yelick J, Jin S, Tian Y, Chiang MSR, Higashimori H, Brown E, Jarvis R, Yang Y. Exosome reporter mice reveal the involvement of exosomes in mediating neuron to astroglia communication in the CNS. *Nat Commun* (2019) 10:4136. doi:10.1038/s41467-019-11534-w

613. Zhou X, Hong Y, Shang Z, Abuzeid AMI, Lin J, Li G. The Potential Role of MicroRNA-124-3p in Growth, Development, and Reproduction of Schistosoma japonicum. *Front Cell Infect Microbiol* (2022) 12:862496. doi:10.3389/fcimb.2022.862496

614. Jiang D, Gong F, Ge X, Lv C, Huang C, Feng S, Zhou Z, Rong Y, Wang J, Ji C, et al. Neuron-derived exosomes-transmitted miR-124-3p protect traumatically injured spinal cord by suppressing

the activation of neurotoxic microglia and astrocytes. *J Nanobiotechnology* (2020) 18:105. doi:10.1186/s12951-020-00665-8

615. Beer L, Mildner M, Gyöngyösi M, Ankersmit HJ. Peripheral blood mononuclear cell secretome for tissue repair. *Apoptosis* (2016) 21:1336–1353. doi:10.1007/s10495-016-1292-8

616. Hathout Y. Approaches to the study of the cell secretome. *Expert Rev Proteomics* (2007) 4:239–248. doi:10.1586/14789450.4.2.239

617. Agrawal GK, Jwa N-S, Lebrun M-H, Job D, Rakwal R. Plant secretome: unlocking secrets of the secreted proteins. *Proteomics* (2010) 10:799–827. doi:10.1002/pmic.200900514

618. Baraniak PR, McDevitt TC. Stem cell paracrine actions and tissue regeneration. *Regen Med* (2010) 5:121–143. doi:10.2217/rme.09.74

619. Vizoso FJ, Eiro N, Cid S, Schneider J, Perez-Fernandez R. Mesenchymal Stem Cell Secretome: Toward Cell-Free Therapeutic Strategies in Regenerative Medicine. *Int J Mol Sci* (2017) 18:1852. doi:10.3390/ijms18091852

620. Liau LL, Al-Masawa ME, Koh B, Looi QH, Foo JB, Lee SH, Cheah FC, Law JX. The Potential of Mesenchymal Stromal Cell as Therapy in Neonatal Diseases. *Front Pediatr* (2020) 8: doi:10.3389/fped.2020.591693

621. Gnecchi M, He H, Liang OD, Melo LG, Morello F, Mu H, Noiseux N, Zhang L, Pratt RE, Ingwall JS, et al. Paracrine action accounts for marked protection of ischemic heart by Akt-modified mesenchymal stem cells. *Nat Med* (2005) 11:367–368. doi:10.1038/nm0405-367

622. Pinho AG, Cibrão JR, Silva NA, Monteiro S, Salgado AJ. Cell Secretome: Basic Insights and Therapeutic Opportunities for CNS Disorders. *Pharmaceuticals* (2020) 13:31. doi:10.3390/ph13020031

623. Martins LF, Costa RO, Pedro JR, Aguiar P, Serra SC, Teixeira FG, Sousa N, Salgado AJ, Almeida RD. Mesenchymal stem cells secretome-induced axonal outgrowth is mediated by BDNF. *Sci Rep* (2017) 7:4153. doi:10.1038/s41598-017-03592-1

624. Pinho AG, Cibrão JR, Lima R, Gomes ED, Serra SC, Lentilhas-Graça J, Ribeiro C, Lanceros-Mendez S, Teixeira FG, Monteiro S, et al. Immunomodulatory and regenerative effects of the full and fractioned adipose tissue derived stem cells secretome in spinal cord injury. *Experimental Neurology* (2022) 351:113989. doi:10.1016/j.expneurol.2022.113989

625. Haider T, Höftberger R, Rüger B, Mildner M, Blumer R, Mitterbauer A, Buchacher T, Sherif C, Altmann P, Redl H, et al. The secretome of apoptotic human peripheral blood mononuclear cells

attenuates secondary damage following spinal cord injury in rats. *Experimental Neurology* (2015) 267:230–242. doi:10.1016/j.expneurol.2015.03.013

626. Zhang B, Lin F, Dong J, Liu J, Ding Z, Xu J. Peripheral Macrophage-derived Exosomes promote repair after Spinal Cord Injury by inducing Local Anti-inflammatory type Microglial Polarization via Increasing Autophagy. *Int J Biol Sci* (2021) 17:1339–1352. doi:10.7150/ijbs.54302

627. Canning DR, Höke A, Malemud CJ, Silver J. A potent inhibitor of neurite outgrowth that predominates in the extracellular matrix of reactive astrocytes. *Int J Dev Neurosci* (1996) 14:153–175. doi:10.1016/0736-5748(96)00004-4

628. Domeniconi M, Cao Z, Spencer T, Sivasankaran R, Wang K, Nikulina E, Kimura N, Cai H, Deng K, Gao Y, et al. Myelin-associated glycoprotein interacts with the Nogo66 receptor to inhibit neurite outgrowth. *Neuron* (2002) 35:283–290. doi:10.1016/s0896-6273(02)00770-5

629. Raspa A, Bolla E, Cuscona C, Gelain F. Feasible stabilization of chondroitinase abc enables reduced astrogliosis in a chronic model of spinal cord injury. *CNS Neurosci Ther* (2019) 25:86–100. doi:10.1111/cns.12984

630. Bradbury EJ, Moon LDF, Popat RJ, King VR, Bennett GS, Patel PN, Fawcett JW, McMahon SB. Chondroitinase ABC promotes functional recovery after spinal cord injury. *Nature* (2002) 416:636–640. doi:10.1038/416636a

631. Steinmetz MP, Horn KP, Tom VJ, Miller JH, Busch SA, Nair D, Silver DJ, Silver J. Chronic enhancement of the intrinsic growth capacity of sensory neurons combined with the degradation of inhibitory proteoglycans allows functional regeneration of sensory axons through the dorsal root entry zone in the mammalian spinal cord. *J Neurosci* (2005) 25:8066–8076. doi:10.1523/JNEUROSCI.2111-05.2005

<u>Chapter 2:</u> The secretome of macrophages has a differential impact on spinal cord injury recovery according to the polarization protocol

---

The results presented in this chapter were published as an original article in the international peer reviewed journal Frontiers in Immunology. This article can be found online at: https://www.frontiersin.org/journals/immunology/articles/10.3389/fimmu.2024.1354479/full

The Supplementary material for this article can be found online at: https://www.frontiersin.org/articles/10.3389/fimmu.2024.1354479/full#supplementary-material

Lentilhas-Graça J, Santos DJ, Afonso J, Monteiro A, Pinho AG, Mendes VM, Dias MS, Gomes ED, Lima R, Fernandes LS, et al. The secretome of macrophages has a differential impact on spinal cord injury recovery according to the polarization protocol. *Front Immunol* (2024) 15: doi:10.3389/fimmu.2024.1354479

The secretome of macrophages has a differential impact on spinal cord injury recovery according to the polarization protocol

José Lentilhas-Graça[1,2,3], Diogo J. Santos[1,2†], João Afonso[1,2†], Andreia Monteiro[1,2], Andreia G. Pinho[1,2], Vera Mendes[3], Marta S. Dias[3,4], Eduardo D. Gomes[1,2], Rui Lima[1,2], Luís S. Fernandes[1,2], Fernando Fernandes-Amorim[1,2], Inês M. Pereira[1,2], Nídia de Sousa[1,2], Jorge R. Cibrão[1,2], Aline M. Fernandes[1,2], Sofia C. Serra[1,2], Luís A. Rocha[1,2], Jonas Campos[1,2], Tiffany S. Pinho[1,2], Susana Monteiro[1,2], Bruno Manadas[3], António J. Salgado[1,2], Ramiro D. Almeida[3,4], Nuno A. Silva[1,2]*

[1]Life and Health Sciences Research Institute (ICVS), School of Medicine, University of Minho, Braga, Portugal

[2]ICVS/3B's Associate Lab, PT Government Associated Lab, Braga, Portugal

[3]CNC—Center for Neuroscience and Cell Biology, University of Coimbra, Coimbra, Portugal

[4]iBiMED- Institute of Biomedicine, Department of Medical Sciences, University of Aveiro, Aveiro, Portugal

[†]These authors contributed equally to this work

*Correspondence: Nuno A. Silva, nunosilva@med.uminho.pt

2.1 Abstract

Introduction: The inflammatory response after spinal cord injury (SCI) is an important contributor to secondary damage. Infiltrating macrophages can acquire a spectrum of activation states, however, the microenvironment at the SCI site favors macrophage polarization into a pro-inflammatory phenotype, which is one of the reasons why macrophage transplantation has failed.

Methods: In this study, we investigated the therapeutic potential of the macrophage secretome for SCI recovery. We investigated the effect of the secretome *in vitro* using peripheral and CNS-derived neurons and human neural stem cells. Moreover, we perform a pre-clinical trial using a SCI compression mice model and analyzed the recovery of motor, sensory and autonomic functions. Instead of transplanting the cells, we injected the paracrine factors and extracellular vesicles that they secrete, avoiding the loss of the phenotype of the transplanted cells due to local environmental cues.

Results: We demonstrated that different macrophage phenotypes have a distinct effect on neuronal growth and survival, namely, the alternative activation with IL- 10 and TGF-β1 (M(IL-10+TGF-β1)) promotes significant axonal regeneration. We also observed that systemic injection of soluble factors and extracellular vesicles derived from M(IL-10+TGF-β1) macrophages promotes significant functional recovery after compressive SCI and leads to higher survival of spinal cord neurons. Additionally, the M(IL-10+TGF-β1) secretome supported the recovery of bladder function and decreased microglial activation, astrogliosis and fibrotic scar in the spinal cord. Proteomic analysis of the M(IL-10+TGF-β1) derived secretome identified clusters of proteins involved in axon extension, dendritic spine maintenance, cell polarity establishment, and regulation of astrocytic activation.

Discussion: Overall, our results demonstrated that macrophages-derived soluble factors and extracellular vesicles might be a promising therapy for SCI with possible clinical applications.

Keywords: spinal cord Injury; macrophages; secretome; neuroimmunology; neuroregeneration

2.2 Background

Spinal cord injury (SCI) is a devastating neurological disorder that strongly affects the physiological, psychological, and social behaviors of affected people. There is an urgent need to develop new therapeutic strategies for SCI repair [1]. The spinal cord trauma, known as "primary injury", triggers a cascade of events, termed "secondary injury", leading to further neurological damage and contributing to regeneration failure after SCI [2]. These include glutamate excitotoxicity, a potent and dysfunctional inflammatory response, release of molecules that inhibit axonal growth, and formation of a glial scar. From all these events, the defective immune response is one of the most important players in SCI pathophysiology. Circulating monocytes infiltrate the spinal cord and differentiate into macrophages in a multiphasic manner, where they should perform multiple functions involved in the wound healing process [3]. It was recently demonstrated that the spleen releases the first monocytes that infiltrate the injured spinal cord [4]. Moreover, Swirsky et al. characterized the splenic monocyte reservoir as a major source of the pro-inflammatory subtype during acute injury [5].

Macrophages can acquire a diverse spectrum of activation states with various functionalities. Macrophage activation can range from the most pro-inflammatory or classically activated phenotype to the anti-inflammatory/pro-repair or alternatively activated phenotype. Pro-inflammatory macrophages are important during the acute response to trauma and facilitate innate immunity to remove wound debris from the injury site. These macrophages release reactive oxygen species (ROS) and pro-inflammatory cytokines, such as IL-1β and TNF-α [6]. Macrophages can acquire this phenotype *in vitro* by stimulating naive macrophages with lipopolysaccharide (LPS) and IFN-γ (commonly known as M1). In contrast, alternatively activated macrophages secrete immunosuppressive cytokines, growth factors, and upregulate ECM components (e.g., IL-10, TGF-β1, and IGF-1) [7, 8]. These macrophages exhibit tissue repair properties by promoting cell proliferation and maturation, tissue remodeling and stabilization, and adjusting and resolving inflammatory processes. These tasks are not performed by a single type of alternatively activated macrophage. Instead, they are subdivided into four distinct subtypes (commonly known as M2a, M2b, M2c, and M2d) that differ in cell surface markers, secreted cytokines, and biological functions [6]. Herein, we focus on two alternatively activated macrophages, the M2a and M2c. The first can be obtained *in vitro* by stimulating naive macrophages with IL-4 and IL-13, and their function is associated with a decrease in the inflammatory response, promotion of cell proliferation and migration, and facilitation of apoptosis. After SCI these cells fail to activate an appropriate proregenerative response [6]. Whereas, the M2c macrophages have functions related to resolving inflammation, ECM synthesis, and promoting tissue maturation/repair. These cells can be obtained by activating naive macrophages

with TGF-β1 and IL-10. The significance of M2c cells in SCI repair remains largely unexplored because these cells do not populate the lesion site, impeding the initiation of the remodeling phase [6]. Overall, the immune response at the initial stages after SCI resembles that in non-CNS injured tissues [9]. However, pro-inflammatory macrophages quickly become the predominant cell type at the injury site [10], and pro-repair macrophages are unable to populate the injured tissue. The pro-inflammatory response is associated with fibrosis, oxidative damage, and neurodegeneration, contributing to wound healing failure [11].

Previous studies transplanted alternatively activated macrophages into the injured spinal cord to promote tissue repair and regeneration [12, 13]. This therapeutic approach reached clinical testing, but failed to show any therapeutic effects (14). The reason behind this clinical trial failure may lie in the spinal cord microenvironment after injury. Indeed, a previous study reported that bone marrow-derived macrophages polarized *in vitro* by IL-4 failed to retain their typical markers when transplanted into the injured spinal cord [10]. Moreover, it was demonstrated that intracellular accumulation of iron by macrophages induces a rapid switch from a pro-regenerative to a pro-inflammatory phenotype in spinal cord tissue [15]. Thus, it is important to find alternative approaches for M2 macrophage transplantation. A possible alternative is to administer the secretome of macrophages instead of transplanting them into the SCI microenvironment. The secretome can be defined as the soluble factors, lipids, and extracellular vesicles secreted by a cell, tissue, or organism into the extracellular space under defined time and conditions [16].

Herein, we explored whether systemic injections of secretome derived from different macrophage phenotypes have a therapeutic effect after SCI.

2.3 Materials and Methods

2.3.1 Macrophages isolation and culture

Macrophages were obtained by differentiating monocytes extracted from the mouse spleens. C57BL/6 mice (~8 weeks old) were sacrificed by cervical dislocation, and their spleen was removed under aseptic conditions and kept on ice-cold VLE-RPMI 1640 (Merck KGaA) with 1% (v/v) penicillin-streptomycin (pen/strep, Gibco). The spleen was mechanically dissociated using two microscope slides until no major fragments were observed. The solution was centrifuged at 1200 rpm for 7 min and the supernatant was discarded. Ammonium-chloride-potassium (ACK) lysis solution was used to lyse erythrocytes (2mL/spleen). After adding HBSS (8mL/spleen, Gibco), centrifugation was performed, and the cell pellet was resuspended in RPMI for hematocytomer cell counting. Cells were plated at a density of 1 million cells/cm^2 in RPMI medium 1% (v/v) pen/strep (Gibco) for 3 h. The monocytes (≈10% of the total cells) are the first to adhere under serum starvation. After this time, the non-adherent cells were discarded and the medium was replaced by RPMI with 10% (v/v) fetal bovine serum (FBS, Millipore), 1% (v/v) pen/strep, and 50 ng/mL of macrophage colony-stimulating factor (M-CSF, Biolegend) to differentiate monocytes into macrophages. The cells were maintained at 37°C and 5% (v/v) CO_2 for a minimum of 7 days, with medium exchanges every 3/4 days. To achieve a proinflammatory phenotype, macrophages were stimulated with IFN-γ (20 ng/mL, Peprotech) and LPS (100 ng/mL, Sigma) for 24 h. One pro-regenerative phenotype was achieved by stimulation with IL-4 (20 ng/mL, Biolegend) and IL-13 (20 ng/mL, Peprotech), and the other phenotype was obtained with IL-10 (20 ng/mL, Peprotech) and TGF-β1 (20 ng/mL, R&D Systems) stimulation. All polarizations were performed in RPMI with 10% FBS, 1% (v/v) pen/strep and 50 ng/mL of M-CSF.

The macrophage secretome was collected after each polarization. Briefly, cells were washed five times with PBS without Ca^{2+} and Mg^{2+} (Merck, KGaA), followed by two washes with RPMI 1% (v/v) pen/strep. After a 12-hour incubation with 16 mL (213ul/cm2) of basal medium (RPMI) with 1% (v/v) pen/strep, the medium was collected, centrifuged at 1200 rpm for 5 min, and the supernatant was snap frozen with liquid nitrogen and stored at -80°C.

2.3.2 qPCR

Macrophage mRNA levels were analyzed using qPCR by extracting RNA from cells grown in T25 flasks. Briefly, 6 h after polarization, TripleXtractor (Grisp) was added to the flasks for 5 min. RNA was extracted and diluted in GRS PCR Grade Water (Grisp) following the manufacturer's instructions. cDNA was synthesized from 1 μg of RNA using the Xpert cDNA Synthesis Supermix (with gDNA eraser, Grisp) protocol. qPCR was performed on these samples using Xpert Fast SYBR blue mastermix (Grisp) with ROX reference dye. After mixing the mastermix with the respective primers (500 nM) and the cDNA on a PCR plate (Nerbe Plus), the reaction was performed on a 7500 Fast Real-Time PCR system (Applied Biosystems). The amplification was performed by heating at 95°C for 2 minutes succeeded by 40 cycles at 95°C for 5 s and 30 s at 60°C. Melt curve analysis was used to assess the specificity of the gene amplification. The primers used are listed in Table 2.1. The target genes were normalized to three reference genes: Gadph, Hprt and 18s. Foldchange levels were calculated using the 2-ΔΔct method relative to non-stimulated macrophages and normalized to the reference genes [17].

Table 2.1: Primers for semi-quantitative Real Time-PCR.

Gene	Forward	Reverse
GAPDH	GGG CCC ACT TGA AGG GTG GA	TGG ACT GTG GTC ATG AGC CCT T
HPRT	GCT GGT GAA AAG GAC CTC T	CAC AGG ACT AGA ACA CCT GC
18s	GTA ACC CGT TGA ACC CCA TT	CCA TCC AAT CGG TAG TAG CG
iNOS	CTC GGA GGT TCA CCT CAC TGT	GCT GGA AGC CAC TGA CAC TT
TNF-α	GCC ACC ACG CTC TTC TGT CT	TGA GGG TCT GGG CCA TAG AAC
EGR2	TTG ACC AGA TGA ACG GAG TG	CCA GAG AGG AGG TGG AAG TG
IRF4	ACA GGA GCT GGA GGG ATT ATG	CTG TCA CCT GGC AAC CAT TT
ARG1	GTG TAC ATT GGC TTG CGA GA	GGT CTC TTC CAT CAC CTT GC
HIF1-α	GCA CTA GAC AAA GTT CAC CTG AGA	CGC TAT CCA CAT CAA AGC AA

2.3.3 Axonal growth assay – dorsal root ganglia

Dorsal root ganglia (DRG) explants were used to study the impact of splenic macrophages on axonal growth. This assay was accomplished following a well-established protocol [18, 19]. Briefly, DRG from thoracic regions of neonatal Wistar Han rat pups (P5-7) were removed and placed on ice-cold HBSS with 1% (v/v) pen/strep. Peripheral nerves attached to the DRG were removed, and the cleaned DRG were used. Two assays were performed. The first consisted of placing the DRG on top of a collagen extracellular matrix gel (3D culture), which was on top of polarized macrophages. Collagen gels were prepared by combining rat tail collagen type I (Corning) at a final concentration of 89.6% (v/v) with 10% (v/v) Dulbecco Modified Eagle Medium (DMEM, Gibco) 10x and 0.4%(v/v) of sodium bicarbonate (7.5% (w/v), Sigma). After forming 30 uL gel droplets at 37°C and 5% (v/v) CO_2 for a minimum of 90 min, the gels were transferred to the macrophages' wells. The other assay consisted of direct placement of the DRG on top of polarized macrophages to study direct cellular interactions (2D culture). Both assays were performed in Neurobasal (Gibco) medium supplemented with 2% (v/v) B27 (Gibco), 2 mM L-glutamine (Invitrogen), 6 mg/mL D-glucose (Sigma), 1% (v/v) pen/strep, and 50 ng/mL of M-CSF with medium changes every two days and maintained at 37°C and 5% (v/v) CO_2 for four (3D) or three (2D) days. The cells were then fixed and immunocytochemistry was performed. The area occupied by the axons in each dorsal root ganglia explant was calculated using the ImageJ (NIH) plugin Neurite-J. Using confocal microscopy, the entire area with positive staining for Neurofilament was acquired. Then, the image was automatically translated to 8 bits and a binary mask was created with the aid of the "Analysis Particles" function which enables the correct segmentation of axonal structures based on an intensity-threshold image coupled with morphological parameters such as structure size and area. The mask generated can then be added as an input to the Neurite-J plugin.

2.3.4 Axonal growth assay –CNS-derived neuronal culture

Cortical neurons were dissected and isolated from Wistar rats E17 embryos as described previously [20]. To physically and fluidically separate distal axons from cell bodies, neurons were plated in microfluidic chambers as described previously [21]. Microfluidic chambers were assembled onto an ibiTreat low wall 50 mm μ-Dish (ibidi) and coated with poly-D-lysine (PDL) 0.1 mg/mL overnight at 37°C and 2 μg/mL laminin for 2 h at 37°C. Cortical neurons were plated in the somal compartment of microfluidic chambers at a density of 50,000 cells per chamber. Cells were maintained in a humidified

5% CO_2 incubator at 37°C and treated with 10 μM 5-Fluoro-2′-deoxyuridine (5'-FDU) on day 4 to inhibit glial cell proliferation.

On day 5, distal axons were submitted to a 20-hour starving and after which axons were treated with $M_{(IL\text{-}10+TGF\text{-}\beta1)}$-derived secretome or control medium. 25 μl of secretome was locally applied to the axonal compartment of the microfluidic chamber for 14 h. Neurobasal medium with 1% penicillin/streptomycin was used for control cultures. A higher volume of culture medium was maintained in the somal compartment to ensure fluidic isolation of the axonal compartment and, therefore, restrict the treatment to distal axons. After 14 h of local treatment, population-wide axonal growth was assessed by live-cell imaging microscopy.

2.3.5 Neurospheres derived from human induced neural stem cells

Neurospheres were generated by culturing human induced pluripotent stem cells (hiPSCs) in vitronectin XF™ treated plates with mTeSR 1 (both from Stem Cell Technology). After 7 days, spontaneous differentiation was initiated by the generation of Embryoid Bodies (EBs). For that, cells were detached by using TrypLE™ Express Enzyme (ThermoFisher) and plate into low attachment 96 well plate in Advanced DMEM/12 supplemented with 15% (v/v) knockout serum replacement (KSR, ThermoFischer), 1% (v/v) non-essential amino acids (NEAA, ThermoFischer), 2% (v/v) glutamax (ThermoFischer), 2-mercaptoethanol (55 mM, ThermoFischer), and Y-27632 (5 mM, Rho-associated protein kinase inhibitor, StemCell Technology). The hole medium was changed every other day. On day 6, 6-9 EBs were transferred from 96 well plates to non-adherent plates (35 mm) and were cultured in Advanced DMEM/12 supplemented with 1% (v/v) non-essential amino acids, 1% (v/v) glutamax, 1% (v/v) of N2 supplement (ThermoFischer), and heparin (1 μg/mL, Sigma-Aldrich) to induce neural differentiation. After 5 days, 6-9 neurospheres were plated into 24 well plates, pre-treated with poly-D-lysin/laminin (76 μg/mL, 20 μg/mL, respectively), and cultured in differentiation media: DMEM/F12: Neurobasal (1:1, both from ThermoFisher), 0.5% of N2 supplement, 1% (v/v) NEAA, 1% (v/v) glutamax, 55 mM 2-mercaptoethanol, 2% (v/v) B27 supplement (ThermoFischer), and insulin (2.5 μg/mL, Sigma). After 2 days, the culture medium was replaced by 500 μl of secretome. Cells were incubated for 2 days and fixed for further analysis using immunofluorescence.

2.3.6 Immunocytochemistry

Cells/DRG/Neurospheres were first incubated with 4% (v/v) PFA for 20 min, and then permeabilized with Triton-X100 0.2% diluted in PBS (PBS-T) for 5 minutes, at room temperature (RT). 10% FBS (Millipore) in PBS was used as a blocking solution for 1 h, followed by the addition of the primary antibodies for 2 h. For macrophages was used the rat anti-CD11b (1:100, BioLegend) and rabbit anti-iNOS (1:100, Abcam), for DRGS the mouse anti-neurofilament (1:200, Millipore) and for neurospheres the Anti-βIII Tubulin (1:100, mouse – Millipore). After washing, Alexa Fluor 488 goat anti-rat (1:1000, Invitrogen) and Alexa Fluor 594 goat anti-rabbit (1:1000, Invitrogen) secondary antibodies were added for another hour, diluted in blocking solution. Finally, the samples were counterstained with 40,6-diamidino-2-phenylindoledihydrochloride (DAPI) (1 μg/mL, Sigma) for 10 min and in the case of DRGs with and Phalloidin (1:500, Sigma) for 45 min at RT. Images were obtained using a confocal microscope (Olympus FV1000) for 3D cultures and an Olympus IX81 fluorescence microscope for 2D cultures. To calculate the axonal area, maximum distance reached by axons, and axonal arborization, ImageJ software was used, as previously described [22].

2.3.7 Live imaging of CNS-derived neurons

Live imaging was performed using a Zeiss LSM 880 microscope with an Airyscan and a Plan-Apo Chromat 20x/0.8 Ph2 objective. During live imaging cells were maintained in a 37°C and 5% CO_2 environment. A tiled phase-contrast image was obtained for each condition immediately before treatment (t=0 h) and after 6, 10 and 14 hours of treatment.

Images were processed and quantified using ImageJ software version 1.51n. A region of interest (ROI) was chosen to encompass the entire length of the axonal compartment, and the same size ROI was used for all samples. The Feature J Hessian plugin was applied with the following settings: largest eigenvalue of the Hessian Tensor, smoothing scale = 2.0). The Local Threshold was adjusted to include all axons in the axonal network. A binary image was generated, and the Skeletonize (2D/3D) plugin was used to obtain a skeletonized image of the axonal network. Finally, the Analyze Skeleton (2D/3D) was applied with the following settings: prune cycle method=none, show detailed info. A Branch Information table was generated using the software, and the sum of all branch lengths was further calculated, giving the population-wide total axonal length. The results were normalized for t=0 under the respective treatment conditions.

2.3.8 Spinal cord injury surgery

All experiments were performed after obtaining consent from the ethical Subcommittee in Life and Health Sciences (SECVS; ID:018/2019, University of Minho) and were conducted in accordance with the local regulations on animal care and experimentation (European Union Directive 2010/63/EU). The ARRIVE guidelines for reporting animal research have been followed [23]. C57BL/6J mice (Charles River) were maintained under sterile conditions and in light, humidity, and temperature-controlled rooms. Food and water were provided *ad libitum*. Animals were handled for 1 week prior to SCI surgery.

Spinal cord surgery was performed as previously described [24]. Briefly, 42 C57BL/6J adult female mice (10-15 weeks age) were used in this study. Anesthesia was delivered intraperitoneally (ip) using Imalgene (ketamine, 75 mg/kg, Richter Pharma AG) and Dormitor (medetomidine, 1 mg/kg, Pfizer). Mice were shaved and disinfected with chlorohexidine. A dorsal midline incision was then made at the thoracic level (T5-T12). The paravertebral muscles were retracted, and the spinal process and laminar arc of T8-T9 were removed to expose the spinal cord. The spinal cord was compressed using fine forceps for 5 seconds. The wound was closed with 9 mm autoclip (Braintree Scientific), and anesthesia was reverted with Antisedan (atipamezole, Orion Corporation) applied subcutaneously. The injured animals were randomly divided into four experimental groups: 1) $M_{(INF\text{-}\gamma+LPS)}$ secretome (n=10); 2) $M_{(IL\text{-}4+IL\text{-}13)}$ secretome (n=11), 3) $M_{(IL\text{-}10+TGF\text{-}\beta1)}$ secretome (n=10), and 4) vehicle (RPMI medium with 1% pen/strep, n=11). Treatment was delivered by intraperitoneal injections (500 μl), and the first injections were administered 3, 6, 9, 14 days post-injury and once a week afterwards. Eight animals did not survive the experimental protocol.

In a separate cohort of animals, we employed the same protocol to induce spinal cord injury, and the same method and schedule to deliver the treatment. However, this time, we utilized (C57BL/6J x CBA)F1 mice expressing the Thy1-GFP transgene. Following spinal cord compression, the injured animals were randomly assigned to two experimental groups: 1) $M_{(IL\text{-}10+TGF\text{-}\beta1)}$ secretome (n=3), and 2) vehicle (RPMI medium with 1% pen/strep, n=3). Treatment was delivered by intraperitoneal injections (500 μl) as described above.

2.3.9 Post-operative care

After surgery and throughout all in vivo experiments, animals were closely monitored and cared for, as previously described [16]. A solution containing the antibiotic enrofloxacin (Baytril, 5 mg/mL, Bayer), the analgesic buprenorphine (Bupaq, 0.05 mg/kg, Richer Pharma AG), vitamins (Duphalyte, Pfizer), and saline (0.09% NaCl) was administered subcutaneously twice a day until the animals showed autonomy and no infections detected. Manual bladder voiding was performed twice a day during the first week and once every day until sacrifice or spontaneous restoration of bladder control was achieved. Food pellets were provided on the cage floor during the first few days to allow easy access. Animals were also monitored for body temperature, correct scarring of the surgical incision, and recovery of general activities (grooming and nesting for example). Five days after surgery, the staples were removed, and the animals were regrouped to promote socialization and decrease anxiety and stress. Animals were monitored during the experiment for humane endpoints: wounds, autophagy behavior, or weight loss (>20% of their baseline weight).

2.3.10 Locomotor analysis

The BMS test was used to evaluate locomotor behavior [25], 3 days post-injury and once a week thereafter for 37 days. The mice were placed in an open arena for 4 min, and their locomotor function was evaluated by two independent observers who were blinded to the experimental groups. Each animal was scored on a scale ranging from 0 to 9. Animals presenting a BMS score greater than 1 in the first BMS assessment (3 dpi) was excluded because of incomplete spinal cord compression.

2.3.11 Bladder function

The bladders were manually voided and the animals were placed in the cage with water provided *ad libitum* overnight. Water weights in the cage bottles were measured before and after the experiment to assess water intake. Bladders were then voided into a beaker and the urine was weighed. The ratio between water intake and urine was calculated to assess bladder control in the different experimental groups. If the amount of urine was less than 0.1 g we considered that the animal regained total bladder control.

2.3.12 Von Frey

The Von Frey test was used to determine tactile sensitivity by measuring how much force is required to elicit movement of the paw fingers, using the up-and-down method with Von Frey monofilaments, as previously described [26]. The experimental setting consisted of placing the mice in an elevated mesh restrained inside a standard perforated box. Before the test started, each animal was habituated to the test conditions. A total of 9 monofilaments were used, ranging from 0.008 to 1.4 g. Both paws were stimulated with the central monofilament (0.16 g). If the animal moved the fingers of the paw, a weaker monofilament was used; otherwise, a stronger monofilament was applied. The test was performed until: 1) observed response to the 0.008 g monofilament, 2) no response to 1.4 g monofilaments, or 3) after a total of five measures around the threshold. 50% threshold was calculated using the formula:

$$50\% \text{ threshold} = \frac{10^{(x\_f+k\delta)}}{10000}$$

Where xf is the value of the final monofilament used (log units), K is the tabular value for the pattern of positive/negative responses, and δ is the mean difference between stimuli (0.267).

2.3.13 Flow cytometry

Nine days post-injury, approximately 50 μL of blood was collected from the tail vein of the animals. Erythrocytes were depleted with ACK lysis solution. The cell pellet was then washed with FACS buffer (PBS, 10% BSA, 0.1% azide). $1x10^6$ cells were stained. The Fc portion was blocked using anti-mouse CD16/CD32 (Biolegend). Cell staining was performed by incubating a cocktail of antibodies for 30min at 4°C (Table 2.2). After washing, the cells were re-suspended in 200 mL FACS buffer. Precision counting beads (Biolegend) were added to the single-cell suspensions according to the manufacturer's instructions to calculate the final cell concentrations. Cells were acquired using an LSRII Flow Cytometer (BD Pharminogen) and analyzed using Flow Jo software version 10.4. The gating strategy used can be found in the Supplementary Data (Supplementary Figure S2.5).

Table 2.2 Flow cytometry analysis summary of markers expressed on different cell populations.

Marker	Fluorochrome	Company	Target	Dilution
CD86	PerCpCy5.5	Biolegend	Myeloid cells	1/100
CD11b	PE	Biolegend	Myeloid cells	1/200
CD11c	BV 605	Biolegend	Mostly dendritic cells	1/100
NK 1.1	BV 510	Biolegend	Natural killer	1/100
CD19	FITC	Biolegend	B lymphocytes	1/200
CD3	APC	Biolegend	T lymphocytes	1/100
CD45	PeCy7	Biolegend	Leukocytes	1/200
Ly6C	BV711	Biolegend	Monocytes	1/100
Ly6G	BV650	Biolegend	Granulocytes	1/100
CD16/32	None	Biolegend	Fc Block	1/25

2.3.14 Spinal cord collection, processing and immunohistochemistry

To understand the molecular and cellular effects of the different treatments on the spinal cord injury environment, an immunohistochemistry protocol to mark GFAP (astrocytes), Iba-1 (macrophages/microglia), PDGFR (fibrosis), and NeuN (mature neurons) was performed on mouse spinal cords. First, at 5 weeks post-injury mice were anesthetized and perfused with 20 mL of cold PBS and then with 4% PFA. A dorsal incision was made to remove the spinal cord with the vertebral column. The isolated spinal cords were then fixed with 4% PFA for 24h at 4°C. After, the tissue was placed on 30% saccharose solution until reaching saturation point, which was then cut into 1 cm fragments centered in the lesion site. Next, the spinal cords were embedded in optimal cutting temperature (OCT) solution and frozen in isopentane and liquid nitrogen. Using a Leica CM 1900 cryostat, the spinal cords were cut into transverse sections of 20 µm and mounted onto microscope slides (SuperFrost Plus) that were stored at -20°C for further use.

On the day of immunohistochemistry, slides with frozen sections were thawed at RT and cleaned with PBS to remove any remaining cryopreservation solution. This was followed by permeabilization with PBS-T 0.2% (v/v) for 10 min and a blocking solution of 5% (v/v) FCS in PBS-T 0.2% (v/v) for 30 min. An overnight incubation at 4°C was then performed with the following primary antibodies: rabbit anti-GFAP (1:200, DAKO), rabbit anti-Iba-1 (1:200, Wako), PDGFR (1:1000, Abcam), and rabbit anti-NeuN (1:200, D4G4O). The next day, after washing, the samples were incubated with Alexa Fluor 594 goat anti-rabbit (1:1000) (Abcam) secondary antibody for 3 h at RT. Cells were then counterstained with DAPI for 20 min before mounting the slides in Immu-Mount® (Thermo Scientific) for subsequent image analysis. A

negative control (primary antibodies omitted) was performed to discard any background as positive staining (Supplementary Figure S2.6).

Imaging was performed using an Olympus Widefield Inverted Microscope IX81. GFAP staining was evaluated by measuring the area of astrogliosis morphology, normalized to the total GFAP area. IBA-1 was evaluated by assessing the area of ramified macrophages/total microglia. Fibrosis was evaluated by assessing the area of PDGFR+ area normalized for total spinal cord area. The location of the spinocerebellar (SCT), rubrospinal (RST) and the corticospinal tracts (CST) were identified using the spinal cord atlas developed by Paxinos, Watson and Kayalioglu [27]. The positive area for Thy1-GFP was calculated and divided for the total area of the tract in each spinal section. Positive Thy1-GFP and total areas were calculated using the plugin Neurite-J from the ImageJ (NIH) software as described above. NeuN staining was measured by counting the number of positive cells in laminae VIII and IX of both ventral horns.

2.3.15 Proteomics Analysis

The secretome was first concentrated (x100) using ultracentrifugation with falcons with 5 kDa cut-off filter (Vivaspin, GE Healthcare). A protein precipitation step using TCA to a final concentration of 20% was performed, and protein pellets were re-suspended in 35μL of Laemmli sample buffer. Protein extracts from each sample were separated by SDS-PAGE for approximately 16 min at 110 V (Short-GeLC Approach) (1) and stained with Coomassie Brilliant Blue G-250. Each lane was divided into three separate gel fractions for a destaining step using a solution of 50 mM ammonium bicarbonate with 30% acetonitrile, followed by overnight protein digestion with trypsin. Peptide extraction from the gel was performed using solutions containing different percentages of acetonitrile (30, 50, and 98%) with 1% of formic acid. For protein identification, each fraction was analyzed separately, and for protein quantification, fractions from each sample were combined, and a single analysis per sample was performed by LC-MS/MS.

Samples were analyzed on a NanoLC™ 425 System (Eksigent) coupled to a Triple TOF™ 6600 mass spectrometer (Sciex) and the ionization source (ESI DuoSpray™ Source). The chromatographic separation was performed on a Triart C18 Capillary Column 1/32" (12 nm, S-3μm, 150 x 0.3 mm, YMC) and using a Triart C18 Capillary Guard Column (0.5 x 5 mm, 3 μm, 12nm, YMC) at 50°C. The flow rate was set to 5 μL/min, and mobile phases A and B were 5% DMSO plus 0.1% formic acid in water and 5% DMSO plus 0.1% formic acid in acetonitrile, respectively. The LC program was performed as follows: 5 – 30% of B (0 - 50 min), 30 – 98% of B (50 - 52 min), 98% of B (52 - 54 min), 98 - 5% of B (54 - 56 min),

and 5% of B (56 - 65 min). The ionization source was operated in the positive mode set to an ion spray voltage of 5500 V, 25 psi for nebulizer gas 1 (GS1), 10 psi for nebulizer gas 2 (GS2), 25 psi for the curtain gas (CUR), and source temperature (TEM) at 100°C. For data-dependent acquisition (DDA) experiments, the mass spectrometer was set to scanning full spectra (m/z 350-2250) for 250 ms, followed by up to 100 MS/MS scans (m/z 100 – 1500). Candidate ions with a charge state between +1 and +5 and counts above the minimum threshold of 10 counts per second were isolated for fragmentation, and one MS/MS spectrum was collected before adding those ions to the exclusion list for 15 s (mass spectrometer operated by Analyst® TF 1.8.1, Sciex®). The rolling collision energy was used with a collision enErgy spread of 5. For SWATH experiments, the mass spectrometer was operated in a looped product ion mode and specifically tuned to a set of 42 overlapping windows, covering the precursor mass range of 350-1400 m/z. A 50 ms survey scan (350-2250 m/z) was acquired at the beginning of each cycle, and SWATH-MS/MS spectra were collected from 100-2250 m/z for 50 ms, resulting in a cycle time of 2.2 seconds.

Protein identification was performed using the ProteinPilot™ software (v5.0.2, Sciex) for each sample. The paragon method parameters were as follows: searched against the reviewed Mus musculus database from SwissProt, cysteine alkylation by acrylamide, digestion by trypsin, and gel-based ID. An independent False Discovery Rate (FDR) analysis using the target-decoy approach provided by Protein Pilot™, was performed to assess the quality of the identifications. SWATH data processing was performed using SWATH™ processing plug-in for PeakView™ (v2.0.01, Sciex®). Relative protein quantification was performed in all samples using information from the Ion-Library search. Quantification results were obtained for peptides with less than 1% of FDR for at least one of the samples by calculating the sum of up to five fragments/peptides. Relative peptide peak areas were normalized to the internal standard peak areas. Protein quantities were obtained by the sum of up to 15 peptides/proteins. Protein–protein interactions and network analysis was constructed using the online STRING database (https://string-db.org) version 11.5, depicting both functional and physical protein associations with a medium confidence level (0.4), and organized into clusters through k means clustering method. All identified proteins were then subjected to an over-representation analysis using the ConsensusPathDB. From a total of 368 proteins identified using LCMS/MS, we focused the analysis on those that presented higher concentrations (fold changes of 2 or higher) between the two groups. These proteins were then grouped by function using the UniProt database and a heat map of their concentration was plotted with a cut off of 5 (ratios higher than 5 were color-expressed as 5). The mass spectrometry proteomics data have been

deposited to the ProteomeXchange Consortium via the PRIDE [28] partner repository with the dataset identifier PXD048453.

2.3.16 LEGENDplex

The concentration of relevant cytokines was evaluated in the secretomes of polarized macrophages using the LEGENDplex™ Mouse Macrophage/Microglia Panel kit according to manufacturer's instructions. The secretome was first concentrated (x10) using ultracentrifugation with falcons with 5 kDa cut-off filter (Vivaspin, GE Healthcare). Then, reagents were prepared from the stocks provided, and standard serial dilutions were prepared to generate a standard curve. Assay buffer (25μL) was added to standard and sample wells in a 1:1 ratio. 25μL of mixed beads were added to each well, and the plate was incubated for 2 hours at RT with continuous agitation at 800 rpm. After a centrifugation of 250g for 5min, beads were washed with 1x wash buffer for 1min. 25μL of detection antibodies was added to each well, followed by 1 hour of incubation at RT with agitation at 800 rpm. 25μL of Streptavidin-phycoerythrin (SA-PE) was added directly to the previous solution, and the plate was incubated for 30 minutes at RT with agitation at 800 rpm. After a wash step with 150μL of 1x wash buffer, the samples were ready to read on the flow cytometer. For that, samples were vortexed, and 300 beads per analyte were acquired in a BD LSRII Flow Cytometer (BD, Pharminogen). The FCS files were analyzed using Biolegend's LEGENDplex™ data analysis software site. Concentration values were subsequently divided by 10 to account for the concentration step, providing an accurate representation of the actual cytokine concentration present in the secretome.

2.3.17 Statistical analysis

Statistical analyses were performed using GraphPad Prism software, version 8.0.1. The normality of the data was evaluated using the Shapiro-Wilk normality test. Gene expression, axonal regeneration *in vitro*, weight loss, bladder function, chronic pain, LEGENDplex, and flow cytometry data were analyzed using One-Way ANOVA followed by Tukey's multiple comparison test. Data from the BMS score, astrogliosis, fibrosis, spinal tracts area, axonal arborization, and ramified microglia were assessed by two-way ANOVA followed by Tukey's multiple comparison test. Live imaging data were assessed by unpaired, non-parametric t-test (Mann-Whitney test). Statistical significance was defined as $p < 0.05$ (95% confidence level). Data are presented as mean ± standard error (SEM).

2.4 Results

2.4.1 Monocytes isolation, differentiation and polarization

To successfully culture spleen-derived macrophages (Sp-MΦ), we isolated monocytes from the spleen and cultured them in the presence of macrophage colony-stimulating factor (M-CSF) to stimulate the survival, proliferation, and differentiation of monocytes into macrophages (Figure 2.1A). Using our protocol, we were able to obtain a highly enriched culture (97% purity) of Sp-MΦ (Figure 2.1B). Without M-CSF, it was impossible to establish and maintain the cells (Supplementary Figure S2.1a), indicating that M-CSF is essential for the Sp-MΦ culture.

To polarize macrophages into different phenotypes, we stimulated macrophages for 24h with 20 ng/mL of IFN-γ plus 100 ng/mL of LPS (classical activation) or with 20 ng/mL of IL-4 plus 20 ng/mL of IL-13 or 20 ng/mL of IL-10 plus 20 ng/mL of TGF-β1 (alternative activation). With immunocytochemistry it was possible to confirm that the classical activation leads to the polarization of 89% of the macrophages (Supplementary Figure S2.1b). Moreover, proteomics analysis of the secreted proteins of each macrophage population revealed that out of 487 proteins identified, 81 were exclusive secreted by $M_{(INF-\gamma+LPS)}$ macrophages, 35 by $M_{(IL-4+IL-13)}$, and 90 by $M_{(IL-10+TGF-\beta1)}$ macrophages (Supplementary Figure S2.1c). Using the Protein Analysis Through Evolutionary Relationships (PANTHER) tool, we further demonstrated distinctions in the protein classes among these populations of proteins (Supplementary Figure S2.1d). Metabolite interconversion enzymes were identified as a common protein class between the different macrophage populations, but as can be observed by the pie charts, the protein class or the percentage of proteins in different classes varied considerably among each cell phenotype (Supplementary Figure S2.1d). Additionally, the phenotypes of each macrophage population was also confirmed by gene expression analysis. qPCR revealed that Sp-MΦ are easily polarized in vitro; namely, when macrophages were stimulated with IL-4+IL-13, they significantly overexpressed *EGR2* and *IRF4*, and these genes were not overexpressed when macrophages were stimulated with IL-10+TGF-β1 (Figure 2.1C). The *ARG1* gene was significantly overexpressed in the two populations of macrophages with alternative activation, however more overexpressed in the $M_{(IL-4+IL-13)}$ phenotype than in the $M_{(IL-10+TGF-\beta1)}$ macrophages. In contrast, the IL-10+TGF-β1 stimulation protocol led to a significant increase in *HIF-1α* expression, and these gene was not overexpressed with the IL-4+IL-13 stimuli. Using gene expression, we also confirm that macrophages under classic activation stimuli significantly overexpressed *iNOS* and *TNF-α* genes (Figure 2.1C). All these genes are known to be specifically overexpressed in these phenotypes [29]. These results showed that we were able to obtain three different subsets of

macrophages, one with classical activation ($M_{(INF-\gamma+LPS)}$) and two with alternative activation ($M_{(IL-10+TGF-\beta1)}$; $M_{(IL-4+IL-13)}$).

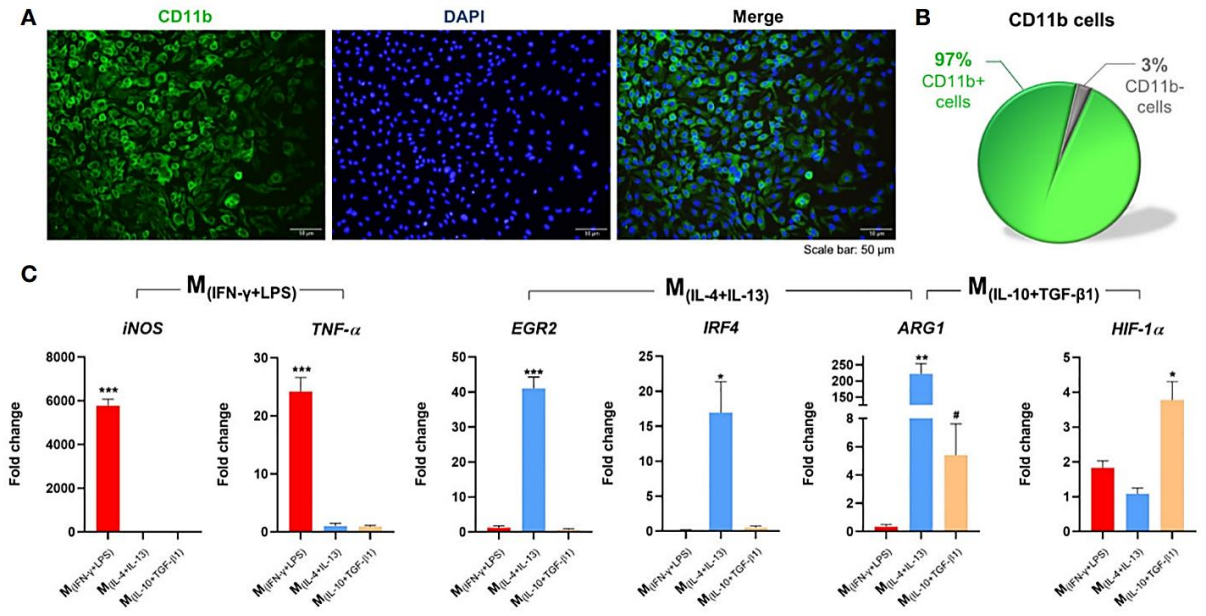

Figure 2.1: Isolation, differentiation, and polarization of macrophages. **(A)** Splenic monocytes cultured with macrophage colony-stimulating factor (M-CSF) for 7 days differentiated into macrophages; **(B)** with a culture purity of 97%. **(C)** Macrophages stimulated for 6 h with INF-γ and LPS significantly overexpressed *iNOS* (2, 7 df, p<0.0001) and *TNF-α* (2, 7 df, p<0.0001). Macrophages stimulated with IL-4 and IL-13 significantly overexpressed *EGR2* (2, 6 df, p<0.0001), *IRF4* (2, 6 df, p=0.0216), and *ARG1* (p=0.0020); and Macrophages stimulated with IL-10 and TGF-β1 significantly overexpressed *ARG1* (p=0.0357), and HIF-1α (2, 8 df, p=0.0032). Target genes were normalized to three reference genes: *GADPH*, *HPRT* and *18s*. Fold-change levels were calculated by the 2-ΔΔct method related to non-stimulated macrophages. In immunocytochemistry photomicrographs macrophages were quantified using the anti-CD11b antibody (green) and nuclei were stained with DAPI (blue). One Way ANOVA followed with Tukey *post-hoc* test was used for statistical analysis. *ARG1* data were analyzed using the Mann Whitney test because normality was not achieved using the Shapiro-Wilk test. Data is presented as mean ± standard error (SEM). df= degrees of freedom, * or #- p< 0.05; **- p< 0.01; ***- p< 0.001. Scale bar=50 µm. n=3. 2 independent experiments were performed.

2.4.2 IL-10 and TGF-β1 activation promotes higher axonal growth

The effects of each macrophage subtype on axonal growth were then investigated. Spleen-derived macrophages polarized into $M_{(INF\text{-}\gamma+LPS)}$, $M_{(IL\text{-}10+TGF\text{-}\beta1)}$ or $M_{(IL\text{-}4+IL\text{-}13)}$ were co-cultured with DRGs growing in three dimensions (Figure 2.2). DRGs cultured without macrophages were used as baseline. The results showed that DRGs co-cultured with $M_{(IL\text{-}10+TGF\text{-}\beta1)}$ and $M_{(IL\text{-}4+IL\text{-}13)}$ macrophages had significantly higher axonal arborization than those co-cultured with $M_{(INF\text{-}\gamma+LPS)}$ or than basal levels (Figure 2.2A). DRGs co-cultured with $M_{(IL\text{-}10+TGF\text{-}\beta1)}$) and $M_{(IL\text{-}4+IL\text{-}13)}$ macrophages also presented significantly longer axons (Figure 2.2B) than those co-cultured with $M_{(INF\text{-}\gamma+LPS)}$). Concerning the total axonal area, only $M_{(IL\text{-}10+TGF\text{-}\beta1)}$ condition showed significant differences from baseline (Figure 2.2C). We also performed a similar experiment with DRGs growing in two dimensions, which did not allow axonal growth in depth, but enabled direct contact between macrophages and DRGs (Supplementary Figure S2.2). Interestingly, under these conditions, only the DRGs co-cultured with $M_{(IL\text{-}10+TGF\text{-}\beta1)}$ macrophages presented significantly higher axonal arborization (Supplementary Figure S2.2a) than those co-cultured with the other subtypes of macrophages, these DRGs also have significantly longest neurite (Supplementary Figure S2.2b), and higher axonal area (Supplementary Figure S2.2c) than $M_{(IL\text{-}4+IL\text{-}13)}$ macrophages. It is important to point out that without the collagen matrix, axonal growth is significantly reduced, and not even the direct contact of the macrophages compensates for the absence of the 3D matrix.

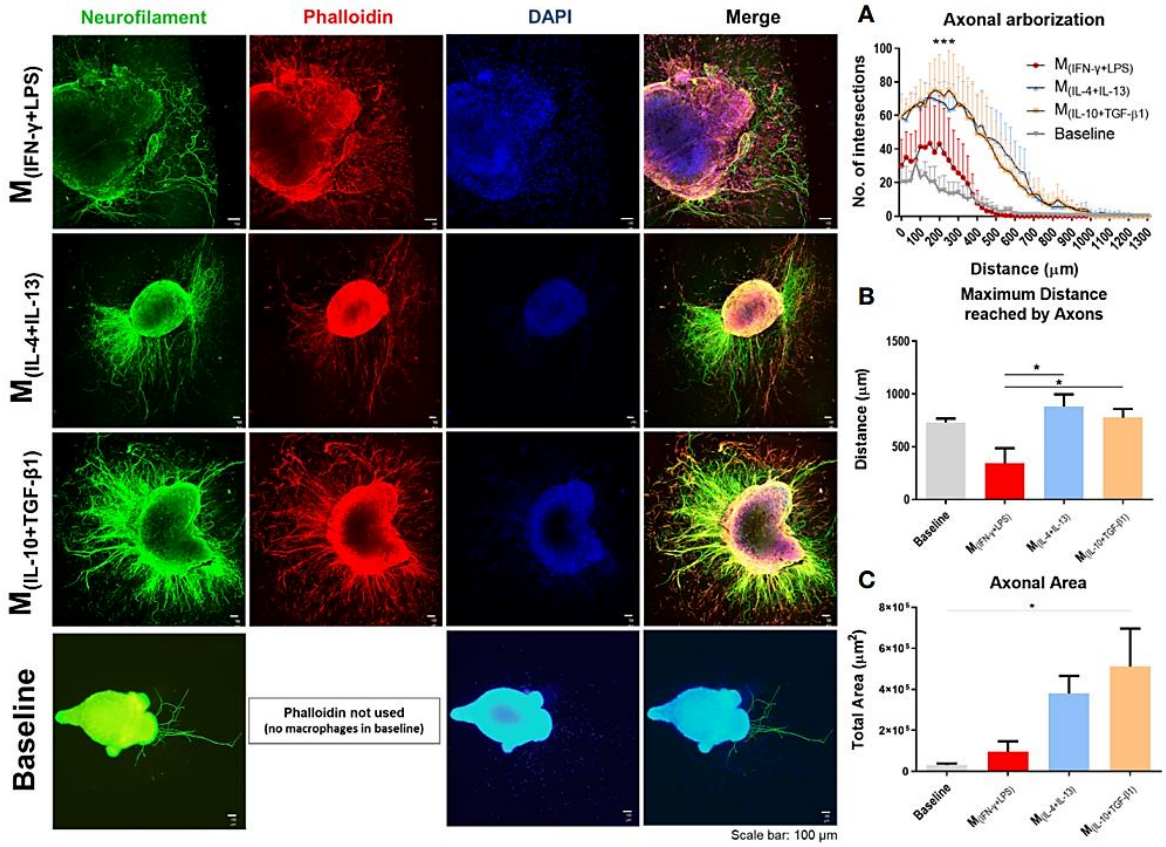

Figure 2.2: Classical ($M_{(INF-\gamma+LPS)}$) or alternative ($M_{(IL-4+IL-13)}$; $M_{(IL-10+TGF-\beta1)}$) activated macrophages co-cultured with dorsal root ganglia (DRGs) in 3D collagen hydrogels. DRGs were stained with Neurofilament (green), Macrophages and DRGs stained with Phalloidin (red) and nuclei counterstained with DAPI (blue). **(A)** DRGs co-cultured with $M_{(IL-4+IL-13)}$ and $M_{(IL-10+TGF-\beta1)}$ macrophages had significantly higher axonal arborization (3, 12 df, $p<0.0001$) and **(B)** significantly longer axons (3, 14 df, $p=0.0172$) than $M_{(INF-\gamma+LPS)}$ group and basal levels. **(C)** $M_{(IL-10+TGF-\beta1)}$ condition also showed significant higher axonal area than basal levels (3, 14 df, $p= 0.0292$). Statistical analysis for axonal arborization employed two-way ANOVA followed by Tukey's multiple comparisons test, while total area and distance were analyzed using one-way ANOVA followed by Tukey's test. Data is presented as mean ± standard error (SEM). df= degrees of freedom, *- $p< 0.05$; ***- $p< 0.001$. Scale bar =100 µm; $M_{(IFN-\gamma+LPS)}$ n= 3; $M_{(IL-4+IL-13)}$ n=5; $M_{(IL-10+TGF-\beta1)}$ n=5. 2independent experiments were performed.

The neuronal effects of the molecules and extracellular vesicles secreted by the different subtypes of splenic macrophages were also tested using human-derived neurospheres obtained from iPSCs. Neurospheres were allowed to differentiate into neurons for two days and then cultured with the secretome derived from each macrophage subtype (Figure 2.3A). It proved challenging to establish the baseline level of neuronal growth devoid of secreted factors as attempts to culture human neurospheres solely in basal medium were unsuccessful, leading to detachment from the culture plates and rendering meaningful analysis unfeasible. Nonetheless, we conducted a positive control using the regular culture medium to provide a comparative reference point. The total axonal area divided by the number of neurospheres was analyzed as described for the DRGs (see materials and methods section). As expected, the positive control group presented an overall neuronal area higher than all the groups, but notably it was only significantly different when compared with the $M_{(INF\text{-}\gamma+LPS)}$ and $M_{(IL\text{-}4+IL\text{-}13)}$ groups, but not with the $M_{(IL\text{-}10+TGF\text{-}\beta1)}$-derived secretome (Figure 2.3B). Results also demonstrated that the $M_{(IL\text{-}10+TGF\text{-}\beta1)}$ secretome significantly promoted more axon preservation/regeneration than $M_{(IL\text{-}4+IL\text{-}13)}$ secretome (Figure 2.3B). Both subtypes are pro-regenerative; however, our *in vitro* results showed that the $M_{(IL\text{-}10+TGF\text{-}\beta1)}$-derived secretome has higher regenerative capabilities. For this reason, we then tested only the secretome derived from this subpopulation in CNS-derived neurons.

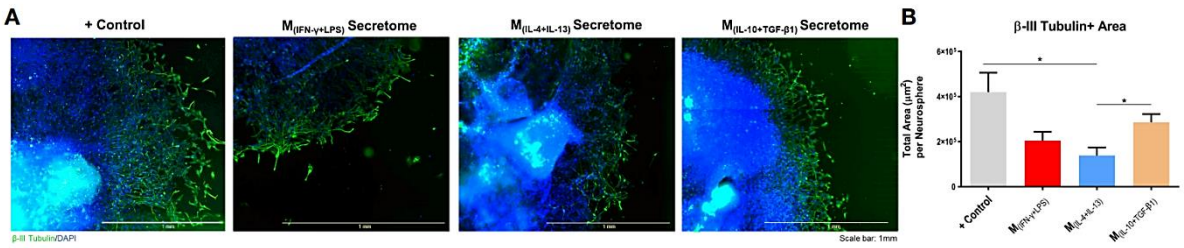

Figure 2.3: Axonal area of differentiated Neural Stem Cells obtained from human induced Pluripotent Stem Cells. **(A)** Axonal area was stained using anti-βIII tubulin antibody (green) and nuclei counterstained with DAPI (blue); **(B)** Statistical analysis demonstrated that the factors secreted by $M_{(IL\text{-}10+TGF\text{-}\beta1)}$ macrophages are able to significantly preserve/regenerate the differentiated neurons (2, 18, p=0.0364) than the $M_{(IL\text{-}4+IL\text{-}13)}$-secreted factors. One Way ANOVA followed by Tukey post-hoc test was used for statistical analysis. Data is presented as mean ± standard error (SEM). *- $p< 0.05$; $M_{(IFN\text{-}\gamma+LPS)}$ n=6; $M_{(IL\text{-}4+IL\text{-}13)}$ n=9; $M_{(IL\text{-}10+TGF\text{-}\beta1)}$ n=6; +Ct n=9. Scale bar=1 mm. 2 independent experiments were performed.

Primary cortical neurons were plated in the soma compartment of microfluidic chambers (Figures 2.4A, B), and neuronal growth was live imaged (Supplementary Video 2.1) in the axonal compartment for 14h (Figures 2.4C, D). The results demonstrated that $M_{(IL\text{-}10+TGF\text{-}\beta1)}$- derived secretome promoted significant axonal regeneration compared with the control medium (Figure 2.4E)

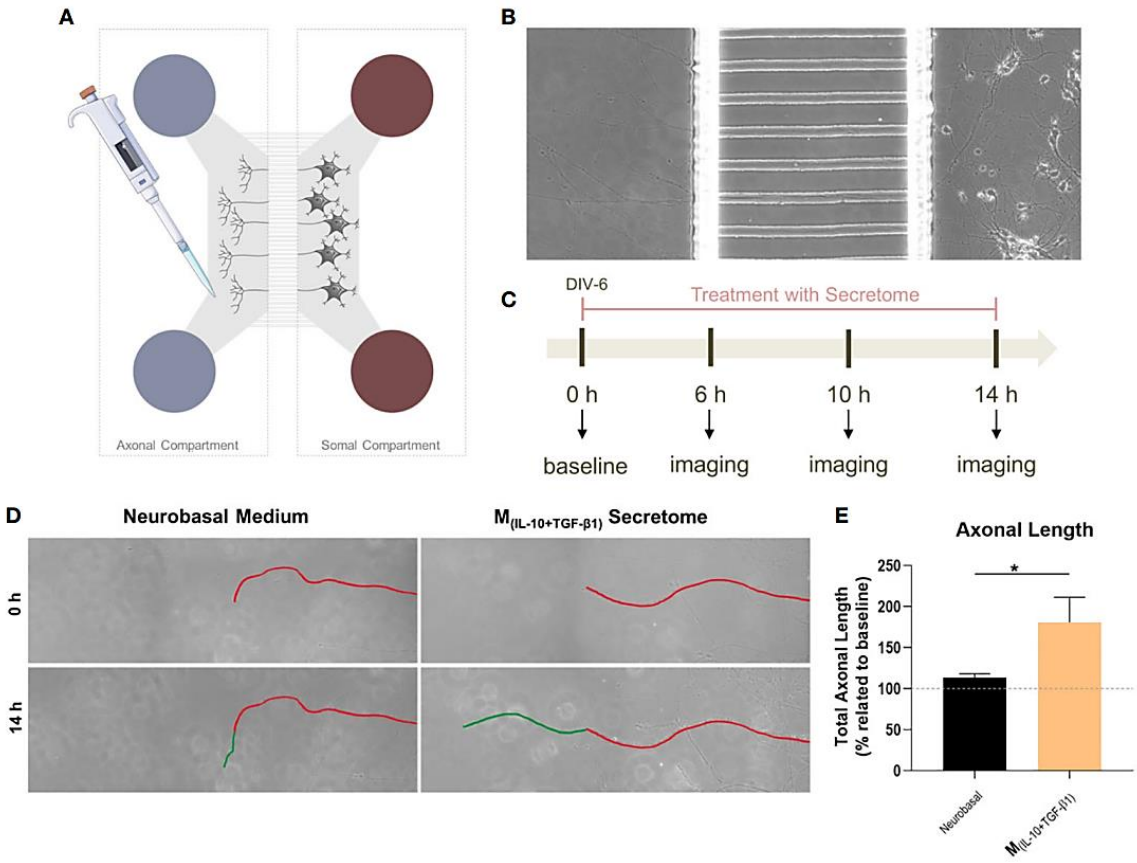

Figure 2.4: The effect of $M_{(IL\text{-}10+TGF\text{-}\beta1)}$-derived secretome on the CNS neurons. **(A)** Schematic representation of the microfluidic chambers used. **(B)** Brightfield images of the axonal and somal compartments of the microfluidic chambers. **(C)** Schematic representation of the workflow used. **(D)** Brightfield images of axons growing under the effect of the soluble factors and extracellular vesicles secreted by $M_{(IL\text{-}10+TGF\text{-}\beta1)}$ macrophages or Vehicle (Neurobasal Medium). In red is represented the length of the axon at baseline and in green after 14h of live imaging. **(E)** The secretome of $M_{(IL\text{-}10+TGF\text{-}\beta1)}$ macrophages promotes significantly axonal regeneration ($p= 0.0286$). Statistical significance tested by unpaired, non-parametric t-test (Mann-Whitney test). Data is presented as mean ± standard error (SEM). *- $p< 0.05$; n=4, DIV= days *in vitro*. 2 independent experiments were performed.

2.4.3 $M_{(IL\text{-}10+TGF\text{-}\beta1)}$ derived secretome promotes functional recovery *in vivo.*

In vitro experiments demonstrated that the soluble factors and extracellular vesicles secreted by macrophages may have therapeutic potential for neural repair. Therefore, we tested whether intraperitoneal injections (500 μL) of macrophage-derived secretome could be used as a therapy for spinal cord injury. Forty-two mice were subjected to compression SCI and 3, 6, 9, and 14 days post-injury (and then once a week up to 28 dpi) were treated with secretome derived from different macrophage subtypes (Figure 2.5A). During the experimental protocol, all animals lost weight without significant differences between groups (Figure 2.5B). To evaluate motor function, we performed the BMS test, in which a higher score indicates higher motor recovery. We found that mice treated with $M_{(IL\text{-}10+TGF\text{-}\beta1)}$ secretome had significantly higher BMS scores than those treated with the vehicle or $M_{(IL\text{-}4+IL\text{-}13)}$ (Figure 2.5C). Only animals treated with this pro-regenerative cocktail ($M_{(IL\text{-}10+TGF\text{-}\beta1)}$ secretome) were able to perform weight-supported plantar stepping, while the other treatment regimens only led to extensive ankle movement recovery without weight support. Interestingly, in the first 2/3 weeks post-injury, mice treated with the pro-inflammatory cocktail ($M_{(INF\text{-}\gamma+LPS)}$ secretome) presented a functional recovery very close to those treated with the $M_{(IL\text{-}10+TGF\text{-}\beta1)}$ secretome, indicating that this pro-inflammatory cocktail may be beneficial in the early phase. However, continuing with $M_{(INF\text{-}\gamma+LPS)}$ secretome treatment, the functional recovery stabilized, and the therapeutic effect disappeared (Figure 2.5C), indicating that the non-resolving nature of chronic exposure to this pro-inflammatory cocktail is detrimental. Four weeks post-injury, we performed the von Frey filament test to assess the mechanical sensitivity function of the animals. We did not detect any statistical differences; however, mice treated with the proinflammatory cocktail ($M_{(INF\text{-}\gamma+LPS)}$ secretome) had lower values, indicating that this treatment may lead to hypersensitivity. In contrast, the vehicle and $M_{(IL\text{-}10+TGF\text{-}\beta1)}$ secretome groups showed higher values in the von Frey filament test (Figure 2.5D), indicating less hypersensitivity. We also analyzed mouse autonomic function, namely bladder function, using the ration between water intake and amount of urine in the bladder. Bladder recovery is an important priority for people living with SCI [30]. Our results showed that mice treated with the $M_{(IL\text{-}10+TGF\text{-}\beta1)}$ secretome had a significant recovery of bladder control compared to those treated with vehicle and $M_{(INF\text{-}\gamma+LPS)}$ secretome (Figure 2.5E). This preclinical trial demonstrated that the therapeutic effect of the molecules and extracellular vesicles secreted by the different subtypes of macrophages varies depending on the phenotype, even when using two pro-regenerative phenotypes.

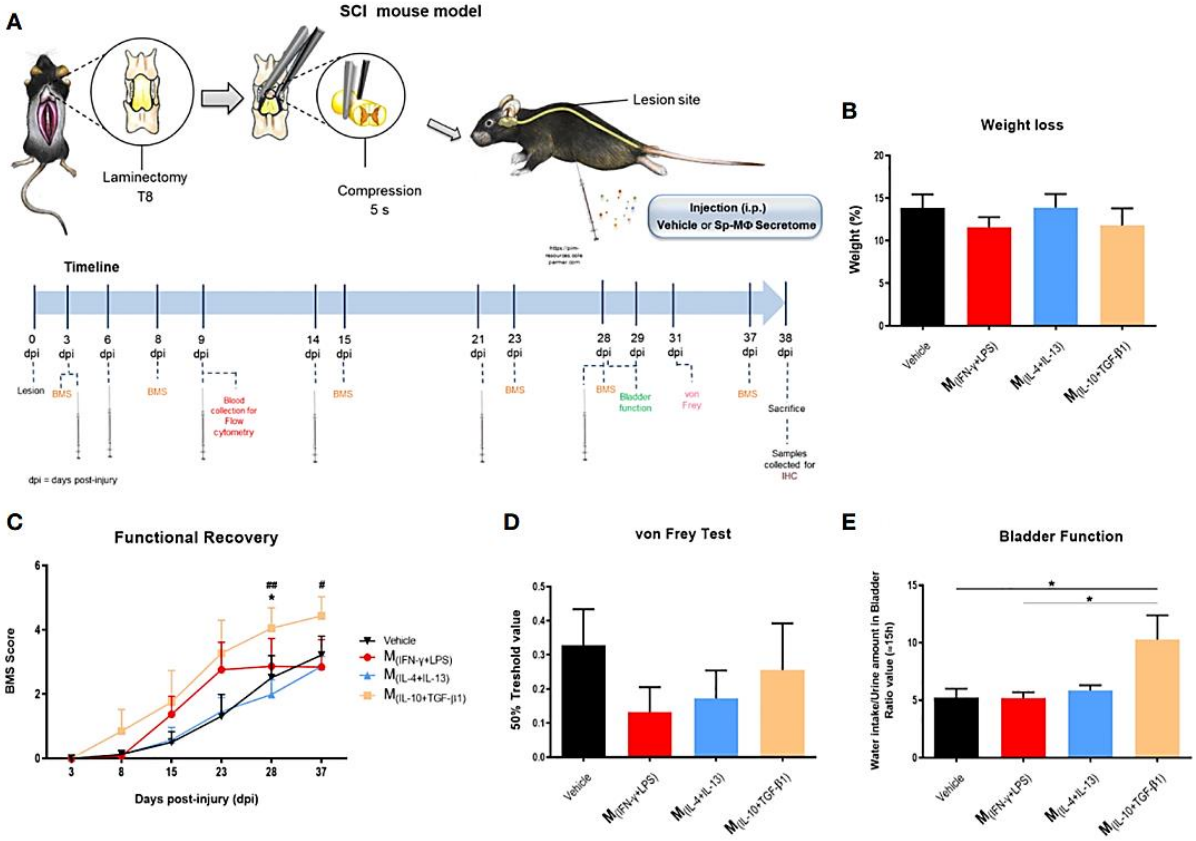

Figure 2.5: Pre-clinical evaluation of macrophages derived secretome using a SCI compression model. **(A)** Schematic layout of the in vivo testing. **(B)** The treatment had no effect on weight of the animals 38 dpi (3, 25 df, p=0.6013). **(C)** Animals treated with $M_{(IL\text{-}10+TGF\text{-}\beta1)}$-derived secretome presented significantly better functional scores than the other treatment groups, namely than the Vehicle (3, 25 df, p=0.0465) and $M_{(IL\text{-}4+IL\text{-}13)}$ group (3, 25 df, p= 0.0047) at 28 days and the $M_{(IL\text{-}4+IL\text{-}13)}$ at 37 days (3, 25 df, p= 0.0359). **(D)** No significantly differences were observed on the hypersensitivity of the animals 38 dpi, however, $M_{(INF\text{-}\gamma+LPS)}$-treated mice presented a tendency to be more hypersensitive (3, 25 df, p=0.5097). **(E)** Animals treated with $M_{(IL\text{-}10+TGF\text{-}\beta1)}$-derived secretome presented significant recovery of the bladder function when assessed 38 dpi (3, 22 df, p= 0.0137). Two-way repeated measure ANOVA was used to analyze statistical differences on the BMS data and One-Way ANOVA was used to analyze statistical differences on the other functional tests followed by the multiple comparison test Tukey. Data is presented as mean ± standard error (SEM). * or #- p< 0.05; ##- p< 0.01; df= degrees of freedom, Vehicle n=8; $M_{(INF\text{-}\gamma+LPS)}$ n=7; $M_{(IL\text{-}4+IL\text{-}13)}$ n=8; $M_{(IL\text{-}10+TGF\text{-}\beta1)}$ n=6. 1 independent experiment was performed.

2.4.4 $M_{(IL\text{-}10+TGF\text{-}\beta1)}$ derived secretome modulates pathophisiological events leading to neuronal survival *in vivo*

To understand the effect of the secretome on the immune response, we collected blood from all groups nine days post-injury and used healthy mice as controls. Flow cytometry was used to verify the inflammatory profile of leukocytes in circulation, which could infiltrate the injured spinal cord. Analysis revealed that mice treated with vehicle, $M_{(INF\text{-}\gamma+LPS)}$ and $M_{(IL\text{-}10+TGF\text{-}\beta1)}$ secretome had a significantly higher frequency of myeloid cells in circulation (Figure 2.6A). Mice treated with the $M_{(INF\text{-}\gamma+LPS)}$ secretome had a significantly higher frequency of monocytes than the $M_{(IL\text{-}10+TGF\text{-}\beta1)}$ secretome (Figure 2.6B). Mice treated with vehicle or $M_{(INF\text{-}\gamma+LPS)}$ secretome had a significantly higher frequency of $Ly6C^{high}$ monocytes (Figure 2.6C). It is noteworthy that the $Ly6C^{high}$ monocytes are prone to become pro-inflammatory macrophages [31]. $M_{(INF\text{-}\gamma+LPS)}$ also presented significantly more $Ly6C^{low\text{-}med}$ monocytes in circulation (Figure 2.6D). All animals with SCI had significantly more circulating neutrophils (Figure 2.6E). Concerning the rest of myeloid cells, $M_{(INF\text{-}\gamma+LPS)}$ also presented significant increase (Figure 2.6F). No differences were observed between the groups for B cells (Figure 2.6G).$M_{(INF\text{-}\gamma\text{-}+LPS)}$ and Vehicle-treated mice had a significantly lower frequency of T cells (Figure 2.6H). Of note, the number of animals used in the flow cytometry analysis varies from that used in functional recovery data because we opted to spare some animals during this sub-acute phase due to their weakened state. To conduct flow cytometry of circulating leukocytes blood collection was necessary, we decide to prioritize the well-being of the animals avoiding unnecessary risks of losing mice.

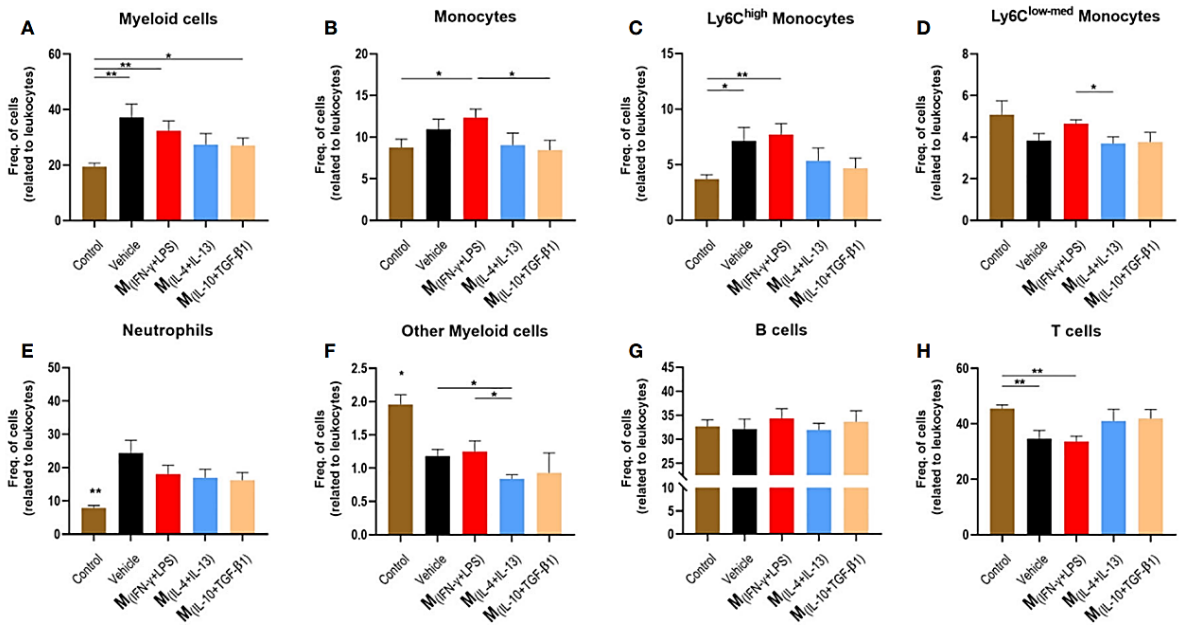

Figure 2.6: Leukocytes in circulation 9 days post injury. Blood was collected from the tail vein and process for analysis using flow cytometry. **(A)** Animals treated with Vehicle, $M_{(INF-\gamma+LPS)}$ and $M_{(IL-10+TGF-\beta1)}$-derived secretome had significantly higher myeloid cells than control mice (4, 17 df, p=0.0240). **(B)** Animals treated with $M_{(INF-\gamma+LPS)}$-derived secretome had significantly higher frequency of monocytes than $M_{(IL-10+TGF-\beta1)}$ secretome group and control (4, 17 df, p=0.0457). (C) Animals treated with Vehicle or $M_{(INF-\gamma+LPS)}$-derived secretome had a significantly higher frequency of $Ly6C^{high}$ monocytes (4, 17 df, p=0.0282) than control mice. **(D)** $M_{(INF-\gamma+LPS)}$ group also had significantly more $Ly6C^{med+low}$ monocytes than $M_{(IL-4+IL-13)}$-treated mice (4, 17 df, p=0.0457). **(E)** Animals without a SCI had significantly lower frequency of Neutrophils (4, 17 df, p=0.0055). **(F)** $M_{(IL-4+IL-13)}$-treated mice had significantly less other myeloid cells than Vehicle and $M_{(INF-\gamma+LPS)}$-treated animals (4, 17 df, p=0.0358). **(G)** No differences were observed for B Cells (4, 17 df, p=0.8721) and **(H)** $M_{(INF-\gamma+LPS)}$ and Vehicle-treated mice had significantly lower frequency of T cells (4, 17 df, p=0.0011) than control mice. One-Way ANOVA was used to analyze statistical differences followed by the multiple comparison test Tukey. Data is presented as mean ± standard error (SEM). *- p< 0.05; **- p< 0.01; df= degrees of freedom, Control n= 5; Vehicle n=5; $M_{(INF-\gamma+LPS)}$ n=4; $M_{(IL-4+IL-13)}$ n=5; $M_{(IL-10+TGF-\beta1)}$ n=4. 1 independent experiment was performed.

Thirty-eight days post-injury, the animals were sacrificed and the spinal cords were collected for histological analysis. IBA-1antibody was used to study the morphology of microglia and distinguish between ramified and amoeboid microglia (Figure 2.7A). Rostral-caudal analysis of the spinal cord showed that mice treated with the pro-regenerative cocktail $M_{(IL\text{-}10+TGF\text{-}\beta1)}$ had a significantly higher percentage of ramified microglia than mice treated with the pro-inflammatory cocktail $M_{(INF\text{-}\gamma+LPS)}$, or the $M_{(IL\text{-}4+IL\text{-}13)}$-secreted factors (Figure 2.7B).

The GFAP antibody was used to analyze astrogliosis. Areas of clustered GFAP overstaining were considered astrogliosis (Figure 2.7C). The analysis revealed that mice treated with the pro-regenerative cocktail, $M_{(IL\text{-}10+TGF\text{-}\beta1)}$) secretome, had significantly lower astrogliosis (Figure 2.7D), which indicate that these animals presented diminished scar.

Neurons from the ventral horns, namely from lamina VIII and IX, were counted using an anti-NeuN antibody (Supplementary Figure S2.3a). Mice treated with $M_{(IL\text{-}10+TGF\text{-}\beta1)}$ secretome have significantly more neurons than animals treated with the proinflammatory-derived secretome (Supplementary Figure S2.3b). Finally, concerning fibrosis, the rostral-caudal analysis did not detect significant differences in the PDGFR+ area (Supplementary Figure S2.3c) between the treated groups when all areas of the spinal cord were analyzed (Supplementary Figure S2.3d); however, caudally to the injury epicenter, mice treated with the $M_{(IL\text{-}10+TGF\text{-}\beta1)}$ secretome have significantly less fibrosis than the other treatments (Supplementary Figure S2.3e).

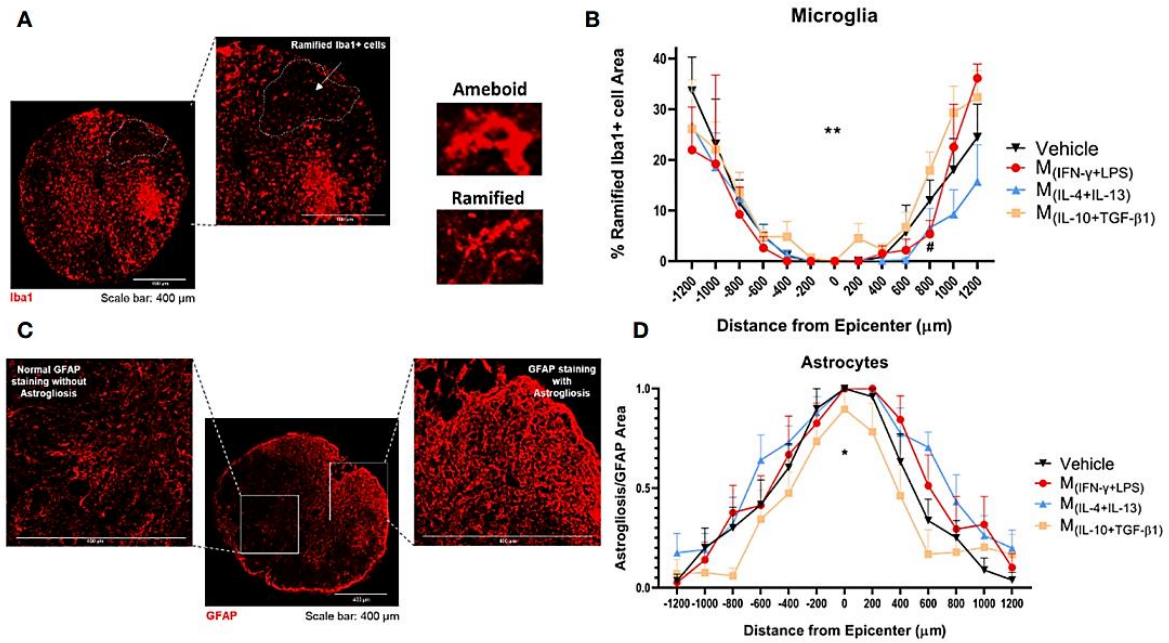

Figure 2.7: Histological analysis of the spinal cord 38 dpi. **(A)** Representative image of microglia from $M_{(IL\text{-}10+TGF\text{-}\beta1)}$-treated group, cells were stained using the antibody anti-IBA-1 (red) and the area of the ramified microglia was analyzed. **(B)** Rostral-caudal analysis demonstrated that the animals treated with $M_{(IL\text{-}10+TGF\text{-}\beta1)}$-derived secretome presented overall significantly more ramified microglia than $M_{(IL\text{-}4+IL\text{-}13)}$ group (3, 239 df, p=0.0058) and presented more ramified microglia than the $M_{(INF\text{-}\gamma+LPS)}$ group at 800 µm caudal to the injury (3, 239 df, p=0.0469). **(C)** Representative image of astrocytes from vehicle-treated group, cells were stained with anti-GFAP antibody (red) and astrogliosis were analyzed by quantification of the area of clustered GFAP overstaining (areas impossible to distinguish individual astrocytes). **(D)** Rostral-caudal analysis demonstrated that mice treated with $M_{(IL\text{-}10+TGF\beta1)}$-derived secretome had significantly less astrogliosis than the animals treated with $M_{(IL\text{-}4+IL\text{-}13)}$ or $M_{(INF\text{-}\gamma+LPS)}$ secretome (3, 231 df p<0.0001). Differences in both microglia and astrocytes analysis were detected using two-way ANOVA followed by Tukey's multiple comparisons test. A total of 284 spinal cord slices were observed to analyze astrogliosis and 301 slices to microglia. Data is presented as mean ± standard error (SEM). * or #- p< 0.05; **- p< 0.01; Vehicle n=7; $M_{(INF\text{-}\gamma+LPS)}$ n=6; $M_{(IL\text{-}4+IL\text{-}13)}$ n=8; $M_{(IL\text{-}10+TGF\text{-}\beta1)}$ n=6. 1 independent experiment was performed.

2.4.5 $M_{(IL\text{-}10+TGF\text{-}\beta1)}$ derived secretome preserved ascending and descending spinal tracts after SCI

Considering the functional and histological outcomes obtained from our pre-clinical trial, we executed a subsequent *in vivo* protocol with a focused objective: to assess the therapeutic efficacy of $M_{(IL\text{-}10+TGF\text{-}\beta1)}$ secretome specifically in the preservation of spinal tracts critical for locomotion. These tracts include the corticospinal tract (CST), rubrospinal tract (RST), and spinocerebellar tract (SCT). Within this cohort of animals, we employed mice harboring the Thy1-GFP transgene, and the percentage of positive area for Thy1-GFP in each distinct spinal tract was calculated (Figure 2.8A). The analysis encompassed a range spanning 600 μm to 2000 μm in both rostral and caudal directions from the epicenter. The vicinity of the epicenter was excluded from the analysis due to challenges in pinpointing the exact location of the spinal tracts. Results demonstrated that the administration of $M_{(IL\text{-}10+TGF\text{-}\beta1)}$ secretome significantly contributes to the preservation of the spinocerebellar tract caudally to the epicenter (Figure 2.8B), both the rostral and caudal portions of the rubrospinal tract (Figure 2.8C), and the preservation of the corticospinal tract (Figure 2.8D) in the rostral region. Significant differences were also observed between the rostral and caudal regions, however, only in the motor tracts (RST and CST). Specifically, the rostral regions exhibited a markedly higher extent of neuronal preservation in comparison to the caudal regions (Figures 2.8C, D).

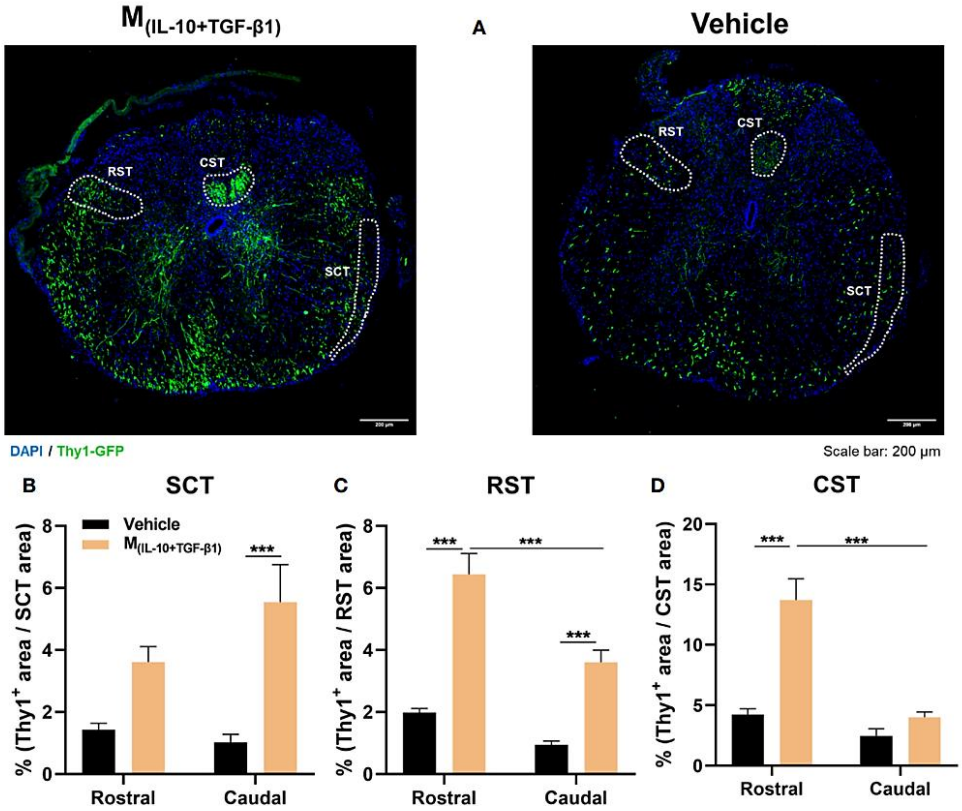

Figure 2.8: Histological analysis of ascending and descending spinal tracts 38 dpi. **(A)** Representative images of Thy1-GFP animals from $M_{(IL\text{-}10+TGF\text{-}\beta1)}$ and Vehicle-treated group. The positive area for Thy1-GFP (green) was calculated and divided for the total area of the tract in each spinal section. The analysis encompassed a range spanning 600 µm to 2000 µm in both rostral and caudal directions from the epicenter. **(B)** The secretome derived from $M_{(IL\text{-}10+TGF\text{-}\beta1)}$ macrophages significantly promoted higher neuronal preservation of spinocerebellar tract (SCT) in the caudal region (3, 65 df, p=0.0007) when compared with Vehicle treatment. **(C)** Animals treated with $M_{(IL\text{-}10+TGF\text{-}\beta1)}$ secretome also revealed a higher preservation of the rubrospinal tract (RST) both in the rostral (3, 64 df, p<0.0001) and in the caudal region (3, 64 df, p=0.0010). Moreover, the treatment effect was significantly higher in the rostral region than in the caudal (3, 64 df, p<0.0001). **(D)** Likewise, the $M_{(IL\text{-}10+TGF\text{-}\beta1)}$ secretome significantly preserved the corticospinal tract (CST) descending axons, namely rostrally from the epicenter (3, 74 df, p<0.0001), and this preservation was significantly higher in the rostral than in the caudal region (3, 74 df, p<0.0001). Two-way ANOVA followed by Tukey's multiple comparisons test was used to analyze statistical differences. A total of 163 spinal cord slices were analyzed. Data is presented as mean ± standard error (SEM). ***- p< 0.001. Vehicle n=3; $M_{(IL\text{-}10+TGF\text{-}\beta1)}$ n=3. 1 independent experiment was performed.

2.4.6 $M_{(IL\text{-}10+TGF\text{-}\beta1)}$ secretome present molecules involved with anti-inflammatory, phagocytosis and tissue repair/remodeling processes

In order to understand which proteins secreted by the different phenotypes of macrophages could be important for the differences observed both *in vitro* and *in vivo*, we identified and quantified the proteins produced by the macrophages using both the bead-based immunoassay LEGENDplex and liquid chromatography with mass spectrometry (LC-MS/MS). LC-MS/MS allows a broader and nontarget analysis; however, it may not detect small and low-concentrated proteins, such as cytokines and chemokines. For this reason, we complemented LC-MS/MS analysis with the immunoassay LEGENDplex. The results demonstrated that proinflammatory cytokines such as TNF-α, G-CSF and IL12p40 were present almost only in the secretome of $M_{(INF\text{-}\gamma+LPS)}$ and were significantly different from the other groups (Supplementary Figure S2.4). These results were expected because these cytokines are characteristic of proinflammatory macrophages. Additionally, the cytokine/hormone G-CSF was also significantly elevated in the $M_{(INF\text{-}\gamma+LPS)}$ secretome (Supplementary Figure S2.4). In turn, TGF-β1, a cytokine with anti-inflammatory properties, was present in higher quantities in the $M_{(IL\text{-}10+TGF\text{-}\beta1)}$ and $M_{(IL\text{-}4+IL\text{-}13)}$ subsets; however, only in the pro-regenerative phenotype $M_{(IL\text{-}10+TGF\text{-}\beta1)}$ that this cytokine reached significant differences (Supplementary Figure S2.4). The macrophage subsets that presented interesting results both *in vivo* and in the LegendPlex assay were the $M_{(IL\text{-}10+TGF\text{-}\beta1)}$ and $M_{(INF\text{-}\gamma+LPS)}$ phenotypes, and therefore, a detailed proteomics analysis was only performed in the secretome derived from these two populations. From a total of 452 proteins identified, we focused the analysis on those that presented higher concentrations (fold changes of 2 or higher) between the two groups. These proteins were grouped by function using the UniProt database, and the results revealed that 14 out of 17 pro-inflammatory proteins were overconcentrated in the $M_{(INF\text{-}\gamma+LPS)}$ secretome, and 3 out of 4 anti-inflammatory proteins were overconcentrated in the $M_{(IL\text{-}10+TGF\text{-}\beta1)}$ secretome (Figure 2.9A). Moreover, the $M_{(IL\text{-}10+TGF\text{-}\beta1)}$ secretome was also enriched in proteins involved in phagocytosis (9 out of 10) and in proteins involved in tissue repair/remodeling (7 out of 8) (Figure 2.9A). These results were expected because the $M_{(INF\text{-}\gamma+LPS)}$ and $M_{(IL\text{-}10+TGF\text{-}\beta1)}$ subsets are classified as pro-inflammatory and anti-inflammatory/repairing, respectively. Finally, protein–protein interaction network analysis was constructed using the online STRING database depicting both functional and physical protein associations and the results revealed that the secretome of $M_{(INF\text{-}\gamma+LPS)}$ contains proteins from just one cluster, which can be considered a cluster related to the inflammatory process, since these proteins are involved in antigen processing and presentation of peptide antigen, T cell-mediated cytotoxicity, and complement activation (Figure 2.9B). In contrast, the $M_{(IL\text{-}10+TGF\text{-}}$

$\beta_{1)}$ secretome contained proteins from three different clusters, a cluster of proteins more related to metabolic processes (Cluster 1), with proteins that participate in Ganglioside and Glycosphingolipid catabolic processes (Figure 2.9B). Two other clusters were identified, with proteins that participate in relevant biological and cellular processes, such as astrocyte activation involved in immune response, regulation of dendritic spine maintenance, and regulation of response to wounding (Cluster 2), and proteins that play a role in axon extension and central nervous system neuron development (Cluster 3), some of which may be responsible for the improvements observed *in vivo* (Figure 2.9B).

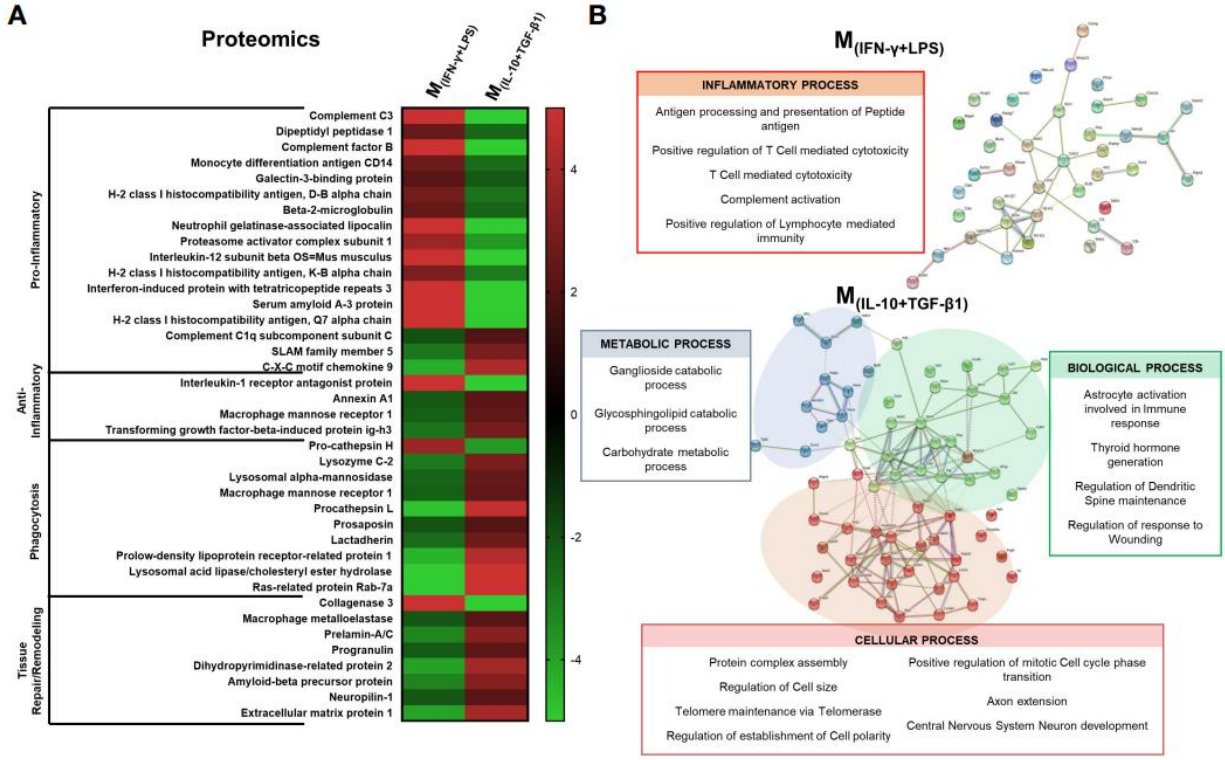

Figure 2.9: Proteomic analysis by LC-MS/MS focused on the proteins that presented higher concentration in the secretome. **(A)** 14 out of 17 pro-inflammatory proteins were overconcentrated in $M_{(INF-\gamma+LPS)}$-derived secretome; 3 out of 4 anti-inflammatory proteins were overconcentrated in $M_{(IL-10+TGF-\beta1)}$ secretome; $M_{(IL-10+TGF-\beta1)}$ secretome was enriched in proteins involved on phagocytosis (9 out of 10) and in proteins involved in tissue repair/remodeling (7 out of 8). **(B)** Cluster analysis using the STRING database revealed that the secretome of $M_{(INF-\gamma+LPS)}$ macrophages only presented proteins related to the inflammatory process (antigen processing and presentation of peptide antigen, T cell mediated cytotoxicity and complement activation); $M_{(IL-10+TGF-\beta1)}$ macrophages secreted proteins were classified into three main clusters: Cluster 1 - proteins related with metabolic process; Cluster 2 - proteins that participate in biological processes, such as, astrocyte activation, involved in immune response, regulation of dendritic spine maintenance and regulation of response to wounding; and Cluster 3 - proteins that play a role in cellular processes such as axon extension and central nervous system neuron development. Proteins were identified using the KEGG Orthology database. 1 independent experiment was performed.

2.5 Discussion

After injury, the immune system is fundamental for promoting adequate tissue repair and regeneration. However, it is well known that the immune response after SCI is dysfunctional and is an important contributor to the secondary damage observed after primary injury. Several therapeutic approaches have been designed to shut down the immune response after SCI; however, more important than shutting it down is to transform a dysfunctional response into a regenerative one. After SCI, splenic and bone marrow-derived monocytes infiltrate the lesion site and differentiate into macrophages [4]. There is abundant literature exploring bone marrow-derived monocytes in an SCI context [10, 32–34], however, less is known about splenic monocytes. The spleen is not just important for erythrocyte recycling and immune response to pathogens. After injury, immune cells in the spleen become rapidly activated and mobilize to sites of damaged tissue. This activation and mobilization was first observed after myocardial ischemia and also demonstrated after SCI [5, 24]. Splenic monocytes infiltrated the spinal cord in the acute phase of the injury, peaking at 7 days, whereas bone marrow-derived monocytes only infiltrated the cord 1 week after injury [4]. Although the spleen has been characterized as the major source of pro-inflammatory monocytes after SCI [4], in ischemic brain injury models, splenic monocytes have been demonstrated to be key effector cells that modulate meningeal and parenchymal immune responses and limit ischemic injury, leading to improved functional outcomes [35]. This indicates a complex interplay between the recruited splenic monocytes and the tissue microenvironment that finally determines the macrophage phenotype.

For these reasons, in this work, we aimed to study and further characterize splenic-derived macrophages in an SCI context, as this cell population may play a key role in tissue repair.

In this study, we used a protocol that led to a highly pure (97%) culture of primary splenic macrophages without the need to use cell sorting or magnetic beads separation kits. It is difficult to compare our purity with other protocols in the literature because the vast majority of studies do not disclaim this value [36–38] or use macrophage cell lines instead of primary cells [39]. We demonstrated that splenic monocytes are similar to monocytes from other origins in terms of plasticity and are easily polarized into pro-inflammatory or pro-regenerative phenotypes. Moreover, we demonstrated that different splenic macrophage phenotypes have distinct effects on axonal growth and neuroprotection. Namely, classical activation (pro-inflammatory) has a detrimental impact, whereas alternative activation promotes axonal regeneration and neuroprotection. To the best of our knowledge, these biological effects were first described in our work for spleen-derived macrophages; however, these effects were also previously

demonstrated in bone marrow-derived macrophages [10, 40]. It is important to point out that the vast majority of the research in the literature only studied one type of alternative activation of macrophages (using IL-4); herein, we showed that activation with TGF-β1 and IL-10 has significantly superior biological effects than activation with IL-4 and IL-13, not only *in vitro* but also in an *in vivo* SCI model.

As previously mentioned, the microenvironment at the SCI site favors predominant and sustained macrophage polarization into a pro-inflammatory phenotype, which is detrimental to tissue repair [15]. Some authors have investigated the therapeutic effect of transplanting alternatively activated macrophages into the damaged spinal cord to balance the ratio between pro- and anti-inflammatory macrophages at the injury site [12, 32]. However, clinical trials have failed to demonstrate a significant therapeutic effect. Clinical results did not support the treatment of acute SCI with autologous incubated macrophage therapy [14]. The reason behind this disappointing result may be that transplanted macrophages fail to retain their pro-regenerative phenotype when transplanted into the injured spinal cord [10]. Kroner and colleagues demonstrated that intracellular accumulation of iron by macrophages induces a rapid switch from a pro-regenerative to a pro-inflammatory phenotype in the spinal cord tissue [15]. Therefore, in this study, we decided to inject the soluble factors and extracellular vesicles produced by macrophages (secretome) instead of transplanting the cells. Herein, we explored whether systemic injections of secretomes derived from different macrophage phenotypes have a therapeutic effect after SCI. We tested the complete secretome rather than separating the soluble and vesicular fractions, because our previous evidence demonstrated that for SCI repair, the secretome as a whole is advantageous over the individual fractions [41]. The local immune response after SCI is known to be dysfunctional; however, SCI also leads to the systemic dysregulation of the immune response. For instance, it was demonstrated that SCI could promote pro-inflammatory responses that damage peripheral organs [42, 43]. Moreover, our group previously demonstrated that the infiltration of neutrophils into the injured spinal cord is affected by neural communication between the spinal cord and the spleen [24]. The combined factors of local environment and systemic dysregulation of the immune response led us to choose the systemic administration of secretome instead of local administration or local transplantation of macrophages. In this way, we not only avoided losing the phenotype of the transplanted cells due to local environmental cues, but we are also able to modulate/prime immune cells even before they infiltrate the spinal cord. Notably, in our experimental animal model, the blood-spinal cord barrier (BSCB) is disrupted due to the mechanical compression, allowing the systemic-injected molecules to reach the spinal cord tissue. However, it is crucial to acknowledge that, even with this

scenario, the majority of systemically delivered secretome is directed towards peripheral organs such as the liver, lungs, and spleen [44–46]. Moreover, in some clinical scenarios, the BSCB may remain intact, in these situations intrathecal administration may be necessary.

In this study, we observed that the $M_{(IL\text{-}10+TGF\text{-}\beta1)}$-derived secretome is the most effective treatment in promoting functional recovery after compressive SCI. Additionally, factors and extracellular vesicles secreted by $M_{(IL\text{-}10+TGF\text{-}\beta1)}$ also supported the recovery of bladder function. Regain of bladder control is an important functional priority for persons living with SCI [30, 47]. Interestingly, up to 3 weeks post-injury, treatment with the proinflammatory secretome, $M_{(INF\text{-}\gamma+LPS)}$, had a similar therapeutic effect to the $M_{(IL\text{-}10+TGF\text{-}\beta_1)}$ secretome; however, the continued injection of molecules derived from the pro-inflammatory phenotype was shown to be detrimental in the long term. In line with this observation, previous research performed by Freria and colleagues demonstrated that preconditioning microglia with LPS injection before ischemic SCI elicits reactive spinal cord microglia and confers neuroprotection, leading to functional recovery [48]. Indeed, a pro-inflammatory response seems to be necessary, at least in the acute phase or before injury; however, our results show that if this pro-inflammatory stimulus continues over time, the therapeutic effect ceases and becomes disadvantageous. We also observed that animals treated with the pro-inflammatory secretome tend to have more neuropathic pain. This data is in accordance with the current literature demonstrating that inflammation in the spinal cord leads to mechanical allodynia [49, 50]. Microglia activation in the spinal cord is critical for developing pain hypersensitivity through the production of pro-inflammatory cytokines, chemokines and extracellular proteases [51]. Activated microglia directly interacts with nociceptors and interneurons by modulating cell surface receptors and ion channels [52].

The identification and quantification of the molecules on the secretome were studied using flow cytometry, through the Legendplex immunoassay kit, and proteomic analysis using LC-MS/MS. Proteomics data were further examined using the STRING database, a web-based open resource that analyzes all known and predicted associations between proteins, including physical and functional interactions [53]. Cluster analysis of the $M_{(INF\text{-}\gamma+LPS)}$-derived secretome revealed that only one class of proteins was functionally enriched. Namely, proteins associated with a proinflammatory response, such as molecules related to positive regulation of T cells cytotoxicity and lymphocytes, mediate immunity, as well as complement activation molecules and proteins involved in antigen processing and presentation of peptide antigen. The immunoassay also revealed that the cytokines TNF-α, IL-12p40, and G-CSF were enriched in the $M_{(INF\text{-}\gamma+LPS)}$ secretome. On the other hand, analysis of the $M_{(IL\text{-}10+TGF\text{-}\beta1)}$-derived secretome

showed that these macrophages secrete a wide variety of proteins structured in three main functional clusters: 1) proteins involved in phagocytosis; 2) proteins involved in tissue remodeling/response to wounding; and 3) proteins with anti-inflammatory properties. Moreover, STRING analysis identified clusters of proteins on the $M_{(IL\text{-}10+TGF\text{-}\beta1)}$ secretome involved in axon extension, dendritic spine maintenance, establishment of cell polarity, and regulation of astrocytic activation. Looking for individual proteins enriched in the $M_{(IL\text{-}10+TGF\text{-}\beta1)}$ secretome, it is possible to find some proteins with a known effect after SCI. For instance, it was demonstrated that Anexinn 1a administration decreased caspase-3 and IL-1β expression, reduced tissue damage, and protected axons of long descending pathways in vivo [54]. In this context, the presence of Anexinn 1a within the secretome likely contributed to the preservation of long descending and ascending spinal tract. Our findings underscore the capacity of the $M_{(IL\text{-}10+TGF\text{-}\beta1)}$ secretome to significantly support the structural integrity of crucial neuronal tracts, including the ascending spinocerebellar tract (SCT) and the descending rubrospinal (RST) and corticospinal tracts (CST). Notably, these tracts assume pivotal roles in locomotion. For instance, the significance of SCT neurons in orchestrating the genesis and perpetuation of locomotor behavior in both neonatal and adult mice has been previously described [55]. SCT neurons exhibit inherent rhythmogenic attributes and intricate circuit connectivity with spinal interneurons within the locomotor central pattern generator [55]. Moreover, the indispensability of this neuronal pathway for motor function restoration in human individuals afflicted with spinal cord injuries has been well documented [56–58].

Likewise, the RST plays a multifaceted role in various components of dexterous motor functions. Disruptions within the RST give rise to deficits in intricate motor tasks such as reaching and grasping, as well as stepping movements [59]. Evidently, the structural soundness of the RST is indispensable for limb coordination during activities encompassing food retrieval and ambulation. Equally pivotal, the contribution of CST neurons to voluntary movement has been extensively elucidated [60, 61], as has the paramount importance of this spinal tract in effecting motor recovery in SCI patients [62, 63]. It is important to note that a higher degree of neuronal preservation was observed within regions that continue to receive afferent neuronal input. Consequently, the rostral portions of the descending tract demonstrate a superior level of neuronal preservation compared to their caudal counterparts due to the enduring reception of supraspinal information. In contrast, the ascending tract exhibits an inverse relationship, wherein higher preservation is evident in caudal regions due to the persistence of afferent input.

Progranulin is another protein enriched in the $M_{(IL\text{-}10+TGF\text{-}\beta1)}$ secretome, which may play a key role in repairing the injured spinal cord. Progranulin deficiency has been demonstrated to promote

neuroinflammation and apoptosis and exacerbate damage [64]. Moreover, progranulin protects lysosomal function and enhances the autophagic flux of microglia, allowing these cells to acquire an anti-inflammatory phenotype [65] and modulate the expression of GFAP, thereby decreasing the pro-inflammatory activation of astrocytes [66, 67]. Indeed, previous studies have demonstrated that microglia respond rapidly to pathological stimuli, influencing then the fate of astrocytes [68, 69]. Additional, using single-cell RNA sequencing, Brennan and colleagues revealed that microglia play a pivotal role in controlling stereotypical astrocyte-specific functions triggered by SCI, including upregulation of inflammatory genes, lipid processing, cell adhesion, and proliferation [70]. Pro-inflammatory microglia release IL-1β, TNF-α, and complement component 1 subcomponent q (C1q), inducing the formation of inflammatory reactive astrocytes, commonly referred to as A1. Conversely, anti-inflammatory microglia promote the induction of pro-regenerative astrocytes, known as A2, thereby mitigating inflammation and exerting neuroprotective effects [68]. Our histological analysis revealed that systemic injections of $M_{(IL\text{-}10+TGF\text{-}\beta1)}$ secretome resulted in fewer amoeboid microglia and reduced astrogliosis in the spinal cord tissue 5 weeks post-injury. The factors present in the secretome likely influenced the microglial phenotype, leading to decreased astrogliosis.

TGF-β1 is elevated in the $M_{(IL\text{-}10+TGF\text{-}\beta1)}$ secretome; however, its role after SCI is more controversial. Some studies have stated that TGF-β1 might have a detrimental role after SCI [71, 72], while others have shown that it may have a therapeutic role [73, 74]. One study described TGF-β1 as an inducer and promoter of fibroblasts distribution and fibrotic scar formation [72]. However, in this study we specifically analyzed the fibrotic scar and observed a significantly reduction of fibrosis on $M_{(IL\text{-}10+TGF\text{-}b1)}$-treated animals; therefore, the systemic administration or the presence of other molecules on the secretome seems to inhibit this effect of TGF-β1 on fibrosis. One possible explanation for this finding is that it may be an indirect effect mediated by the modified microglia, similar to the mechanism observed in astrogliosis. It was demonstrated that microglia activated with anti-inflammatory factors can attenuate neuroinflammation-induced scarring by rescuing the expression of Arf and Rho GAP adapter protein 3 [75]. Additionally, transplantation of neonatal microglia and single-cell RNA sequencing studies have highlighted the crucial role of microglia in scar-free healing [76]. It is also important to point out that PDGFR+ cells may play a multifaceted role after spinal cord injury, with conflicting findings reported in the literature. As a major pericyte marker, PDGFRβ has been associated with the proliferation of scar-forming cells [77]. Studies suggest that inhibiting the proliferation of PDGFRβ+ pericytes reduces fibrotic

scar formation by fibroblasts, thereby promoting axon regeneration and functional recovery following SCI [78]. On the contrary, evidence also indicates a positive role for PDGFRβ+ pericytes in sealing the lesion core after SCI, aiding in injury containment and protecting neural tissue [77, 79]. However, it was demonstrated that PDGFR+ cells that contribute to normal tissue healing and regeneration return to their physiological niche, and that their prolonged presence in the tissue resulted in tissue fibrosis and aberrant healing [80]. Our analysis was performed 38 days after injury, which may indicate that these cells are contributing to tissue fibrosis instead of tissue healing.

Finally, Dihydropyrimidinase-related protein 2, also known as Collapsin Response Mediator Protein-2 (CRMP2), is recognized for its affinity for tubulin heterodimers and functions in regulating the microtubule network, playing an important role in neuronal polarity establishment and axonal guidance [81]. Several authors have identified CRMP2 as a crucial molecule for axonal regeneration [82, 83]. The presence of this protein in the $M_{(IL\text{-}10+TGF\text{-}\beta1)}$ secretome may be crucial for explaining the regeneration observed when using DRGs. *In vivo* CRMP2 was also identified as a contributor to the maintenance of spinal-cord regenerative ability [84], playing a key role in promoting axonal regeneration and leading to functional motor improvements [85]. Recently, the function of CRMP2 was also described in human cells. The GADD45G/p38 MAPK/CDC25B signaling pathway promotes dephosphorylation of phosphorylated CRMP2 which in turn facilitates microtubule polymerization and leads to neurite outgrowth in human neurons [86].

Identifying the mechanism of action of our therapeutic approach is challenging; most likely, several proteins and extracellular vesicles have a distinct therapeutic action over time. Nonetheless, future experiments will focus on blocking some of the most promising candidates to understand whether the beneficial effects of the $M_{(IL\text{-}10+TGF\text{-}\beta1)}$ secretome have one or several origins. In the first week after SCI, most of the monocytes circulating in the blood will be derived from the spleen reservoir (4), so in a putative clinical situation there is no need to obtain monocytes from the spleen of the person with SCI, a sample of blood will work. However, in future experiments, we will also have to test whether the $M_{(IL\text{-}10+TGF\text{-}\beta1)}$ secretome obtained from monocytes isolated from blood has the same therapeutic action as those obtained directly from the spleen. Finally, in this study, we started the treatment 3 days after injury, which means that in a clinical scenario patients need to receive injections of the allogeneic derived secretome. For autologous treatment, we will need to assess whether the $M_{(IL\text{-}10+TGF\text{-}\beta1)}$ secretome maintains its therapeutic effect when administered at least 10 days post-injury.

2.6 Conclusions

In this study, we demonstrated that different splenic macrophage phenotypes secrete factors and extracellular vesicles with distinct therapeutic effects. We conclude that systemic injection of the $M_{(IL-10+TGF-\beta1)}$ secretome is the most effective treatment in promoting functional motor recovery after compressive SCI. Additionally, the $M_{(IL-10+TGF-\beta1)}$ secretome supported the recovery of bladder function. Proteomic analysis showed that these macrophages secrete a wide variety of proteins involved in axon extension, dendritic spine maintenance, establishment of cell polarity, and regulation of astrocytic activation. The results presented herein are promising, and additional research is needed to optimize and characterize this therapy so that it can be translated to clinical use.

2.7 Data availability statement

The original contributions presented in the study are included in the article/Supplementary Material. Further inquiries can be directed to the corresponding author. The mass spectrometry proteomics data have been deposited to the ProteomeXchange Consortium via the PRIDE partner repository with the dataset identifier PXD048453.

2.8 Ethics statement

The animal study was approved by ethical Subcommittee in Life and Health Sciences (SECVS; ID:018/2019, University of Minho). The study was conducted in accordance with the local legislation and institutional requirements.

2.9 Author contributions

JL-G: Formal analysis, Investigation, Writing – original draft. DS: Formal analysis, Investigation, Writing – review & editing. JA: Formal analysis, Investigation, Writing – review & editing. AM: Writing – review & editing. AP: Formal analysis, Investigation, Writing – review & editing. VM: Formal analysis, Investigation, Writing – review & editing. MD: Formal analysis, Investigation, Writing – review & editing. EG: Investigation, Writing – review & editing. RL: Investigation, Writing – review & editing. LF: Formal analysis, Investigation, Writing – review & editing. FF-A: Formal analysis, Investigation, Writing – review & editing. IP: Investigation, Writing – review & editing. NdS: Investigation, Writing – review & editing. JRC: Investigation, Writing – review & editing. AF: Investigation, Writing – review & editing. SS: Investigation, Writing – review & editing. LR: Investigation, Writing – review & editing. JC: Formal analysis, Investigation, Writing – review & editing. TP: Investigation, Writing – review & editing. SM: Investigation, Writing – review

& editing. BM: Formal analysis, Writing – review & editing. AS: Funding acquisition, Writing – review & editing. RA: Formal analysis, Investigation, Writing – review & editing. NS: Conceptualization, Funding acquisition, Project administration, Resources, Supervision, Writing – original draft, Writing – review & editing.

2.10 Funding

The author(s) declare financial support was received for the research, authorship, and/or publication of this article. This work has been funded by National funds, through the Foundation for Science and Technology (FCT) - project UIDB/50026/2020 (DOI 10.54499/UIDB/50026/2020), UIDP/50026/2020 (DOI 10.54499/ UIDP/50026/2020), LA/P/0050/2020 (DOI 10.54499/LA/P/0050/2020) and EXPL/MED-PAT/0931/2021. Financial support was also provided by Prémios Santa Casa Neurociências–Prize Melo e Castro for Spinal Cord Injury Research (MC-18-2021) and by Wings For Life Spinal Cord Research Foundation (WFL-PT-14/23). Imaging acquisition was performed in the LiM facilities of iBiMED and at the ICVS Scientific Microscopy Platform, both are members of the national infrastructure PPBI - Portuguese Platform of Bioimaging (PPBI-POCI-01-0145-FEDER-022122).

2.11 Acknowledgments

We would also like to acknowledge the FCT for the Scientific Employment Stimulus to NAS and SM (CEECIND/04794/2017 and CEECIND/01902/2017) and for grants to JL-G (PD/BD/127820/2016), MSD(SFRH/BD/141092/2018). José Graça would like to acknowledge the PhDOC – Inter-University Doctoral Program in Ageing and Chronic Disease.

2.11 Conflict of interest

The authors declare that the research was conducted in the absence of any commercial or financial relationships that could be construed as a potential conflict of interest.

The author(s) declared that they were an editorial board member of Frontiers, at the time of submission. This had no impact on the peer review process and the final decision.

2.12 Supplementary material

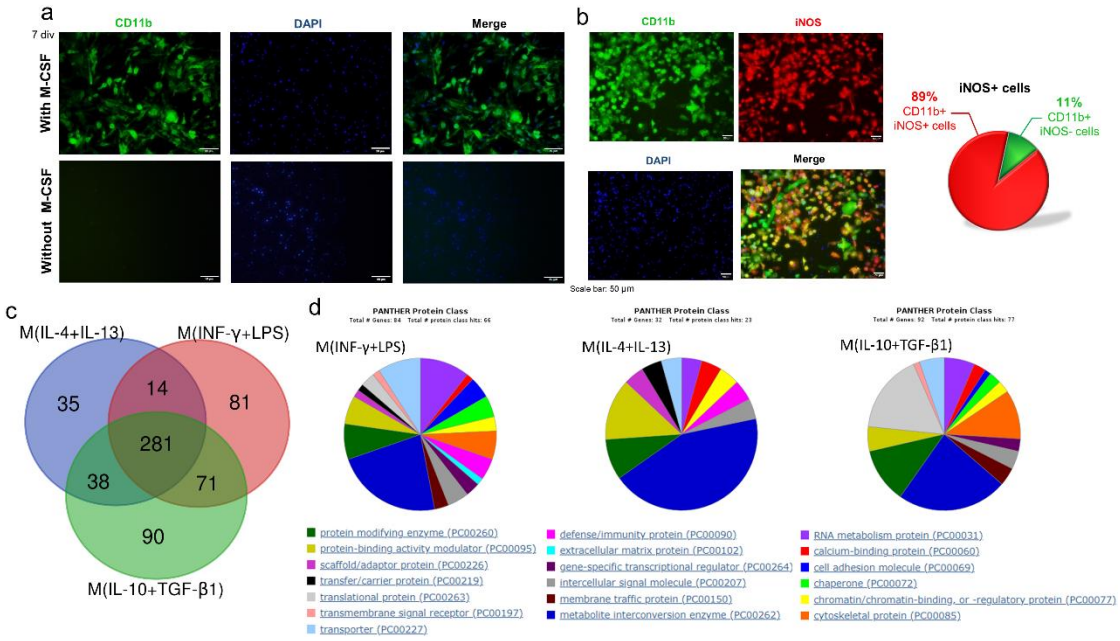

Supplementary Figure S2.1: Splenic macrophages characterization. **a)** MCS-F is essential for the survival and proliferation and differentiation of splenic monocytes into macrophages. **b)** After 24h of polarization with the pro-inflammatory molecules LPS and INF-γ, 89% of the macrophages expressed iNOS. **c)** A total of 487 proteins identified, 81 were exclusive to the secretome of $M_{(INF-\gamma+LPS)}$ macrophages, 35 to $M_{(IL-4+IL-13)}$, and 90 to $M_{(IL-10+TGF-\beta1)}$. **d)** Using the PANTHER tool was possible to identified metabolite interconversion enzymes (dark blue) as a common protein class between the different macrophage populations, but as can be observed by the pie charts, the protein class and the percentage of proteins in different classes varied considerably among each cell phenotype. Anti-CD11b antibody was used to identify macrophages (green), anti-iNOS antibody was used to confirm the polarization (red) and nuclei was counterstained with DAPI (blue). Scale bar =50 µm. 2 independent experiments were performed for the in vitro data and 1 independent experiment for proteomics analysis.

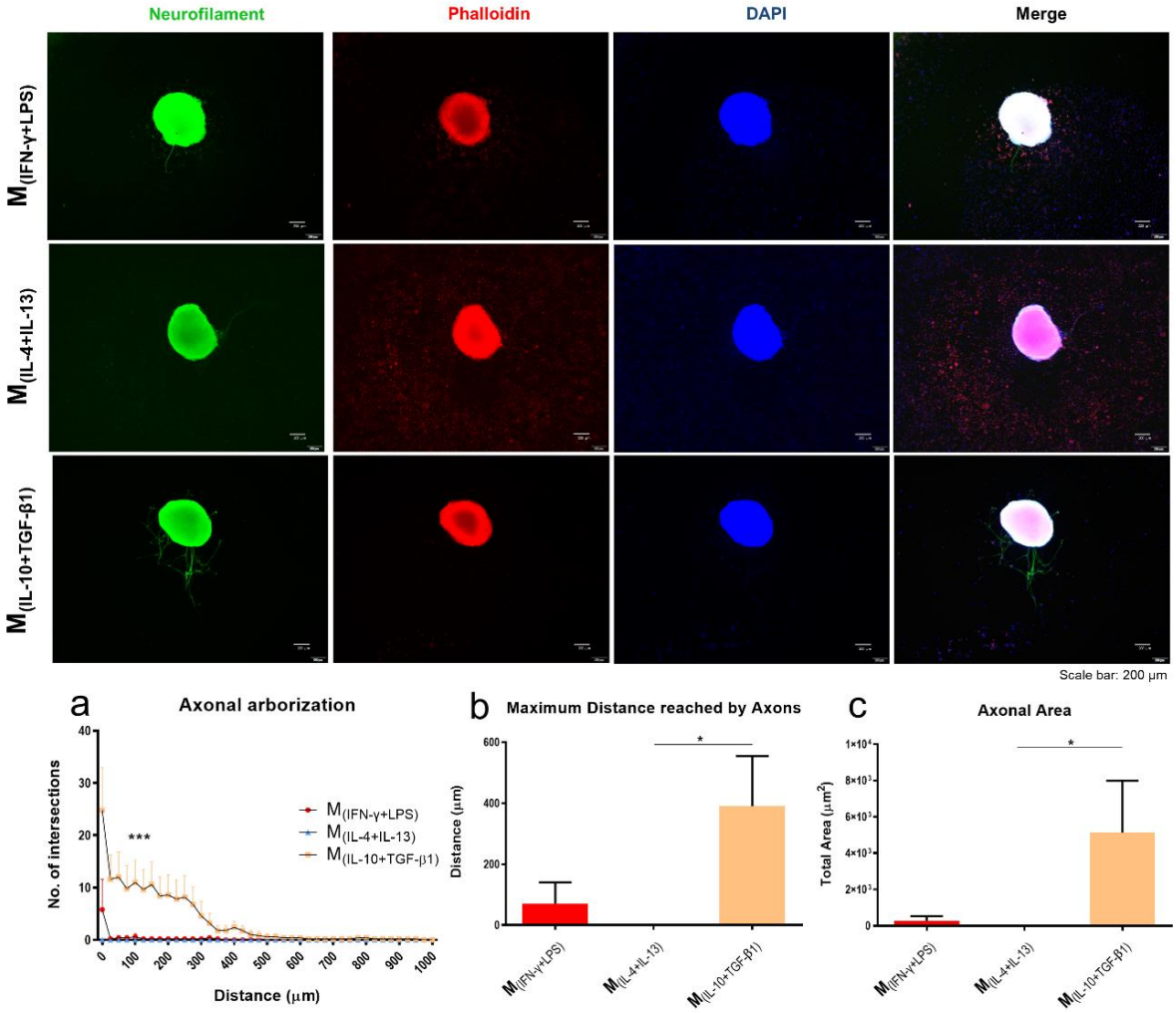

Supplementary Figure S2.2: Classical ($M_{(INF-\gamma+LPS)}$) or alternative ($M_{(IL-4+IL-13)}$; $M_{(IL-10+TGF-\beta1)}$) activated macrophages co-cultured with dorsal root ganglia (DRGs) in 2D. DRGs stained with Neurofilament (green), Macrophages and DRGs stained with Phalloidin (red) and nuclei counterstained with DAPI (blue). **a)** DRGs co-cultured with $M_{(IL-10+TGF-\beta1)}$ macrophages had significantly higher axonal arborisation (3, 17 df, $p<0.0001$) and **b)** significantly longer axons ($p=0.0247$) than the than $M_{(IL-4+IL-13)}$. **c)** $M_{(IL-10+TGF-\beta1)}$ also had significant more axonal area (0.0240) than the $M_{(IL-4+IL-13)}$. Two way ANOVA followed by Tukey post-hoc test was used for axonal arborization analysis and Kruskal-Wallis test followed by Dunn's multiple comparisons test was used for longer distance and axonal area analysis. Data is presented as mean ± standard error (SEM). *- $p < 0.05$; ***- $p < 0.001$. Scale bar =200 µm; $M_{(INF-\gamma+LPS)}$ n=5; $M_{(IL-4+IL-13)}$ n=4; $M_{(IL-10+TGF-\beta1)}$ n=5. 2 independent experiments were performed.

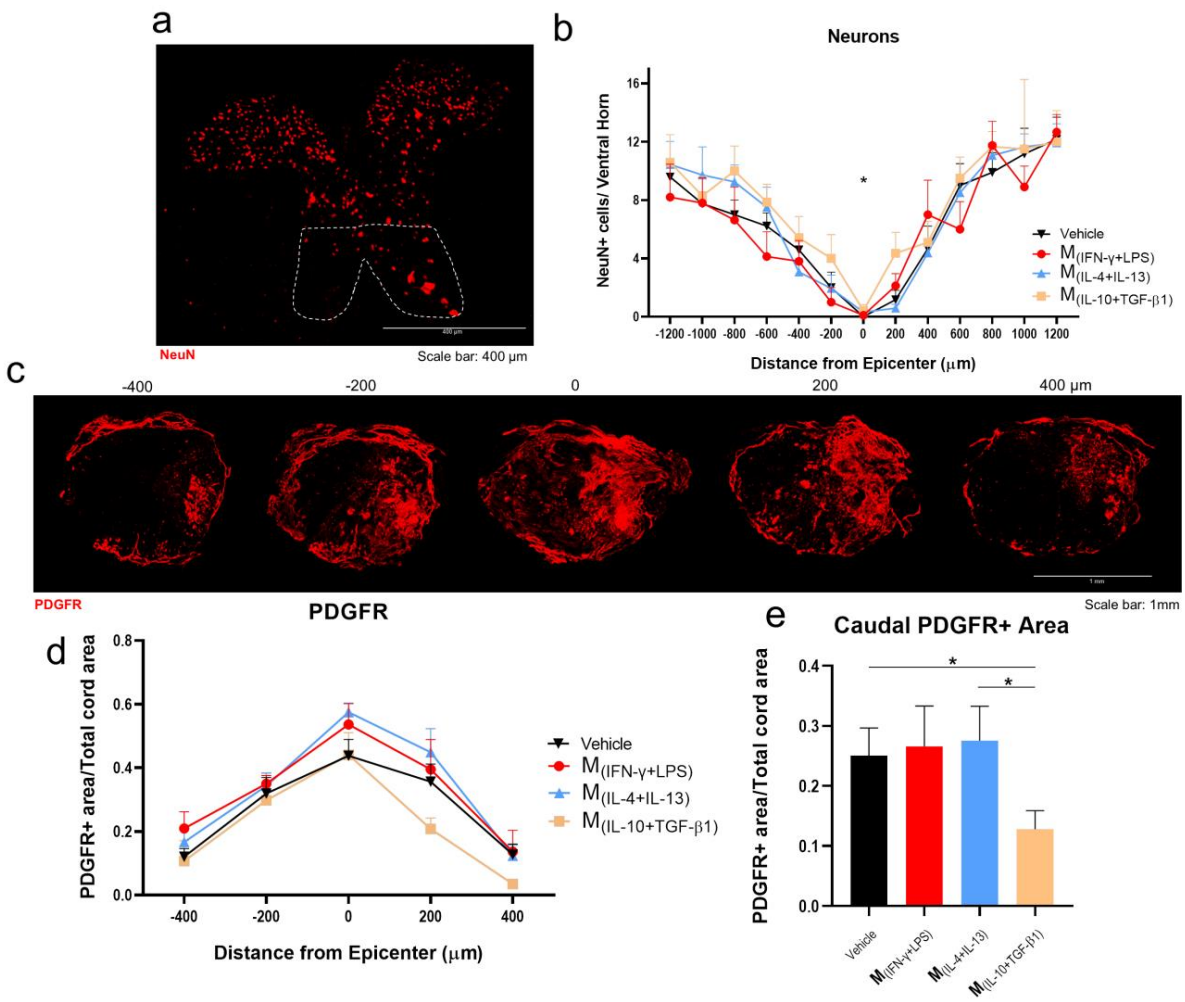

Supplementary Figure S2.3: Histological analysis of the spinal cord. **a)** Representative image of gray matter neurons from $M_{(IL\text{-}10+TGF\text{-}\beta1)}$-treated group, cell bodies were measured by counting the number of positive NeuN cells (red) in laminae VIII and IX of both ventral horns. **b)** Rostral-caudal analysis demonstrated that the secretome derived from $M_{(IL\text{-}10+TGF\text{-}\beta1)}$ cells significantly promoted neuronal survival at the ventral horns (3, 253 df, p= 0.0438) when compared with $M_{(IFN\text{-}\gamma+LPS)}$. **c)** Representative image of fibrotic scar from vehicle-treated group, anti-PDGFRβ antibody (red) was used to analyse fibrosis in the spinal cord. **d)** Although there are not significant differences in PDGFRβ+ total area between treated groups, **e)** rostral caudal analysis show that mice treated with $M_{(IL\text{-}10+TGF\text{-}\beta1)}$-derived secretome had significantly less fibrosis caudally to the injury area (3, 49 df, p= 0.0370). ANOVA followed by the Tukey post-hoc test was used to analyse statistical differences. A total of 312 spinal cord slices were observed to analyse neuronal survival and 134 slices (53 for the caudal calculation) for fibrosis. Data is presented as mean ± standard error (SEM). *- $p < 0.05$. Vehicle n=7; $M_{(INF\text{-}\gamma+LPS)}$ n=6; $M_{(IL\text{-}4+IL\text{-}13)}$ n=8; $M_{(IL\text{-}10+TGF\text{-}\beta1)}$ n=6. 1 independent experiment was performed.

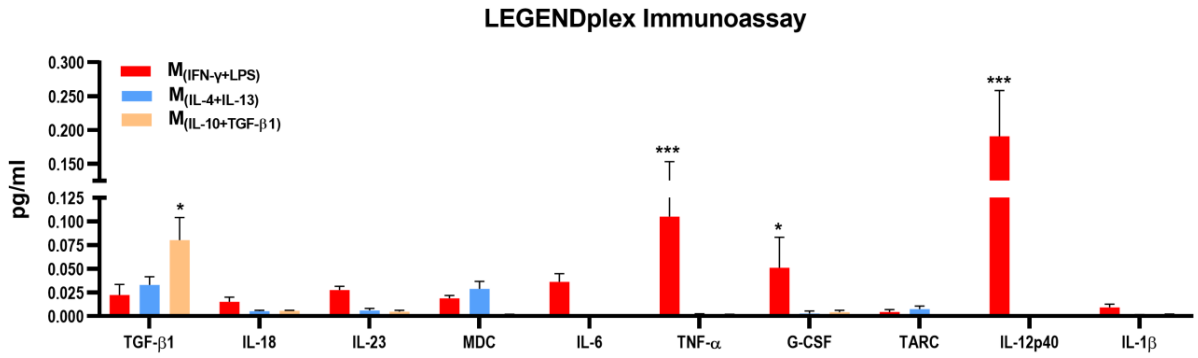

Supplementary Figure S2.4: LEGENDplex immunoassay. The pro-inflammatory cytokines TNF-α, G-CSF and IL12p40 were significantly concentrated on the secretome of $M_{(INF\text{-}\gamma+LPS)}$. The cytokine/hormone G-CSF was also significantly concentrated on the $M_{(INF\text{-}\gamma+LPS)}$-derived secretome. TGF-β1, a cytokine with anti-inflammatory properties was significantly concentrated in the $M_{(IL\text{-}10+TGF\text{-}\beta1)}$-derived secretome. Data was analysed using the two-way ANOVA (2, 130 df, $p<0.0001$) followed by the Tukey's multiple comparisons test. Data is presented as mean ± standard error (SEM). *- $p < 0.05$; ***- $p < 0.001$, $M_{(IFN\text{-}\gamma+LPS)}$ n=4; $M_{(IL\text{-}4+IL\text{-}13)}$ n=6; $M_{(IL\text{-}10+TGF\text{-}\beta1)}$ n=6. Concentration values plotted in the graph were divided by 10 to account for the concentration step performed before the analysis. The values for CXCL-1, IL-12p70, and IL-10 were below the limit of detection and were consequently excluded from the analysis. 1 independent experiment was performed.

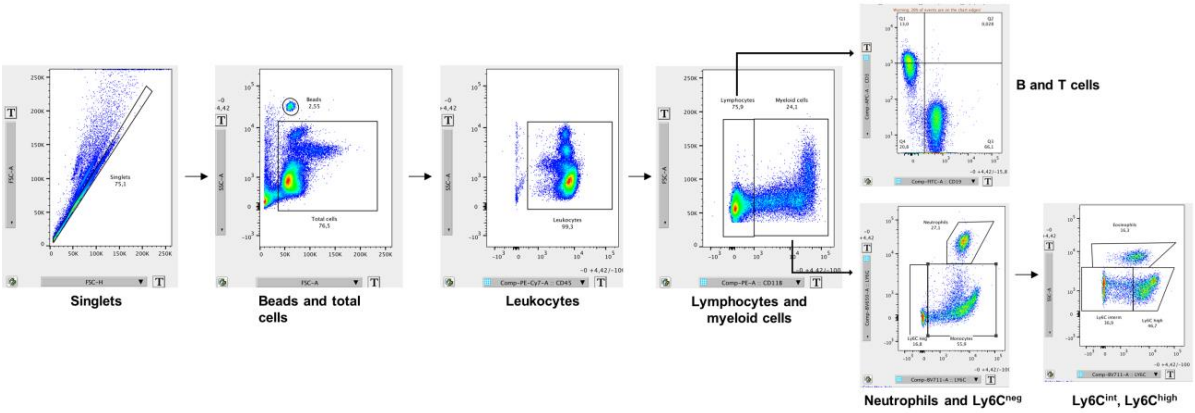

Supplementary Figure S2.5: Gating strategy used for flow cytometry analysis of mice blood cells. Doublets were excluded by FSC-A vs FSC-H scatter. Blood total cells were gated by SSC-A vs FSC-A scatter. Leukocytes were gated by $CD45^+$ cells and on this population lymphocytes and myeloid cells were distinguished by CD11b expression. In lymphocytes population, $CD3^+CD19^-$ cells were defined as T cells and $CD3^-CD19^+$ cells were defined as B cells. In myeloid cell population, Ly6G vs Ly6C allowed the selection of neutrophils ($Ly6G^+Ly6C^+$) and monocytes ($Ly6G^-Ly6C^+$). The selection of eosinophils vs monocytes Ly6C intermediate vs monocytes $Ly6C^{high}$ was made based on Ly6C vs SSC-A gating.

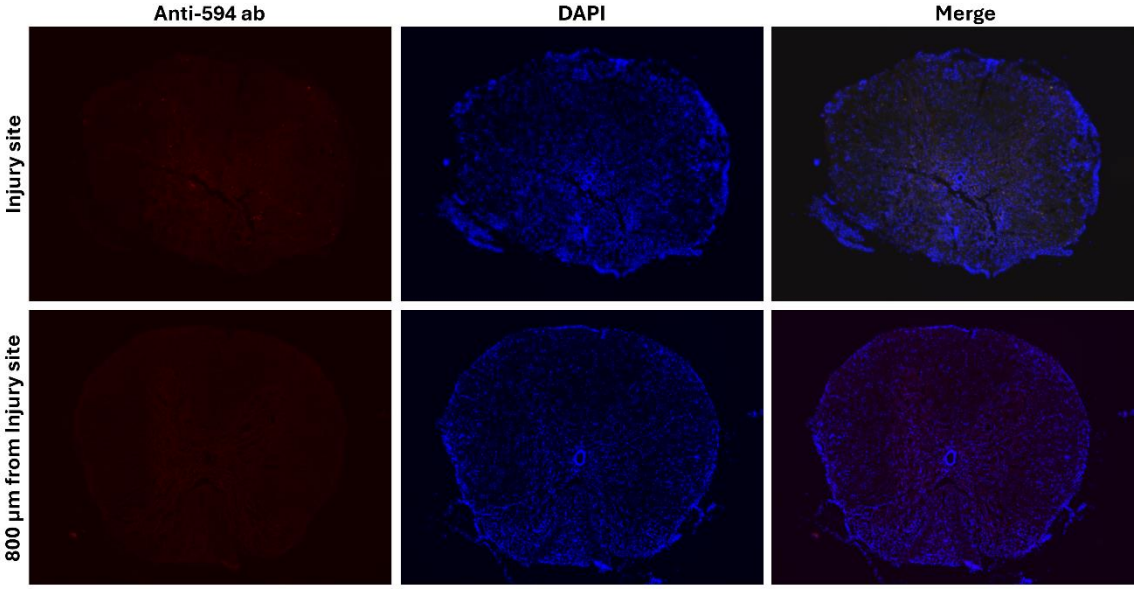

Supplementary Figure S2.6: Negative control fluorescence images of the Alexa Fluor 594 goat anti-rabbit antibody (red) both at the injury site and 800µm from the injury site. DAPI (blue) was used as structural marker.

Supplementary Video 2.1: The Supplementary video 2.1 can be found online at: https://www.frontiersin.org/articles/10.3389/fimmu.2024.1354479/full#supplementary-material

2.13 References

1. Silva NA, Sousa N, Reis RL, Salgado AJ. From basics to clinical: a comprehensive review on spinal cord injury. *Prog Neurobiol* (2014) 114:25–57. doi: 10.1016/j.pneurobio.2013.11.002
2. Silva NA, Sousa RA, Pires AO, Sousa N, Salgado AJ, Reis RL. Interactions between Schwann and olfactory ensheathing cells with a starch/polycaprolactone scaffold aimed at spinal cord injury repair. *J BioMed Mater Res A* (2012) 100:470–6. doi: 10.1002/jbm.a.33289
3. Milich LM, Ryan CB, Lee JK. The origin, fate, and contribution of macrophages to spinal cord injury pathology. *Acta neuropathologica* (2019) 137:785–97. doi: 10.1007/s00401-019-01992-3
4. Blomster LV, Brennan FH, Lao HW, Harle DW, Harvey AR, Ruitenberg MJ. Mobilisation of the splenic monocyte reservoir and peripheral CX(3)CR1 deficiency adversely affects recovery from spinal cord injury. *Exp Neurol* (2013) 247:226–40. doi: 10.1016/j.expneurol.2013.05.002
5. Swirski FK, Nahrendorf M, Etzrodt M, Wildgruber M, Cortez-Retamozo V, Panizzi P, et al. Identification of splenic reservoir monocytes and their deployment to inflammatory sites. *Science* (2009) 325:612–6. doi: 10.1126/science.1175202
6. Gensel JC, Zhang B. Macrophage activation and its role in repair and pathology after spinal cord injury. *Brain Res* (2015) 1619:1–11. doi: 10.1016/j.brainres.2014.12.045
7. Galli SJ, Borregaard N, Wynn TA. Phenotypic and functional plasticity of cells of innate immunity: macrophages, mast cells and neutrophils. *Nat Immunol* (2011) 12:1035–44. doi: 10.1038/ni.2109
8. Mosser DM, Edwards JP. Exploring the full spectrum of macrophage activation. *Nat Rev Immunol* (2008) 8:958–69. doi: 10.1038/nri2448
9. Shechter R, Schwartz M. CNS sterile injury: just another wound healing? *Trends Mol Med* (2013) 19:135–43. doi: 10.1016/j.molmed.2012.11.007
10. Kigerl KA, Gensel JC, Ankeny DP, Alexander JK, Donnelly DJ, Popovich PG. Identification of two distinct macrophage subsets with divergent effects causing either neurotoxicity or regeneration in the injured mouse spinal cord. *J Neurosci* (2009) 29:13435–44. doi: 10.1523/JNEUROSCI.3257-09.2009
11. Monteiro S, Salgado AJ, Silva NA. Immunomodulation as a neuroprotective strategy after spinal cord injury. *Neural Regener Res* (2018) 13:423–4. doi: 10.4103/ 1673-5374.228722
12. Schwartz M, Lazarov-Spiegler O, Rapalino O, Agranov I, Velan G, Hadani M. Potential repair of rat spinal cord injuries using stimulated homologous macrophages. *Neurosurgery* (1999) 44:1041–5. doi: 10.1097/00006123-199905000-00057

13. Schwartz M, Yoles E. Macrophages and dendritic cells treatment of spinal cord injury: from the bench to the clinic. *Acta Neurochir Suppl* (2005) 93:147–50. doi: 10.1007/3-211-27577-0_25
14. Lammertse DP, Jones LA, Charlifue SB, Kirshblum SC, Apple DF, Ragnarsson KT, et al. Autologous incubated macrophage therapy in acute, complete spinal cord injury: results of the phase 2 randomized controlled multicenter trial. *Spinal Cord* (2012) 50:661–71. doi: 10.1038/sc.2012.39
15. Kroner A, Greenhalgh AD, Zarruk JG, Passos dos Santos R, Gaestel M, David S. TNF and increased intracellular iron alter macrophage polarization to a detrimental M1 phenotype in the injured spinal cord. *Neuron* (2014) 83:1098–116. doi: 10.1016/j.neuron.2014.07.027
16. Pinho AG, Cibrão JR, Silva NA, Monteiro S, Salgado AJ. Cell secretome: basic insights and therapeutic opportunities for CNS disorders. *Pharm (Basel)* (2020) 13 (2):31. doi: 10.3390/ph13020031
17. Livak KJ, Schmittgen TD. Analysis of relative gene expression data using realtime quantitative PCR and the 2(-Delta Delta C(T)) Method. *Methods* (2001) 25:402–8. doi: 10.1006/meth.2001.1262
18. Gomes ED, Mendes SS, Leite-Almeida H, Gimble JM, Tam RY, Shoichet MS, et al. Combination of a peptide-modified gellan gum hydrogel with cell therapy in a lumbar spinal cord injury animal model. *Biomaterials* (2016) 105:38–51. doi: 10.1016/j.biomaterials.2016.07.019
19. Gomes ED, Mendes SS, Assuncao-Silva RC, Teixeira FG, Pires AO, Anjo SI, et al. Co-transplantation of adipose tissue-derived stromal cells and olfactory ensheathing cells for spinal cord injury repair. *Stem Cells* (2018) 36:696–708. doi: 10.1002/stem.2785
20. Pinto MJ, Pedro JR, Costa RO, Almeida RD. Visualizing K48 ubiquitination during presynaptic formation by ubiquitination-induced fluorescence complementation (UiFC). *Front Mol Neurosci* (2016) 9:43. doi: 10.3389/fnmol.2016.00043
21. Pinto MJ, Alves PL, Martins L, Pedro JR, Ryu HR, Jeon NL, et al. The proteasome controls presynaptic differentiation through modulation of an on-site pool of polyubiquitinated conjugates. J Cell Biol (2016) 212:789–801. doi: 10.1083/jcb.201509039
22. Rocha LA, Gomes ED, Afonso JL, Granja S, Baltazar F, Silva NA, et al. *In vitro* evaluation of ASCs and HUVECs co-cultures in 3D biodegradable hydrogels on neurite outgrowth and vascular organization. *Front Cell Dev Biol* (2020) 8:489. doi: 10.3389/fcell.2020.00489
23. Percie du Sert N, Hurst V, Ahluwalia A, Alam S, Avey MT, Baker M, et al. The ARRIVE guidelines 2.0: Updated guidelines for reporting animal research. *BMC veterinary Res* (2020) 16:242. doi: 10.1186/s12917-020-02451-y

24. Monteiro S, Pinho AG, Macieira M, Serre-Miranda C, Cibrao JR, Lima R, et al. Splenic sympathetic signaling contributes to acute neutrophil infiltration of the injured spinal cord. *J Neuroinflamm* (2020) 17:282. doi: 10.1186/s12974-020-01945-8

25. Basso DM, Fisher LC, Anderson AJ, Jakeman LB, McTigue DM, Popovich PG. Basso Mouse Scale for locomotion detects differences in recovery after spinal cord injury in five common mouse strains. *J Neurotrauma* (2006) 23:635–59. doi: 10.1089/neu.2006.23.635

26. de Sousa N, Pinho AG, Monteiro S, Liberato V, Santos DJ, Campos J, et al. Acute Baclofen administration promotes functional recovery after spinal cord injury. *Spine J* (2022) 23(3):379–91. doi: 10.1016/j.spinee.2022.09.007

27. Watson C, Paxinos G, Kayalioglu G, Heise C. Chapter 16 - atlas of the mouse spinal cord. In: Watson C, Paxinos G, Kayalioglu G, editors. *The Spinal Cord*. Academic Press, San Diego (2009). p. 308–79.

28. Perez-Riverol Y, Bai J, Bandla C, García-Seisdedos D, Hewapathirana S, Kamatchinathan S, et al. The PRIDE database resources in 2022: a hub for mass spectrometry-based proteomics evidences. *Nucleic Acids Res* (2022) 50:D543–d552. doi: 10.1093/nar/gkab1038

29. Lu J, Cao Q, Zheng D, Sun Y, Wang C, Yu X, et al. Discrete functions of M2a and M2c macrophage subsets determine their relative efficacy in treating chronic kidney disease. *Kidney Int* (2013) 84:745–55. doi: 10.1038/ki.2013.135

30. Lo C, Tran Y, Anderson K, Craig A, Middleton J. Functional priorities in persons with spinal cord injury: using discrete choice experiments to determine preferences. *J Neurotrauma* (2016) 33:1958–68. doi: 10.1089/neu.2016.4423

31. Kalinski AL, Yoon C, Huffman LD, Duncker PC, Kohen R, Passino R, et al. Analysis of the immune response to sciatic nerve injury identifies efferocytosis as a key mechanism of nerve debridement. *eLife* (2020) 9:e60223. doi: 10.7554/eLife.60223

32. Arai K, Harada Y, Tomiyama H, Michishita M, Kanno N, Yogo T, et al. Evaluation of the survival of bone marrow-derived mononuclear cells and the growth factors produced upon intramedullary transplantation in rat models of acute spinal cord injury. *Res Vet Sci* (2016) 107:88–94. doi: 10.1016/j.rvsc.2016.05.011

33. Kim SJ, Ko WK, Jo MJ, Arai Y, Choi H, Kumar H, et al. Anti-inflammatory effect of Tauroursodeoxycholic acid in RAW 264.7 macrophages, Bone marrow-derived macrophages, BV2 microglial cells, and spinal cord injury. *Sci Rep* (2018) 8:3176. doi: 10.1038/s41598-018-21621-5

34. Norden DM, Faw TD, McKim DB, Deibert RJ, Fisher LC, Sheridan JF, et al. Bone marrow-derived monocytes drive the inflammatory microenvironment in local and remote regions after thoracic spinal cord injury. *J Neurotrauma* (2019) 36:937–49. doi: 10.1089/neu.2018.5806
35. Garcia-Bonilla L, Brea D, Benakis C, Lane DA, Murphy M, Moore J, et al. Endogenous protection from ischemic brain injury by preconditioned monocytes. *J Neurosci* (2018) 38:6722–36. doi: 10.1523/JNEUROSCI.0324-18.2018
36. Bauer C, le Saux O, Pomozi V, Aherrahrou R, Kriesen R, Stolting S, et al. Etidronate prevents dystrophic cardiac calcification by inhibiting macrophage aggregation. *Sci Rep* (2018) 8:5812. doi: 10.1038/s41598-018-24228-y
37. Chao H-H, Li L, Gao X, Wang C, Yue W. CXCL12 expression in aborted mouse uteri induced by IFN-g: Potential anti-inflammatory effect involves in endometrial restoration after abortion in mice. *Gene* (2019) 700:38–46. doi: 10.1016/j.gene.2019.02.089
38. Yu ZY, Chen DW, Tan CR, Zeng GH, He CY, Wang J, et al. Physiological clearance of Abeta by spleen and splenectomy aggravates Alzheimer-type pathogenesis. *Aging Cell* (2022) 21:e13533. doi: 10.1111/acel.13533
39. Li Y, Li X, Chen X, Sun X, Liu X, Wang G, et al. Qishen Granule (QSG) Inhibits Monocytes Released From the Spleen and Protect Myocardial Function via the TLR4-MyD88-NF-kappaB p65 Pathway in Heart Failure Mice. *Front Pharmacol* (2022) 13:850187. doi: 10.3389/fphar.2022.850187
40. Zhang K, Lu WC, Zhang M, Zhang Q, Xian PP, Liu FF, et al. Reducing host aldose reductase activity promotes neuronal differentiation of transplanted neural stem cells at spinal cord injury sites and facilitates locomotion recovery. *Neural Regener Res* (2022) 17:1814–20. doi: 10.4103/1673-5374.330624
41. Pinho AG, Cibrao JR, Lima R, Gomes ED, Serra SC, Lentilhas-Graca J, et al. Immunomodulatory and regenerative effects of the full and fractioned adipose tissue derived stem cells secretome in spinal cord injury. *Exp Neurol* (2022) 351:113989. doi: 10.1016/j.expneurol.2022.113989
42. Bao F, Bailey CS, Gurr KR, Bailey SI, Rosas-Arellano MP, Dekaban GA, et al. Increased oxidative activity in human blood neutrophils and monocytes after spinal cord injury. *Exp Neurol* (2009) 215:308–16. doi: 10.1016/j.expneurol.2008.10.022
43. Gris D, Hamilton EF, Weaver LC. The systemic inflammatory response after spinal cord injury damages lungs and kidneys. *Exp Neurol* (2008) 211:259–70. doi: 10.1016/j.expneurol.2008.01.033

44. Aimaletdinov AM, Gomzikova MO. Tracking of extracellular vesicles' Biodistribution: new methods and approaches. *Int J Mol Sci* (2022) 23(19):11312. doi: 10.3390/ijms231911312

45. Driedonks T, Jiang L, Carlson B, Han Z, Liu G, Queen SE, et al. Pharmacokinetics and biodistribution of extracellular vesicles administered intravenously and intranasally to Macaca nemestrina. *J extracellular Biol* (2022) 1 (10):e59. doi: 10.1002/jex2.59

46. Wiklander OPB, Nordin JZ, O'Loughlin A, Gustafsson Y, Corso G, Mäger I, et al. Extracellular vesicle in vivo biodistribution is determined by cell source, route of administration and targeting. *J Extracell Vesicles* (2015) 4:26316. doi: 10.3402/jev.v4.26316

47. Anderson KD. Targeting recovery: priorities of the spinal cord-injured population. *J Neurotrauma* (2004) 21:1371–83. doi: 10.1089/neu.2004.21.1371

48. Freria CM, Brennan FH, Sweet DR, Guan Z, Hall JC, Kigerl KA, et al. Serial systemic injections of endotoxin (LPS) elicit neuroprotective spinal cord microglia through IL-1-dependent cross talk with endothelial cells. *J Neurosci* (2020) 40:9103. doi: 10.1523/JNEUROSCI.0131-20.2020

49. Narita M, Kuzumaki N, Narita M, Kaneko C, Hareyama N, Miyatake M, et al. Chronic pain-induced emotional dysfunction is associated with astrogliosis due to cortical d-opioid receptor dysfunction. *J Neurochem* (2006) 97:1369–78. doi: 10.1111/j.1471-4159.2006.03824.x

50. Hains BC, Saab CY, Klein JP, Craner MJ, Waxman SG. Altered sodium channel expression in second-order spinal sensory neurons contributes to pain after peripheral nerve injury. *J Neurosci* (2004) 24:4832–9. doi: 10.1523/JNEUROSCI.0300-04.2004

51. Tansley S, Uttam S, Ureña Guzmán A, Yaqubi M, Pacis A, Parisien M, et al. Single-cell RNA sequencing reveals time- and sex-specific responses of mouse spinal cord microglia to peripheral nerve injury and links ApoE to chronic pain. *Nat Commun* (2022) 13:843. doi: 10.1038/s41467-022-28473-8

52. Schomberg D, Olson JK. Immune responses of microglia in the spinal cord: Contribution to pain states. *Exp Neurol* (2012) 234:262–70. doi: 10.1016/j.expneurol.2011.12.021

53. Szklarczyk D, Gable AL, Nastou KC, Lyon D, Kirsch R, Pyysalo S, et al. The STRING database in 2021: customizable protein-protein networks, and functional characterization of user-uploaded gene/measurement sets. *Nucleic Acids Res* (2021) 49:D605–12. doi: 10.1093/nar/gkaa1074

54. Liu NK, Zhang YP, Han S, Pei J, Xu LY, Lu PH, et al. Annexin A1 reduces inflammatory reaction and tissue damage through inhibition of phospholipase A2 activation in adult rats following spinal cord injury. *J neuropathology Exp Neurol* (2007) 66:932–43. doi: 10.1097/nen.0b013e3181567d59

55. Chalif JI, Martínez-Silva ML, Pagiazitis JG, Murray AJ, Mentis GZ. Control of mammalian locomotion by ventral spinocerebellar tract neurons. *Cell* (2022) 185:328–344.e326. doi: 10.1016/j.cell.2021.12.014

56. Lei Y, Perez MA. Cerebellar contribution to sensorimotor adaptation deficits in humans with spinal cord injury. *Sci Rep* (2021) 11:2507. doi: 10.1038/s41598-020-77543-8

57. Formento E, Minassian K, Wagner F, Mignardot JB, Le Goff-Mignardot CG, Rowald A, et al. Electrical spinal cord stimulation must preserve proprioception to enable locomotion in humans with spinal cord injury. *Nat Neurosci* (2018) 21:1728–41. doi: 10.1038/s41593-018-0262-6

58. Matson KJE, Russ DE, Kathe C, Hua I, Maric D, Ding Y, et al. Single cell atlas of spinal cord injury in mice reveals a pro-regenerative signature in spinocerebellar neurons. *Nat Commun* (2022) 13:5628. doi: 10.1038/s41467-022-33184-1

59. Morris R, Whishaw IQ. A proposal for a rat model of spinal cord injury featuring the rubrospinal tract and its contributions to locomotion and skilled hand movement. *Front Neurosci* (2016) 10:5. doi: 10.3389/fnins.2016.00005

60. van den Brand R, Heutschi J, Barraud Q, DiGiovanna J, Bartholdi K, Huerlimann M, et al. Restoring voluntary control of locomotion after paralyzing spinal cord injury. *Science* (2012) 336:1182–5. doi: 10.1126/science.1217416

61. Borton D, Bonizzato M, Beauparlant J, DiGiovanna J, Moraud EM, Wenger N, et al. Corticospinal neuroprostheses to restore locomotion after spinal cord injury. *Neurosci Res* (2014) 78:21–9. doi: 10.1016/j.neures.2013.10.001

62. Jo HJ, Richardson MSA, Oudega M, Perez MA. Paired corticospinal-motoneuronal stimulation and exercise after spinal cord injury. *J spinal cord Med* (2021) 44:S23–s27. doi: 10.1080/10790268.2021.1970908

63. Jo HJ, Perez MA. Corticospinal-motor neuronal plasticity promotes exercise-mediated recovery in humans with spinal cord injury. *Brain* (2020) 143:1368–82. doi: 10.1093/brain/awaa052

64. Wang C, Zhang L, Ndong JC, Hettinghouse A, Sun G, Chen C, et al. Progranul in deficiency exacerbates spinal cord injury by promoting neuroinflammation and cell apoptosis in mice. *J Neuroinflamm* (2019) 16:238. doi: 10.1186/s12974-019-1630-1

65. Shi Q, Wu Y, Zhang B, Wu S, Wang X, Lin F, et al. Progranulin promotes functional recovery in rats with acute spinal cord injury via autophagy-induced anti-inflammatory microglial polarization. *Mol Neurobiol* (2022) 59:4304–14. doi: 10.1007/s12035-022-02836-0

66. Kuse Y, Tsuruma K, Mizoguchi T, Shimazawa M, Hara H. Progranulin deficiency causes the retinal ganglion cell loss during development. *Sci Rep* (2017) 7:1679. doi: 10.1038/s41598-017-01933-8
67. Menzel L, Kleber L, Friedrich C, Hummel R, Dangel L, Winter J, et al. Progranulin protects against exaggerated axonal injury and astrogliosis following traumatic brain injury. *Glia* (2017) 65:278–92. doi: 10.1002/glia.23091
68. Liddelow SA, Guttenplan KA, Clarke LE, Bennett FC, Bohlen CJ, Schirmer L, et al. Neurotoxic reactive astrocytes are induced by activated microglia. *Nature* (2017) 541:481–7. doi: 10.1038/nature21029
69. Jha MK, Jo M, Kim J-H, Suk K. Microglia-astrocyte crosstalk: an intimate molecular conversation. *Neuroscientist* (2019) 25:227–40. doi: 10.1177/1073858418783959
70. Brennan FH, Li Y, Wang C, Ma A, Guo Q, Li Y, et al. Microglia coordinate cellular interactions during spinal cord repair in mice. *Nat Commun* (2022) 13:4096. doi: 10.1038/s41467-022-31797-0
71. Lv C, Zhang T, Li K, Gao K. Bone marrow mesenchymal stem cells improve spinal function of spinal cord injury in rats via TGF-beta/Smads signaling pathway. *Exp Ther Med* (2020) 19:3657–63. doi: 10.3892/etm.2020.8640
72. Pan D, Yang F, Zhu S, Li Y, Ning G, Feng S. Inhibition of TGF-beta repairs spinal cord injury by attenuating EphrinB2 expressing through inducing miR-484 from fibroblast. *Cell Death Discovery* (2021) 7:319. doi: 10.1038/s41420-021-00705-8
73. Nakazaki M, Morita T, Lankford KL, Askenase PW, Kocsis JD. Small extracellular vesicles released by infused mesenchymal stromal cells target M2 macrophages and promote TGF-beta upregulation, microvascular stabilization and functional recovery in a rodent model of severe spinal cord injury. *J Extracell Vesicles* (2021) 10:e12137. doi: 10.1002/jev2.12137
74. Tyor WR, Avgeropoulos N, Ohlandt G, Hogan EL. Treatment of spinal cord impact injury in the rat with transforming growth factor-beta. *J Neurol Sci* (2002) 200:33–41. doi: 10.1016/s0022-510x(02)00113-2
75. Xu Y, He X, Wang Y, Jian J, Peng X, Zhou L, et al. 5-Fluorouracil reduces the fibrotic scar via inhibiting matrix metalloproteinase 9 and stabilizing microtubules after spinal cord injury. *CNS Neurosci Ther* (2022) 28:2011–23. doi: 10.1111/cns.13930
76. Li Y, He X, Kawaguchi R, Zhang Y, Wang Q, Monavarfeshani A, et al. Microgliaorganized scar-free spinal cord repair in neonatal mice. *Nature* (2020) 587:613–8. doi: 10.1038/s41586-020-2795-6
77. Göritz C, Dias DO, Tomilin N, Barbacid M, Shupliakov O, Frisén J. A pericyte origin of spinal cord scar tissue. *Science* (2011) 333:238–42. doi: 10.1126/science.1203165

78. Dias DO, Kim H, Holl D, Werne Solnestam B, Lundeberg J, Carlén M, et al. Reducing pericyte-derived scarring promotes recovery after spinal cord injury. *Cell* (2018) 173:153–165.e122. doi: 10.1016/j.cell.2018.02.004
79. Narang A, Zheng B. To scar or not to scar. *Trends Mol Med* (2018) 24:522–4. doi: 10.1016/j.molmed.2018.04.007
80. Santini MP, Malide D, Hoffman G, Pandey G, D'Escamard V, Nomura- Kitabayashi A, et al. Tissue-resident PDGFRa(+) progenitor cells contribute to fibrosis versus healing in a context- and spatiotemporally dependent manner. *Cell Rep* (2020) 30:555–570.e557. doi: 10.1016/j.celrep.2019.12.045
81. Moutal A, White KA, Chefdeville A, Laufmann RN, Vitiello PF, Feinstein D, et al. Dysregulation of CRMP2 post-translational modifications drive its pathological functions. *Mol Neurobiol* (2019) 56:6736–55. doi: 10.1007/s12035-019-1568-4
82. Kondo S, Takahashi K, Kinoshita Y, Nagai J, Wakatsuki S, Araki T, et al. Genetic inhibition of CRMP2 phosphorylation at serine 522 promotes axonal regeneration after optic nerve injury. *Sci Rep* (2019) 9:7188. doi: 10.1038/s41598-019-43658-w
83. Liz MA, Mar FM, Santos TE, Pimentel HI, Marques AM, Morgado MM, et al. Neuronal deletion of GSK3beta increases microtubule speed in the growth cone and enhances axon regeneration via CRMP-2 and independently of MAP1B and CLASP2. *BMC Biol* (2014) 12:47. doi: 10.1186/1741-7007-12-47
84. Gogel S, Lange S, Leung KY, Greene ND, Ferretti P. Post-translational regulation of Crmp in developing and regenerating chick spinal cord. *Dev Neurobiol* (2010) 70:456–71. doi: 10.1002/dneu.20789
85. Tsuchida M, Nakamachi T, Sugiyama K, Tsuchikawa D, Watanabe J, Hori M, et al. PACAP stimulates functional recovery after spinal cord injury through axonal regeneration. *J Mol neuroscience: MN* (2014) 54:380–7. doi: 10.1007/s12031-014-0338-z
86. Kase Y, Sato T, Okano Y, Okano H. The GADD45G/p38 MAPK/CDC25B signaling pathway enhances neurite outgrowth by promoting microtubule polymerization. *iScience* (2022) 25:104089. doi: 10.1016/j.isci.2022.104089

Chapter 3: General discussion of the study and future perspectives

3.1 Discussion and Perspectives

Spinal cord injury (SCI) is a devastating neurological disorder, in which the reduced axonal regeneration is an important problem. Additionally, there are no satisfactory treatment strategies for SCI and thus, there is an urgent demanding in the development of novel therapeutic strategies for this disorder.

One of the reasons why macrophage transplantation strategy has failed, is because the microenvironment at the SCI site favors macrophage polarization into a pro-inflammatory phenotype,

On the other hand, spleen houses a monocyte reservoir [1] and Blomster et al. [2] showed that the majority of infiltrating monocytes at 7 days post-SCI originate from the spleen.

Taking advantage of these facts, we considered appealing to polarize the spleen monocyte-derived macrophages into alternatively-activated anti-inflammatory and repairing phenotypes and use them to promote recover after SCI. Therefore, in this study, we investigated the therapeutic potential of the spleen macrophage secretome for SCI recovery, and instead of transplanting the cells, we injected the paracrine factors and extracellular vesicles that these macrophages secrete,

Now, in this section we will discuss about this study and therapeutic strategy that we developed.

First, in this study, we extracted the spleen from mice to obtain the monocytes to differentiate in macrophages, however, in case of humans and other animals it would be unethical obtain these spleen monocytes by extraction of the spleen. Therefore, since the spleen monocytes are released from the spleen to circulation, and they are in the injured cord within the first week after injury [2,3,4], to obtain the monocytes, it will be feasible to collect them in blood stream and then differentiate them in macrophages.

In this study we used rat DRGs *in vitro*, instead of mouse DRGs, for two reasons: the first was because in previous experiments we tried to use mouse DRGs to assess the axonal growth, however, much of the DRGs did not growth, probably because these mouse DRGs are very small, and due to that, their extraction and manipulation is more difficult than those of rats, what could cause damage to neurons and prevented their growth. The second reason was because the use of rat DRGs is a very well implemented model of axonal growth in our laboratory. We also used CNS neurons, namely rat cortical neurons, because the use of these rat neurons is also a very well implemented model in Doctor Ramiro's laboratory.

In the *in vivo* experiments we choose to inject intraperitoneally the secretomes, instead of injecting the secretomes intraspinally, because the injection in the injured spinal cord, could increase tissue

distension, exacerbating the damage. However, and despite we choose the intraperitoneal administration, we never characterized the biodistribution of the secretomes, what could be important, to know the amount of those that really arrive to the lesion site of the spinal cord, to adjust the dosage, and to know what portion and in what organs the secretomes were retained, in order to study in the future, if the retained secretomes have some impacts in these organs, and if reciprocally these organs can affect the lesion or some outcomes.

The results of the *in vivo* revealed the $M_{(IL\text{-}10+TGF\text{-}\beta1)}$-derived secretome is the most effective treatment in promoting functional recovery after compressive SCI, however, Interestingly, in the first 2/3 weeks post-injury, mice treated with the pro-inflammatory cocktail ($M_{(INF\text{-}\gamma+LPS)}$ secretome) presented a functional recovery very close to those treated with the $M_{(IL\text{-}10+TGF\text{-}\beta1)}$ secretome, indicating that this pro-inflammatory cocktail may be beneficial in the early phase. Therefore, in future studies, it will be considered to inject first this pro-inflammatory secretome, alone or in combination with the $M_{(IL\text{-}10+TGF\text{-}\beta1)}$-derived secretome and then proceed just with $M_{(IL\text{-}10+TGF\text{-}\beta1)}$-derived secretome to see the outcomes. This fact seems to have some connection with the early phases of normal and SCI healing, in which pro-inflammatory macrophages are present and secrete pro-inflammatory citokines, to attract other immune cells and increase inflammatory response to facilitate removal of damaged tissue.

Last but not the least, the proteomic analysis of the $M_{(IL\text{-}10+TGF\text{-}\beta1)}$-derived secretome revealed some proteins that could explain the results in the *in vivo*, however, we did not analyse this secretome and the other secretomes in terms of soluble factors, and extracellular vesicles like exossomes. This analysis would be important to know the constitution of them, and if the proteins are soluble factors, or if for instance they encapsulated in exossomes. This knowledge would also be important because the locations of the proteins, could take to isolation of the specific fractions where they are present and be administered separately to know the outcomes.

Concluding, we conducted a study where we developed a therapeutic strategy for SCI recover, with promising results. With these results, new and pertinent questions arose, that could be explored and answered in future studies and experiments. With all this, we know that this could be just the beginning of another journey in the complex and hard world of SCI treatment.

3.2 References

1. Swirski FK, Nahrendorf M, Etzrodt M, et al. Identification of Splenic Reservoir Monocytes and Their Deployment to Inflammatory Sites. *Science*. 2009;325(5940):612-616. doi:10.1126/science.1175202
2. Blomster LV, Brennan FH, Lao HW, Harle DW, Harvey AR, Ruitenberg MJ. Mobilisation of the splenic monocyte reservoir and peripheral CX3CR1 deficiency adversely affects recovery from spinal cord injury. *Experimental Neurology*. 2013;247:226-240. doi:10.1016/j.expneurol.2013.05.002
3. Popovich PG, Wei P, Stokes BT. Cellular inflammatory response after spinal cord injury in Sprague-Dawley and Lewis rats. *J Comp Neurol*. 1997;377(3):443-464. doi:10.1002/(sici)1096-9861(19970120)377:3<443::aid-cne10>3.0.co;2-s
4. Sroga JM, Jones TB, Kigerl KA, McGaughy VM, Popovich PG. Rats and mice exhibit distinct inflammatory reactions after spinal cord injury. *J Comp Neurol*. 2003;462(2):223-240. doi:10.1002/cne.10736